



esa

ESA-ESO Working Groups

Report No.4 Galactic Populations, Chemistry and Dynamics June 2008



Chair: Catherine Turon
Co-chair: Francesca Primas

Report by the ESA-ESO Working Group on Galactic populations, chemistry and dynamics

Abstract

Between the early 40s, when Baade showed the first evidence for the existence of two distinct stellar populations, and today, with our Galaxy surprising us with new substructures discovered almost on a monthly basis, it is clear that a remarkable progress has been achieved in our understanding of the Galaxy, of its structure and stellar populations, and of its chemical and dynamical signatures. Yet, some questions have remained open and have proven to be very challenging.

The main task of this Working Group has been to review the state-of-the-art knowledge of the Milky Way galaxy, to identify the future challenges, and to propose which tools (in terms of facilities, infrastructures, instruments, science policies) would be needed to successfully tackle and solve the remaining open questions. Considering the leadership position that Europe has reached in the field of Galactic astronomy (thanks to the Hipparcos mission and the Very Large Telescope) and looking at the (near-)future major initiatives it has undertaken (VISTA and VST survey telescopes, Gaia mission), this work clearly has been very timely.

It is of uttermost importance for European astronomy to keep and further consolidate its leading position. This Working Group has made recommendations that would allow dissecting our backyard laboratory, the Galaxy, even further. ESO survey telescopes about to become operational and the upcoming ESA Gaia mission are a guarantee for opening new horizons and making new discoveries. We, the astronomers, with the support of our funding agencies, are ready to fully commit to the best exploitation of the treasure that is ahead of us. The main recommendations this Working Group has made to ESA and ESO are to guarantee the expected tremendous capabilities of these new facilities, to vigorously organise their synergies and to jointly give ways to European astronomers to be leaders in the exploitation of their output data.

Background

Following an agreement to cooperate on science planning issues, the executives of the European Southern Observatory (ESO) and the European Space Agency (ESA) Science Programme and representatives of their science advisory structures have met to share information and to identify potential synergies within their future projects. The agreement arose from their joint founding membership of EIROforum (www.eiroforum.org) and a recognition that, as pan-European organisations, they serve essentially the same scientific community.

At a meeting at ESO in Garching during September 2003, it was agreed to establish a number of working groups that would be tasked to explore these synergies in important areas of mutual interest and to make recommendations to both organisations. The chair and co-chair of each group were to be chosen by the executives but thereafter, the groups would be free to select their membership and to act independently of the sponsoring organisations.

The following membership and terms of reference for the working group on “Galactic populations, chemistry and dynamics” was agreed on:

Membership

Catherine Turon (Chair)	catherine.turon@obspm.fr
Francesca Primas (Co-Chair)	fprimas@eso.org
James Binney	binney@thphys.ox.ac.uk
Cristina Chiappini	cristina.chiappini@obs.unige.ch
Janet Drew	j.drew@herts.ac.uk
Amina Helmi	ahelmi@astro.rug.nl
Annie Robin	annie@obs-besancon.fr
Sean Ryan	s.g.ryan@herts.ac.uk

Additional contributors: Yveline Lebreton, Françoise Combes

Organisation and coordination: Wolfram Freudling

Thanks and acknowledgments

Thanks are also due to Ted Dame, Mike Irwin, Sergio Molinari, Toby Moore, Stuart Sale, Eline Tolstoy, and Sandro D’Odorico who provided figures or advanced information on their work.

Terms of Reference

- (1) To outline the current state of knowledge of the field. (This is not intended as a free-standing review but more as an introduction to set the scene.)
- (2) To review the observational and experimental methods used or envisaged for the characterisation of the Galactic population and dynamics.
- (3) To perform a worldwide survey of the relevant programmes and associated instruments that are operational, planned or proposed, both on the ground and in space.
- (4) For each of these, to summarise the scope and specific goals of the observation/experiment and to point out the limitations and possible extensions;
- (5) Within the context of this global effort, examine the role of ESO and ESA facilities; analyse their expected scientific returns; identify areas of potential overlap and thus assess the extent to which the facilities complement or compete; identify open areas that merit attention by one or both organisations and suggest ways in which they could be addressed.
- (6) Make an independent assessment of the scientific cases for large facilities planned or proposed.
- (7) Propose sets of recommendations on how ESO and ESA, both separately and together, can optimise the exploitation of current and planned missions, and how the agencies can collaborate in the planning of future missions.
- (8) The chair of the working group is appointed by ESO and ESA. The chair will select a co-chair. Other working group membership will be established by the chair and co-chair. The resulting views and recommendations made in the final report will be the responsibility of the group alone.

A final report should be submitted to ESO and ESA by mid-2008.

Catherine Cesarsky(ESO)

Alvaro Giménez (ESA)

December 2006

Contents

Membership	ii
Terms of Reference	iii
1 Executive summary	1
2 Introduction	3
3 Outline of the current state of knowledge of the field	7
3.1 The main structures of the Galaxy	7
3.1.1 The halo	8
3.1.2 The bulge	9
3.1.3 The disc	11
3.1.4 Fossil populations	15
3.1.5 Gas and dust content	16
3.1.6 OB associations and open clusters	18
3.1.7 The globular clusters	19
3.1.8 The satellites	21
3.2 Present day star-formation census	22
3.2.1 The present day initial mass function	23
3.2.2 Environmental factors in star formation	24
3.2.3 Star formation as a structure tracer	26
3.2.4 Star clusters and the cluster mass function	30
3.2.5 Star formation profile along the Galactic plane	31
3.2.6 Interactions with the intergalactic medium (IGM)	34
3.3 Dynamics	37

3.3.1	The central few parsecs	38
3.3.2	The bar/bulge	39
3.3.3	The rotation curve	42
3.3.4	The solar neighbourhood	45
3.3.5	Spiral structure	46
3.3.6	Tidal shredding	48
3.3.7	The warp	49
3.3.8	Dark matter	51
3.4	Composition, kinematics and ages of stellar populations	55
3.4.1	Age determinations	55
3.4.2	Stellar yields	59
3.4.3	Timescales	60
3.4.4	Primordial nucleosynthesis	62
3.4.5	Ages, kinematics, and chemical abundances	67
3.4.6	Comparative studies in the Local Group	70
3.5	Galaxy assembly and evolution	74
3.5.1	History of the halo	75
3.5.2	History of the bulge	76
3.5.3	History of the disc	78
3.5.4	History of the globular-cluster system	82
4	The Galaxy and the Local Group as templates	84
4.1	To constrain stellar evolution models and their uncertainties	84
4.2	To constrain population synthesis models	92
4.3	To constrain galaxy formation models	94

4.4	To constrain dynamical models and theories of the nature of dark matter and gravity	95
4.5	To interpret observations of galaxies beyond the Local Group	98
5	Top questions, and proposed solutions	101
5.1	Global questions and proposed solutions	101
5.1.1	Which stars form and have been formed where?	101
5.1.2	What is the mass distribution throughout the Galaxy? . . .	102
5.1.3	What is the spiral structure of our Galaxy?	103
5.1.4	How is mass cycled through the Galaxy?	104
5.1.5	How universal is the initial mass function?	106
5.1.6	What is the impact of metal-free stars on Galaxy evolution? . . .	107
5.1.7	What is the merging history of the Galaxy?	108
5.1.8	Is the Galaxy consistent with Λ CDM?	109
5.2	The central pc	111
5.2.1	Open questions	111
5.2.2	Tools and tracers	111
5.2.3	Facilities	112
5.3	The bar/bulge	112
5.3.1	Open questions	112
5.3.2	Tools and tracers	113
5.3.3	Facilities	114
5.4	The thin disc	114
5.4.1	Open questions	115
5.4.2	Tools and tracers	116
5.4.3	Facilities	116

5.5	The thick disc	117
5.5.1	Open questions	118
5.5.2	Tools and tracers	119
5.5.3	Facilities	119
5.6	The stellar halo	120
5.6.1	Open questions	120
5.6.2	Tools and tracers	121
5.6.3	Facilities	122
5.7	The globular cluster system	122
5.7.1	Open questions	122
5.7.2	Tools and tracers	123
5.7.3	Facilities	124
5.8	The dark matter	124
5.8.1	Open questions	124
5.8.2	Tools and tracers	125
5.8.3	Facilities	125
6	Relevant programmes and associated instruments, ground-based and space	127
6.1	Astrometric surveys	127
6.2	Spectroscopic surveys	132
6.3	Photometric surveys	136
6.4	Other ground-based facilities	143
7	Recommendations	147
	References	152
	List of abbreviations	172

1 Executive summary

ESA and ESO initiated a series of Working Groups to explore synergies between space and ground-based instrumentation in astronomy. The first three working groups dealt with Extra-Solar Planets (Perryman et al., 2005), the Herschel-ALMA Synergies (Wilson & Elbaz, 2006) and Fundamental Cosmology (Peacock et al., 2006). This, the fourth Working Group concentrated on Galactic stellar populations, Galactic structure, dynamics, chemistry and history.

This work was especially timely given the planning currently being undertaken for Gaia by ESA and the impending first-light of dedicated survey telescopes (VISTA and VST) in the optical and near-infrared by ESO. Moreover, in the future E-ELT era, new utilisations of 4- and 8-meter telescopes and instrumentation can be envisaged.

In this context, a few remarks should be highlighted:

- the volume and quality of data that Gaia will provide will revolutionise the study of the Galaxy even more than Hipparcos revolutionised the study of the solar neighbourhood
- there is a need for very large statistically-significant samples in order to undertake many of the dynamical, kinematic and compositional studies of the Galaxy
- it will be important to develop the capabilities to cover what Gaia will not, such as high-resolution spectroscopy follow-up for a large number of targets selected from Gaia data, medium-resolution spectroscopy for a large number of selected faint stars for which no spectroscopic data will be obtained from Gaia, or achieving wide wavelength coverage in photometry and spectroscopy
- advances in infrared (IR) astronomy will allow us to tap the benefits of infrared wavelengths for astrometric, spectroscopic and photometric observations of the obscured Galactic bulge and Galactic central region
- stellar population science needs access to the visible (including blue) spectrum of stars in the Galaxy, and not to just the IR which is favoured by much cosmological work.
- the cost of these forthcoming data justify, and indeed demand, significant improvements to underlying theory, modelling and analysis techniques

Europe is now poised to take a leading position in Galactic research thanks to an ambitious space mission and to innovative ground-based telescopes. The

major recommendations resulting from this Working Group are for ESA to pay a particular attention to guaranteeing the expected tremendous capabilities of Gaia; for ESO to consider the construction of highly multiplexed spectrographs for follow-up and complementary observations of selected Gaia targets; and for ESA and ESO to jointly organise the exploitation of synergies between Gaia and ground-based observations, and consider ways to give European astronomers a lead in the exploitation of the Gaia catalogue. Detailed recommendations are given in Section 7.

2 Introduction

The blackout of Los Angeles from 1942 enabled Walter Baade (1944) to resolve the brightest stars in M31 and two of its companions. He found them to be red giants, similar to those seen in globular clusters, rather than the blue giants that are the most luminous stars near the Sun. Baade concluded galaxies comprise two stellar populations, *Population I* typified by the Solar neighbourhood, and *Population II* typified by globular clusters. He assumed that blue giants are young because they are associated with dust and gas, so he inferred that Population I is still being formed, while Population II was formed in the past.

In the years between Baade's seminal paper and the Vatican conference in 1958 the concept of a stellar population struck deep roots. Spectroscopic observations and the emerging theory of stellar evolution showed that Population I contains young, metal-rich stars, whereas Population II stars are all old and metal-poor. Population I stars are all on nearly circular orbits, whereas Population II stars are generally on highly inclined and/or eccentric orbits. Moreover, within Population I the ages, metallicities and random velocities of stars are correlated in the sense that younger, more metal-rich stars have orbits that are more nearly circular than those of older, more metal-poor stars.

Thus by 1958 Baade's original simple dichotomy had blossomed into a concept that connects stellar evolution and the progressive enrichment of the interstellar medium (ISM) with heavy elements, to the pattern of star formation in the Galaxy and the Galaxy's dynamical evolution. Much of contemporary astrophysics is still concerned with using this connection to infer the history of galaxies, especially our own.

At this point it is useful to define two terms. A *simple stellar population* is a group of stars that are formed at a single time from gas of given chemical composition. Globular clusters are the objects that most nearly realise the definition of single stellar population. Galaxies always have more complex stellar populations. For example, the Galactic bulge contains stars that have a measurable spread in age, even though they are all old, and cover a significant range in metallicity. We can consider a *compound population* such as that of the bulge to be a superposition of a large number of simple stellar populations. The population of the solar neighbourhood is a compound population that differs from that of the bulge in that it contains very young stars as well as old ones.

An obvious question is whether the compound population of the solar neighbourhood can be represented as a sum of simple stellar populations, one for each time in the history of the disc. Remarkably this is not possible because the stars of a given age have a significant spread in metallicity.

Within any annulus around the Galactic centre, interstellar gas is believed to be well mixed and to have a well-defined metallicity, which increases over time, most rapidly at small galactocentric radii. Therefore the stars that form in an annulus within a small time interval constitute a simple stellar population. The spread in metallicity of the stars near the Sun that have a given age implies that the simple stellar populations that form in different annuli mix over time. This mixing is probably driven by spiral structure and the Galactic bar, so by decomposing the compound stellar population of the disc into simple stellar populations and taking account of the uncertainties affecting metallicities and stellar ages, it should be possible to learn about the Galaxy's dynamical and chemical history.

So far the word *metallicity* is used as if it were a one-dimensional variable. In fact, while stars that are deficient relative to the Sun in, say, iron by a factor 100 will be strongly deficient in sodium or magnesium by a substantial factor, that factor may differ appreciably from 100, and we can learn a lot from what that factor actually is.

The basic application of this idea is to measure $[\alpha/\text{Fe}]^1$, which is the abundance relative to iron of the α nuclides (^{16}O , ^{20}Ne , ^{24}Mg , ^{28}Si , ^{32}S , ^{36}Ar and ^{40}Ca). The α nuclides are synthesised alongside Fe in stars more massive than $\sim 8 M_{\odot}$ that explode as *core-collapse* supernovae $\lesssim 30$ Myr after the star's birth, scattering a mixture of α nuclides and Fe into the interstellar medium (ISM). Consequently, any episode of star formation that lasts longer than 30 Myr will contain stars with both α nuclides and Fe synthesised in massive stars that formed earlier in the episode. Some fraction of stars with masses $< 8 M_{\odot}$ explode as type Ia supernovae ~ 1 Gyr after the star's birth, and these supernovae scatter mainly Fe into the ISM. So if a star-formation episode lasts longer than 1 Gyr, it can lead to the formation of stars enhanced in Fe relative to the α nuclides, or low $[\alpha/\text{Fe}]$. In general, Population II stars have higher $[\alpha/\text{Fe}]$ than Population I stars, indicating that the objects to which they belong formed on timescales shorter than 1 Gyr. In the case of globular clusters this deduction can be verified by showing that the cluster's stars are distributed in the colour-magnitude diagram as we would expect if they were all formed at the same time. This time-scale of 1 Gyr is well established in the solar vicinity, but might be much smaller in other environments and other types of galaxies.

The gas clouds that give rise to low-mass star clusters and associations may be enriched by only a handful of supernovae, with the result that many of the cluster's stars have abundance patterns that reflect peculiarities of the enriching supernovae. Thus if one looks in great detail at the abundances of stars in a given cluster, one may see a pattern that is unique to the cluster, in the same way that

¹where the bracket notation $[\text{X}/\text{Y}]$ refers to the logarithmic ratio of the abundances of elements X and Y in the star minus the same quantity in the Sun

the members of a particular tribe may reveal a characteristic genetic sequence. Moreover, clusters and associations are subject to disruption, and stars that were once in a cluster may now be widely distributed within the Galaxy. By looking for abundance patterns – genetic fingerprints – in field stars, it may be possible to identify members of a cluster that was disrupted long-ago.

Thus depending on the criteria used to define a stellar population, it can range in scale from the members of a disrupted star cluster to Baade’s original Population I, which is made up of stars formed over 10 Gyr from material that has a wide range of abundances of Fe and the α nuclides. However, in every case the members of a stellar population have a common history and similar dynamics; moreover, with appropriate observational material they can usually be identified from their spectra with little regard to their phase-space positions. Galaxy models of the sophistication that will be required in the middle of the next decade to make sense of the Gaia catalogue, will probably interpret the Galaxy as made up of a series of related populations, each with its own distribution function (DF) $f(x, v, t)$ that gives the probability density with which the population’s stars are distributed in phase space at time t . As the Galaxy ages, diffusive phenomena will cause f to become less sharply peaked in phase space, and therefore the DFs of different populations to overlap more and more. Notwithstanding the overlapping of their DFs, the populations will retain their integrity because their member stars will be identifiable by their chemical imprints.

Observational techniques which have traditionally been restricted to targets in the Galaxy are becoming feasible for increasingly distant objects. In particular, we are beginning to be able to study the stellar populations of Local Group galaxies in sufficient detail to be able to decipher their hosts’ star-formation histories. This work gives insight into the histories of galaxies that cover a wide range of morphological types, from gas-rich star-forming galaxies such as the Large Magellanic Cloud and IC 1613, to red and dead galaxies such as M32. Moreover, a large fraction of the current star-formation in the Universe takes place in groups similar to the Local Group, and in fact in galaxies similar to our own, so understanding the Local Group is the key to understanding a significant fraction of the Universe.

The smaller galaxies of the Local Group show abundant evidence of interactions with the Group’s two massive members, M31 and the Galaxy, so studies of Local Group stellar populations should reveal the impact that interactions have on star-formation rates and the build up of heavy elements.

A cosmological framework is essential for any discussion of galaxy formation, and the Lambda cold dark matter (Λ CDM) theory provides the standard framework. In this theory baryons comprise $17 \pm 1\%$ of the matter in the Universe (Spergel et al., 2007), the rest being made up of matter that does not experience

strong or electromagnetic interaction but at redshift 3100 begins to clump and eventually forms the dark halos within which visible galaxies form after redshift ~ 10 . Vacuum energy ('dark energy'), currently dominates the mean cosmic energy density: it contributes $76.3 \pm 3.4\%$ of the energy density with $\sim 24\%$ of the energy density contributed by matter (Spergel et al., 2007); baryons account for only 4.6% of the energy density. On account of the repulsive gravitational force that vacuum energy generates, the expansion of the universe has been accelerating since a redshift ~ 0.5 .

Events similar to those we hope to uncover through studies of Local Group stellar populations, can be observed as they happen at redshifts 0.5–3. These facts make it important to address the question 'what does the Local Group look like to observers who see it at redshifts 0.5, 2 or 3?' This is a thoroughly non-trivial question, but one that could be answered given a sufficient understanding of the Local Group's stellar populations. Answering this question would enable our understanding of high-redshift observations to take a big step forward, for we would then know which objects were evolving towards analogues of the Local Group, and which will merge into rich clusters of galaxies. So the stellar populations of the Local Group are templates from which a much broader understanding of the Universe can be fashioned.

In this Report, we examine the issues raised above as follows. In Section 3 we examine the current state of our knowledge of the structure of the Galaxy, and our knowledge of the processes which have shaped and which continue to shape its stellar populations and gas. At the end of Section 3 we sketch the current picture of how the Galaxy was assembled from its building blocks. In Section 4 we describe how the Galaxy can be used as a laboratory in which to study the processes that shape galaxies, and to constrain theoretical models of galaxy formation and evolution. In the course of Sections 3 and 4, we identify a number of limits on our current knowledge, and hint at future work that would overcome these. These issues are brought into sharp focus in Sections 5 and 7, where we identify the top remaining questions, and suggest how possible solutions might be provided by investment in new facilities, planned and yet to be planned. In Section 6 we review ground- and space-based facilities that have played and/or will play a major role in achieving our scientific goals. The major recommendations of the Working Group are drawn together in Section 7.

Since the original motivation for this Report was a desire on the part of ESO and ESA to consider projects that would complement the Gaia mission, the panel's expertise lays primarily in stellar and dynamical astronomy and this fact may have led to a relative neglect of such important areas as high-energy astrophysics and studies of the interstellar medium.

3 Outline of the current state of knowledge of the field

3.1 The main structures of the Galaxy

Our Galaxy is a late-type spiral, as is directly evident from the high concentration of stars, gas and dust into a narrow strip strung across the night sky. Just as directly, we know from the changing surface brightness of this flattened structure with longitude, that the Sun is at a significant distance from the centre of the Galaxy. Our best estimate of that distance has been lowered gradually over the time-scale of a generation of astronomers: the most recent value for 7.62 ± 0.32 kpc (Eisenhauer et al., 2005), to be compared with the figure of 10 kpc accepted 40 years ago.

The Galaxy is conventionally decomposed into: (i) a bar/bulge that has a luminosity $1 \pm 0.3 \times 10^{10} L_{\odot}$ and extends out to ~ 3 kpc (Launhardt et al., 2002); (ii) a nearly spherical halo that extends from with the bulge out to of order 100 kpc and is studded with globular clusters; (iii) a disc that defines the Galactic plane and is probably confined to radii $R \lesssim 15$ kpc. The disc is often decomposed into two components, a *thin disc*, in which the density falls with distance $|z|$ from the plane exponentially with scale height ~ 300 pc and a *thick disc*, which is characterised by a vertical scale height ~ 900 pc (Cabrera-Lavers et al., 2005; Jurić et al., 2008). The thin disc is patterned into spiral arms but even now, the final word on the number and positioning of the arms present has not been spoken. Beyond the Sun the thin disc is warped.

The baryonic mass of the Galaxy is thought to be less than $\sim 10^{11} M_{\odot}$, with 3/4 of it in the Galactic disc, and nearly all the rest in the bulge. Sgr A*, the black hole at the centre of the Galaxy, is estimated to have a mass of $(3.6 \pm 0.3) \times 10^6 M_{\odot}$ (Ghez et al., 2005, adopting the Eisenhauer et al. (2005) distance).

The major mass component in the Galaxy is believed to be the *dark-matter halo*. This is constrained by measurements of the space motions of Galactic satellites and remote globular clusters, and is thought to be $1 - 3 \times 10^{12} M_{\odot}$ (Wilkinson & Evans, 1999; Sakamoto et al., 2003; Battaglia et al., 2005). The mass within 50 kpc, i.e. the distance to the Large Magellanic Cloud (LMC), is only about a quarter of the total (Sakamoto et al., 2003, $5 - 5.5 \times 10^{11} M_{\odot}$). The dark-matter radial profile is much shallower (roughly $\propto R^{-2}$) than that of the luminous Galactic disc component for which is modelled by an exponentially decreasing surface density, with scale length 2 – 3 kpc (e.g. Drimmel & Spergel, 2001; Robin et al., 2003; Jurić et al., 2008).

3.1.1 The halo

The halo comprises old stars that have heavy-element abundances less than a tenth of the solar value. Its radial density profile is close to a power law $\rho \propto r^{-2.8}$ and it is slightly flattened at the Galactic poles to axis ratio ~ 0.8 (Jurić et al., 2008). Despite being flattened, near the Sun its net rotation is consistent with zero (Figure 1); further out it may rotate slightly in the opposite sense to the disc (Carollo et al., 2007).

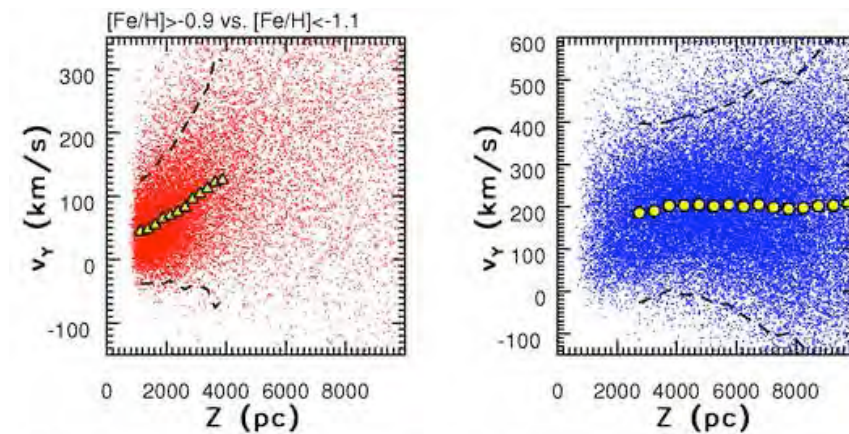


Figure 1: Top row Fig 11 of Ivezić et al. (2008). The rotational velocities of 18 000 stars with $[Fe/H] > -0.9$ (left) or $[Fe/H] < -1.1$ (right) plotted against height $|z|$. Symbols indicate medians and dashed lines 2σ boundaries at fixed $|z|$. Stars plotted in the left panel are associated with the disc and those in the right panel with the halo (see Figure 3).

Bell et al. (2008) find that a smooth model of the halo’s luminosity density can account for only $\sim 60\%$ of the total luminosity: the halo is rich in substructure. Some substructures are certainly the debris of objects that have been tidally shredded by the Galaxy (Section 3.3.6 below), as is evidenced by the tidal streams of the Sgr dwarf spheroidal galaxy, which wraps more than once around the Galaxy (Chou et al., 2007) and of the Magellanic Clouds, which arches right over the southern hemisphere (Putman et al., 2003). The globular clusters Pal 5 and NGC 5466 are known to have significant tidal tails (Odenkirchen et al., 2002; Belokurov et al., 2006a) and an exceptionally long and narrow tail suffers from disputed parenthood (Belokurov et al., 2007b; Jin & Lynden-Bell, 2007; Sales et al., 2008).

The majority of halo stars are on plunging orbits, so near the Sun we see stars that spend most of their time at large galactocentric radii as well as stars that

spend time well inside the solar circle. On account of the prevalence of plunging orbits, any gradients in the halo are of necessity weak.

The metallicity distribution of halo stars is broad, but peaks at abundances far below solar: in the inner halo the peak lies around $[\text{Fe}/\text{H}] = -1.6$, while further out it lies near $[\text{Fe}/\text{H}] = -2.2$ (Carollo et al., 2007). Near the Sun, halo stars are found with metallicities down to at least $[\text{Fe}/\text{H}] = -5.5$ (Frebel et al., 2005). Recently Carollo et al. (2007) revived the idea that out to distances ~ 4 kpc, the stellar halo may be described by two broadly overlapping components. The inner component has a peak metallicity $[\text{Fe}/\text{H}] = -1.6$, is flattened and with a small amount of prograde rotation, while the outer component has a lower peak metallicity ~ -2.2 , is rounder and in net retrograde rotation. The dominance of the inner-halo population in the solar neighbourhood would explain why extremely metal-poor stars in magnitude limited objective-prism surveys are so rare.

Extremely metal-poor stars (*EMP stars*) are of special interest as they give insight into the formation of the first stars. They show some surprising properties:

- Around 20% of EMP stars show unexpected large $[\text{C}/\text{Fe}]$ and often $[\text{N}/\text{Fe}]$ enhancements with respect to the Sun (the so-called *carbon-enhanced metal-poor stars*, Beers & Christlieb, 2005). For the most metal-poor ones, this has been taken as evidence of a different initial mass function (IMF), or for pollution by stellar winds from massive stars even at $Z = 0$, as may be possible if such stars were fast rotators (Meynet, 2007).
- Cayrel et al. (2004) showed that normal (i.e., not C-enhanced) stars with $-4 < [\text{Fe}/\text{H}] < -2$ display a striking degree of chemical homogeneity (Figure 2). This uniformity challenges the view that the whole Galactic halo formed from the successive swallowing of smaller stellar systems with independent evolutionary histories (Gratton et al., 2003).
- Those same stars have large $[\text{N}/\text{O}]$ ratios, and show a large scatter in $[\text{N}/\text{O}]$ (roughly 1 dex) as well as in the r- and s-process elements (Spite et al., 2005). This observation has triggered the development of models of the effect of rotation on stellar evolution at very low metallicity (Meynet, 2007; Limongi & Chieffi, 2007).

3.1.2 The bulge

The bulge dominates the Galaxy interior to ~ 3 kpc. Unfortunately, much of it is highly obscured at optical wavelengths, so it has been intensively studied

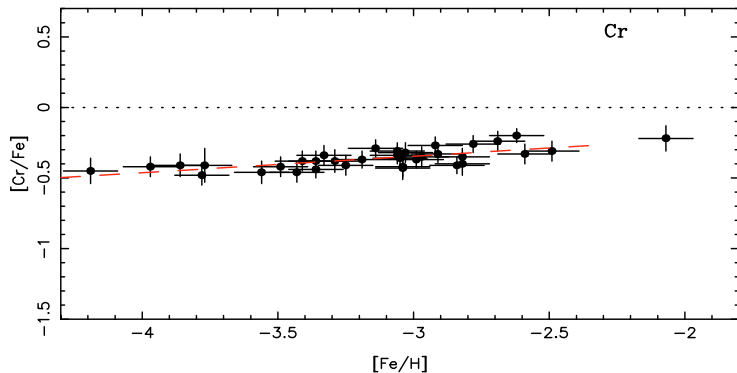


Figure 2: $[Cr/Fe]$ vs. $[Fe/H]$ measured in extremely metal-poor stars by Cayrel et al. (2004). Note that the very small scatter in these abundance ratios can be completely explained by the observational uncertainties, thus suggesting the absence of intrinsic scatter. The reality of the $[Cr/Fe]$ trend with metallicity is still a matter of debate.

along a restricted set of lines of sight that are less obscured. These intersect the bulge $\gtrsim 300$ pc above or below the plane, so the region in which the disc and bulge intersect has still to be adequately explored. Lines of sight to the bulge contain many disc stars in the foreground, especially at the lowest latitudes. Distance errors can lead to these stars contaminating “bulge” samples. The bulge is geometrically and chemically complex: its main body is barred, gas-poor and comprised of old stars with a wide spread in metallicity, while its inner region is gas-rich and the site of active star formation.

The bulge has the peanut shape that in external galaxies is associated with a bar, and both photometry (Blitz & Spergel, 1991; Binney et al., 1997; Stanek, 1995; Babusiaux & Gilmore, 2005) and gas kinematics (Binney et al., 1991; Bissantz et al., 2003) confirm that it is barred. The bar is oriented such that the near end of the bar lies at positive longitudes, and at its extremities it may become less thick and blend into the disc. The key parameters are its semi-major axis length a , its axis ratios and the angle ϕ between the bar’s major axis and the Sun-centre line. Bissantz & Gerhard (2002) find $a \sim 3.5$ kpc, $15^\circ < \phi < 30^\circ$, and axis ratios 1:0.35:0.3, while López-Corredoira et al. (2005) find $20^\circ < \phi < 35^\circ$ and axis ratios 1:0.5:0.4. Most recently Rattenbury et al. (2007) find $24^\circ < \phi < 27^\circ$ and ratios 1 : 0.35 : 0.26. With these parameters the nearer end of the bar is ~ 5 kpc away along $l = 17^\circ$.

Outside the innermost $\sim 1^\circ$, the bulge mainly comprises an old population; the dispersion in ages is small (Ortolani et al., 1995; Zoccali et al., 2003). The distribution of abundances is wide, ranging from $[Fe/H] = -1$ to 0.5 and peaking at $[Fe/H] \sim -0.2$ (Fulbright et al., 2007; Lecureur et al., 2007; Zoccali et al., 2008). In the bulge, $[\alpha/Fe]$ remains high to a higher $[Fe/H]$ than in the disc; in

Section 3.4.3 we shall see that this indicates that the timescale of star formation was shorter in the bulge than in the disc. Zoccali et al. (2008) have demonstrated that the metallicity decreases by 0.25 dex along the minor axis between $b = -4^\circ$ and $b = -12^\circ$, suggesting a mix of different bulge populations.

Within 1° of the Galactic centre, the nature of the bulge changes dramatically because here the *central molecular disc* contains dense, cold gas from which stars continue to form. Because it is so highly obscured, this region is best known from radio-frequency studies of the ISM (Section 3.1.5) and little is known about its stars.

3.1.3 The disc

With a mass $\sim 5 \times 10^{10} M_\odot$ the disc is the most massive stellar component of the Galaxy and the site of most current star formation. It defines the Galactic plane, and holds most of the Galaxy's stock of gas. Dust in this gas hides most of the disc from optical telescopes. The Sun lies near the outer edge of the optically luminous part of the disc, within ~ 15 pc of the plane.

Ivezic et al. (2008) probed the Galaxy with stars that were selected in the colour-magnitude plane to be predominantly fairly distant F and G dwarfs. In Figure 3 from their work there is a triangular region in the lower half of the diagram within which halo stars fall (stars fainter than $g = 18$ and more metal-poor than $u - g = 1$) while disc stars occupy an elliptical region at upper right (brighter than $g = 17.5$ and more metal-rich than $u - g = 1$). Spectroscopic calibrations of the $u - g$ metallicity indicator imply that halo stars are more metal-poor than $[\text{Fe}/\text{H}] = -1$ and disc stars more metal-rich. Hence the disc covers the same metallicity range as the bulge. At top right of Figure 3 the ridge-line of the disc stars slope up and slightly to the right, indicating that the disc becomes more metal-rich as the plane is approached. Unfortunately the photometry (from the *Sloan Digital Sky Survey; SDSS*) provides poor discrimination of metallicity in the region $[\text{Fe}/\text{H}] \sim -0.5$ so it is hard to determine from it the upper limit on the metallicity of disc stars. Thus although the disc extends at least 2.5 kpc above the plane, chemistry clearly separates it from the halo.

Near the Sun the disc's vertical density profile is accurately fitted by the sum of two exponentials in $|z|$ (Gilmore & Reid, 1983) with scaleheights $h_{\text{thin}} = 300$ pc and $h_{\text{thick}} = 900$ pc (Jurić et al., 2008). This observation led to the idea that the disc is a superposition of distinct components, the thin and thick discs. Obscuration within the plane makes it difficult to determine the radial density profiles of these components with confidence, but by analogy with external galaxies the vertical scaleheights are assumed to be independent of radius and the densities are assumed

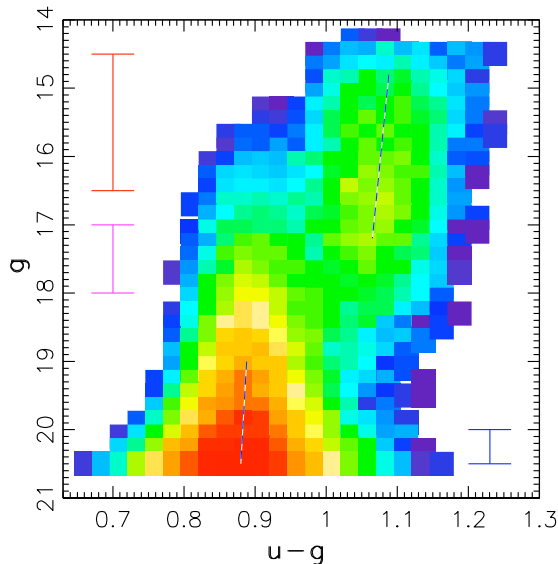


Figure 3: The $u - g, g$ plane for F and G stars ($0.2 < g - r < 0.4$) from Ivezić et al. (2008).

to decrease exponentially with radius. With these assumptions Robin et al. (2003) conclude from near infrared (NIR) star counts that the thin disc has scale length $L_{\text{thin}} = (2.53 \pm 0.1) \text{ kpc}$, while from SDSS photometry Jurić et al. (2008) find $L_{\text{thick}} = 3.6 \text{ kpc}^2$. An outer limit to the stellar thin disc at $15 \pm 2 \text{ kpc}$ has been inferred from the DENIS NIR star counts (Ruphy et al., 1996). Less is known about the extent of the thick disc.

The physical reality of the distinction between the thin and thick discs is hotly debated, and the debate is confused by a lack of agreement as to how these structures should be defined. If we define the thick disc to be a structure that has a double-exponential density profile with the parameters determined from SDSS photometry, then $\sim \frac{1}{4}$ of disc stars belong to the thick disc, which accounts for essentially all disc stars at $|z| > 1.5 \text{ kpc}$. The fraction of local stars that belong to the thick disc is very uncertain: estimates range between 2% (Robin et al., 2007) and 12% (Jurić et al., 2008) depending on the assumed value of h_{thick} (the larger h_{thick} is, the smaller the proportion of local stars that belong to the thick disc). When the thick disc has been defined in terms of the vertical density profile, the question is whether it is possible to identify which local stars belong to the thick disc in a physically well motivated way. A kinematic criterion such as that illustrated in Figure 4 is often used to separate thin and thick disc stars near the

²Jurić et al. (2008) also find $L_{\text{thin}} = 2.6 \text{ kpc}$ in agreement with Robin et al. (2003), although the thin disc does not contribute heavily to the SDSS star counts.

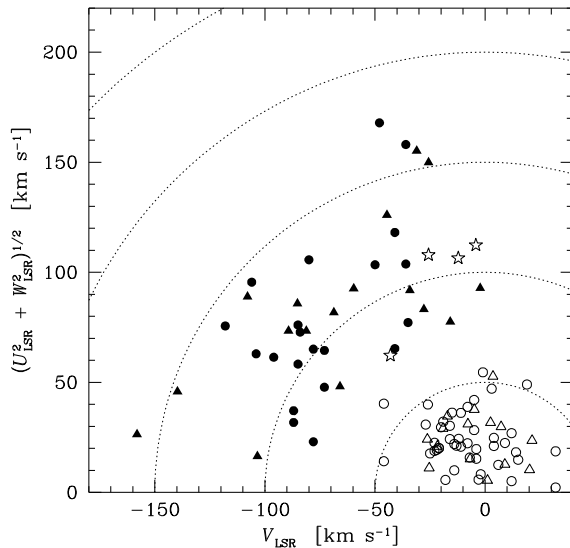


Figure 4: *Fig 1 of Bensby et al. (2005) showing stars near the Sun kinematically identified as belonging to the thin disc (open symbols) and thick disc (filled symbols). The stars mark ‘transition objects’.*

Sun. Dynamical models would connect the spatial and kinematic definitions of the two discs, but we currently lack models of sufficient sophistication to forge this connection.

Spectroscopic determinations of abundances in nearby stars are interpreted as showing that thick-disc stars (identified by their kinematics) have higher $[\alpha/\text{Fe}]$ than thin-disc stars (Fuhrmann, 2008; Soubiran & Girard, 2005). On the other hand, there is a large overlap in iron abundance between the two populations. It is still a matter of debate whether the iron abundance of the thick disc extends up to the solar value – Bensby et al. (2007) argue that it extends to above solar, while in the volume-complete sample of Fuhrmann (2008) the most metal-rich thick-disc stars have $[\text{Fe}/\text{H}] \sim -0.2$.

Within the distance range 7–9 kpc that they probed, Edvardsson et al. (1993) found a slight inward increase in $[\alpha/\text{Fe}]$. It is unclear whether this phenomenon reflects a gradient within the thin disc or changes with radius in the proportions of stars belonging to the two discs (Nissen, 2005). To resolve this question, $[\alpha/\text{Fe}]$ must be determined in much larger samples of stars spanning a larger galactocentric range, with a precision ~ 0.05 dex.

In the solar neighbourhood the velocity distributions of disc stars are approximately Gaussian in the radial and vertical directions, but skew in the direction of Galactic rotation (Figure 5 and Section 3.3.4). Both the velocity dispersion and

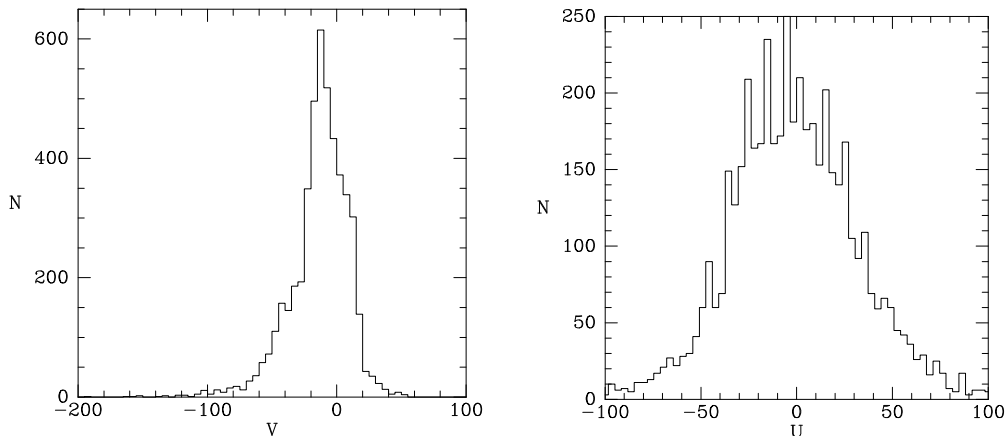


Figure 5: *Distributions of U and V in the Geneva-Copenhagen Survey (from data published in Nordström et al., 2004). Stars with $V > 0$ move round the Galaxy faster than the local circular orbit.*

surface density of disc stars are thought to increase inwards, and these increases inevitably make the V distribution skew because many more stars have their apocentres near the sun and pericentres far in, than there are with pericentres near the Sun and apocentres far out.

Figure 1 shows that the further from the plane you go, the more strongly the median rotation of the disc lags behind that of the Sun. This figure, which is consistent with the findings of Girard et al. (2006), suggests that the entire thick disc lags solar rotation, and that near the Sun thick-disc stars can be identified by their low rotation. The rotational lag of the thick disc has been variously reported as -100 km s^{-1} (Wyse & Gilmore, 1986), -50 km s^{-1} (Fuhrmann, 2004) to as low as -20 km s^{-1} (Norris, 1987). The slope of the line of median symbols in Figure 1 provides an explanation of this ambiguity.

The further a star rises above the plane, the larger its vertical velocity W as it crosses the plane, so Figure 1 implies that near the Sun stars with large $|W|$ should tend to have strongly negative V . Such a trend is not evident in the sample of Nordström et al. (2004).

The clearest relation of this type is Stromberg’s linear relationship between $\langle V \rangle$ and the square of the total velocity dispersion of main-sequence stars bluewards of $B - V = 0.6$ (e.g. Dehnen & Binney, 1998). Such stars have lifetimes smaller than the age of the Galaxy and are generally considered to be members of the thin disc.

There is clear evidence of coherent streams in the thick disc (Helmi et al.,

2006). For example, the Monoceros ring is a structure in the outer disc with a nearly circular orbit, and it is probably related to the Canis Majoris over-density (Martin et al., 2004). It is not yet clear whether the thick disc is dominated by streams or if these are just froth on a smooth background (Gratton et al., 2003). The stars in streams are believed to have formed outside the Galaxy (Section 3.5.3).

Whereas all thick-disc stars are thought to be older than ~ 9 Gyr, freshly formed stars have been added to the thin disc at a fairly constant rate over at least the last 9 Gyr (Section 3.5.3). Stars are now formed on nearly circular orbits that do not go far from the plane. Gradually the fluctuating gravitational fields of spiral arms and giant molecular clouds increase orbital eccentricities and inclinations, so that the random velocities of disc stars increase with age.

Standing shocks in the ISM along the leading edges of spiral arms are thought to be responsible for much of the star formation in the disc. Hence the density of the youngest stars (e.g., OB stars), is strongly peaked along spiral arms (Figure 9).

3.1.4 Fossil populations

Stars with initial masses smaller than $\sim 8 M_{\odot}$ eventually produce white dwarfs. Slightly more massive stars end their lives as neutron stars. Both types of fossil can make a noticeable contribution to the mass density in their local environments. For example, in the solar neighbourhood white dwarfs are believed to contribute $\sim 6\%$ to the local mass-density (Flynn et al., 2006). In high-density environments, two-body interactions will cause fossil stars that are more massive than living stars to sink towards the gravitational centre of the system, where they can begin to dominate the mass density. This effect is most relevant to neutron stars, which have masses $\sim 1.4 M_{\odot}$, and will sink towards the centre of a globular cluster or, indeed, the Galactic centre star cluster in which Sgr A* is located (Freitag et al., 2006).

The neutron stars, when radiating as pulsars, provide an additional service as probes of the free electron density distribution within the Galaxy: essentially, pulsar radio-flux dispersion measures can be combined with H II region data (treated as spiral arm tracers) and independent distance determinations to pulsars in the Galactic plane and in globular clusters to establish a map of n_e (Taylor & Cordes (1993) since updated by Cordes & Lazio (2002)). One of the more arresting results first obtained by Taylor & Cordes (1993) is the existence of a broad ring of free electrons with mean Galactocentric radius of 3.7 kpc, and typical n_e comparable to that found in spiral arms. However the impact of their explosive origins on the kinematics of neutron stars and the short lifetimes of supernova remnants mean such objects are not directly useful as tools for Galactic archaeology. Both super-

nova remnants and high-mass X-ray binaries are of value in tracing present day star formation.

In contrast, white dwarfs are too faint to have any role as tracers of Galactic structure, but they do provide a valuable record of a stellar system's star formation history, simply because they cool so very slowly. It is in principle possible to determine age from a white dwarf's luminosity and colours, as long as the effects of mass and chemistry on the cooling and atmospheric properties are known. The main impediments to obtaining good statistics on white dwarf masses and ages, from which rates of star formation in earlier epochs might be inferred, are sample incompleteness (because old white dwarfs are extremely faint) and difficulties in modelling the properties of the coolest white dwarfs. Nevertheless, this approach has been used with success recently to date globular clusters (Hansen et al., 2004, see also Section 3.4.1), underlining its considerable potential for studies of the star-formation and dynamical histories of the solar neighbourhood. In a similar fashion very old, unevolved low mass stars are also fossils in the sense of encoding within their surface abundance patterns the physical conditions prevailing at the time and place of their formation.

3.1.5 Gas and dust content

The gas and dust content of the Galaxy is mainly concentrated in the Galactic thin disc along with most of the stars, contributing around one-fifth of the disc mass.

The main gas phases are the cold molecular phase at temperatures of 10–50 K, encountered most strikingly in the densest regions associated with spiral arms, and the warmer (~ 80 K) atomic phase of the diffuse clouds that show a related distribution. Mapping of these phases has been accomplished mainly through CO and HI 21cm radio emission surveys that have also become key tools in uncovering the Galactic rotation law and for distance estimation. The works of Dame et al. (2001) and Kalberla et al. (2005) are recent comprehensive examples. While, to lowest order, the velocity field described by such surveys is well modelled as created by rotation on circular orbits, there are also signs of influence by the bar, and peculiar effects due to spiral arms and the warp.

The basic properties of the HI gas layer are largely as summarised by Dickey & Lockman (1990). The HI scale height in the solar neighbourhood, at 100–200 pc, is somewhat smaller than that of the stellar thin disc, but shows strong growth outside the Solar Circle – a characteristic shared with the stellar disc. Also in an analogy to the distinction between the stellar thin and thick discs, there is evidence that atomic gas persists to above ~ 1 kpc from the plane. But these averages hide

a lot of structure on smaller scales. The radial extent of the gas disc may be greater than that of the stellar disc: Levine et al. (2006) trace spiral structure out to ~ 25 kpc. But this is not accompanied by much molecular gas, since very little CO is found outside the Solar Circle. The local molecular scale-height, at under 40 pc, is appreciably less than that of H I (Stark & Lee, 2005).

Looking inwards, up the density gradient, the gas surface density peaks at galactocentric radius $R \sim 4$ kpc, where a large fraction of the gas is molecular rather than atomic (the *molecular ring*). Within the molecular ring there is a dearth of gas because here the bar eliminates circular orbits. Any gas that leaks into this radius range from outside is quickly driven in to $R < 400$ pc, where it accumulates in the central molecular disc. As a consequence of the high density of molecular gas in this central disc, it is a region of active star formation. This star formation is so far not fully explored because this region is highly obscured by dust.

There is a greatly improving picture of the distribution of dust within the Galactic plane: from COBE/DIRBE data we have a useful mapping of column-integrated extinctions (Schlegel et al., 1998) and, with the aid of 2MASS data, much better semi-empirical three-dimensional maps (Drimmel & Spergel, 2001; Marshall et al., 2006). The dust distribution largely follows that of H I.

Ionised (H II) regions exist in close association with molecular clouds and are the classic markers of star forming regions seated mainly in the thin disc. They are known from radio recombination line and continuum surveys and have also been picked out, now at \sim arcsecond spatial resolution, in recent H α surveys (Parker et al., 2005; Drew et al., 2005). At lower spatial resolutions a more global picture emerges that essentially reproduces the spatial scales derived from mapping neutral gas, but there is much structural detail, at both high and low Galactic latitudes, often linked to star-forming activity. This is revealed particularly vividly in WHAM data (Haffner et al., 2003) which combines sensitive imaging with velocity information.

The hottest gaseous phase of the Galactic ISM is made up of the loops and bubbles of $\sim 10^6$ K coronal-phase gas that betray supernova blastwaves and similar. They are seen to higher Galactic latitudes than most cool gas. But such break-outs may take with them filaments of cold gas at speeds of up to 100 km s^{-1} , as described in the *galactic fountain* model (Bregman, 1980). The extent to which coronal-temperature gas carries metals out of the Galaxy into the intergalactic medium is not known, but X-ray observations of clusters of galaxies suggest that this may be a major process.

Some of the best evidence for the mainly out-of-plane high velocity clouds comes from studies based on H I 21 cm data (e.g. Kalberla & Haud, 2006). For

decades after their discovery, the distances to these clouds and their origin was uncertain (van Woerden et al., 2004), but it is becoming clear that most are not as distant or as massive as was once speculated – almost all are at $R \lesssim 20$ kpc and have masses $M \lesssim 10^7 M_\odot$. Some are filaments of H I that have been ejected from the disc by ejecta from young stars, while others are so metal-poor that they must be dominated by material that is entering the Galaxy for the first time (Wakker et al., 2007a).

3.1.6 OB associations and open clusters

Short-lived luminous O and B stars – often but not always associated with H II regions – map out regions of currently high star formation rate (the spiral arms), while lower-mass, longer-lived stars have a much more uniform azimuthal distribution, and more accurately map out the Galactic disc’s mass distribution. Yet the disc contains stellar groupings on a variety of scales that introduces a rich irregular substructure. Broadly speaking, this substructure will have descended from the preceding gas distribution, given that stars form where over-densities of gas are able to collapse. Three particular levels of clustering are recognised: in order of increasing spatial scale and overall mass, these are the open clusters, OB associations and moving groups.

Open clusters are the most easily discerned of these three classes because of their small size and moderate youth, which results in a higher surface density of stars being seen, within a small angular extent on the sky. Their chemical composition is, to a good approximation, uniform (e.g. Paulson et al., 2003; De Silva et al., 2007), and the age spreads of one to a few million years that can sometimes be found within them are negligible from the perspective of Galactic archaeology. The catalogue of open clusters by Dias et al. (2002) lists 1629 of them, with the ages of most being under 1 Gyr, and only a few as old as 10 Gyr. They serve as precious but biased records of stellar and Galactic evolution. The oldest open clusters provide a lower limit to the age of the thin disc. These tend to be found at high galactocentric radius and/or larger distance from the Galactic plane, where they are less subject to the disruptive interactions that are otherwise frequent. Nevertheless, the opportunity to access bound clusters spanning a wide age range has been crucial in revealing a lack of evidence for an age-metallicity relation within the Galactic disc (e.g. Friel, 1995, and the many other papers by this author) which constrains theories of its origin and evolution.

In addition open clusters provide important constraints on the stellar initial mass function (see further discussion in Section 3.2). Recently Kroupa (2007) has provided arguments as to why no open cluster on its own perfectly exhibits the stellar IMF: to recover this it is important to combine observations of numerous

clusters and support the endeavour with some theoretical modelling.

OB associations are recognisable as over-densities of rare, massive stars on spatial scales up to 100 pc, often subtending several degrees on the sky. They are more extended than open clusters. Even though the massive stars appear to be so prominent within them, it has come to be recognised that the IMF in OB associations appears to be essentially the same as in less massive clusters (Massey et al., 1995, and works since). Despite their relative youth ($\lesssim 50$ Myr), the stellar space densities within them are sufficiently low that the members are readily unbound through interactions with other disc objects. Indeed, direct measurements of the expansion have been made for a number of OB associations. Furthermore age spreads are more apparent (Massey et al., 1995) hinting at more complex origins. It has been shown to be useful to independently measure the dynamical and evolutionary ages of OB associations, as this can expose the dissolution process that undoubtedly affects star clusters on all scales (Brown, 2002).

It has recently become evident that the Galaxy is home to some examples of brilliant, very massive and compact clusters analogous to the super star clusters that were first picked out in external galaxies. As in the extragalactic examples these are contained within the inner disc and bulge: they are more massive than $10^4 M_{\odot}$, only a few parsecs across, and are usually highly obscured. The Arches cluster near the Galactic Centre is an example (Figer et al., 2002). Westerlund 1 located in the inner disc is another, and has been mooted as a globular cluster progenitor (Clark et al., 2005). They are mainly distinguished from more common OB associations by their compactness.

3.1.7 The globular clusters

About 160 globular clusters orbit within the Galaxy (Harris, 1996). Each one contains from several thousand to in excess of a hundred thousand stars. They show little if any rotation and are named for being rather nearly spherical. Their radial profiles display a wide range of central concentration from M15, in which the central density continues to rise towards the centre down to the smallest radii probed, to fluffy clusters such as Pal 5. Their velocity dispersions, centrally as large as 12 km s^{-1} , decrease outwards – consistent with all the cluster matter being in stars.

Although globular clusters are often thought of as halo objects, at least 20% of them seem to be associated with the thick disc (Zinn, 1985). The bimodal metallicity distribution of the globular-cluster population (Figure 6), with its peaks at $[\text{Fe}/\text{H}] \simeq -0.5$ and $[\text{Fe}/\text{H}] \simeq -1.5$ ties in with this. When chemical properties are used to decompose the cluster population into metal-rich and metal-poor compo-

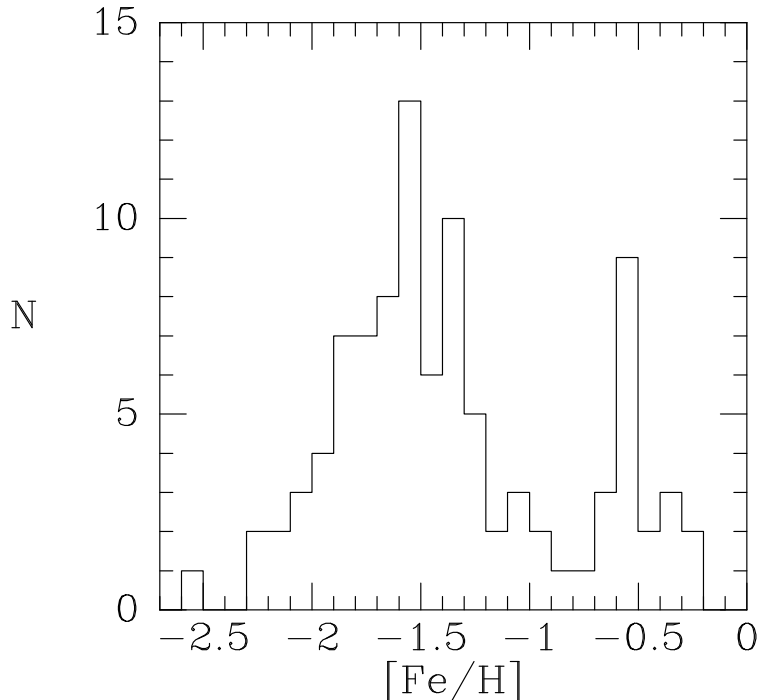


Figure 6: *Metallicity distribution of the Galaxy's globular clusters (from data published in Armandroff, 1989).*

nents, it is found that the two components also have distinct spatial and kinematic properties: the metal-rich population is confined in space to distances from the Galactic plane $|z| < 3$ kpc and $R < 8$ kpc and has significant rotation (the disc clusters), while the metal-poor population is approximately spherically distributed and extends out to $R \simeq 100$ kpc (the halo clusters). All globular clusters are α -enhanced relative to the Sun.

High precision spectroscopic studies do not reveal star-to-star variations in a cluster as far as heavy elements like Fe-peak, s- and r-elements are concerned. In contrast, a wide star-to-star variation is detected for light elements from Li to Al (Gratton et al., 2004; Sneden, 2005). The scenario now accepted is that the first generation of stars in globular clusters would have abundance patterns similar to the ISM from which the protocloud formed (with abundances of the light elements compatible to those observed in their field contemporaries), whereas the second generation contains stars born out of material polluted to different degrees by the ejecta of either asymptotic giant branch (AGB) stars (e.g. D'Antona & Ventura,

2007) or fast rotating massive stars (Decressin et al., 2007). The choice of the right polluters is currently debated and it is clear that to advance in this field it will be necessary to couple both the dynamical and chemical aspects of the globular cluster formation and evolution. If rapidly rotating massive stars are the right polluters, then the evidence for two generations implies a small age spread of ~ 10 Myr, whereas if AGB stars are the polluters the age spread could be larger.

The halo clusters are all extremely old – the data for the large majority of clusters are consistent with ages equal to the cosmologically-determined age of the Universe, 13.4 Gyr. Significantly smaller ages (~ 10 Gyr) are obtained for a minority of clusters (Pal 12 for instance) whose assignment to the halo is controversial (Pritzl et al., 2005). There is no evidence that, among halo clusters, age is correlated with either $[\text{Fe}/\text{H}]$ or galactocentric distance (Richer et al., 1996).

Many globular clusters are on eccentric orbits along which the strength of the Galaxy’s tidal pull varies strongly. With accurate photometry from the SDSS survey it became possible to track streams of stars that have been torn from clusters at pericentre, where the Galactic tide is strong (Odenkirchen et al., 2001). Streams of stars that have been tidally stripped from globular clusters and dwarf spheroidal galaxies offer one of the most promising tools for probing the Galaxy’s gravitational field far from the disc.

Finally, it should not escape attention that some globular clusters are very peculiar, showing extended horizontal branch morphologies and evidence of multiple stellar populations. The well-known long-standing example of this is the cluster ω Cen, but more recent work is beginning to identify an appreciably longer list of clusters presenting similar phenomenology (Lee et al., 2007). These may be construed as the signatures of accretion or satellite-galaxy merger events (Mackey & Gilmore, 2004; Lee et al., 2007).

3.1.8 The satellites

The Galaxy, as a dominant member of the Local Group, has its fair share of dwarf galaxy satellites. They are low-metallicity gas-poor objects, showing patterns of alpha-element enhancement that are different from those seen within the Galaxy or its globular cluster system. The Large and Small Magellanic Clouds (LMC and SMC) are the most massive and best known of these satellites at distances of respectively 50 kpc (Freedman et al., 2001) and 61 kpc (Hilditch et al., 2005). The LMC’s dynamical mass at $\sim 6 \times 10^9 M_{\odot}$ (Kunkel et al., 1997) amounts to just ~ 1 % of the Galaxy’s mass within a radius of 50 kpc. These dwarf irregulars are important as sites of extensive star-forming activity at average metallicities significantly below those of the Galactic disc ($[\text{Fe}/\text{H}] \sim -0.5$ and ~ -0.8 for the

LMC and SMC respectively). The Magellanic Stream, a debris trail of neutral gas and stars, was recognised as linking the Clouds to the Galaxy by Mathewson et al. (1974). This highly extended filamentary structure can be seen in retrospect as prototypical of high velocity clouds. Interestingly, recent proper motion measurements of both the LMC and SMC have raised the question as to whether they may be experiencing their first passage past the Galaxy (Besla et al., 2007).

The list of low mass mainly dwarf-spheroidal satellites has reached double figures and, at the present time, is growing very fast – along with identifications of streams linked to them (see e.g. Belokurov et al., 2007a). There is little doubt that we are presently in a vigorous phase of discovery. There is nevertheless still a shortfall in that predictions would indicate up to ~ 500 might be found (e.g. Moore et al., 1999). The Fornax dwarf-spheroidal galaxy is among the most distant satellites at ~ 150 kpc, and retains its own modest system of globular clusters.

3.2 Present day star-formation census

The question of how stars form, and what factors may determine the result of the process, is a central preoccupation in astrophysics. It is pertinent to all epochs in the history of the Universe and poses problems on many length scales. It is detected at high redshift in the youngest galaxies accessible to us and it is clearly an important part of galaxy formation. A more central issue to this report is that we live in a galaxy within which star formation is a prominent and continuing process that strongly shapes its present-day properties. Because the business of planet-building is caught up in the process of star birth, we are driven also to understand it at the (astronomically) more intimate scale exemplified by the Solar System.

Within the Galaxy we can access worked examples of individual objects near the Sun, as well as open up sites of star formation for inspection on the scales of either star clusters or of spiral arms winding around the Galactic thin disc. The outline picture of how stars form through progressive cloud collapse and disc-mediated accretion is well-established for low mass stars, for which there has long been good access to an array of nearby young clusters. The Taurus-Auriga star-forming region, ~ 140 pc away, was the first to be intensively studied, giving rise to this standard paradigm for lower mass star formation. In recent years this has begun to be broadened out, as the ability to analyse more distant, more massive star-forming regions has grown.

Nevertheless, there are very many unsettled questions of a quite general nature about the process of star formation which - if answered - would make a significant contribution to understanding how our own and other galaxies have evolved over

time. Much effort has been going into modelling and observations from optical to radio wavelengths of the collective behaviour in young Galactic clusters in order to gain insight into the factors determining the stellar content of clusters – essentially, the form of the stellar initial mass function (IMF) – and the factors shaping their early histories. This is set to continue. An important concern is the role that Galactic environment and metallicity might play, and whether the outcome carries any memory of whether the star formation was rapid, triggered or more quiescent in character. An increasingly related, small-scale, but very challenging problem is whether star formation at masses exceeding $\sim 10 M_{\odot}$, where radiation pressure might halt collapse is essentially the same process as at solar and lower masses. To work out the astrophysics of this, the disc of the Galaxy is the crucial laboratory for the simple reasons of proximity and angular scale. Similarly the process of fragmentation, the origins of stellar multiplicity, and the efficiency with which gas is turned into stars, remain open questions and must be studied locally.

3.2.1 The present day initial mass function

For the discussion here, the stellar IMF is defined as the distribution function $dN(M)/dM \propto M^{-\alpha}$, where $N(M)$ is the number of stars within a specified population, in the mass interval M to $M + dM$. In this formulation the Salpeter (1955) value of the power law index, α , is 2.35.

The stellar IMF is at once simple, and quite elusive. Down to stellar masses of about $0.5 M_{\odot}$ it appears that the power law proposed by Salpeter (1955) serves well in many applications. Measured indices commonly fall within a few tenths of the canonical value, but – as argued by Kroupa (2007) – individual measurements are always problematic. Also there is strong evidence that, for the galactic disc, $\alpha \sim 2.7$ and hence steeper than the Salpeter one (Romano et al., 2005; Kroupa, 2008, and references therein). This is into agreement with the suggestion that the *integrated galactic initial mass function* (IGIMF) might differ from the IMF inferred observationally from stellar clusters, being steeper for masses above $\sim 1.5 M_{\odot}$ (Weidner & Kroupa, 2006). In the lower mass range, down to the hydrogen burning limit at $M \sim 0.08 M_{\odot}$, cluster studies have provided evidence of flattening of the IMF with respect to the Salpeter slope to $\alpha \simeq 1.3$, followed by a turnover or still further flattening into the substellar mass domain. The substellar extension of the IMF is still hard to quantify and it is probably more intrinsically variable. Setting this aside, the measured variations in the IMF are small and, inevitably, subject to stochastic effects proportionate to the number of stars in any given cluster. The data are commonly seen as consistent with the concept of a universal IMF (Kroupa, 2001, 2007), in which the main feature is the ‘knee’ mass ($\sim 0.5 M_{\odot}$) at which the IMF first flattens. It has been argued that this prominent but not so variable feature of the IMF may carry a weak sensitivity to the initial Jeans mass

of the collapsing cloud (Bonnell & Bate, 2006).

Interestingly, metallicity has not yet been isolated as a significant influence on the IMF, given that comparative studies of the Magellanic Clouds and the Galaxy have yet to pick out distinctive IMF differences that require such a cause (Scalo, 1998; Massey, 2003). But it may turn out that very low metallicity populations within the Galaxy – simply because they are so old – may have sprung from a different IMF, brought about by their forming in an environment bathed in a warmer cosmic microwave background (CMB): Larson (2005) has suggested that warmer backgrounds in the past, through their impact on the Jeans mass, could have resulted in IMFs with raised characteristic masses. This concept has been taken up by Tumlinson (2007) and used in exploring the abundance patterns of Galactic carbon-enhanced metal poor stars.

In terms of direct evidence, there seem to be two limiting cases of the stellar IMF seen mainly outside the confines of the Galaxy that do provide evidence of departures from a universal IMF. One of these cases may be the densest regions (giant molecular clouds, and super star clusters seen in the nuclear regions of other galaxies). Despite the improving quality of observations, an impression persists that the high-end IMF is systematically somewhat flatter than Salpeter and/or actually truncated at intermediate masses ('top-heavy' mass functions, see e.g. Smith & Gallagher, 2001). Similar behaviour has been noted in the Galactic Centre (e.g. Blum et al., 2003). At the same time, there is a list of good physical and observational reasons why this impression cannot be accepted automatically as proof that environment alters the IMF. Two of the more interesting physical considerations are that mass segregation after the main collapse has completed would hinder a good accounting of the intrinsic IMF, and that loss of lower mass members might occur. At the opposite extreme, there is some tentative evidence that the IMF is all-round steeper in the case of very low density galactic environments, e.g. Lee et al. (2004).

So whilst there is a powerful impetus to regard the IMF in the near Universe, at least, as an invariant characteristic of all newly created single stellar populations, it is a concept that never ceases to come under scrutiny, fraught with difficulty though that scrutiny is.

3.2.2 Environmental factors in star formation

The major environmental debate at the present time is over the available modes of star formation: knowledge of the IMF (universal or not) does not in itself imply a working model of *how* stars form. A recent effort to unify ideas on this has been presented by Elmegreen (2007), building particularly on the earlier work of

Hartmann et al. (2001). Elmegreen (2007) proposes limiting the classical concepts of slow field expulsion through ambipolar diffusion and gradual collapse to lower density ‘sub-critical’ environments (e.g. as in low surface brightness galaxies). In contrast, dense compact molecular cores may be seen as collapsing and forming stars very rapidly, within a cloud-crossing time, in supercritical conditions wherein self-gravity overwhelms magnetic support. A third mode of star formation described by Elmegreen (2007) – that might be permitted in between these extremes – corresponds to blast-wave triggering of the later collapse of cloud envelopes in the wake of a supercritical massive cloud core event. This way of thinking brings with it the possibility to also begin to explain how the age spreads often seen within massive clusters are set up (Massey et al., 1995). Whether this synthesis is right in all or only some of its component parts remains to be seen.

Figure 7 presents an attractive worked example of massive cluster production, which would involve the two more spectacular modes of star formation. Star-forming regions within the Galaxy are being examined closely in order to set constraints on early-stage gas clump mass functions and star formation efficiencies, as well as on final stellar IMFs. A nice recent example is provided by a sub-millimetre study of W3, a dense cloud in the Perseus Arm, that points out the distinction, within one part of the complex, between triggered star formation in the compressed interface with a neighbouring H II region, and more quiescent processes at lower density well away from the interface (Figure 8). Whilst it is known that the prestellar gas clump mass function bears a close resemblance to the stellar IMF, understanding the linkage between the two remains a challenge (Clark et al., 2007; Goodwin et al., 2008).

The picture of essentially three modes and time-scales for cloud collapse gives a sharpened context, and a raised significance to the debate on the origin of massive stars (Krumholz & Bonnell, 2007). Those preferring final star masses to be limited to that available from the initial collapsing fragment find reason to question the concept of fast supercritical collapse in dense environments (Krumholz & Tan, 2007). On the other hand, proponents of competitive accretion – in which star-forming fragments in nascent cluster cores continue to gain mass as they collapse and accrete onto a central object – find it more natural (Bonnell & Bate, 2006).

Before the concept of supercritical modes of star formation can achieve wide acceptance, there needs to be (i) a convincing census of the Galactic population of dense molecular clouds to establish what proportion is inert, and (ii) a convincing description of how molecular clouds are produced quickly from a pre-existing population of H I clouds by the passage of a spiral density wave or other flow. With regard to the second of these issues, there is a problem in that the accepted time-scale for the dust-grain surface chemistry conversion of H I to H₂ is about a factor of 10 greater than is available within the fast collapse scenario (Goldsmith &

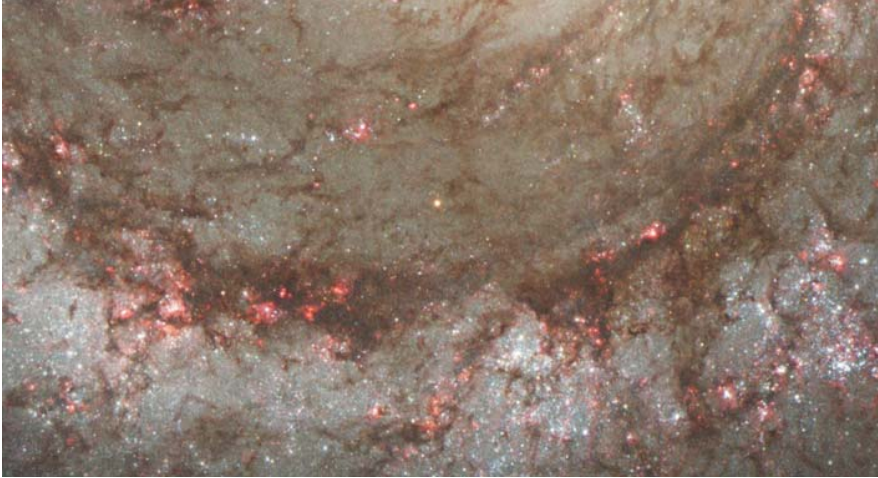


Figure 7: *An unimpeded view, from almost 10 Mpc, of star formation and spiral arm structure: an excerpt from the Hubble Heritage image of M51, discussed by Elmegreen (2007). This illustrates rapid and triggered star formation in action. Matter in the disc of this galaxy enters from upper left into the presumed density wave. Accordingly the brightest and youngest compact H II regions that are formed promptly are entangled in the densest part of the dust lane to the left, while more extensive, evolved and less obscured clusters are moving away from the compression zone in the middle-right of the picture. The latter are seen surrounded by shredded remnants of their former molecular cloud envelopes, triggered into star-forming action.*

Li, 2005). Toward the centre of the Galaxy, where molecular gas is more plentiful in the first place and more easily shielded, this is probably a less serious issue. Tracing the evolution of the Galaxy's reservoir of cold interstellar gas through the earlier stages of the star formation process, to answer (i) above, is a major driver for surveying the Galactic disc with Herschel (HiGAL open time survey), and also of surveys at sub-millimetre wavelengths.

3.2.3 Star formation as a structure tracer

It can be demonstrated from examples like M51, a beautiful nearly face-on grand design spiral (Figure 7), how precisely brilliant young H II regions sit on major spiral arm features. The same has long been presumed to be true of the disc of the Galaxy, but this has not so much been demonstrated as been taken as an axiom. If this were already a settled matter, there might not be the niggles and challenges that persist regarding the number and disposition of the major spiral arms. The majority view, based mainly on a mix of optical OB association data, radio and CO data, favours 4 major spiral arms picked out by these tracers (see Figure 9 and Vallée, 2005, see also Section 3.3.2 and Figure 12). Points at issue begin close to home: is the Sun in a separate minor arm (the Orion Arm), or is this structure

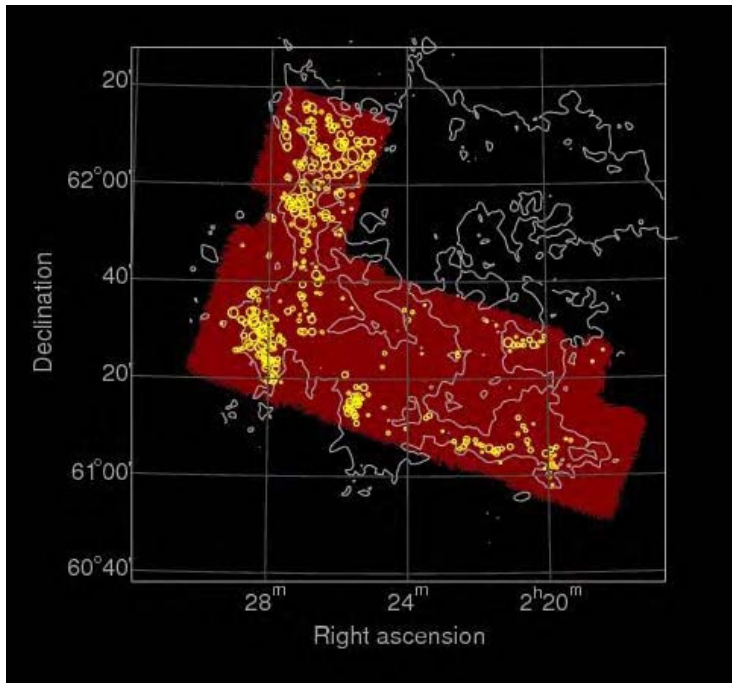


Figure 8: *Star formation on the scale of a single cloud. A submillimetre continuum map of the star-forming cloud W3 showing a dense zone of triggered collapse on the east (left) flank, along with quiescent collapse in the south west. 316 point-source density peaks are picked out in yellow, down to a completeness limit estimated to be $13M_{\odot}$. The gas clump mass functions in the two regions seem very similar. From Moore et al. (2007).*

a spur off the major Sagittarius Arm (the so-called ‘local arm’ feature, Figure 9)? It gets worse further away: a recent unsettling discovery, in Spitzer/GLIMPSE stellar data, has been the absence of an obvious stellar over-density in the sky at $\ell \sim 49^{\circ}$, where the Sagittarius arm tangent is supposed to be (Benjamin et al., 2005, see also Section 3.2.5).

Outside the Solar Circle, mapping of spiral-arm or indeed any other kind of *stellar* structures are just not as well developed. Is there an Outer Arm? Maybe. The evidence is presently suggestive rather than conclusive. Also it is not clear whether the claim of the stellar density cut-off at a Galactocentric radius of ~ 15 kpc (Ruphy et al., 1996) is fully compatible with claims of more distant star clusters and gaseous structures in the Galactic plane (e.g. Digel et al., 1994; McClure-Griffiths et al., 2004; Levine et al., 2006; Brand & Wouterloot, 2007). These unsettled questions arise in part from limited attention to the outer structure of the Galactic plane. There are difficulties also. On the one hand, problems persist in the absolute magnitude calibrations for OB stars – an issue of general significance. But there are also well-known and noticeable departures from uni-

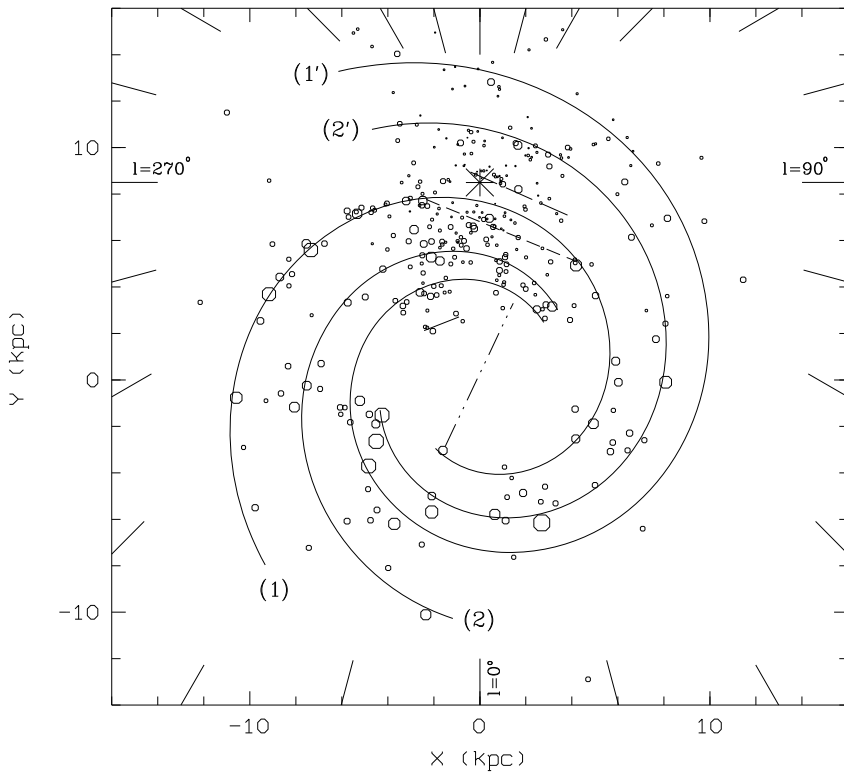


Figure 9: A four arm model for the Galactic disc superimposed on the distribution of known OB associations. The Sun is centre top, marked as an asterisk. The bar is marked by the dash-dotted line. The four arms are plotted. 1: Sagittarius-Carina arm, 2: Scutum-Crux arm, 1': Norma-Cygnus arm and 2': Perseus arm. The dashed lines mark the local arm feature. From Russeil (2003), assuming $R_{\odot}=8.5\text{kpc}$. See also Russeil et al. (2007).

form Galactic rotation (Fich et al., 1989). Furthermore, the declining presence of CO in the outer Galaxy (Figure 10, note the weak non-zero velocity signatures there) is one factor in the generally poorer state of kinematic data beyond the Solar Circle.

Only now is fully empirical 3D extinction mapping on the scale of a few arcminutes becoming achievable via high spatial resolution digital surveys such as IPHAS (Drew et al., 2005) and UKIDSS/GPS (Lucas et al., 2007). Less deep 2MASS data have already been exploited to semi-empirically map the disc both within the Solar Circle (Marshall et al., 2006), and beyond (Froebrich et al., 2007). An example of how the state of the art is changing is shown as Figure 11. As this capability improves, so will the reliability with which lines of sight passing through the Galactic plane can be disentangled to give a more certain spatial

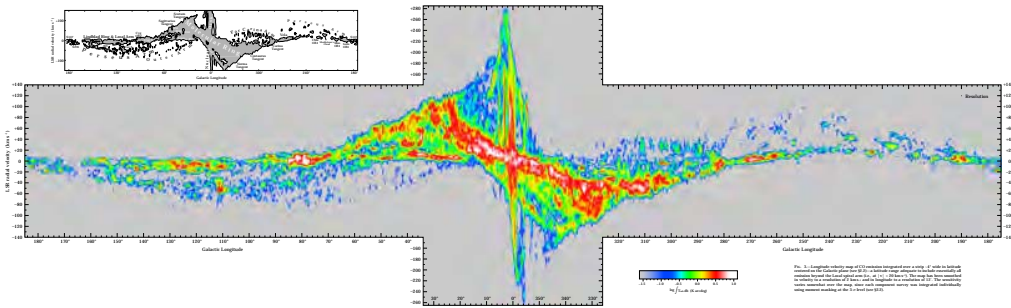


Figure 10: The longitude-velocity map derived from CO observations of the Galactic plane. The data shown have been integrated over a latitude range of 4° . From Dame et al. (2001).

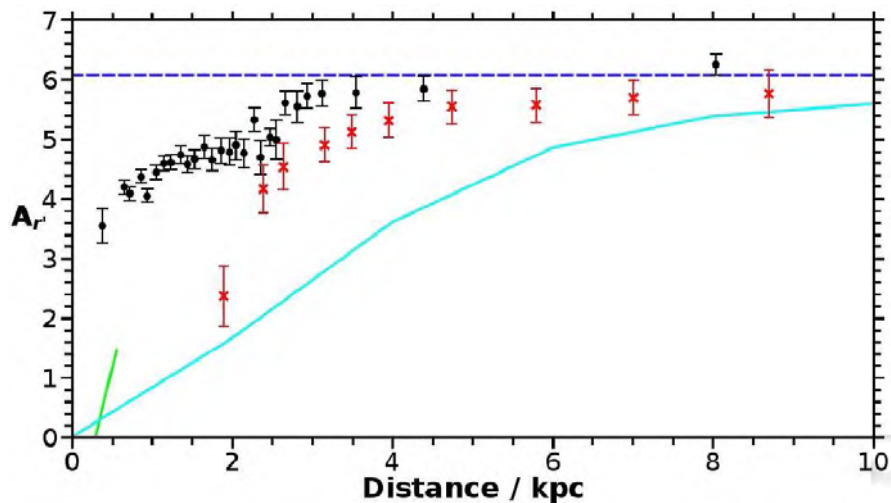


Figure 11: The changing status of extinction mapping within the disc of the Galaxy. This figure, for Galactic coordinates $(\ell, b) = (32, +2)$, compares the early 3D-extinction map of Neckel et al. (1980) (green line) based on early-type stars, through the semi-empirical maps of Drimmel et al. (2003) (cyan line) and Marshall et al. (2006) (red points), to the more fully empirical mapping beginning to emerge from IPHAS stellar photometry (black points). The dashed blue line identifies the asymptotic extinction derived for this sightline from the data of Schlegel et al. (1998). The available spatial resolution is becoming much better: for Neckel et al. (1980) it was several square degrees, for Marshall et al. (2006) it was 30×30 arcmin², while the IPHAS mapping refers to a sky area of 10×10 arcmin² (Sale et al, submitted). The most recent mapping is sensitive to the Aquila Rift at ~ 500 pc (responsible for the sharp initial reddening rise), while the Sagittarius arm is apparent within it as the gradient change at 2.5 to 3 kpc.

sequencing of the structures seen. At the same time, the necessity will remain to determine extinction well for individual objects to place them correctly in context – very often this will involve continuing access to a range of single and multi-object

optical/NIR spectroscopic facilities (both north and south), capable of delivering spectrophotometric data.

Overall it would be fair to say that the present image of the relationship between young star-forming regions within the Galactic disc and large-scale stellar and gaseous structures is sound but greatly lacking in convincing detail. This much is true of the $\sim 2/3$ of the Galactic plane currently open to investigation. About the remaining $1/3$, Vallee's (2005) 'terra incognita' on the far side of the Galactic Centre, we do indeed know nothing.

3.2.4 Star clusters and the cluster mass function

In the hierarchy of astronomical structure, star clusters are the next rung up from the stars. Their masses range from a few tens of solar masses up to $\sim 10^5 M_{\odot}$ for a small number of spectacular clusters in the inner Galaxy. Up to a point, cluster size correlates with mass in that open clusters are lower in mass than OB associations and are generally appreciably smaller and more concentrated too. However the fact that the analogues to the super-star-clusters in the inner Galaxy are both massive *and* very compact, shows that environment is an important determinant of cluster properties also. The solar neighbourhood, out to a distance of a few hundred parsecs, is not notable for particularly massive clusters.

Cluster initial mass functions (CIMF) are, in general, harder to derive for the simple reason that the individual clusters within a population of clusters (unlike the stars within them) are not expected to be coeval – thus requiring individual cluster ages to be modelled out from present-day observed luminosity functions. As with the stellar IMF, there is a prevailing sense of a universal CIMF, with little or no metallicity dependence, of the form $\xi(M) \propto M^{-\alpha}$, where $\alpha \simeq 2$ (Elmegreen & Efremov, 1997). The power law index is not far off the Salpeter value, and the devil is once again in the detail. Recent modelling of the Galaxy's globular cluster system suggests a CIMF index of $1.7 - 2$ (Kravtsov & Gnedin, 2005). Hunter et al. (2003) obtained 2 to 2.4 for the LMC and SMC. The Lada & Lada (2003) result for embedded clusters in the Galactic disc within 2 kpc of the Sun is $\alpha \simeq 2$, for a sample limited to the mass range $50 - 1000 M_{\odot}$.

Star clusters are fragile objects prone to rapid disruption and strong luminosity evolution. A very striking result due to Lada & Lada (2003) is that there appears to be an order of magnitude mismatch between the embedded cluster birthrate in the Milky Way disc and the rate of appearance of visible open clusters – proving early life up to 5–10 Myrs is perilous. The more recent modelling of clusters in the solar neighbourhood by Lamers et al. (2005) scales this dramatic death rate down to around 50%. Significant factors in this mortality are tidal

effects (in all clusters), and the stellar evolution of the most massive members. In more massive OB associations, this second effect is particularly dramatic, since the massive-star content will yield powerful winds and explosions that serve to drive out any gas left over from star formation, greatly modifying the cluster potential (see e.g. Goodwin & Bastian, 2006). Few clusters survive the slow expansion they are subject to, or indeed the dynamical buffeting they receive from encounters with giant molecular clouds, and when they pass through density waves.

Simulations of cluster evolution yield estimates of the current surface star formation rate and its recent history. For the present rate, Lamers et al. (2005) obtain $5 \times 10^{-10} M_{\odot} \text{ yr}^{-1} \text{ pc}^{-2}$, as compared with the Lada & Lada (2003) figure of $7 - 10 \times 10^{-10} M_{\odot} \text{ yr}^{-1} \text{ pc}^{-2}$. Regarding the historical rate, Lamers et al. (2005) find evidence of a phase of increased cluster formation 250 to 600 Myrs ago. On the basis of a different, slightly larger cluster sample, de La Fuente Marcos & de La Fuente Marcos (2004) find evidence for a similar event, as well as for four earlier periods of enhanced cluster formation spanning the last 2 Gyrs.

Understanding the life cycle of clusters clearly will remain an important astrophysical goal, given the expectation that most stars are born in them, and the window they provide on the stellar IMF and the past. They are inherently complex systems that, in well chosen cases, will warrant careful spectroscopic dissection, in order to establish their membership, reddening variations, structure and dynamical status. Depending on age and location within the Galaxy, both optical and NIR multi-object work will be required. A supporting area of science of great relevance to work on massive clusters is the evolution of massive stars - our understanding of this is still weak, and requires both theoretical and observational work.

3.2.5 Star formation profile along the Galactic plane

The profile of ongoing star formation within the Galaxy begins right in the centre. It came as a surprise when, first, Allen et al. (1990) found a luminous emission line object of type WN9/Ofpe, close to Sgr A*, and then Krabbe et al. (1991) reported a compact group of emission line objects detected via emission in H I 2.06μ . These Wolf-Rayet like objects were clear evidence of star-forming activity only a few million years old, in what is now referred to as the Central Cluster. From these beginnings, much effort has been poured into describing and understanding the stellar environment right at the heart of our Galaxy and its vigorous star formation activity. Currently, the Central Cluster, along with the nearby Arches and Quintuplet clusters, contain no less than 20% of the Galaxy's known Wolf-Rayet population (60 out of 298: van derHucht, 2006).

The central 500 pc of the Galaxy has been described by Launhardt et al.

(2002) on the basis of what can be learned from IRAS and COBE/DIRBE infrared data. This central region appears as a mini-version of the main Galactic disc and bulge, wherein the central nucleus has an R^{-2} stellar density profile, contained within a radius of ~ 30 pc which is embedded within a disc component of scale length ~ 230 pc that is much better populated with molecular clouds. See also Section 3.3.1. Although the central nucleus as a whole contains less interstellar matter, the Central Cluster does have its own compact reservoir of molecular gas within a few parsecs of Sgr A* - which in turn is disc-like. Paumard et al. (2006) have shown that this tiny structure consists of two counter-rotating discs, and confirm the earlier result of Blum et al. (2003) of an apparently top-heavy IMF (truncated at $\sim 0.7 M_{\odot}$). Another notable feature of star formation in and around the centre of the Galaxy is the presence of several seemingly extremely massive stars ($> 100 M_{\odot}$, e.g. Figer et al., 1998, 2002). The engine for all this activity, which is seen superposed on an older population of stars, is very likely to be mass inflow drawn toward the central black hole (see e.g. Morris & Serabyn, 1996).

Star formation within the thin disc of the Galaxy, from a radius of ~ 3 kpc outwards, is on the whole not quite as dramatic, being driven mainly by either spiral density waves or the stirring at the inner edge by the central bar. There is a strong radial gradient on this activity as is well-illustrated by the distribution of known massive Wolf-Rayet stars – nearly all of them are found inside the Solar Circle (van der Hucht, 2001; van derHucht, 2006). This is despite the greater impact reddening is likely to have on the completeness of the available sample for sightlines towards the inner Galaxy. van der Hucht (2001) has estimated that we should expect around 1600 of them, to be compared with the latest figure of 298. This strong trend is no doubt linked to the strong radial gradient in gas density. Of course, this particular tracer emphasises the very top end of the stellar mass spectrum, given that massive Wolf-Rayet stars are in the main likely to be the end states of stars more massive than $\sim 20 M_{\odot}$.

Supernova remnants as tracers of present-day star formation rate lower the threshold of stellar mass detection to $\sim 8 M_{\odot}$. Recent studies of respectively the northern and the southern distributions of large H I shells have been carried out by Ehlerová & Palouš (2005) and McClure-Griffiths et al. (2002). The approach taken by Ehlerová & Palouš (2005) was aimed to be more statistical and so allowed them to deduce a typical exponential scale length within the Galactic disc that is not very different from that of the stellar content as a whole (i.e. ~ 3 kpc). This remains in keeping with much older work in this area by Rana & Wilkinson (1986) who collected together data on H II regions, pulsars and supernova remnants. Inevitably, given the problems with distance determination outside the Solar Circle, the identified trends are more reliable within it.

What is less clear at this time is how far the Galaxy is right-left symmetric

with regard to its star formation activity. It can be seen in Figure 9 that the Carina arm in the 4th quadrant is clearly marked out by a well developed chain of H II regions, while neither the Sagittarius or Perseus arms in the first quadrant are very evident at all. This is backed up by an imbalance in the emission line star counts available from the Stephenson & Sanduleak (1971) and Kohoutek & Wehmeyer (1999) surveys covering the southern and northern hemispheres respectively, down to a red magnitude of ~ 12 : e.g. data from these surveys obtainable via SIMBAD reveal around twice as many emission line stars at negative Galactic longitudes (in the south) as at positive longitudes. This is unlikely to be more than partially attributable to a reddening asymmetry given that the complexes identified in Figure 9 are drawn from radio mapping at least as much as from optical data. If spiral density waves are the main drivers of star formation, this raises the question as to why the waves creating the Sagittarius and Cygnus arms are less efficacious than that responsible for Carina.

3.2.6 Interactions with the intergalactic medium (IGM)

There are several reasons why late-type galaxies such as ours must be accreting gas.

- Accretion of metal-poor gas is the standard solution to the ‘G-dwarf problem’ discussed in Section 3.5.3.
- The relatively high abundance of deuterium, which is destroyed by stars, implies that the disc’s stock of deuterium is constantly replenished by accretion of unstrated gas (e.g. Prodanovic & Fields, 2008). See also Section 3.4.4.
- The current rate of star formation ($\sim 1M_{\odot} \text{ yr}^{-1}$; above) would exhaust the current supply of cool gas ($\sim 10^9 M_{\odot}$) in a time that is short compared to the age of the disc. Moreover, in the past the star-formation rate is likely to have been higher (Just & Jahreiss, 2007), so either we happen to live right at the end of the Galaxy’s star-forming life, or the Galaxy constantly replenishes its gas supply. Given that the Galaxy’s star-formation rate and gas supply are in line with the values estimated for many external galaxies, it seems unlikely that star-formation is about to cease.
- It has recently been established that lenticular galaxies (S0 galaxies) are simply spiral galaxies in which star formation ceased a few Gyr ago, since when their discs have faded and reddened (Bedregal et al., 2006). These galaxies are concentrated in clusters of galaxies, and the cessation of star formation in them explains the observed evolution in the colours of cluster galaxies. Theoretically it is expected that a galaxy loses its gas supply when it falls into a cluster, so there is a strong implication of a connection between the cessation of star formation and the interruption of the gas supply.

If the Galaxy is accreting gas, where is it coming from? Cosmology predicts that majority of baryons are in extragalactic gas (Section 3.3.8 below), so there is no shortage of baryons to accrete. It is thought that most of these baryons must be at the Local Group’s virial temperature ($\gtrsim 10^6 \text{ K}$) and form the *warm-hot intergalactic medium* (*WHIM*).

At the low densities ($n < 10^{-4} \text{ cm}^{-3}$) expected of the Local Group’s store of virial-temperature gas, the gas is hard to detect in emission. At slightly cooler temperatures ($1 - 3 \times 10^5 \text{ K}$) the relatively abundant elements CNO are present as the ions C IV, N V and O VI that have UV absorption lines that allow these ions to be detected at very low column densities by absorption against a background source. O VI absorption was extensively studied with the FUSE satellite (Sembach

et al., 2003). More than half the 102 sources observed showed O VI absorption at velocities within 500 km s^{-1} of the Local Standard of Rest. Sembach et al. estimate that along these sight lines the column density of the associated H II exceeds 10^{18} cm^{-2} , well in excess of the column densities of H I seen in high-velocity clouds (Section 3.1.5). On the other hand, sight lines that pass close to high-velocity clouds usually show O VI absorption at the cloud's velocity. The natural interpretation of this fact is that the O VI lies in the interface between the cold H I and the WHIM. Various line ratios favour collisional- over photo-ionisation, so the widespread existence of O VI absorption provides strong circumstantial evidence for the existence of the WHIM. The rms velocity of O VI absorption systems is least when referred to the rest frame of the Local Group, which is consistent with the WHIM being confined to the Local Group rather than the Galaxy, as it must be if it is to contain a significant fraction of the baryons that are not accounted for by the Galaxy, M31 and the smaller Local-Group galaxies.

Although in the Local Group the WHIM is probably too rarefied to be detected in emission, Pedersen et al. (2006) detected a distribution of virial-temperature gas around a more massive spiral galaxy, NGC 5746. It seems likely that the Local Group has a similar halo. Is the Galaxy's supply of H I constantly topped up with gas that cools from this halo?

An argument against this proposition is that the X-ray emission observed around NGC 5746 is rather spherical and incompatible with gas accreting onto the disc rather than the bulge. In fact observations of 'cooling flows' strongly suggest that once gas reaches the virial temperature of a dark-matter halo, it is prevented from forming stars by the halo's central black hole, which acts like a thermostat (Binney, 2004). If this is so, galaxies must form from gas that falls in cold.

The low metallicities of some high-velocity clouds (Section 3.1.5) prove that they have not been ejected from the disc, and they have a net negative radial velocity of $\sim 50 \text{ km s}^{-1}$. With current estimates of their distances, the inferred accretion rate is $\sim 0.1 M_{\odot} \text{ yr}^{-1}$, smaller than the current rate of gas consumption through star formation, but given the large uncertainties not entirely negligible. Peek et al. (2008) show that in a cosmological simulation of the formation of a galaxy like our own, there is a population of clouds that moves through the WHIM towards the galaxy, accreting mass from the WHIM as they go. They argue that the distribution of these clouds is consistent with the observed properties of the high-velocity clouds, and that they imply an accretion rate of $0.2 M_{\odot} \text{ yr}^{-1}$. The masses of high-velocity clouds are at or below the resolution limit of the best current simulations of galaxy formation. Moreover, the interface between cold clouds that move through a hot ambient medium poses a very complex dynamical problem, and the ability of the *Smooth Particle Hydrodynamics* technique used

by Peek et al. to handle such problems has been questioned (Agertz et al., 2007). Hence the results of Peek et al. must be considered tentative, but the astronomical evidence does seem to point to some of the Galaxy’s supply of cold gas coming from the WHIM via high-velocity clouds.

The cold gas we see around star-forming galaxies is not simply being accreted. Deep HI surveys of NGC 891, which is similar to our Galaxy, have revealed a halo of HI that contains $\sim 30\%$ the system’s total stock of HI (Oosterloo et al., 2007). Most of the HI is only a few kpc from the disc, and if it were simply infalling, it would hit the disc in a few tens of Myr, and endow NGC 891 with an implausibly high accretion rate, $\gtrsim 30M_{\odot} \text{ yr}^{-1}$. Other star-forming galaxies that have been studied in similar detail suggest that they too have HI halos like that of NGC 891 (Fraternali et al., 2007; Sancisi et al., 2008). It seems inevitable that HI halos are predominantly made up of gas that has been ejected from the disc. Most of this gas will return to the disc as in a fountain, but some may mix with the coronal gas that is presumed to fill the Local Group.

Thus studies of external galaxies indicate that cold gas flows both out of and into star-forming discs. It is still unclear exactly how this works out in the case of the Galaxy. The heliocentric velocities of most of the fountain gas are probably insufficiently anomalous for the gas to qualify as ‘high-velocity’ gas, but some may be catalogued as ‘intermediate-velocity’ gas. Chemical evolution models need to take into account the existence of a fountain, since the fountain moves gas outwards, and this motion must be balanced by an inward flow within the disc. Thus the fountain mixes gas radially. However, recent 3D hydrodynamical simulations of typical fountains powered by 100 SN II have recently shown that the majority of gas lift up by the fountains fall within 0.5 kpc from the place where the fountain originated, suggesting this mechanism to be less efficient in mixing gas along the disc than previously thought (Melioli et al., 2008). If such distances are confirmed, the impact of galactic fountains on the large scale radial abundance gradients would be minor.

From the earliest days of cold dark matter (CDM) cosmology, it has been recognised that the theory requires star formation to be effective in driving outflows (Blumenthal et al., 1984) – were this condition not fulfilled, most of the baryons would be in objects much smaller than observed galaxies. Objects that are currently experiencing starbursts are observed to be ejecting gas at rates comparable to their rates of star formation (Strickland & Heckman, 2007; Rix et al., 2007). The efficiency of mass ejection is thought to decrease with increasing mass, but in rich clusters of galaxies, where the majority of stars and thus presumably nucleosynthesis are contributed by relatively luminous galaxies, about a half of the heavy elements are in the intergalactic medium and must have been ejected (Renzini, 1997). Thus whatever the current rate of mass ejection from the Galaxy,

in the past the rate must have been significant, and models of population synthesis cannot safely ignore this process.

3.3 Dynamics

The purple arrow identifies the integrated extinction derived from the data of Schlegel et al. (1998).

There are three distinct reasons to study the dynamics of stars in the Galaxy:

- (i) To determine the gravitational field throughout the Galaxy, and thus through Poisson's equation (or its equivalent in a non-standard theory of gravity) to determine the mass distribution in the Galaxy. Comparing this with the distribution of visible mass, we can determine the distribution of dark matter.
- (ii) To identify stars seen at different locations that are on the same orbits with different phases, and thus to connect the kinematics of each population with its spatial distribution. The Galaxy's components have many overlapping regions and dynamical analysis provides an essential tool for disentangling them. Also when a satellite is tidally shredded by the Milky Way, its stars are left on similar orbits, and much can be learned by identifying populations of stars that are related in this way.
- (iii) To understand how stars are scattered between orbits, for example by spiral arms, molecular clouds, star clusters or massive black holes. Such understanding both provides constraints on the population of scatterers and enables us to relate the present orbits of stars to the orbits on which they were born – or to conclude that a region of phase space is so strongly mixed that we cannot infer the original orbits of the stars that are now in it.

Underlying all three tasks is a fundamental assumption that must be challenged: that the Galaxy is effectively in a steady state in the sense that its gravitational potential does not change substantially in a dynamical time, and the changes that do occur are predominantly fluctuations that average to zero. This assumption is fundamental to task (i) because the data consist of the present phase-space coordinates of stars, and *any* gravitational field is consistent with a given body of data if the steady-state assumption is dropped: if the field vanishes, the stars fly apart, while if it is stronger than it would be in a steady state, the system rapidly contracts. The field we infer is the one that enables the system to evolve into a configuration that is statistically identical with its present one.

Sufficiently far from the centre, we expect the Galaxy to deviate significantly from a steady state, and the recently published results of the 2MASS (Majewski et al., 2004) and SDSS surveys (Belokurov et al., 2006b; Bell et al., 2008) show that the stellar distribution in the outer Galaxy is by no means in a steady state. Getting a better understanding of the nature of this disequilibrium, especially its radial distribution, and how it is related to the warp of the Galactic disc, are important tasks. Within the solar circle it is probable that the Galaxy is nearly in a steady state and we must address the linked tasks (i) and (ii) above.

To date, the large-scale structure of the Galaxy’s gravitational field has been most effectively probed by observations of the radio-frequency lines of HI and CO, which are not obscured by dust. Unfortunately, the objects observed lie overwhelmingly in the plane, with the consequence that we have very little knowledge of the gravitational field away from the plane. Mapping the field outside the plane is a key task for Gaia.

We start our survey of the dynamics of the Galaxy at the centre and work our way out.

3.3.1 The central few parsecs

The very compact continuum radio source Sgr A* has long been suspected to mark the centre of the Galaxy. Only relatively recently has it been detected in the near-IR and X-ray bands (Baganoff et al., 2003; Genzel et al., 2003b). Its radiation is significantly polarised and is variable on timescales down to 15 m (Trippe et al., 2008), the variability being greatest in X-rays. Its spectrum is featureless and likely dominated by the synchrotron process.

Observations in the near IR that use adaptive optics have made it possible to follow stars as they move around Sgr A* and come closer than 10^{-3} pc to Sgr A*. These objects are on accurately Keplerian orbits and establish beyond reasonable doubt that Sgr A* is a black hole of mass $(3.6 \pm 0.3) \times 10^6 M_\odot$ (Eisenhauer et al., 2005; Ghez et al., 2005). By combining proper-motion and radial velocity measurements of a star that is on a short-period orbit around Sgr A*, Eisenhauer et al. (2005) deduce that the distance to the Galactic centre is $R_0 = 7.62 \pm 0.35$ kpc.

Sgr A* sits at the centre of the anomalous Central Star Cluster. From star counts, Genzel et al. (2003a) reached the following conclusions:

- (i) The counts are consistent with the cluster’s density profile having the form

$$j(r) \propto \begin{cases} r^{-1.4} & \text{for } r < 0.39 \text{ pc} \\ r^{-2} & \text{otherwise,} \end{cases} \quad (1)$$

with the central star density exceeding $3 \times 10^7 M_{\odot} \text{pc}^{-3}$. The two-body relaxation time in the cluster is estimated to be shorter than the cluster's age.

- (ii) The cluster largely comprises an old metal-rich population, to which a sprinkling of young stars has been added.
- (iii) The luminous stars are concentrated into two counter-rotating discs that are highly inclined with respect to each other and the Galactic plane. These stars have lifetimes of $\lesssim 10$ Myr. This finding suggests that the stars formed where we now see them, notwithstanding the strong tidal field of Sgr A*.

Maness et al. (2007) consider it likely that the Central Star Cluster has been the site of top-heavy star formation throughout the life of the Galaxy.

In the dense environment of the central star cluster strong encounters are relatively common. The hypervelocity stars recently found in the halo (Brown et al., 2005) may testify to this. Their very fast motions suggest that they experienced a three-body encounter, being the result of either the tidal disruption of a binary system by the super-massive black hole in Sgr A*, or from the encounter with a binary black hole (Yu & Tremaine, 2003; Gualandris et al., 2005). Such hypervelocity stars are unique probes of the mass distribution at large radii. Their trajectories may deviate from being exactly radial because of the shape of the Galactic potential (Gnedin et al., 2005).

In the inner few parsecs, two-body relaxation, star-formation and stellar collisions make for an extremely complex dynamical situation.

3.3.2 The bar/bulge

Until fairly recently it was thought that bulges were scaled-down versions of elliptical galaxies, but it has become clear that the bulges of late-type galaxies are complex objects that can differ profoundly from a typical elliptical galaxy. Moreover, it is widely suspected that the bulges of late-type galaxies and elliptical galaxies form in completely different ways: elliptical galaxies are the products of mergers, while the bulges of late-type galaxies formed when the embedding disc became bar unstable and buckled (e.g. Patsis et al., 2003). The bulges of some early-type spirals may be similar to elliptical galaxies; such bulges are called *classical bulges* to distinguish them from *pseudobulges*, which form from buckling discs.

The bulges of late-type galaxies, including our own, are challenging objects to study because their spatial and velocity scales are small, and they are often

significantly obscured by dust. Consequently, major uncertainties attach to the nature of bulges. Data for both our own and external galaxies, and from N-body models, point to the existence of three dynamically related zones: the innermost zone is approximately circular, fairly flat and rich in gas and star formation; the middle zone is strongly barred, thicker, and often peanut-shaped in projection; the outermost section is again strongly barred but thinner. Thus, confusingly, two of the three parts of a ‘bulge’ are nearly planar.

Studies of the distribution and kinematics of gas in the bar/bulge region are reviewed by Ferrière et al. (2007) and Launhardt et al. (2002) and summarised in Section 3.1.2. Starcounts from GLIMPSE at $|l| > 10^\circ$ and $|b| < 1^\circ$ are markedly asymmetric in l to at least $|l| = 30^\circ$, and from this fact Benjamin et al. (2005) and López-Corredoira et al. (2007a) infer that at $R \sim 4$ kpc the disc is elongated along a line inclined to the Sun-centre line by ϕ , where $35^\circ < \phi < 55^\circ$. The misalignment between the major axis of the bulge and this elongation of the disc implies that the disc is leading the bar, as it would do if there were offset dustlanes (and associated star formation) along the leading edge of the bar, as is frequently observed in external galaxies.

Pseudobulges are observed to rotate much more rapidly than classical bulges. The rotation rate of the Galactic bulge can be determined from the proper motions of stars in bulge fields. Most such measurements are in good agreement with the predictions of N-body models of the Galactic bar (Bissantz et al., 2004), although recently a conflicting data set has appeared (Rich et al., 2007). In the coming years measurements of the radial velocities and proper motions of bulge stars will contribute much to our understanding of the Galaxy’s gravitational field and mass distribution.

Current thinking on galaxy formation suggests that most galaxies should have at least a small classical bulge even if their central regions are dominated by a pseudobulge. Perhaps in the coming years, careful analysis of the spectroscopic and kinematic properties of stars deep in the bulge will reveal that the Galaxy has a small classical bulge.

Gas clouds tend to follow stable closed orbits, and in a barred potential such as that of the Galaxy there are two important families of such orbits (e.g. Binney & Tremaine, 2008): at low energies, orbits of the x_2 family are only mildly elliptical, with their major axes aligned with the bar’s minor axis. Collectively these orbits form the x_2 disc. At higher energies, orbits of the x_1 family are more elongated, with their major axes aligned with the bar. Gas spirals inwards through a series of x_1 orbits of increasing elongation, until at a critical radius it suffers a strong shock and collapses onto the x_2 disc, where it tends to accumulate. In the Galaxy, the x_2 disc has a semimajor axis length ~ 200 pc and is gas rich (Ferrière et al., 2007).

In external galaxies the shocks coincide with dust lanes parallel to the bar, and the rim of the x_2 disc is often dotted with luminous H II regions (Athanasoula, 1992). In N-body models, the x_2 disc does not participate in the buckling of the bar, and observations do indicate that the inner ~ 200 pc is fairly thin and lies in $b = 0$. The distribution of gas in the disc is markedly lop-sided, with $\sim \frac{3}{4}$ of the CO emission observed at positive longitudes, so it is likely that the flow is strongly time-dependent at these radii (Fux, 1999). The x_2 disc is the site of star formation, much of it concentrated into two giant clusters, the Arches and Quintuplet clusters (Stolte et al., 2005). The gas that lies outside the x_2 disc but inside corotation moves on elongated orbits that are inclined by $\sim 7^\circ$ with respect to the Galactic plane in the sense that their further ends are at $z > 0$ and their nearer ends are at $z < 0$ (Ferrière et al., 2007). The cause of this tilt is not understood.

Stars that resonate with the bar’s rotating gravitational field are probably observed in the solar neighbourhood as the ‘Hercules stream’. From the central velocity of this stream, Dehnen (1999) estimates the bar’s pattern speed to be $(53 \pm 3) \text{ km s}^{-1} \text{ kpc}^{-1} = (54 \pm 3) \text{ Gyr}^{-1}$, in good agreement with the findings of Bissantz et al. (2004), who studied the motion of gas at $R \lesssim 4$ kpc for an assumed pattern speed of $56 \text{ km s}^{-1} \text{ kpc}^{-1}$. This pattern speed places corotation at 3.4 kpc, close to the likely end of the bar. A bar with corotation so close to its end is classified as ‘fast’.

Searches for microlensing events (moments when a background star is lensed and made brighter by the gravitational field of a foreground object) provide important constraints on the mass distribution in the inner Galaxy, and especially the bar. The particular importance of microlensing derives from two facts: (i) it measures the mass density contributed by stars alone rather than the combined density of stars, gas and dark matter, and (ii) it enables us to determine the mass function of stellar objects down to extremely low masses, way below the minimum mass for hydrogen burning. Results of microlensing surveys are reported in terms of the *optical depth* in each field, which is the probability that a given star will be microlensed at a given time. The first optical depths to be reported were implausibly high (Binney et al., 2000) but more recent measurements (Popowski et al., 2005; Hamadache et al., 2006; Sumi et al., 2006), which minimise the effects of ‘blending’, are yielding optical depths in excellent agreement with the predictions of models of the Galactic bar in which *all gravitating matter is in stars*. The distribution of event durations is consistent with natural extensions of the initial mass function of stars to low masses (Bissantz et al., 2004; Wood & Mao, 2005; Hamadache et al., 2006).

Interstellar gas that is located at ~ 3 kpc shows remarkably large radial velocities $\sim 120 \text{ km s}^{-1}$ as it passes in front of the Galactic centre. The bar provides much of the torque required to produce these velocities, but Englmaier & Gerhard

(1999) and Bissantz et al. (2003) conclude that significant contributions come from spirals arms that can just be discerned in near IR photometry (Drimmel & Spergel, 2001). The data are best fit with four arms (see Figure 12). Inside corotation they are likely connected to the ultraharmonic (4:1) resonance, but outside corotation they probably have a lower pattern speed than the bar.

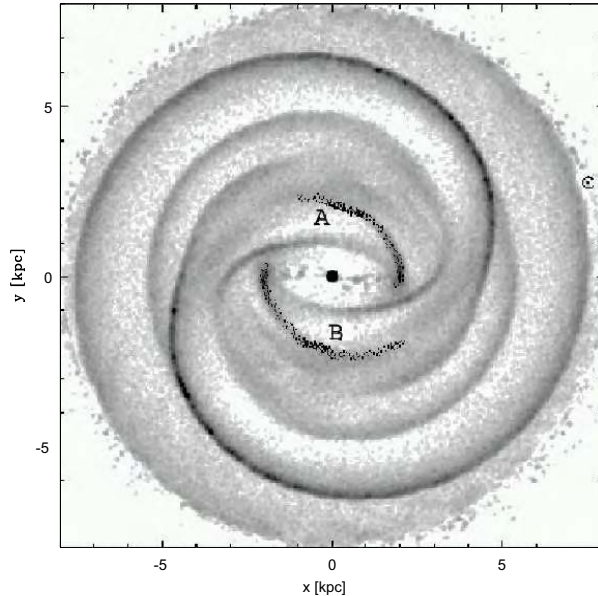


Figure 12: Gas flow model of the Milky Way from Bissantz et al. (2003). The location of the Sun is marked by the dot in a circle above the middle of the right-hand border.

3.3.3 The rotation curve

The rotation curves of external spiral galaxies have played a key role in convincing us that either most matter is dark (van Albada et al., 1985) or Newtonian gravity does not apply at low accelerations (Sanders & McGaugh, 2002). In most respects the Milky Way is the galaxy we know best, but the rotation curve is an exception to this rule. There are three problems: (i) to determine the rotation curve from measurements of heliocentric velocities, we need to know the azimuthal speed of the Sun Θ_0 , which is hard to measure, (ii) beyond the solar circle we need to know the distance to a tracer whose radial velocity has been measured before we can infer the circular speed at its location, and (iii) the Galaxy does not have an extended HI disc. Within the disc, heliocentric radial velocities are easily determined from radio-frequency lines, but distance determinations are difficult

on account of interstellar absorption. Fortunately, at $R < R_0$ the rotation curve can be determined from the radial velocities alone.

Figure 13 shows the data from which the rotation curve is derived for $R < R_0$. The upper curves in Figure 14 show the rotation curves derived from these data under the assumption that $\Theta_0 = 229 \text{ km s}^{-1}$ (full curve) or 200 km s^{-1} (dashed curve). The wiggles in these curves reflect the wiggles in the data, which are presumably caused by spiral structure. From Figure 14 we see that the rotation curve inside R_0 is probably rising, and the higher Θ_0 is, the faster it rises. The lower curve in Figure 14 shows the rotation curve of the exponential disc that was fitted to the solar neighbourhood data plotted in Figure 13; clearly this disc generates much less centripetal acceleration than the data require.

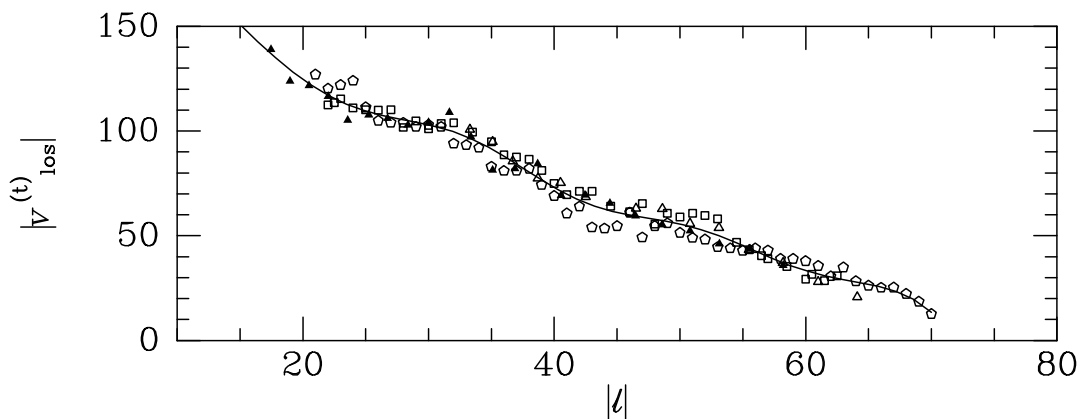


Figure 13: *The points show measurements of the terminal velocity of emission by HI (open symbols) and CO (filled symbols) from Bania & Lockman (1984), Weaver & Williams (1973, 1974), Malhotra (1995) and Kerr et al. (1986). The curve is a polynomial fit to the data. The undulations probably reflect perturbation of the flow field by spiral structure.*

Outside R_0 errors in the distances to tracers cause R and v_c to be correlated in a way that makes it unclear whether the rotation curve is rising, but there is no evidence that it is (Figure 15).

The most direct way to determine Θ_0 is from the proper motion of Sgr A*, the compact radio source associated with the Galaxy's central black hole. Reid & Brunthaler (2005) find $\mu_{A^*} = 6.37 \pm 0.02 \text{ mas yr}^{-1}$. If Sgr A* is stationary in the Galaxy's rest frame (and its motion perpendicular to the plane is $< 2 \text{ km s}^{-1}$), then $\mu_{A^*} = [\Theta_0 + V_\odot]/R_0$, where V_\odot is the peculiar velocity of the Sun in the direction of Galactic rotation ($5.2 \pm 0.6 \text{ km s}^{-1}$; Dehnen & Binney, 1998), so $\Theta_0 = (240 \pm 1)(R_0/8 \text{ kpc}) \text{ km s}^{-1}$. Using $R_0 = 7.62 \pm 0.35 \text{ kpc}$ from Eisenhauer et al. (2005) one finds $\Theta_0 = (229 \pm 10) \text{ km s}^{-1}$.

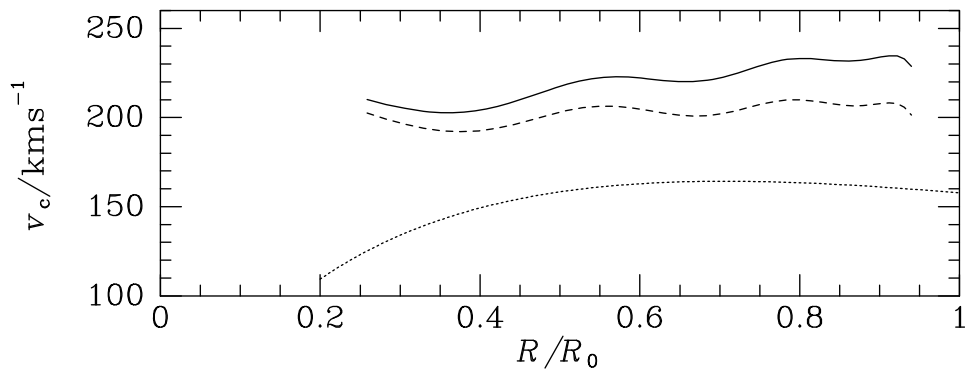


Figure 14: Upper curves: the rotation curves at $R < R_0$ derived from the curve in Figure 13 if $\Theta_0 = 229 \text{ km s}^{-1}$ (full) or 200 km s^{-1} (dashed). The lower curve is the rotation curve of an exponential disc with scale length 2.5 kpc and mass $4.0 \times 10^{10} M_\odot$.

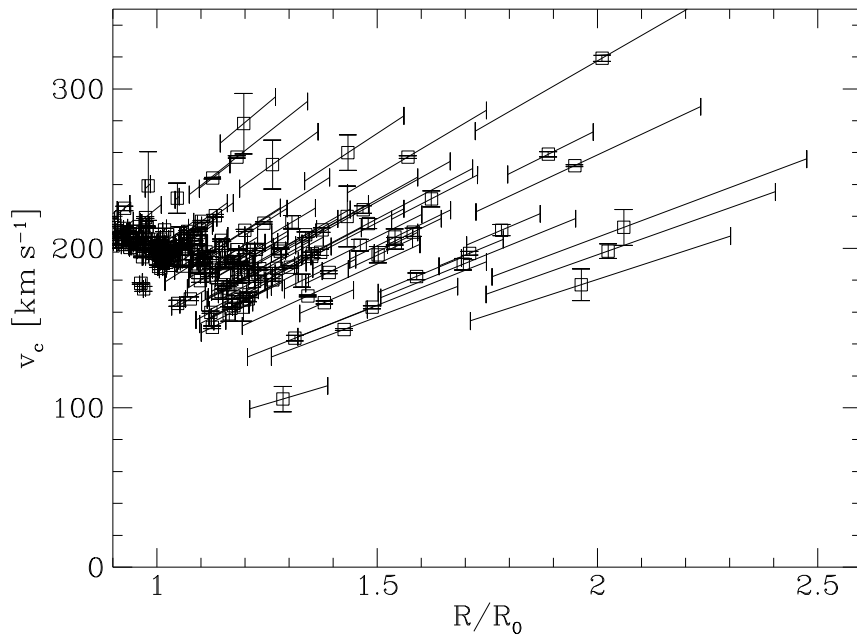


Figure 15: The rotation curve at $R > R_0$ from the radial velocities of tracers tabulated by Brand & Blitz (1993) and assuming $\Theta_0 = 220 \text{ km s}^{-1}$. The uncertain distances to the tracers produce correlated uncertainties in the rotation speed. (Binney & Dehnen, 1997, after).

3.3.4 The solar neighbourhood

The Sun sits ~ 14 pc above the plane (Binney et al., 1997), while the vertical scale-height of the dominant disc is $z_0 \sim 250 - 300$ pc. So the mass density near the Sun, ρ_0 , is the central (mid-plane) density of the disc. By combining the proper motions of stars seen near $b = 0$ with counts of A and F stars in fields near $b = 90^\circ$, Creze et al. (1998) and Holmberg & Flynn (2000) find that $\rho_0 = (0.076 \pm 0.015)M_\odot \text{pc}^{-3}$ and $(0.10 \pm 0.01)M_\odot \text{pc}^{-3}$, respectively. If we assume that the density drops exponentially with distance from the plane with the scale height $z_0 = 300$ pc, characteristic of the thin disc, $\rho_0 = 0.1M_\odot \text{pc}^{-3}$ corresponds to a surface density of $60M_\odot \text{pc}^{-2}$. In reality the vertical density profile is more complex than an exponential because the disc contains a thick stellar disc and a thin gas disc in addition to the thin disc. By counting directly observed stars and gas Flynn et al. (2006) infer that the total surface density is $\Sigma_0 = 49M_\odot \text{pc}^{-2}$ and that the local disc has mass-to-light ratio $\Upsilon_I = (1.2 \pm 0.2)M_\odot/L_\odot$. From radial velocities of K dwarfs observed at $b \approx -90^\circ$, Kuijken & Gilmore (1989) estimated that the total gravitating mass within 1.1 kpc of the plane is $\Sigma_{1.1} = (71 \pm 6)M_\odot \text{pc}^{-2}$, while from K giants Holmberg & Flynn (2004) obtained $\Sigma_{1.1} = (74 \pm 6)M_\odot \text{pc}^{-2}$. These measurements are significantly larger than the directly observed surface density of the disc. Moreover, if we assume by analogy with external galaxies that the disc has an exponential radial profile, the mass of the disc, $M_d = 2\pi R_d^2 \Sigma_0 e^{R_0/R_d}$, follows once one knows the scale length R_d of the disc. From NIR starcounts, Robin et al. (2003) obtain $R_d = (2.53 \pm 0.1)$ kpc; adopting $R_d = 2.5$ kpc and $R_0 = 7.6$ kpc we find $M_d \simeq 4.0 \times 10^{10}M_\odot$, and this disc generates a circular speed 156 km s^{-1} at the position of the Sun. If we add in the acceleration contributed by the bulge, taking the bulge mass to be $1.5 \times 10^{10}M_\odot$, we obtain a circular speed of 181 km s^{-1} , which is smaller than any plausible value of Θ_0 ; the gravitational acceleration is actually only 0.62 of that required by $\Theta_0 = 229 \text{ km s}^{-1}$. Moreover, the circular speed of the exponential disc is declining at $R_0 = 3R_d$, in conflict with Figure 14. In summary, stars and gas dominate the mass density near the Sun but provide only $\sim 62\%$ of the required radial acceleration. In standard gravity the balance must be generated by a substantially rounder and less centrally concentrated distribution of matter.

The Hipparcos satellite showed that in the solar neighbourhood the distribution of stars in velocity-space is full of structure (Dehnen, 1998; Famaey et al., 2005). The gross structure was already known: with increasing velocities in the radial and vertical directions, the density of stars declines in a roughly Gaussian manner with dispersions $\sigma_R \simeq 38 \text{ km s}^{-1}$ and $\sigma_z \simeq 19 \text{ km s}^{-1}$, while the density of stars is very skew in $v_\phi - \Theta_0$ because Jeans' theorem predicts that for fixed $|v_\phi - \Theta_0|$, the number of stars near apocentre (which have $v_\phi < \Theta_0$) exceeds the number at pericentre, having $v_\phi > \Theta_0$. The surprise in the Hipparcos data was the richness of the star streams that are imposed on this smooth background distri-

bution. The Hercules stream associated with the bar has already been mentioned. Several other streams have been shown to also contain stars of different ages and metallicities (Famaey et al., 2005), so they cannot be dissolving star clusters; they must have a dynamical origin. They are probably associated with spiral structure (De Simone et al., 2004; Quillen & Minchev, 2005), but conclusive proof has yet to be delivered, and the pattern of star streams has not been connected to the observed morphology of spiral arms.

There is a very well defined correlation between the ages and velocity dispersions of stellar populations (e.g. Wielen, 1977; Dehnen & Binney, 1998; Nordström et al., 2004). Spiral structure plays an important role in establishing this correlation by exciting stars at resonances, predominantly at the inner Lindblad resonance (ILR) (Carlberg & Sellwood, 1985; Sellwood & Binney, 2002). Molecular clouds also play an important role by scattering stars (Spitzer & Schwarzschild, 1953; Lacey, 1984). The role of molecular clouds is particularly important in relation to the increase in σ_z with time because spiral structure only endows stars with random motions in the plane, and it is molecular clouds that enable σ_z to increase (Lacey, 1984; Jenkins & Binney, 1990).

3.3.5 Spiral structure

Dissipation causes gas clouds to move on nearly circular orbits that do not stray far from the plane, so freshly formed stars are on similar orbits. A self-gravitating stellar disc in which most stars are on such orbits is said to be *cold*; the dimensionless measure of the temperature of a stellar disc is the parameter (Toomre, 1964)

$$Q \equiv \frac{\sigma_R \kappa}{3.36 G \Sigma},$$

where σ is the rms radial velocity of stars, κ is the frequency of radial oscillations about a circular orbit and Σ is the disc's surface density. For the disc near the Sun we adopt $\kappa = 37 \text{ km s}^{-1} \text{ kpc}^{-1}$, $\sigma_R = 38 \text{ km s}^{-1}$ and $\Sigma = 49 M_\odot \text{ pc}^{-2}$ and find that $Q \simeq 1.9$.

Disks with $Q < 1$ are unstable, and ones with $1 < Q \lesssim 2$ are extremely responsive, because when most of the stars in a given volume are on similar orbits, most stars will respond in a similar way to a perturbing gravitational field. For example, a giant molecular cloud that is on a circular orbit in a cold disc gathers a stellar wake about it that takes the form of a trailing spiral. The wake's mass depends sensitively on Q , diverging as $Q \rightarrow 1$, and for $Q = 1.4$ is about a factor 10 larger than the cloud's mass (Julian & Toomre, 1966). Thus in a cold disc, spiral structure is readily excited by seed inhomogeneities.

Cold discs are fragile because their stars are crammed into a small part of the energetically available phase space, and even a weak scattering process can profoundly modify the phase-space distribution by moving stars to previously empty parts of phase space, which will in practice thicken and/or heat the disc. For example, in the situation described above, the combined gravitational field of the cloud and its wake transfers angular momentum from stars with guiding-centre galactocentric radii R_g smaller than the cloud's radius R_c , to stars that have $R_g > R_c$. This outward transfer of angular momentum reduces the amount of energy associated with the circular orbits of the guiding centres, and the surplus energy manifests itself as increased velocity dispersion in the disc. Thus a massive object such as a cloud can heat a stellar disc without transferring any energy to it, by mediating an outward transfer of angular momentum. Spiral structure is at once a manifestation of this process and its cause.

It follows that spiral structure heats the disc, thus increasing Q and making the disc less responsive – in a purely stellar disc, spiral structure will fade as the disc heats and becomes less responsive. A disc can maintain its responsiveness and spiral structure only if star formation constantly rebuilds the peak in the distribution function around circular orbits that spiral structure depletes. S0 galaxies lack spiral structure because they no longer form significant numbers of stars.

By pushing gas clouds from circular to elliptical orbits, spiral structure causes the clouds to crash into one another in long spiral shocks. These shocks are a major driver of star formation. In most cases, the kinetic energy that is thermalized in shocks is taken from the orbits of the clouds, so spiral structure causes clouds to drift inwards. This inward drift is potentially important for models of the Galaxy's chemical evolution.

In addition to responding to external stimuli, stellar discs are capable of carrying self-sustaining, running spiral waves. In the standard theory of spiral structure (e.g. Binney & Tremaine, 2008), waves propagate between the inner Lindblad resonance and near the corotation resonance. Both leading and trailing waves are present, but as waves are converted from leading to trailing form, they are amplified. Consequently, the overall appearance of the disc is dominated by the large-amplitude trailing waves. Since the waves are largely confined inside the corotation resonance, gas and stars overtake individual spiral arms and stream through them from their concave sides to their convex sides. The energy carried by the waves increases the random velocities of stars in the neighbourhood of the inner Lindblad resonance.

This picture has little or no empirical backing; it is the fruit of applying linear analysis to some idealised models. These calculations are hard to carry out with rigour, and have usually involved questionable approximations, such as

the tight-winding approximation, which yields an algebraic connection between the perturbed density and its gravitational field. N-body simulations have been used to test the theory to a limited extent, but the simulations are also very challenging technically, and their results can be hard to interpret in terms of the theory. Moreover, the mass distribution in a real galaxy is much more complex than those of the models used to develop the theory – at the minimum one should include the bar, a disc with a complex velocity distribution and a non-negligible quantity of gas. Ideally, one would include coupling to the dark halo.

Extensive measurements of the phase-space distribution of disc stars and gas would enable us to test the theory properly, and stimulate essential extensions of the theory to include realistic stellar distribution functions and gas dynamics. This exercise would explore how closely gas and stars work together – is the main role of the gas to repopulate near-circular orbits? or can much spiral structure be treated as wakes of concentrations of gas? How global and/or stationary is the Galaxy’s spiral structure? What spiral waves does the bar excite? How rapidly do they slow the bar? What is the radial inflow of gas that spiral structure drives? Do giant molecular clouds arise naturally in the shocks that spiral structure generates?

3.3.6 Tidal shredding

In the Λ CDM theory, galaxies grow via mergers and acquisitions. As a satellite is captured by the Galaxy, it suffers strong gravitational tidal forces that progressively strip its outer layers. Simultaneously, dynamical friction exerts a drag on its motion that is proportional to the square of its remaining mass, so the orbit decays as the mass dwindles (Binney & Tremaine, 2008). Initially massive satellites spiral in quickly and reach the Galactic centre before being completely disrupted. Less massive objects are disrupted before they reach the centre. The length of time that a less massive system orbits within the Galaxy before being disrupted, depends on its compactness, and can exceed the Hubble time.

Satellites are typically captured from plunging orbits. On such an orbit the tidal forces are strongly peaked around pericentre, so at each pericentre passage a new layer of stars is stripped from the satellite. These stars continue to move through the Galaxy on orbits that are similar to the orbit of the Satellite at the moment they were stripped. However, the orbits of stripped stars have radial periods that are either shorter or longer than the period of the satellite’s orbit. A leading tidal tail is formed by stars with shorter periods, while the other stripped stars form a trailing tidal tail. The tidal tails lengthen at a rate that increases with the mass of the satellite, in some cases they are known to wrap more than once around the Galaxy. As Figure 16 illustrates, numerical simulations show that tidal tails persist for a Hubble time, so with sufficiently rich observational material

it should be possible to detect many tens, perhaps hundreds, of them.

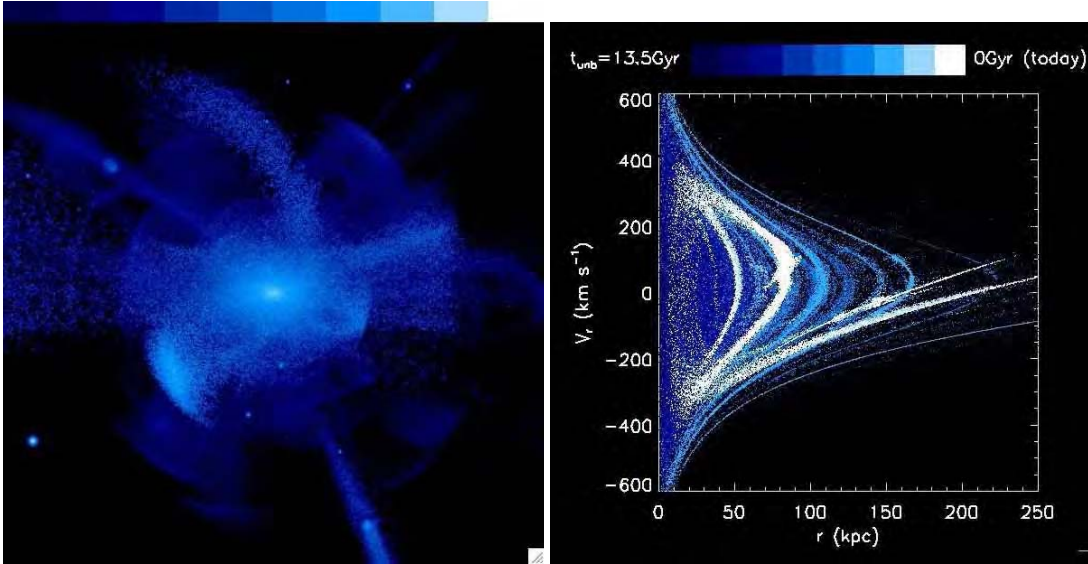


Figure 16: Model of the stellar halo built up from the mergers of satellites. The expected spatial structure (left panel) and (radial) phase-space structure (right panel) offer a direct test of cosmological models. In the left panel, the colour-coding indicates surface brightness: from 23 (white) to 38 mag/arcsec² (dark blue / black). In the panel on the right, the colour code reflects the time when each particle became unbound from its parent satellite: white points correspond to the last 1.5 Gyr, while dark blue is more than 12 Gyr ago. From Bullock & Johnston (2005).

Tidal tails are extremely interesting objects. First because they betray the existence of objects that were destroyed long ago and thus reveal the Galaxy’s accretion history. Second, they delineate individual orbits through the Galaxy, and by reconstructing such orbits one can strongly constrain the Galaxy’s gravitational potential and mass distribution (e.g. Jin & Lynden-Bell, 2007; Binney, 2008). In the outer halo the dynamical time is long and streams are stretched more slowly than in the inner Galaxy, where the dynamical time is short. Consequently, streams should be easier to detect at large radii, and in fact a significant fraction of the halo’s luminosity may be contributed by streams (Sections 3.1.1 and 3.5.1). A low-luminosity stream that has been stretched to great length becomes impossible to detect in real space, but may still be observable in phase space (Helmi & White, 1999; Helmi et al., 1999).

3.3.7 The warp

The H I disc of the Milky Way is warped (Kerr, 1957; Hartmann & Burton, 1997), as are the H I discs of many external galaxies (Bosma, 1978). Within $\sim R_0$ the

disc is flat (discounting the distortion of the gas disc between the x_2 disc and corotation), and further out the ‘line of nodes’ is defined to be the curve in which the disc cuts the plane of the inner disc. The Sun happens to sit on the line of nodes, which is approximately straight – in external galaxies it becomes an open leading spiral at large radii (Briggs, 1990). At $R \simeq R_0$ the disc rises above the plane as one moves around a circle from the Sun in the direction of Galactic rotation, and falls below the plane in the opposite direction. The maximum distance above the plane, $z_+(R)$ increases with R , while the maximum distance below the plane, $z_-(R)$ peaks at $R \simeq 2R_0$ (Hartmann & Burton, 1997). Thus near the Sun the Galaxy has an ‘integral-sign’ warp, which is characterised by $m = 1$ symmetry, while further out components associated with $m = 0$ and $m = 2$ become important (e.g. Binney & Merrifield, 1998).

The warp is not easily traced in the stellar disc, but its signature has been identified in both Hipparcos velocities, (Dehnen, 1998) and near IR star counts (López-Corredoira et al., 2002). The existence of warp in the stellar disc rules out (magneto)hydrodynamical explanations of the warp such as that of Kahn & Woltjer (1959).

We can now also rule out the theory that the warp is a steady wave in the disc driven by misalignment of the disc and the dark halo (Toomre, 1983; Sparke & Casertano, 1988). The problem with this theory is that the halo is not a rigid structure but one that responds readily to the disc. In fact if an N-body disc starts from what would be a steady wave for a rigid halo, the dynamical response of the halo causes the warp to wind up on a dynamical time (Binney et al., 1998).

Thus it seems that the Galaxy on its own cannot sustain a warp; the warp must be externally driven. The Galaxy should be constantly accreting matter that brings with it angular momentum, and we do not expect the direction of the angular momentum that is now being accreted to be aligned with the spin axis of the inner disc (Quinn & Binney, 1992). In the inner region, in which the orbital time is shorter than the time-scale of angular-momentum reorientation, torques cause the stellar system to slew almost as if it were a rigid body (Binney & May, 1986). However, as the system slews, it must be (temporarily) distorted from axisymmetry because torques have to carry off-axis angular momentum from the outside inwards. The disc will be most strongly distorted where its surface density is lowest and its thickness greatest, so the largest offset is required to produce a given gravitational torque between adjacent rings (Ostriker & Binney, 1989). Beyond the Sun both the low surface density and the flare of the disc are expected to lead to significant misalignments, and at some radius a warp must become pronounced. Numerical simulations confirm that warps similar in form and amplitude to that observed are generated when appropriate torques are applied to the outer Galaxy (Jiang & Binney, 1999; Shen & Sellwood, 2006).

We have yet to identify the body (or bodies) that are applying the torque – in view of the indications from the SDSS that the stellar halo is very lumpy, it is not clear that it will be possible to establish unambiguously what is torquing the inner Galaxy, but we should at least understand what torques are applied by the Magellanic Clouds, the Sgr dwarf, and the object that produced the recently discovered Monoceros ring (Newberg et al., 2002; Martinez-Delgado Hans-Walter Rix, 2007).

Assessing these torques is hard for two reasons: (i) Any galaxy has most of its mass in an invisible dark halo around it. We can only guess as to the masses of the dark halos of the Clouds and the Sgr dwarf, and the halo of the latter will by now have been tidally stretched into a tube that wraps more than once around the Galaxy. (ii) A satellite excites a wake of comparable mass in the dark halo of the Galaxy, and the wake is likely to exert a greater torque on the inner Galaxy than the satellite itself because it is closer to the inner Galaxy. Consequently, the Magellanic Clouds may be able to generate the observed warp unaided (Weinberg & Blitz, 2006) contrary to the classical conclusion of Hunter & Toomre (1969) that the Clouds are too remote.

The recent spate of discoveries of low-mass satellites around the Galaxy and M31 has led to controversies about whether features seen at low Galactic latitudes arise from the warp or companions (e.g. López-Corredoira et al., 2007b). Clearly if any of these features is a satellite, at some level it must contribute to the warp by exciting vertical oscillations in the disc. Another unresolved question is the role of gas accretion (e.g. López-Corredoira et al., 2008).

3.3.8 Dark matter

Extragalactic astronomy provides abundant evidence for either the existence of dark matter or that Einstein’s theory of general relativity is invalid at small accelerations. Of these two possibilities, dark matter is by far the most extensively developed and widely accepted. Observations of the microwave background, galaxy clustering and distant supernovae are all compatible with the Λ CDM model (Section 2) in which 84% of matter is contained in weakly interacting particles, and baryons contribute only $\sim 16\%$ of the matter (Spergel et al., 2007).

External galaxies are believed to have dark-matter halos because at radii $\gtrsim 3R_d$ their rotation curves do not fall as expected from their baryonic contents (e.g. van Albada et al., 1985). As explained above, the Galaxy’s rotation curve is ill-determined beyond the Sun, so we cannot be certain that the Galaxy has a dark halo, although we have seen that in the solar neighbourhood visible matter accounts for $\sim 62\%$ of the measured centripetal acceleration. Moreover, the escape

velocity that is inferred from nearby halo stars, $v_e \gg \sqrt{2}\Theta_0$ (Smith et al., 2007), which implies that a much larger fraction of the total mass lies beyond the Sun than the fraction of the light out there. So we *assume* that the Milky Way is surrounded by a dark halo of the type predicted by Λ CDM. In simulations of the clustering of dark matter in the absence of baryons, halos form with $\rho_{\text{DM}}(r) \sim r^{-1}$ at small r regardless of the power spectrum of the initial density perturbations. That is, the density diverges at small r rather than tending to a finite central value, and one says that the dark-matter density has a *cusp*. It is not certain how adding baryons will affect this cusp, but a naive treatment leads one to expect baryons to make a cusp steeper (Sellwood & McGaugh, 2005), and it has not been convincingly demonstrated that a dark-matter cusp can be smoothed out by such features as baryon-dominated satellites or bars (Sellwood, 2008). In the cusp the phase-space density of dark-matter particles may be sufficiently high to produce a detectable γ -ray flux through the mutual annihilation of dark-matter particles (Stoehr et al., 2003; Strigari et al., 2007).

Neglecting any modification of ρ_{DM} by baryons, the dark-matter density may be taken to follow the *NFW profile* (Navarro et al., 1997)

$$\rho_{\text{DM}}(r) = \frac{\rho_1 a^3}{r(r+a)^2}, \quad (2)$$

where a is a scale radius. The simulations provide a correlation between ρ_1 and a , so there is in effect a one-parameter family of NFW halos. The parameter can be taken to be the halo's peak circular speed $v_{\text{max}} = 1.65a(G\rho_1)^{1/2}$, which occurs at $r = 2a$. Klypin et al. (2002) favour a halo that has $a = 21.5$ kpc and $v_{\text{max}} = 163$ km s $^{-1}$. At the solar radius this halo's density is $\rho_{\text{DM}}(R_0) = 0.007M_\odot \text{pc}^{-3}$, a factor 14 smaller than the measured total mass density, but it contributes $15.4M_\odot \text{pc}^{-2}$ to $\Sigma_{1.1}$ and a fraction 0.29 of the acceleration required by $\Theta_0 = 229$ km s $^{-1}$. Thus with this halo the inner Galaxy is very much baryon-dominated as studies of the dynamics of gas and microlensing imply. If the Milky Way were an external galaxy, we should say that it has a 'maximum disc'.

An obvious way to test this model is to study the dynamics of satellites such as dwarf spheroidals and globular clusters at large radii, where the gravitational field is dominated by the halo. The limiting factor in such studies is the availability of accurate proper motions for satellites: line-of-sight velocities alone provide only a lower limit on the halo's mass because they essentially determine only the components of velocity towards the Galactic centre, which for any mass can be made as small as one pleases by assuming tangentially biased velocity dispersions. With all available data Wilkinson & Evans (1999) were only able to constrain the Galactic mass inside 50 kpc to $5.4_{-3.6}^{+0.2} \times 10^{11} M_\odot$, to be compared with $3.1 \times 10^{11} M_\odot$ in the Klypin et al. (2002) halo and $0.58 \times 10^{11} M_\odot$ in the exponential disc. More recently, Battaglia et al. (2005) compiled a significantly larger sample including

~ 100 halo stars located at large radii, and argued that beyond 50 kpc the radial velocity dispersion declines from $\sim 100 \text{ km s}^{-1}$ to $\sim 50 \text{ km s}^{-1}$, so either the mass of the halo lies at the lower end of the range given by Wilkinson & Evans, or the velocity dispersion becomes markedly tangential at large radii.

The total mass of the Galaxy is hard to estimate, but a secure lower limit can be placed on the mass of the Local Group by a timing argument due to Kahn & Woltjer (1959). The other massive member of the Local Group, M31, is approaching us with a Galactocentric speed $\sim 125 \text{ km s}^{-1}$. The minimum mass required to locally reverse the initial expansion of the Universe and produce this infall velocity within the available time can be calculated by imagining that the entire mass of the system is concentrated in point masses associated with M31 and the Galaxy. Taking into account the impact of vacuum energy, this mass turns out to be $5.3 \times 10^{12} M_{\odot}$ (e.g. Binney & Tremaine, 2008). In Λ CDM 16.3% of matter is baryonic, so the smallest baryonic mass that the Local Group could have started with is $8.6 \times 10^{11} M_{\odot}$. The overwhelming majority of the Local Group's stellar mass is contained in the Galaxy and M31, and between them they cannot contribute more than $2 \times 10^{11} M_{\odot}$ in stars and gas, so Λ CDM predicts that at least three quarters of the baryons originally in the Local Group are missing. The most plausible hypothesis is that this material is contained in a hot low density corona that extends more than 1 Mpc from the centre of the Local Group. In rich clusters of galaxies, X-ray observations of thermal emission from gas at the virial temperature directly show that a similar fraction of the baryons are in intergalactic gas. In the case of the Local Group, X-ray emission from the gas is probably too faint to detect because the density of the gas is very low.

Determining the shape of the Galaxy's gravitational field provides an important probe of the dark halo. In cosmological simulations with only dark matter, halos are generically triaxial (Gao et al., 2004). There are many indications that the complex physics of baryons has yet to be properly handled in a cosmological simulation, so we are not sure what to expect in real life. However, in simulations that include baryons, halos tend to become axisymmetric and oblate near the centre (Kazantzidis et al., 2004). The rate at which an orbit precesses increases with the oblateness of the potential. Hence using the connection between orbits and tidal streams (Section 3.3.6) we should be able to determine the shape of the potential. The stream that can be followed furthest around the Galaxy is that of the Sgr dwarf (Ibata et al., 2001; Majewski et al., 2004); unfortunately, from the morphology of this stream the halo has been argued to be oblate (Johnston et al., 2005), prolate (Helmi, 2004) and spherical (Fellhauer et al., 2006). This discordance probably reflects the fact that a gravitational potential has yet to be identified that is consistent with all the available data.

A cuspy halo has non-negligible density where the Galactic bar moves around,

and in this region its particles will pick up energy from the bar's rotating gravitational field (Tremaine & Weinberg, 1984; Debattista & Sellwood, 2000). This transfer of energy causes the bar to lose angular momentum and the halo to be set spinning on a time-scale that is longer than the dynamical time by of order the ratio of the total mass in the bar region to the contribution of the halo to that mass. For the Klypin et al. (2002) halo this ratio is ~ 5 . Since the dynamical time in this region is $\lesssim 0.1$ Gyr, the bar-halo interaction is rapid.

As the bar loses angular momentum its pattern speed decreases, and the question arises of whether such slowing is consistent with the Galaxy having a fast bar as we saw above. Given that in the bar region the halo has much less mass than the bar, a possibility is that this mass early on became effectively corotating with the bar and the drag on the bar ceased. A likely problem with this interpretation is that interactions within the halo transfer angular momentum from the inner halo outwards, so the drag on the bar is sustained.

Λ CDM predicts that the dark halo is rich in substructure, right down to solar-system scales. That is, equation (2) describes the spherically averaged density only when smoothed on scales $\sim r$. About 10% of the mass is concentrated into subhalos that orbit in the primary dark halo (Gao et al., 2004). This robust prediction of Λ CDM has several important implications. First, the Galaxy should have many more satellites than are known, perhaps because many subhalos carry no stars. Second, the presence of subhalos makes the gravitational field more lumpy and time-dependent than it would otherwise be, and this noise may perturb fragile structures such as wide binaries or thin tidal tails to a detectable extent (Johnston et al., 2002; Ibata et al., 2002). Laboratory experiments to detect DM may see more or less DM than equation (2) implies, depending on whether the Sun is currently in or out of a subhalo (Diemand et al., 2005).

The gravitational fields of the Galaxy's dwarf spheroidal (dSph) satellites are dominated by dark matter (Walker et al., 2007), while dynamical studies of globular clusters reveal no evidence of dark matter.

3.4 Composition, kinematics and ages of stellar populations

Our Galaxy and the other Local Group galaxies are the ideal test-ground for galaxy formation models because of the exquisitely detailed information that is uniquely available for these systems. The ages, kinematics and elemental abundances of individual stars are directly measurable and can be used to infer their evolutionary paths. For example, the study of chemical abundance patterns provides strong constraints on the history of star formation, the initial mass function, the infall/outflow of gas and the merger history of a galaxy (Pagel, 1997; Matteucci, 2001). Such a detailed approach is very powerful and especially warranted in an era when large volumes of high quality abundance measurements can be combined with kinematic information from ongoing and upcoming surveys (e.g. RAVE, SEGUE, Gaia), and new facilities such as the E-ELT come online.

We start this section by reviewing the principles that are used to determine the basic astrophysical parameters – ages, stellar yields and star-formation time-scales – from observations of individual stars.

3.4.1 Age determinations

Measuring ages is the only way directly to trace the history and evolution of the Galaxy. Ages are difficult to measure absolutely; more often it is possible to establish the relative ages of two objects. Stars of a given age generally have abundances of the interstellar medium at the moment and place of their birth. Their kinematics are also slightly linked with the place of birth (external/internal part of the disc, the halo, etc.) but are more sensitive to the dynamical history of their parent population since their birth.

It is possible to infer stellar ages from the relative abundances of radioactive isotopes that have lifetimes longer than $\sim 10^7$ years or, more precisely, the time since the last significant nucleosynthesis event. Radioactive dating relies on comparing the present abundance ratios of radioactive and stable nuclear species to the theoretically predicted ratios of their production (Goriely & Arnould, 2001). The uncertainties in the production ratios decrease if the two elements used have similar mass numbers, and so are close to one another in the nucleosynthetic network (Cayrel et al., 2001). One example is the work of Hill et al. (2002), using Th and U in two extremely metal-poor stars that exhibit a strong enhancement of r-process elements relative to iron. From the U/Th ratio the star's ages were found to be 14 ± 2.4 Gyr, consistent with the age of the Universe independently obtained from the Wilkinson Microwave Anisotropy Probe (WMAP) and globular clusters isochrones. For the Galactic disc in the solar vicinity, del Peloso et al. (2005),

using Th and Eu, estimated an age of 8.8 ± 1.7 Gyr. However, until we have a precise understanding of the nucleosynthesis models able to provide the isotopic or elemental yields for the adopted radionuclides, and of the chemical evolution models able to describe the evolution of these nuclides in the solar neighbourhood, this method will not furnish high-precision stellar ages.

Asteroseismology is potentially very powerful in improving stellar age determinations since oscillation frequencies carry direct information on the distribution of the density of matter in the stellar interiors, which is continuously modified by evolution. Depending on the mass and evolutionary state of the oscillator (to be obtained from other observations), different seismological diagnostics can be used to probe the internal structure and estimate the age. The relevant diagnostics can be either a suitable combination of the frequencies of pressure modes or the use of modes of mixed pressure and gravity character (see e.g. Christensen-Dalsgaard, 1988; Christensen-Dalsgaard et al., 1995; Roxburgh & Vorontsov, 2003). The method requires that a sufficient number of oscillation frequencies are measured with high accuracy. This is the case for the Sun where Gough (2001) used seismic analysis to infer a value of the solar age in good agreement with the age obtained from meteorites. For stars other than the Sun, spectroscopy and/or photometry give access to a limited number of oscillation modes. New ground-based and space-borne instrumentation like the HARPS spectrograph at VLT and the MOST, CoRoT and (future) Kepler space missions are increasing the number of objects with measured frequencies, and the accuracy of those frequencies.

A popular method to estimate the age of a field star is to fit an isochrone to its position in the Hertzsprung-Russel diagram (HR diagram). However, this technique also relies on stellar-structure modelling. Calculations of stellar evolution are generally quite reliable up to the first ascent of the giant branch. Thereafter the calculations become sensitive to several loosely-constrained parameters relating to transport processes and mass loss at various stages in the star's evolution. Here, asteroseismology will also play a role, by constraining the physical processes at work in stellar interiors. Transport processes are one of the dominant sources of uncertainty in describing stellar interiors. These processes modify the internal composition profiles and the fuel available for a star, which has an impact on the age that is estimated from stellar models. For instance Lebreton et al. (1995) have shown that the uncertainty on the determination of the size of the convective core in low mass A-F stars is responsible for an uncertainty on the age of roughly 20%. This could be reduced by a factor of 5 if high quality asteroseismic data were available, because they can constrain the density profile within the star.

So better stellar models resulting from asteroseismic analysis combined with accurate observations of the stellar global parameters (distances, magnitudes, temperatures, abundances) are expected to lead to a considerable reduction of the

errors in age determination from inversion of theoretical isochrones in the HR diagram. Absolute measurements of luminosity are currently restricted to stars with good Hipparcos parallaxes, which generally lie within 100 pc of the Sun. With the accuracies of Gaia on distance and apparent magnitude together with parallel improvements in the accuracies of the bolometric corrections, the uncertainty on stellar absolute luminosities will have a negligible impact on the age determination of stars within a few hundreds of parsecs. The effective temperature can be determined from good quality photometry, if possible including the near infrared. Chemical composition to 0.2-0.3 dex can be obtained from spectra with low-to-middle resolving power (SEGUE: $R=2000$; RAVE: $R=7500$), but obtaining an accurate determination (to 0.1 dex or better) of the abundances of a range of elements requires spectra with resolving power of at least $R=30\,000$, ideally higher. The accuracy of age estimates also depends on the extent to which the star has evolved, so are unreliable for low-mass main-sequence stars.

It is worth noting that subgiant stars can play an important role for stellar ages. The reason is that a precise knowledge of their effective temperature is not required (Sandage et al., 2003; Bernkopf et al., 2001). From a volume-complete sample of FGK stars (Fuhrmann, 2008), it was found that among the few subgiants of the local disc, 70 Vir is probably the oldest with an age of 8.1 ± 0.6 Gyr (Bernkopf et al., 2001). Using the same method for three other subgiants of the thick disc, the latter authors found a relatively small age interval 12.5-13.8 Gyr, while the kinematics remains inconclusive with respect to the population status, the chemistry of these stars implies they are thick disc members - see Section 3.5.3. A similar conclusion is reached by Mashonkina & Gehren (2001).

Chromospheric activity provides a useful if indirect method of determining stellar ages: young stars tend to be rapidly rotating, and their rotation generates more intense coronal activity than occurs in more slowly rotating stars of the same mass. As the star ages, its wind carries angular momentum away, so the coronal activity decays. The rate of decay cannot be calculated from first principles, but by using other methods to determine the ages of stars with coronal activity, indicators of coronal activity can be established, such as the flux emission in the core of the K line of Ca II, and then used to date other stars. Chromospheric activity has been widely studied in field stars (e.g. West et al., 2008). Unfortunately, significant dispersion in the chromospheric activity-age relation is found even among coeval stars (Pace & Pasquini, 2004). In addition, Pace & Pasquini (2004) noticed that two intermediate-age clusters (~ 1.7 Gyr) in their sample have chromospheric activity levels comparable to older clusters (~ 5 Gyr). These two observational facts indicate that chromospheric ages for field stars older than ~ 1.5 Gyr could be very uncertain.

For a coeval population (e.g. open and globular clusters³), an isochrone can be fitted without prior knowledge of the distance (and yields a distance modulus), so isochrone fitting is widely used. Unfortunately, the errors on ages determined from isochrones are generally correlated with errors in chemical composition and extinction. This complicates the analysis of relations between ages and abundances. The uncertainties on the absolute ages of globular clusters are still ~ 1 Gyr.

An alternative method to determine the age of globular clusters is offered by white dwarfs. By measuring the white dwarf cooling sequence, it is possible to assign an age by modelling the rate at which these objects cool (Hansen et al., 2004). Recently, this method became very attractive thanks to the very deep colour-magnitude diagrams obtained with the Hubble Space Telescope (HST), which allows the detection of very faint white dwarfs (Hansen et al., 2002, 2007). In fact, data at the fainter end can better constrain several other parameters such as distance, extinction, and masses directly from the fit to the full cooling sequence. This method was successfully applied to two globular clusters (M4 and NGC 6397) yielding age constraints which are tighter than the traditional main-sequence-turnoff method (MSTO). For M4, the closest globular cluster to the Sun, this method yielded an age of 12.7 ± 0.7 Gyr (2 sigma error), similar to the latest MSTO analysis by Krauss & Chaboyer (2003) of $12.6_{-2.2}^{+3.4}$ Gyr. For NGC 6397 an age of 11.47 ± 0.47 Gyr at 95% confidence was obtained with the white dwarf method (Hansen et al., 2007). However, the prospects of extending this methodology to other clusters is limited by the extreme faintness of the oldest white dwarfs.

Moreover, the determination of an age from the white dwarf luminosity function allows a direct comparison between the globular clusters and the Galactic disc. There appears to be a gap of ~ 2 Gyr between the ages of globular clusters and the oldest open clusters (e.g. Jimenez et al., 1998; Sandage et al., 2003), which may reflect a delay in the formation of the disc, or simply the failure of any open clusters to survive destruction for the disc's whole life (Section 3.1.6). Current age estimates for the local thin disc by other methods (without taking into account the white dwarf-based estimates) range from 8 to 12 Gyr (e.g. Jimenez et al., 1998; Binney et al., 2000). On the other hand, the recent results coming from white dwarf-based estimates seem to confirm the existence of a significant delay between globular clusters formation and the onset of star formation in the Galactic disc (Hansen et al., 2007). The most definitive proof that the local disc white dwarfs are younger than the oldest halo stars was the discovery by Hansen et al. (2002) that the white dwarfs of M4 extend to approximately 2.5 mag fainter than the peak of the local thin disc white dwarf luminosity function. A caveat remains: the white dwarf luminosity function of the thin disc needs to be obtained down to

³In most if not all globular clusters there is evidence for two stellar generations, albeit with a very small ($\simeq 10$ Myr) age spread, questioning the simple hypothesis that these systems are real simple stellar populations (see Section 3.1.7)

the faintest magnitudes, requiring large areas of the sky to be covered in order to acquire a large white dwarf (WD) sample (Harris et al., 2006).

Elsewhere disc globular clusters seem to have a similar age to the ones found in the halo, providing evidence that the star formation in these two classes of object began at roughly the same time (in line with the conclusions obtained from the study of thick disc and halo abundance patterns - see Section 3.5.3).

The bulge age is a harder question. While generally thought to be more than 10 Gyr old, as expected from an early formation and in agreement with the chemical abundances (see Section 3.5.2), there is intense star formation in the plane at $R < 100$ pc, and hence a younger population inhabits the central region of the Galaxy (traced by OH/IR stars and other objects mostly confined to the Galactic plane). However, the deepest colour-magnitude diagram of the bulge to date, obtained with Advanced Camera for Surveys (ACS) at HST (Sahu et al., 2006; Minniti & Zoccali, 2008) is consistent with the interpretation that the bulk of the bulge is old.

3.4.2 Stellar yields

Gaining an understanding of the origin of the chemical elements must be counted one of the great scientific advances of the 20th century. Since the seminal paper of Burbidge et al. (1957), only very few nuclear processes have been added to the ones suggested in that work, but many very detailed calculations based on complex fundamental physics have been carried out (Meynet, 2007; Limongi & Chieffi, 2007; Siess, 2007, for recent reviews). It has become possible to confront the theory with observations of a wide variety of stars. The Galaxy and Local Group galaxies offer the unique opportunity to constrain stellar yields because they are resolved in individual stars and it has now become possible to confront theory with observations of a wide variety of stars in different environments (see Sec. 4.1).

Massive stars produce almost all the nuclides from carbon to the Fe-peak, as well as many of the nuclides heavier than iron (the light s-, r- and p- nuclides), and eject them into the ISM through stellar winds and core-collapse supernova explosions. The predicted abundances of nuclides are affected by uncertainties in the hydrostatic burning phases (such as mass-loss rates and mixing process), and in explosive nucleosynthesis (such as the location of the mass cut, the energy of explosion, and the extent of fallback). For most nuclides, the yields computed for massive stars of solar metallicity by different authors are in agreement within a factor of two. The discrepancies among different groups are more severe towards lower metallicities, not only for secondary elements (as expected) but also for some

primary elements whose nucleosynthesis depends on earlier stellar evolutionary processes such as mass loss and mixing. Moreover, it has been suggested that the explosion energy is a function of metallicity (Nomoto et al., 2006), which would then affect the yields of nuclides located near the mass cut.

Thermonuclear supernovae are important contributors to the enrichment of the ISM with Fe-peak nuclei and some intermediate mass nuclei (from Si to Ca). The deflagration model W7 is used most widely, and it successfully reproduces observed spectra (Nomoto et al., 1997). Most models are spherically symmetric, but turbulence is expected to play an important role at all stages of a thermonuclear supernova, so the 3D calculations that have started to appear are necessary if stellar yields are to be determined from first principles.

Intermediate-mass stars are the main producers of heavy s-process nuclides and also contribute large amounts of several other nuclides (Siess, 2007), notably carbon and nitrogen during their AGB phase. The yields of intermediate-mass stars are more uncertain than those of massive stars: dredge-up and hot-bottom burning lead to large uncertainties because these processes require detailed computations of transport mechanisms and depend strongly on stellar lifetimes, which in turn depend on the mass-loss rate. Hence, for intermediate-mass stars, large discrepancies between authors are found even at solar metallicity.

At very low metallicities only core-collapse supernovae had time to enrich the ISM, so extremely metal-poor stars (EMP stars) put stringent constraints on the stellar yields of massive stars. The above discussion illustrates the difficulty in extrapolating yields calibrated in the solar vicinity (with stars of near-solar metallicity) to lower metallicities at which observational constraints are scarce or non-existent. Obtaining such observational constraints on nucleosynthesis at low metallicities is an important task for the future; we need spectra at resolving power $R \sim 40000$ and $S/N \sim 100-200$ in the optical, of statistically significant stellar samples at a range of metallicities, and then the spectra must be analysed in a homogeneous way.

3.4.3 Timescales

The ISM was enriched faster in elements produced by short-lived massive stars and more slowly in elements mainly produced by low- and intermediate-mass stars and thermonuclear supernovae. By measuring the ratio of two elements that are returned to the interstellar medium on different time-scales – such as oxygen and iron – as a function of metallicity, it is possible to infer how fast the metal enrichment proceeded and the time-scale over which a particular Galactic component was formed. With a range of stellar masses contributing elements in different

proportions, and star formation and evolution being a protracted, continuous process, it is necessary to model the various contributions throughout the history of the Galaxy. Chemical evolution models that are able to trace the evolution of a large number of chemical elements can be used to unravel the history of the Milky Way and other galaxies. The enrichment time-scale of other galaxies containing a resolved stellar population can be elucidated by the same technique.

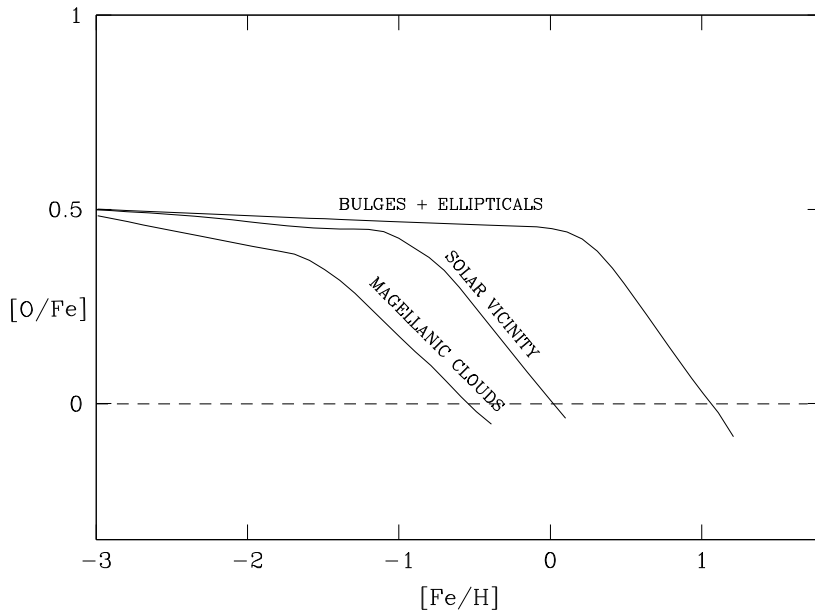


Figure 17: A sketch of the predicted $[O/Fe]$ vs. $[Fe/H]$ relations in different systems as a consequence of their different enrichment time-scales. Stars in our Galaxy’s bulge formed during an intense star formation burst that enriched its interstellar medium in a short time-scale essentially with products of SN II. Hence, they should have a large oxygen-to-iron ratio up to higher metallicities. In contrast, dwarf galaxies like the Magellanic Clouds form stars very gradually, so most of their stars have a higher proportion of iron (coming from SN Ia) relative to other metals. Thin-disc stars near our Sun are an intermediate case (Matteucci, 2001).

This is illustrated schematically in Figure 17: systems in which the chemical enrichment was faster than in the solar vicinity attain a metallicity larger than solar in a very short time-scale, before the iron-rich ejecta of thermonuclear SN diluted the oxygen. In this case the $[O/Fe]$ plateau extends to higher metallicities than in the solar vicinity, as in the case of old systems such as the Galactic bulge and elliptical galaxies. On the other hand, systems in which star formation is less efficient, e.g. in Magellanic irregular galaxies, the opposite occurs, and thermonuclear SN start contributing to the chemical enrichment even at low metallicities, and essentially no plateau is observed. The initial level of $[O/Fe]$ at very low

metallicities gives us an idea of the IMF. In the example shown in Figure 17, all three systems have the same IMF, and hence all the curves start at the same value of $[O/Fe] \sim +0.5$.

Figure 18 shows a comparison of abundance data of the Milky Way with those of Local Group dwarf spheroidal galaxies obtained with the VLT (Venn et al., 2004). The abundance pattern observed in dwarf spheroidal galaxies is interpreted as indicating that the star formation in these objects proceeded much slower than in the Galactic halo. Detailed models of the abundance patterns of different elements in each of these galaxies, able to reproduce their observed metallicity distribution (Lanfranchi & Matteucci, 2007) seem to confirm this interpretation and show that their enrichment history was affected by galactic winds.

3.4.4 Primordial nucleosynthesis

The relic abundances of light elements synthesised during the first few minutes of the evolution of the Universe provide unique probes of cosmology and constitute the starting point for stellar and galactic chemical evolution. Recent WMAP analyses of the angular power spectrum of the temperature fluctuations in the cosmic microwave background, combined with other relevant observational data, have yielded very tight constraints on the baryon density. Fixing this permits a detailed, quantitative confrontation of the predictions of standard Big Bang Nucleosynthesis (BBN) with the primordial abundances inferred from observational data. Figure 19 clearly indicates a tension between BBN predictions and observed abundances of ${}^7\text{Li}$ in the sense that the observed abundances tend to be lower. In contrast, for D the observations and BBN models seem to agree well with each other. Considering the large uncertainty associated with ${}^4\text{He}$ observations, the agreement with CMB+BBN is fair. The calculated ${}^3\text{He}$ value is close to its Galactic value suggesting that its abundance has little changed during Galactic chemical evolution.

Deuterium is a very sensitive chemical marker of the gas consumption in a given locale. All of the deuterium in the Universe was created in the Big Bang. Stars destroy deuterium, so mass-loss from stars reduces the D abundance in the ISM, while accretion of pristine material from intergalactic space increases it. Given that we know the primordial D abundance, $D/H = (2.60_{-0.17}^{+0.19}) \times 10^{-5}$, measurements of the current D abundance at any location in the Galaxy would constrain the local IMF and the star-formation and infall histories there.

Unfortunately, it is extremely hard to determine the abundance of deuterium securely: D gives rise to many observable spectral lines, but conversion of the line strengths into abundances is hard because one needs to know what fraction of the

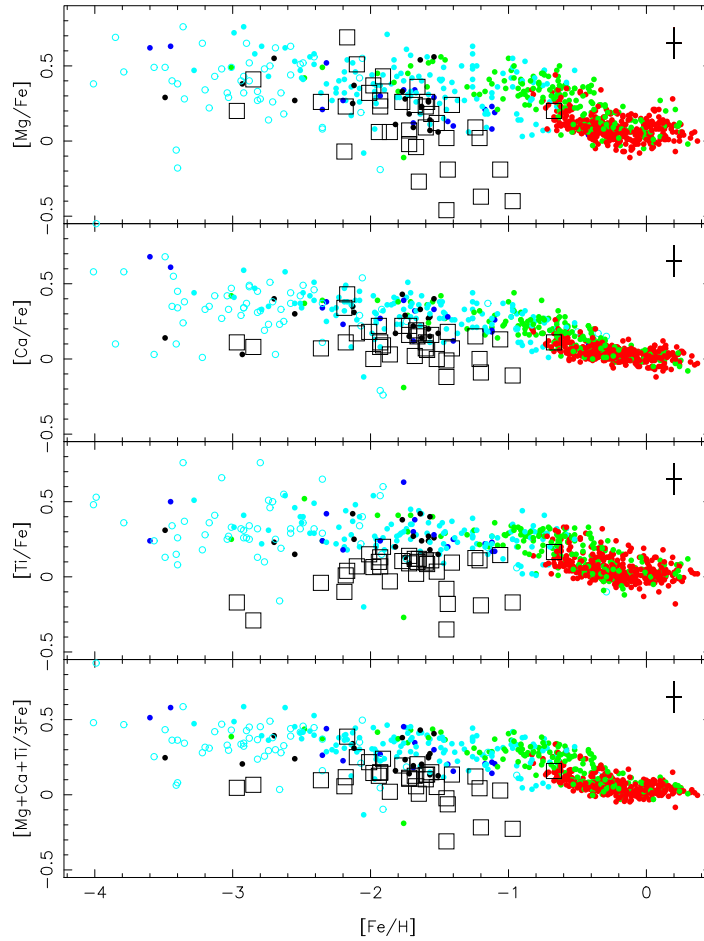


Figure 18: $[\alpha/\text{Fe}]$ versus metallicity for the α elements Mg, Ca, Ti and the mean of the three (Venn et al., 2004). Small symbols show stars in the Milky Way thin disc (red), thick disc (green) and halo (blue/cyan). Small black symbols represent stars on retrograde orbits. The large black squares show the abundance pattern of dwarf spheroidal galaxies and clearly lie below most of Galactic data. This is interpreted as showing that star formation in dwarf spheroidal galaxies was less efficient than in our Galactic halo, similar to the Magellanic Clouds curve shown in Figure 17.

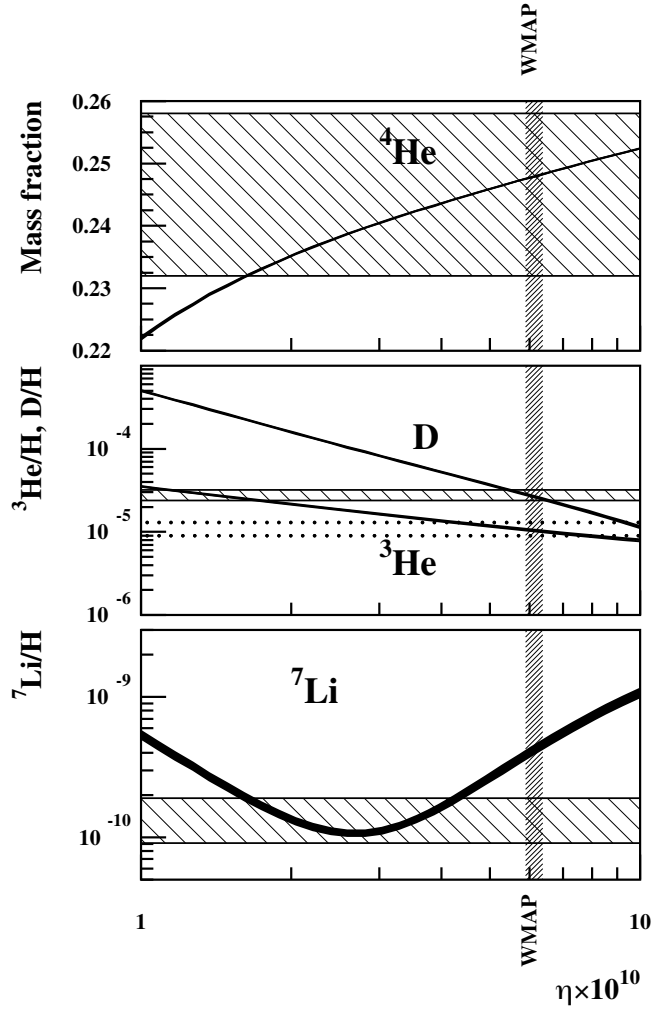


Figure 19: Solid curves show the primordial values of the ${}^4\text{He}$ mass fraction (Y) and the D , ${}^3\text{He}$ and ${}^7\text{Li}$ abundances by number relative to hydrogen, predicted as functions of the baryon to photon ratio ($\eta_{10} = 10^{10}\eta$) by standard BBN. The thickness of each curve reflects the nuclear uncertainties. The horizontal lines represent the limits on the primordial abundances deduced from observations, while the vertical stripe represents the WMAP estimate of η_{10} (Coc, 2008).

available deuterium is in the phase observed, and this involves complex chemistry that depends on the physical conditions (density, flux of ionising radiation, electron temperature etc.) in the region observed (Linsky et al., 2006). As a consequence of these difficulties, there are only two measurements of deuterium in the Galaxy outside the solar neighbourhood. From the measurement of the 327 MHz line of deuterium Rogers et al. (2005) obtained a D abundance close to the primordial value at a Galactocentric distance 10 kpc. In the Galactic centre one expects vigorous star formation and a dearth of accreted pristine material to lead to a low deuterium abundance. In fact, from a line of DCN, Lubowich et al. (2000) found the $[D/H] = 1.7 \pm 0.3 \times 10^{-6}$. While this abundance is the lowest value measured in the Galaxy, it is several orders of magnitude larger than the value predicted by models of chemical evolution that neglect cosmic infall.

Models of the chemical evolution of the solar vicinity that reproduce the major observational constraints predict only moderate D depletion, by at most a factor of two (Romano et al., 2006). Interpretation of the available data is complex for the reasons given above, but Linsky et al. (2006) conclude that $[D/H] = (2.31 \pm 0.24) \times 10^{-5}$, which is smaller than the primordial value by only a factor ~ 1.2 . Measurements of D (or of the D/O ratio) in different parts of the Galactic disc could put stringent constraints on the Galactic disc formation history. Chiappini et al. (2002) predict a Galactocentric gradient for $d \log(D/O)/dR = 0.13$ dex/kpc. According to Hébrard & Moos (2003), given the typical error bars, such gradients would be detectable with FUSE. However, this signature was not detected because the sample of distant targets was still poor, with few targets sampling regions more distant than 500 pc. The FUSE satellite was decommissioned in October 2007.

Standard models of stellar evolution predict stars of 1–2 M_{\odot} to be net producers of ${}^3\text{He}$. Galactic chemical evolution models adopting such prescriptions predict a strong increase of the ${}^3\text{He}$ abundance in the ISM over the last few Gyr. Neither this increase nor a spatial gradient in the abundance of ${}^3\text{He}$ is observed. Instead, observations show that the abundance of ${}^3\text{He}$ remained almost constant in the ISM at a value close to that predicted by WMAP (Balsler et al., 1999). Some of the ${}^3\text{He}$ predicted by standard models is probably destroyed by a non-canonical mixing occurring during the red giant phase (Charbonnel, 1995). To reproduce the observed abundances, Galactic chemical evolution models require this non-canonical mixing to occur in at least 93% of stars in the 1–2 M_{\odot} range (Chiappini et al., 2002; Galli, 2006). This leaves room to accommodate the two planetary nebulae whose progenitors are believed to have been in the 1–2 M_{\odot} range and show large ${}^3\text{He}$ abundances, compatible with the standard prediction (Balsler et al., 2007).

Until very recently, a self-consistent stellar model that explained why this extra mixing occurs in many but not all low-mass stars was missing. This is now explained by a threshold magnetic field of 10^4 – 10^5 Gauss, above which a process

called *thermohaline mixing* is inhibited in red giants located at or above the bump (Charbonnel & Zahn, 2007). As fields of that order are expected in the descendants of the Ap stars, it remains to be checked whether the magnetic stars are sufficient in number to account for the $\sim 7\%$ of red giants which are spared from thermohaline mixing.

The abundance of ${}^4\text{He}$ plays a fundamental role in testing BBN and constraining non-standard models, if it can be determined with a 0.001 precision or better. Combining the BBN predictions with the WMAP baryon density, a primordial helium abundance $Y_p = 0.2482 \pm 0.0007$ is obtained (Figure 19). However, due to systematic effects, the uncertainty in the primordial ${}^4\text{He}$ abundance is still large, $\sim 1\text{-}3\%$ (Olive & Skillman, 2004; Peimbert et al., 2007). Might there be alternative approaches to estimating Y_p that are competitive with the current method of measuring the helium abundance in extragalactic, low-metallicity H II regions? One approach would be to use chemical evolution models, tied to the solar helium and heavy element abundances, to extrapolate back to the relic abundance of ${}^4\text{He}$ (Steigman, 2006). At present this approach appears to be limited by theoretical uncertainties related to the stellar yields of He of massive stars and its dependency on the adopted mass loss.

Since the pioneering paper of Spite & Spite (1982) the constant lithium abundance of metal-poor ($[\text{Fe}/\text{H}] \leq -3$) stars has been interpreted as the primordial lithium value. However, even in the most recent estimates of the *Spite plateau* the observed value is ~ 0.5 dex below the primordial ${}^7\text{Li}$ abundance suggested by WMAP+BBN (Asplund et al., 2006). To reconcile the observations of ${}^7\text{Li}$ with the values indicated by WMAP, various processes have been invoked. These range from the reduction of surface ${}^7\text{Li}$ by diffusion in low-mass stars (Korn et al., 2006), to the dilution of ${}^7\text{Li}$ in the ISM by material ejected from stars prior to the formation of the stars we now observe (Piau et al., 2006). Another interesting piece of the lithium puzzle is the discovery of ${}^6\text{Li}$ in metal-poor halo stars (Smith et al., 1993, 1998). The observed high ${}^6\text{Li}$ abundance at very low metallicities cannot be explained by standard BBN, nor by Galactic cosmic-ray spallation and α -fusion reactions. In addition, the presence of ${}^6\text{Li}$ in metal-poor stars sets strong constraints on any theory of Li depletion in such stars, since ${}^6\text{Li}$ is destroyed at lower temperatures than ${}^7\text{Li}$. Some of the solutions proposed so far to explain the lithium problem(s) have consequences on other research areas, e.g. BBN nuclear rates (Coc et al., 2004). However, measurements of ${}^6\text{Li}$ are extremely challenging, and some uncertainties could falsely mimic the existence of ${}^6\text{Li}$ as recently shown by Cayrel et al. (2007). This is an open and exciting area of research.

3.4.5 Ages, kinematics, and chemical abundances

One of the crucial observations that could in principle constrain the different galaxy formation models is the existence of a correlation between age and metallicity – the age-metallicity relation (AMR). This has so far only been extensively investigated for the solar vicinity, and even in this case the results are quite controversial. The AMR in different regions of M31 was determined by Brown et al. (2006). Studies that estimate ages from chromospheric activity find a rather tight correlation of age and metallicity (Rocha-Pinto et al., 2000). Edvardsson et al. (1993) obtained very high-quality data for a small and biased sample of stars and found a large scatter in the age–metallicity plane. The Geneva-Copenhagen Survey (Nordström et al., 2004) provides photometric metallicities, ages, Hipparcos kinematics, and Galactic orbits for a complete, magnitude-limited, all sky sample of $\sim 14\,000$ F and G dwarfs brighter than $V \sim 8.3$. With this much larger and unbiased sample, Nordström et al. (2004) also found a large scatter in the age–metallicity plane. A reappraisal by Pont & Eyer (2004) of the ages assigned to the stars by Nordström et al. suggest again the existence of an AMR, but a similar exercise by Holmberg et al. (2007) reaffirmed the absence of an AMR. Recently, the AMR has also been derived from observations of field (da Silva et al., 2006) and clump giants (Soubiran et al., 2008). In the latter case a much lower dispersion was found.

A major unresolved issue is the extent to which stars are observed at radii significantly different from their radii of birth. Older stars can be on quite eccentric orbits, and can consequently be observed at a range of radii that can be several kiloparsecs in extent in the case of old stars that formed well inside R_0 , where the velocity dispersion is thought to be large.

A star oscillates in radius around its guiding centre. If this guiding-centre radius lies near the corotation resonance of a transient spiral structure, the star can become resonantly trapped and have its guiding centre shifted a significant distance inwards or outwards (Sellwood & Binney, 2002). This process (*churning*) is most important for stars on nearly circular orbits, that would otherwise not move radially.

Radial migration of stars through these two processes brings to the solar neighbourhood stars that were born elsewhere, so stars of a given age will have a spread in metallicity equal to the radial spread in the metallicities of the ISM at their time of birth. Thus we do not expect to observe a tight AMR. An additional source of scatter in the AMR at the Sun arises because local samples contain a mixture of thin- and thick-disc stars (Fuhrmann, 2008).

Haywood (2005) estimates that the AMR (and hence the star formation history) can be recovered adequately once metallicities, temperatures and parallaxes

are measured with a precision of 0.05 dex, 50 K and 10%, respectively. Gaia will in principle get such high precision for the last two parameters, depending on the accuracy of the extinction and reddening corrections, but metallicities of the required precision will have to be obtained from the ground. Gaia will also allow a better discrimination of thick- and thin-disc stars.

In so far as the random velocities of disc stars increase with time, the velocity dispersion of a population can be used as a proxy for age, and velocity dispersions can be extracted from proper motions (e.g. Dehnen & Binney, 1998) or low-dispersion spectra (e.g. Steinmetz et al., 2006) while ages are hard to measure for most stars. Moreover, models of chemical evolution typically predict average properties of the stellar population in a vertical column through the disc at the position of the Sun, while observations refer to a roughly spherical volume centred on the Sun. The motions of stars must be known to allow for this difference (Holmberg et al., 2007). A good knowledge of stellar motions also allows for a better correction of selection effects that arise in kinematically selected samples.

Kinematics and age play an important role in constructing samples of field thick-disc and halo stars, helping to distinguish them from the more numerous thin-disc stars in the solar neighbourhood. At present, there is a lack of consensus concerning how to distinguish thick- from thin-disc stars. The assignment criteria can depend on poorly known quantities such as the fraction of thick-disc stars in the solar neighbourhood, the impact of disc heating, and contamination by the Hercules stream (Holmberg et al., 2007).

One way to distinguish the thin and thick disc is by their different velocity dispersion and asymmetric drift values (both larger for the thick disc). In the literature the asymmetric drift of the thick disc covers a large range: from -100 km s^{-1} (Wyse & Gilmore, 1986) to about -50 km s^{-1} (Fuhrmann, 2004) and -20 km s^{-1} (Norris, 1987). For nearby field stars, the kinematic criterion most commonly used is based on a decomposition of the local velocity distribution into Gaussians corresponding to the thin and thick disc and assuming values for the asymmetric drift and U , V , W velocity dispersions for each. Membership probabilities to either disc are assigned for each star, based on the observed space motion (Bensby et al., 2004). According to Holmberg et al. (2007) a more robust separation of the thick- and thin-disc stars is obtained if the kinematic parameters chosen for the thin disc correspond to its oldest stars.

A different approach was adopted by Fuhrmann (2008) who built a volume-complete sample of FGK stars that had been observed with the FOCES echelle spectrograph at the Calar Alto Observatory and exposed to S/N values of at least 200. For this sample, which has no kinematic or chemical pre-selection, Fuhrmann (2008) was able to show that, as opposed to the kinematic overlap

of thick- and thin-disc stars, a very different picture is visible in a $[\text{Fe}/\text{Mg}]$ vs. $[\text{Mg}/\text{H}]$ diagram (see Figure 20). Together with the age-dating of key subgiants by Bernkopf & Fuhrmann (2006) and Bernkopf et al. (2001) (see Section 3.4.1), this result provides another prime argument for the genuine distinctness of the two local disc populations. It also suggests chemical signature to be a useful tool to assign a star to either the thick or thin-disc components.

The existence of the Hercules stream in local samples (Famaey et al., 2005; Seabroke & Gilmore, 2007) is also a source of contamination for the thick disc population which renders the selection of a pure population even more difficult. The RAVE survey should help in this but will be limited to radial velocities and to distances close to the Sun. A larger and extended kinematic survey including 3D velocities and distances (for example Gaia) would help clarify the situation.

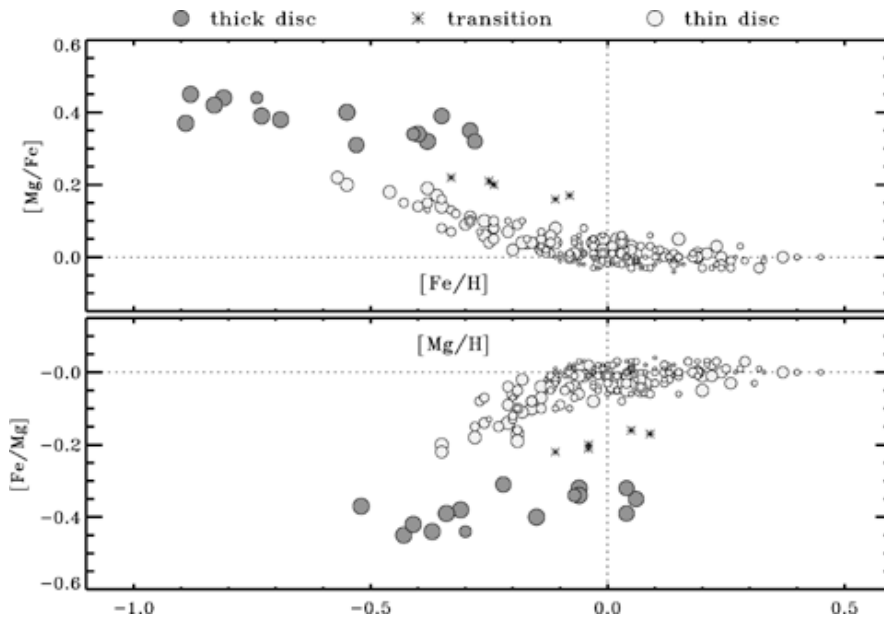


Figure 20: Iron and magnesium abundances for more than 200 FGK stars within 25 pc. Circle diameters are proportional to the age estimates, i.e. small diameters correspond to young stars. Light and dark circles represent members of the thin disc and thick disc, respectively. This figure suggests a gap in star formation in between the youngest thick-disc and the oldest thin-disc stars. From Fuhrmann (2008).

With well defined samples, important questions can be addressed. One is whether the velocity dispersion of disc stars continues to increase throughout the lifetime of the disc, or whether it saturates after some time. The answer can be found in the observed age-velocity relation. Quillen & Garnett (2001) obtained an almost flat relation between velocity dispersion and age for stars younger than ~ 9 Gyr. This result implies that the disc stars suffered little heating or dispersion

between 3 and 9 Gyrs ago. In addition, they proposed that the Milky Way suffered a minor merger 9 Gyrs ago, responsible for the creation of the thick disc. However, this analysis conflicts with results obtained for a much larger sample of Hipparcos stars by Binney et al. (2000) and the analysis of a similar sample by Holmberg et al. (2007): in these studies, the velocity dispersion σ increases with age τ roughly as $\sigma \propto \tau^{1/3}$ throughout the life of the disc (Figure 21).

The bulge kinematics are mainly derived from K-giant radial velocity. The bulge has a peak rotation of about 75 km s^{-1} (Minniti & Zoccali (2008) and references therein) and a large velocity dispersion. Proper motions were measured in Baade's window confirming the high velocity dispersion of M-giants. One of the goals in the future is to be able to distinguish between a possible inner disc/halo component and the true bulge (Minniti & Zoccali, 2008).

It is again clear, from the discussion in this section, that sufficiently large samples of high quality data would have a profound impact on our views of how the Galaxy formed. The work of Norström et al. shows a preview of what will be achieved with Gaia for a much large number of stars, sampling a much larger region of our Galaxy. The impact of this research is guaranteed by the large number of stars and hence the adequate statistics for selecting subsets of stars defined by age, metallicity or abundance, and kinematics. Moreover, Gaia will not only increase the volume sampled but will also enable a better assignment of stellar ages.

3.4.6 Comparative studies in the Local Group

The Galaxy is not isolated, but inhabits the Local Group, a rather average environment in the Universe. The Andromeda galaxy is our nearest large neighbour, a rather typical spiral but one that shows some interesting differences when compared to the Milky Way. Orbiting within the Local Group are several tens of dwarf galaxies, ranging from irregular and gas rich systems to spheroidals almost devoid of cold gas. These neighbouring galaxies give us the opportunity to study the differences and similarities in the evolutionary path of galactic systems, and also how they depend on scale. For these objects, star formation histories may be obtained, detailed chemical abundance patterns measured, fossil streams discovered, and their mass distribution and dark matter content mapped in great detail. Indeed, we are moving into an era when data on Local Group objects will be comparable to what we had a generation or less ago on the Galaxy. A key task for the coming decade is then to upgrade the Local Group data so that we can understand as fully as possible the differences and similarities between the populations of Local Group objects, including our Galaxy, and relate these to their different masses and environments.

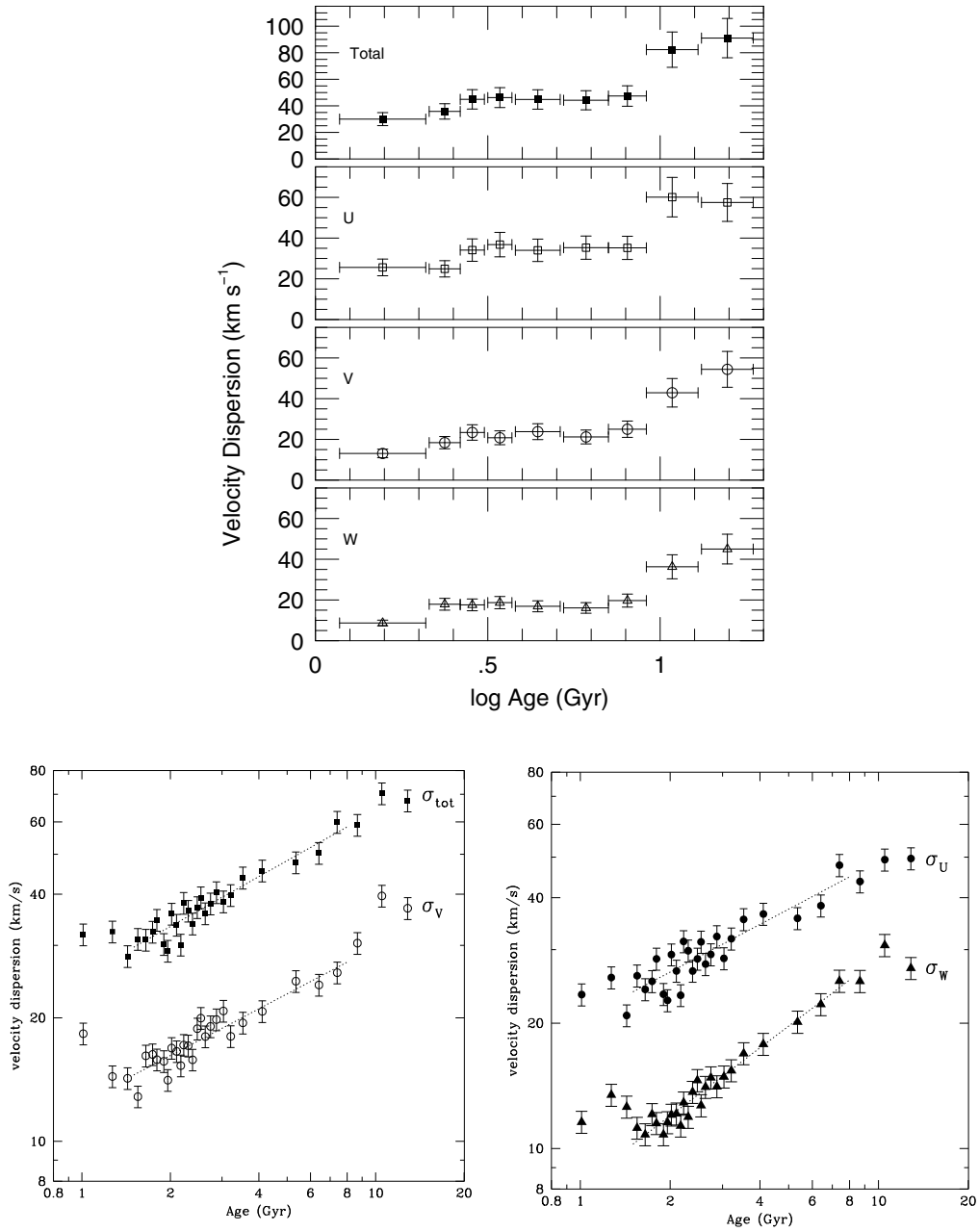


Figure 21: *Velocity dispersion vs. age for stars in the Galactic disc. The upper panel shows the results obtained by Quillen & Garnett (2001), whereas in the lower panels the recent results of Holmberg et al. (2007) are shown.*

Andromeda is an early type disc galaxy, with a rather prominent bulge component (see Figure 22). This bulge is relatively metal-rich and has similar properties to an elliptical galaxy (which makes it particularly interesting to study in detail). A metal-poor and faint halo is also present in this spheroid (Kalirai et al., 2006). Just as for the Milky Way, a giant stellar stream, analogous to the Sgr stream, has also been found (Ibata et al., 2001b). Furthermore, our external view of Andromeda has allowed us to observe a very extended disc whose outskirts are very rich in substructure, presumably due to accreted satellite galaxies (Ferguson et al., 2002; Ibata et al., 2007). Such features would have remained largely hidden in the outer disc of the Galaxy, because of the large amounts of extinction at low Galactic latitudes. However, it is very possible that structures like the Monoceros ring (Newberg et al., 2002; Ibata et al., 2003) are the counterparts of those that we see in Andromeda. A basic comparison with the Milky Way therefore suggests that our neighbour has probably had a more active merging history.

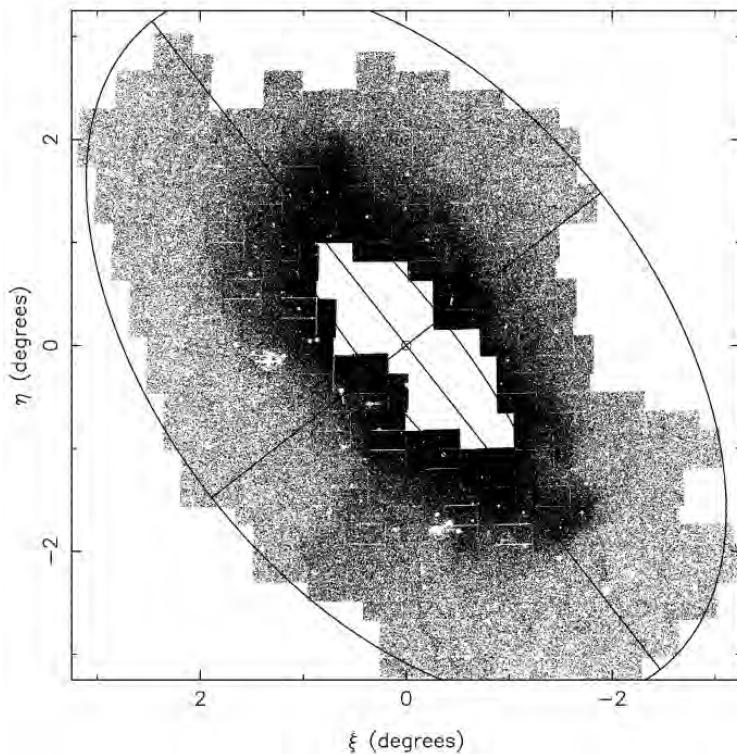


Figure 22: *Projection of the surface density of blue red giant branch (RGB) stars across a 25 deg^2 survey area of the Andromeda galaxy. The optical disc of Andromeda lies well within the inner ellipse. Note the large amount of substructure seen at large radii, including the giant stellar stream and stellar over-densities at both extremes of the major axis (from Ferguson et al., 2002).*

Dwarf galaxies are the most common type of galaxy in the Universe, and

similarly they dominate the number counts in the Local Group. In recent years the number of known satellites has doubled both for the Milky Way (Belokurov et al., 2007a) and for Andromeda (Martin et al., 2006). However, this tally is still far below the number of bound substructures found in cold dark-matter simulations (Klypin et al., 1999; Moore et al., 1999). This ‘missing satellites problem’ can be solved if there is a mass-scale below which luminous satellites do not form. This can either be because gas is unable to cool and form stars (e.g. due to a UV ionising background, Bullock et al., 2000), or because the mass-spectrum has a low-mass cutoff (as for warm or self-interacting dark matter, e.g. Spergel & Steinhardt, 2000). To understand the cause of this large discrepancy it is therefore fundamental to measure the masses of dwarf galaxies. There is currently some evidence that there may be a lower mass limit which is not far below $10^7 M_{\odot}$ (e.g. Strigari et al., 2007b; Gilmore et al., 2007).

The spatial distribution of dark-matter depends on its nature. Dwarf galaxies have such high mass-to-light ratios that they are excellent dark-matter laboratories. While there is now circumstantial evidence favouring a cored profile for a few systems (e.g. Sculptor, see Battaglia et al., 2008), most dwarfs are consistent with both cuspy and cored profiles given that only radial velocities are available. The measurement of the slope of the density profile relies on assumptions regarding the (completely unknown) orbital distribution of stars in these systems. Breaking this degeneracy requires accurate proper motion measurements of individual stars, but this may be out of the question with Gaia (although SIM will be better in this respect). By binning Gaia proper motions near the centre and separately in the outskirts, it may however be possible to roughly constrain the orbital structure of these systems.

Not just the dynamics, but also the star formation and chemical evolution histories of dwarf galaxies should be compared to those of large galaxies like the Milky Way or Andromeda. This is particularly relevant in the context of the hierarchical paradigm where large galaxies are the result of the merging of smaller systems. Clearly we would like to know how the stellar populations in these dwarf systems compare to the building blocks of the Milky Way. Given that we expect such building blocks to have contributed stars both to the thick disc and particularly to the stellar halo, a comparison of these components is certainly worthwhile.

Such studies have begun to show a more complex picture than initially envisioned. There is no significant contribution to the Galactic stellar halo from present-day dwarf spheroidal galaxies (Unavane et al., 1996), since their detailed chemical abundance patterns are too different from that of any component in the Milky Way (Venn et al., 2004). The metallicity distribution is also puzzling. Although still based on small number statistics, it seems that the dwarf galaxies lack

a population of very metal-poor stars below $[\text{Fe}/\text{H}] \sim -3$ dex, whereas such stars are present in the stellar halo of the Galaxy. This may imply that the dwarfs formed from pre-enriched material, and even perhaps from the building blocks of our Galaxy (Helmi et al., 2006b).

Studies of the stellar populations in the dwarfs allow us to explore how galaxy evolution is affected by mass. For example, objects whose potential well is relatively shallow may be unable to retain their gas and perhaps even metals (Ferrara & Tolstoy, 2000). Environment is probably also an important driver of evolution, since tides and ram-pressure stripping will affect the ability of satellites to retain the fuel needed to form new generations of stars (Mayer et al., 2001). Furthermore, it may be possible to observe the imprints of re-ionisation on these small systems, in the sense that it could well be that (some of) the dwarfs were only able to start forming stars below a redshift $z \sim 3 - 5$. However, this requires very precise age dating, and may be difficult to achieve. At present all we know is that all dwarfs contain ancient stellar populations, i.e. older than 10 Gyr (Grebel & Gallagher, 2004). The initial mass function (IMF) could also be different in these tiny galaxies. On the one hand, the low star-formation rates characteristic of these systems could limit the formation of very massive stars, effectively truncating the high-mass end of the IMF (Tolstoy et al., 2003). On the other hand, it is also possible that the IMF depends on metallicity, since cooling occurs via metal-lines in molecular clouds. Therefore, by studying these galaxies, we can get a handle on the variation of the IMF with environment and also in time.

The globular clusters are at the bottom end of the mass function of the Local Group. With the recent discovery of extremely faint dwarf spheroidal galaxies, the boundary between these and the globular clusters has become hazier. The two populations have similar absolute magnitudes, but the faint dwarf galaxies are significantly more extended (Belokurov et al., 2007a), and show evidence of multiple star formation episodes and a metallicity spread. The internal kinematics of these objects are now beginning to be explored, but large mass-to-light ratios are already apparent (Martin et al., 2007). Whether these have been induced by tides, or are evidence of large amounts of dark matter, remains to be seen. However, it is clear that dwarf galaxies are somehow different from globular clusters, and this difference presumably reflects different formation paths, which may be associated with the presence of dark matter or lack thereof.

3.5 Galaxy assembly and evolution

We now outline our still fragmentary picture of how the Galaxy was assembled. The discussion makes extensive use of the clues provided by relations between the ages, abundances and kinematics of stars. This methodology has its roots in the

paper of Eggen et al. (1962) and has recently been extended to searches for groups of stars with similar chemistry and kinematics (e.g. Freeman & Bland-Hawthorn, 2002). We start with the halo. Its stars are as old as any known, but as a structure the halo was possibly not the first component to form – in a certain sense it is still forming – but at least formed from relatively pristine material (because it is metal-poor) (Section 3.1.1). Then we discuss the bulge, which being the densest part of the Galaxy, may have formed first, before moving to the disc, which is still a work in progress. Finally we discuss the origin of the globular clusters, which is still rather obscure and involves connections with all the three other components of the Galaxy.

3.5.1 History of the halo

Given the number and extent of the tidal streams that have now been detected in the halo (Section 3.1.1), and the prediction of the Λ CDM theory that much of the growth of galaxies is driven by tidally shredding accreted satellites (Section 3.3.6), one first asks whether the entire halo is made up of such debris.

Halo stars are very similar to the stars of halo globular clusters, from which we see tidal streams (Section 3.1.1). Moreover, globular clusters lose stars by evaporation in addition to tidal shredding. In fact, the observed globular clusters occupy the whole of the parameter space in which clusters of mass $\lesssim 3 \times 10^6 M_\odot$ can orbit for a Hubble time without either evaporating or being tidally shredded (Gnedin & Ostriker, 1997). Is the halo made up of destroyed globular clusters? Two difficulties that such a theory has to overcome are (a) that globular cluster metallicities extend no lower than $[\text{Fe}/\text{H}] = -2.5$ (Figure 6), and (ii) in some globular clusters the abundances of light elements from Li to Al show wide variations between stars that have no parallel in field stars.

If the halo did consist of debris from globular clusters, the similarity of the halo's radial density profile with that of the globular-cluster system implies that tidal shredding was not the dominant process for the destruction of the clusters: the probability per unit time that a given cluster will be tidally destroyed decreases strongly with increasing galactocentric distance, so tidal destruction implies that the ratio of cluster to halo light should increase outwards. However, it is possible that the halo formed from a population of low-mass clusters that have all evaporated. Since the luminosity of the halo is ~ 100 times larger than the aggregate luminosity of the existing clusters, this picture requires the mass function for globular clusters to be extremely strongly weighted to low masses. The streams formed by evaporating clusters would be too numerous and individually contain too few stars to make the halo luminosity density as lumpy as it appears to be.

The tidal stream with by far the largest quantity of stars is that of the Sgr dSph. However the halo cannot comprise the debris of such objects because field halo stars are more α -enriched than the stars of dSph galaxies (Venn et al., 2004, see Figure 18). Moreover, in a sample of four dSph galaxies there is a dearth of stars more metal-poor than $[\text{Fe}/\text{H}] = -3$ (Helmi et al., 2006b), whereas halo stars are found down to $[\text{Fe}/\text{H}] = -5.5$.

Hence the conjecture that the halo consists of tidally shredded globular clusters and dSph galaxies does not readily explain evidence that $\sim \frac{1}{2}$ of the halo's luminosity is contributed by irregularities (Bell et al., 2008, and Section 3.1.1). The lumpiness points to halo stars forming in relatively massive objects that have been destroyed, but star formation in those objects must have been short lived. A possibility that we should consider is that the surviving dSph galaxies are a biased subset of the original population. In fact, the first satellites to be tidally destroyed will have been those with the lowest physical densities and/or the shortest-period orbits. These will also have been the objects least able to retain gas after their first burst of star formation, and least likely subsequently to accrete a fresh supply of gas. Hence they would be the satellites least able to sustain star formation long enough to have incorporated Fe from type Ia supernova into stars.

If the inner halo were made of debris from satellites that were tidally destroyed early in the Galaxy's life, the debris would be chemically distinct from that of current dSph galaxies since the latter are known to have formed stars for several gigayears. Simulations suggest that major tidal streams live on in phase space long after they have become undetectable in real space (Figure 16). Hence we should be able to detect these streams in full phase-space data.

We conclude that while disrupted globular clusters and dSph galaxies have certainly contributed to the halo, there must have been substantial contributions to the halo from other sources. The most likely source is a population of relatively massive satellites that were disrupted early on. We can test this conjecture by identifying and studying moving groups in the inner halo. A scarcity of such groups might signal that many halo stars formed in situ when the halo was briefly gas-rich.

3.5.2 History of the bulge

There are probably two fundamentally different modes of star formation. During mergers gas clouds that are on highly eccentric orbits collide, are violently shocked and convert a significant fraction of their gas into stars. At low redshift this process can be observed in some detail in rare ultra-luminous infrared galaxies (*ULIRGs*). The extreme luminosities of these objects suggest that in them the IMF is top-

heavy (Baugh et al., 2005). Cold gas does not remain on highly eccentric orbits for much longer than a dynamical time, either because feedback from massive stars blows it away, or because dissipation causes it to settle to a disc. Hence the system’s dynamical time ($\ll 1$ Gyr) forms an upper bound on the duration of any episode of star formation in this mode, and it follows that the stars formed will have high $[\alpha/\text{Fe}]$ ratios, and their chemistry may show the imprint of a top-heavy IMF. Moreover, the stars will not be on circular orbits, so they will form a spheroid. The central, cuspy regions of elliptical galaxies with stellar masses below $3 \times 10^{10} M_{\odot}$ are thought to be largely made in such starbursts (Nipoti & Binney, 2007). It is likely that the bulges of some spiral galaxies were also formed this way – such bulges are called “classical bulges” (Section 3.3.2).

The present-day Galactic disc exemplifies the second mode of star formation. Molecular clouds on nearly circular orbits collide gently, provoking a small fraction of the gas to form stars with a normal IMF. Newly-formed stars then disperse most of the gas, so in each dynamical time only a small fraction of the gas is converted into stars. The stars formed in this way are initially on nearly circular orbits, so they form a thin disc. After a time, the gas dispersed after each minor episode of star formation finds its way into new molecular clouds, which themselves suffer collisions and produce young stars. Since star formation is sustained over several gigayears, most stars in the disc have low $[\alpha/\text{Fe}]$ ratios. Hence the chemical and dynamical properties of discs and spheroids are naturally explained by the two modes of star formation.

In numerical simulations of galaxy formation, mergers occur frequently. If gas is present during a merger, tidal torques drive much of it towards the centre of the remnant, where it is expected to fuel rapid star formation and contribute to growth of the bulge. If the progenitors have stellar discs, these are shattered by the merger and will either form a thick disc (if the merger is relatively minor and the heating weak) or, in the case of a major merger, contribute to the bulge and the halo, depending on radius. Thus galaxy-formation simulations suggest that bulges should be conspicuous and contain a mixture of stars that formed in each star-formation mode. The Galaxy’s near neighbour, M33, is problematic for this theory because it has no measurable bulge and an extremely low-luminosity halo. This result implies that *none* of the progenitors of the M33 dark halo accumulated a significant body of gas or sustained much star formation. Miraculously the M33 halo came into existence fully formed with scarcely a baryon in its possession, and then stars began to form quiescently in the gaseous disc that grew around it.

The Galaxy is also problematic for the theory because, although the Galaxy has a luminous bulge, it is a “pseudo-bulge”, which should have formed when a vertically thin stellar bar buckled (Section 3.3.2). Hence theory says that most bulge stars formed in the disc.

This conclusion does not exclude the possibility that classical bulge is mixed in with the conspicuous pseudobulge, and an important task for the future is either to detect the classical bulge or to place limits on its luminosity. In fact, several facts are consistent with the observationally accessible outer regions of the bulge being part of a classical bulge: in Section 3.1.2 we saw that the stars are all old and have high values of $[\alpha/\text{Fe}]$, so they must have formed in the first \sim Gyr of the Galaxy's life. The wide spread in values of $[\text{Fe}/\text{H}]$ measured for bulge stars implies that substantial chemical enrichment must have taken place at this time, which is consistent with the indications that the IMF was top-heavy.

When did the disc buckle and give rise to the present bulge? One possibility is that the disc was largely gaseous when it buckled. Then conditions under which stars formed would not have been so different from the conditions in a modern ULIRG: many very massive gas clouds moved to highly non-circular orbits by the bar, were strongly shocked and rapidly formed stars with a top-heavy IMF. On account of the rapid, top-heavy star formation and the rapid inward motion of gas that bars drive, the gas quickly became exhausted and in the main body of the bulge star formation only lasted a few dynamical times, leaving the stellar population α -enhanced. In this case the bulge is old, and its present structure could differ significantly from its original structure as a result of angular-momentum loss to the dark halo (which makes a bar grow stronger and less rapidly rotating) and angular-momentum gain from gas (which has the opposite effect) (Athanasoula, 2003).

Another possibility is that the disc did not buckle until several gigayears after the present bulge stars were formed. That is, the large age of the bulge stars does not necessarily imply a large age for the bulge itself. This scenario would be favoured if the long-term dynamical stability of a barred bulge were an issue (for a discussion of the role of transitory bars in simulations of galaxy formation, see Heller et al., 2007).

The dynamics of the bulge are such that gas accumulates in the central x_2 disc (Section 3.3.2), and star formation continues there to this day. Little is known about the history of star formation in this region or the current spatial distribution of the stars that formed there.

3.5.3 History of the disc

Near the Sun we see stars of all ages, from the Hubble time down to zero (Edvardsson et al., 1993; Holmberg et al., 2007). The mix of stars suggests a star-formation rate that has been fairly constant or gently declining with time through most of the life of the Galaxy (Binney et al., 2000; Just & Jahreiss, 2007). Hernandez et al.

(2000) find that superimposed on this background rate there is a cyclic variation of period ~ 0.5 Gyr.

Models of the chemical evolution of the disc connect the history of gas inflow and outflow (Section 3.2.6), the IMF and the past star-formation rate to the current properties of the ISM and the stellar population of the disc. They predict the abundances in both the ISM and stars of various ages of nuclides that are produced in different types of stars. Consequently, the models are strongly constrained by data and provide valuable insights into the history of the disc. A general conclusion from these models is that near the Sun, the star-formation rate has been constant or at most slowly declining over the last ~ 9 Gyr and that it has been sustained by inflow of metal-poor gas at a rate that has also been steady or slowly declining (Chiappini et al., 1997), consistent with the rather uncertain predictions of the Λ CDM theory (Sommer-Larsen et al., 2003; Naab & Ostriker, 2006). The low values of $[\alpha/\text{Fe}]$ measured for most disc stars is a natural consequence of a long timescale for thin-disc formation. With an IMF similar to that of Kroupa (2002), Chiappini et al. (2003) are able to satisfy most observational constraints, in particular the observed abundances of a large number of elements within a factor of two, both now in the ISM and at the time of the formation of the Sun. In view of the large abundance range covered by different elements in the Sun – by more than a factor of 10^6 (Prantzos, 2007) – this result must be considered a great success of both chemical evolution theory and stellar evolution models.

Besides explaining the relatively high deuterium abundance and low $[\alpha/\text{Fe}]$ near the Sun, sustained cosmic infall resolves the classical G-dwarf problem, which is the scarcity of unevolved stars with $[\text{Fe}/\text{H}] \lesssim -0.5$. If the thin disc originally had the same surface density as it does now but was made exclusively of pristine gas, about half of the local dwarf stars would have $[\text{Fe}/\text{H}] < -0.5$, regardless of what star-formation history reduced the surface density of gas to its present value. The actual density of such stars is much smaller. If most of the disc's mass has been accreted since star-formation started in the disc, only a small number of metal-poor dwarfs are predicted because a few stars were required to raise the metallicity of the initial low-surface density disc to near solar abundance.

At a given age, stars near the Sun are widely scattered in metallicity (Edvardsson et al., 1993; Holmberg et al., 2007, Section 3.4.5). This is at first sight surprising because the ISM appears to be well mixed in azimuth, so at any given time and radius, newly-formed stars should all have the same metallicity. The resolution of this paradox lies in the interplay between a radial gradient in the metallicity of the ISM and the radial migration of stars: on account of the latter, the birthplaces of stars with age say 6 Gyr that we see near the Sun are widely distributed in R , and by virtue of the metallicity gradient in the ISM are scattered in metallicity. Unfortunately, the extent of radial migration is not well deter-

mined, and few chemical-evolution models include it. Most recently, Haywood (2008) showed that signatures of radial migration can be identified and may be responsible for the high metallicity dispersion in the age-metallicity distribution. In particular the low and high metallicity tails of the thin disc are populated by objects which orbital properties suggest an origin in the outer and inner galactic disc, respectively.

As each generation of open clusters ages, its members disperse. Long after a star cluster has dispersed, its stars remain identifiable by the similarity of their orbits (Sections 3.1.6, 3.1.7 and 3.3.6). As each generation of stars within the disc ages, its velocity dispersion increases (Section 3.3.4 and Figure 21), with the result that the vertical distribution of the stars broadens. It follows that the mean stellar age should increase as one moves away from the plane.

Given that the disc formed by a coeval population of disc stars steadily thickens and all thick-disc stars are old, it is natural to ask whether the thick disc is just the oldest, therefore thickest part of the thin disc. This proposal encounters two difficulties. First, thick-disc stars have a completely different chemistry from that of thin-disc stars. In fact, the abundance patterns in the thick disc closely resemble those in the bulge (Meléndez et al., 2008). The second objection is that the secular acceleration of stars seen at ages $\lesssim 8$ Gyr does not extend to the velocity dispersions $\gtrsim 60 \text{ km s}^{-1}$ associated with the thick disc (Figures 1 and 21). In other words, although its internal dynamics causes the thin disc to thicken with age, by itself it will not produce the thick disc. Production of the thick disc appears to require an external agency.

In a widely cited conference proceeding, Quillen & Garnett (2001) argued that acceleration of stars within the disc saturates after ~ 3 Gyr, and a further increase in velocity dispersion occurs abruptly at an age of ~ 9 Gyr (Figure 21). This picture is not supported by analyses of much larger samples of Hipparcos stars (Binney et al., 2000; Holmberg et al., 2007, Figure 21), but it meshes nicely with a popular scenario in which an ancient thin disc was puffed up when a satellite was accreted from a low-inclination orbit (Carney et al., 1989). Numerical simulations show that this process does indeed form an object that is consistent with the observed thick disc (Quinn et al., 1993). It might be possible to identify stars from the satellite as a moving group within the thick disc, or a chemically distinct sub-population. The accretion of several massive satellites on low-inclination orbits has been investigated by Abadi et al. (2003). In their simulation, the majority of the thick-disc stars are tidal debris from disrupted satellites. The thick disc is observed to contain substructures that are probably remnants of accreted satellites (Section 3.1.3) but we do not know what fraction of the thick disc can be accounted for in this way.

In the satellite-accretion scenario, the kinematic characteristics of the thick disc strongly depend on the original orbit of the satellite and the location at which the final disruption occurred. This may explain the variety of values for the scale lengths and rotation velocities measured for the thick discs of external galaxies (Yoachim & Dalcanton, 2005).

As in our discussion of the possibility that the halo consists of debris from accreted satellites, so here the population of accreted satellites must have differed from that of the observed dSph galaxies: the latter have lower $[\alpha/\text{Fe}]$ at a given value of $[\text{Fe}/\text{H}]$ than the disc (Venn et al., 2004, and Section 3.4.3). Again this difference is not unexpected given that the thick disc was formed within the first $\sim 2 \text{ Gyr}$ of the Galaxy's life and the satellites must have been taken from short-period orbits.

Kroupa (2002b) has argued that his model of disc heating (Section 3.3.4) through the expansion of star-forming regions is capable of generating the thick disc.

An alternative model for the origin of thick discs has been suggested by Bournaud et al. (2007). In such models an early fast accretion of gas leads to highly turbulent gas rich discs in which big clumps are formed and high star formation efficiencies are achieved. Once the big clumps dissolve and/or merge into the bulge the remaining gas settles into a thinner disc. Elmegreen & Elmegreen (2006) argue that in the Hubble Ultra Deep Field we can see thick discs forming in this way. Another model forming the thick disc from gas rich mergers was suggested by Brook et al. (2005). The latter authors present numerical simulations in which their thick discs have properties similar to those of observed thick discs, although with larger metallicities. In addition these models predict thick discs with smaller scale length than that of the thin disc, whereas the measured thick disc scale length is ~ 1.4 times that of the thin disc (Section 3.1.3). Perhaps a simulation with slightly different parameters would have produced a thick disc that lacked these defects.

In all these formation scenarios the thick disc is older than the entire thin disc. The observed difference in the thick and thin disc abundances in iron and α -elements are consistent with a delay in the onset of the formation of the thin disc (Chiappini et al., 1997; Reddy et al., 2006; Bernkopf & Fuhrmann, 2006; Gratton et al., 2003), which would make the thin disc $\sim 2 \text{ Gyr}$ younger than either the inner halo or the thick disc. However, the existence of such an age offset is controversial (see Section 3.4.1). Haywood (2008) argues that, if stars born outside the solar neighbourhood are excluded, the thin disc at R_\odot contains only stars with iron abundances in the range $[-0.2, 0.2]$ while thick disc stars have abundances $[\text{Fe}/\text{H}] < -0.2$. This tends to prove that the thick disc episode of formation was clearly

distinct and occurred before the thin disc starts to form.

3.5.4 History of the globular-cluster system

It is still very unclear how globular clusters formed. Models are strongly influenced by observations of the globular-cluster systems of external galaxies, which reveal the following facts (Harris, 1991):

- The luminosity function of clusters in any system can be fitted with a universal log-normal distribution.
- The number of globular clusters per unit luminosity is highest in dense environments in general, and in early-type galaxies in particular (Bridges & Hanes, 1990).
- The bimodal distribution of cluster colours first seen in the Galaxy (Figure 6) is widespread but not universal. The Galaxy's blue (halo) clusters are extremely old and metal poor, and the data for external galaxies are consistent with their blue clusters having similar ages and metallicities. The red clusters of external galaxies are analogous to the Galaxy's disc clusters in being only moderately metal-poor, but in some cases they may not be extremely old (e.g. Kotulla et al., 2008).
- In some systems young clusters are observed that are expected to evolve into globular clusters.
- The mean colours of the blue and red clusters increase with the host's luminosity.

The metal-poverty and extreme age of the halo clusters suggests that they formed at redshifts $z \gtrsim 3$, before the Galaxy as we know it had been assembled: at $z = 5$ the masses of the dominant dark-matter haloes were smaller than they are now by a factor $10^3 - 10^4$ (e.g. Binney & Tremaine, 2008, Fig. 9.8). Hence in the Λ CDM model the halo clusters should have started as the property of (gas-rich) dwarf galaxies, from which they were stripped when these galaxies were accreted by the growing Galaxy. In an update of the seminal paper of Searle & Zinn (1978), Côté et al. (2000) showed that this expectation is consistent with the clusters' metallicity distribution providing the mass function of the protogalactic fragments was steep ($dN/dM \sim M^{-2}$) as Λ CDM predicts. It is also consistent with the observations that the galaxy with the largest number of clusters per unit luminosity is the Fornax dwarf galaxy, and three clusters are likely to have been stripped from the Sgr dwarf galaxy (Bellazzini et al., 2003; Geisler et al., 2007).

Of course, at early times these dwarfs would have been gas rich, so we should not think of the halo clusters as just being stripped from dSph galaxies.

The presence of young clusters in galaxies as different in morphology and environment as NGC 1275, the central-dominant galaxy at the centre of the Perseus cluster, and the LMC, imply that globular-cluster formation is not restricted to the early Universe and low metallicities. On the other hand, the failure of the Galaxy to produce a single new globular cluster over the last ~ 9 Gyr implies that an essential trigger for cluster formation has been missing locally.

Schweizer (1986) and Ashman & Zepf (1992) suggested that that condition was strong tidal disturbance associated with a merger. This hypothesis is consistent with both the age of the thin disc and the similarity of the thick-disc's metallicity distribution function (MDF) to that of the disc globular clusters: since the thin disc would be shattered by any significant merger, we can be confident that the Galaxy inside R_0 has led a quiet life for $\gtrsim 9$ Gyr. So with this hypothesis, the last time globular clusters could form was during the merger event that probably formed the thick disc (Section 3.5.3), and the similarity of the two MDFs has a natural explanation.

The formation of the halo clusters may also have been driven by merger events, which were extremely common at early times (Binney & Tremaine, 2008, Fig. 9.13).

Physically, the idea is that globular clusters form when large-scale flows of cool, dense gas collide and form a dense knot of gas that implodes under its own gravity. Any dark matter that was associated with the gas will have separated from the gas after the collision because it did not experience hydrodynamical forces, so the final cluster is essentially dark-matter free, as observations imply. Hence in this picture globular clusters are fundamentally different from low-luminosity galaxies, which form when gas falls into the gravitational potential of a dark-matter halo.

When a globular cluster forms, star formation must be extremely efficient: if less than half the gas were turned into stars, the cluster would be disrupted when massive stars dispersed the remaining gas. As in Section 3.5.2, we see a connection between efficient star formation and violently colliding gas clouds.

It is possible that ω -Cen, which has stars that formed at several well separated epochs, is in reality the nucleus of a galaxy that has been stripped of the vast majority of its mass.

4 The Galaxy and the Local Group as templates

At this stage in the Report, we have discussed our current understanding of the structure and formation of the Galaxy and evolutionary processes at work within it. Galactic studies also serve an important role in constraining underlying theories which also have applications in the study of other galaxies. In this section, we summarise those applications before looking at possible solutions to the outstanding problems.

4.1 To constrain stellar evolution models and their uncertainties

Theoretical estimates of nucleosynthetic yields are widely used to infer the chemical evolution of galaxies, the enrichment of the intracluster medium and to predict the behaviour of abundances in First Stars. However, the stellar prescriptions are still incomplete due to important uncertainties in stellar evolution models (see below) and due to the fact that only in recent years has it become possible to compute models with detailed 3D numerical hydrodynamic simulations (e.g. Arnett et al., 2005). Among the most important uncertainties are the mass loss, the accurate description of mixing processes (most notably, convection) and the role of magnetic fields in stellar evolution. In addition, the dependence of these processes on metallicity and other properties (e.g. rotation) still needs to be better determined. In particular, mixing processes can be constrained by surface abundance measurements in stars of different masses, metallicities and environment (field vs. clusters) and by how they correlate with other properties such as rotational velocity and magnetic fields.

In what follows we discuss some of the main constraints on stellar evolutionary models for single stars, and finish with some comment on the more challenging problem of binary star evolution. Thanks to modern instrumentation on a broad range of telescopes up to and including 8m apertures, observational work in this area is no longer limited to the solar neighbourhood, having moved onto exploration of both the inner and outer regions of our Galaxy, and also other galaxies of the Local Group. Additional important constraints are beginning to emerge from interferometry and asteroseismology.

For low- and intermediate-mass stars in their late stages, dredge-up episodes and hot-bottom burning are still poorly understood. Theoretically, detailed computations of transport mechanisms are required, and their impact is in turn dependent on stellar lifetimes and mass-loss. Many of these processes can be tested against detailed surface abundance measurement in stars of different metallicities.

ties (either in the inner and outer regions of our Galaxy or in nearby metal-poor galaxies). In addition, important constraints come from the comparison of different samples of planetary nebulae (PNe) in different galaxies or components of our own Galaxy (such as the LMC and SMC, the solar vicinity or the bulge). For instance, current data from LMC and SMC PNe confirm the larger efficiency of mixing processes taking place in low and intermediate mass stars at lower metallicities (e.g. Leisy & Dennefeld, 2006). Complementary information can be obtained from the surface abundances of post-AGB stars (objects that have already ejected their envelopes but are not yet hot enough to ionise them), the initial-final mass relation, the white-dwarf mass distribution and carbon star luminosity function (Charbonnel, 2005).

The larger scale patterns measured as abundance gradients can also be used as constraints on stellar evolution. For instance, the existence or not of an [N/O] gradient in spiral galaxies can help to better define both the efficiency and metallicity dependency of hot bottom burning and dredge-up processes (Chiappini et al., 2003). While the results for the Galaxy are still controversial, in other spirals an [N/O] gradient is clearly observed.

There is evidence that additional mixing processes not included in standard models also occur: these are mixing due to gravity waves, rotational mixing and thermohaline mixing. For instance, at the beginning of the RGB phase, the first dredge up modifies the surface chemical composition and this has been tested against observations. For low-mass stars it was shown that the observed lithium depletion and the conversion of ^{12}C into ^{13}C and ^{14}N after the first dredge-up exceeded the levels predicted by standard models (Charbonnel, 2005; Gratton et al., 2000), suggesting that an extra mixing process might be at work. Statistical studies of RGB stars have shown that $\sim 96\%$ of low mass stars require this additional process, whereas less than 4% have their evolution well described by the standard models (as observed in some PNe with low-mass progenitors, Palla et al., 2002). This has recently been explained by a process called *thermohaline mixing* that may be set up in the presence of chemical gradients, but would be inhibited by fossil magnetic fields in red giant stars descending from main-sequence Ap stars (see Section 3.4.4 and Charbonnel & Zahn, 2007). It remains to be checked whether the magnetic stars are in sufficient number to account for the $\sim 7\%$ of red giants which are spared from thermohaline mixing by observing Ap stars not only in the Galaxy but also in the LMC (e.g. Paunzen et al., 2006).

Gravity waves are believed to have a strong impact on stellar rotation by redistributing angular momentum and hence determining the extent and magnitude of rotation-induced mixing. A theoretical effort is underway to assess the impact of such waves on stars of different masses and evolutionary stages. Gravity waves were shown (Talon & Charbonnel, 2003) to explain the so-called *Lithium dip* (a

strong lithium depletion in a narrow region of ~ 300 K in effective temperature, centred around $T_{\text{eff}}=6700$ K) observed in several galactic open clusters as well as in the field. The impact of gravity waves on rotation-induced mixing for stars of different mass still has to be estimated.

Rotation seems to play a fundamental role in the evolution of massive stars (Meynet & Maeder, 2005). For instance, models without rotation predict no surface enrichment before the red supergiant stage for stars less massive than $40 M_{\odot}$, clearly in contradiction with recent observations. And it has been argued that the retention of high angular momentum might be the key ingredient explaining why the ratio of blue to red supergiants drops sharply at low metallicities (Maeder & Meynet, 2001). The recent development of theoretical models including rotation has triggered large surveys of massive stars to test them (Meynet, 2007). The availability of multi-object spectrographs has been key in facilitating this. Recent observations have focused on the following properties of O, B and Be stars: the distribution of rotational velocities and the dependency on metallicity and environment (cluster or field stars); the variation of rotational velocity as a function of stellar age, the correlation between rotation rate and the existence of equatorial discs; the measurements of surface enrichments of N and He and the role of binaries. The preferred approach has been to measure projected rotational velocities in O, B and Be stars in the different metallicity environments of the Galaxy, LMC and SMC (e.g. Hunter et al., 2008, – from a survey carried out with FLAMES at VLT). Other important studies in this area, using FLAMES or other multi-object instruments such as Hydra at WIYN, include the works of Martayan et al. (2007), Wolff et al. (2007), and Huang & Gies (2006).

A result of the VLT-FLAMES survey and Martayan et al. (2007) is that the mean rotational velocity of O, B and Be stars tend to be larger in the LMC than in the Galaxy, and even larger in the SMC. In this way, the conjecture that rotational velocities increase as metallicity falls, is supported. The suspected cause of this is that mass loss may promote angular momentum loss, and radiation driving (mediated by spectral lines) will be less efficient at lower metallicity. Evidence of this reduced efficiency has been provided by comparison of the O-type wind velocities in the Galaxy and SMC (they are much lower in the latter). It has also been found that the most massive objects, which have the stronger winds, rotate more slowly than their less massive counterparts.

But there are complications. Huang & Gies (2006) present evidence that the more massive B stars spin down during their main-sequence phase, but at the same time find that the rotational velocity distribution appears to show an increase in the numbers of rapid rotators among clusters with ages of 10 Myr or higher. The authors suggest that some of these rapid rotators may have been spun up through mass transfer in close binary systems. Similarly, there are suggestions

that the rotational velocities of OB stars in clusters are greater than those of stars belonging to less dense systems such as associations or the field (e.g. Keller, 2004; Wolff et al., 2007).

Important results have also been obtained with respect to massive-star surface enrichments in N and He. Results from the VLT-FLAMES survey indicate that rotation can qualitatively account for the observed helium enrichment in O-type stars in SMC, but the observed helium increase is in many cases much stronger than predicted by stellar evolution models (Mokiem et al., 2006). Huang & Gies (2006b) also find, for a sample of Galactic OB stars, evidence for an increased helium abundance among the objects with larger rotational velocities. Hunter et al. (2008) obtained the chemical composition (C, N, O, Mg and Si) for 135 B-type stars in the LMC with projected rotational velocities up to ~ 300 km/s. They find that models with rotation can account for roughly 60% of the surface enhancements. However the authors find a significant population of highly nitrogen-enriched intrinsic slow rotators, along with some relatively unenriched fast rotators. These last results suggest that rotational mixing does not tell the full story and that binarity or fossil magnetic fields are required to explain the data.

It is clear that rotation plays a key role in stellar evolution but its impact is linked to other factors such as mass, age, metallicity, environment, binarity, magnetic fields, etc. Large spectroscopic surveys, exploiting multi-object instruments on 8m-class telescopes are evidently beginning to unpick how these factors combine. More constraints could be obtained from the exploration of more distant galaxies, that would allow a wider range of properties such as metallicity to be examined. With instruments such as the FOcal-Reducer Spectrograph (FORS) on the VLT, detailed analysis of massive stars in galaxies at 1-2 Mpc is currently possible (Evans, 2007), although at lower spectral resolutions than those now deployed in studies of the Galaxy, LMC, SMC and some of the Local Group galaxies. In such cases, the loss of information needs to be mitigated by comparing the observed spectra with synthetic spectra. Studies of stars in the Galaxy and nearby galaxies are then required to test and calibrate the spectral synthesis. By this means, it is possible to study the spatial distribution of several elements in external galaxies, probing their current ISM composition for those elements not affected by the evolution of the star, while constraining the stellar models using modified elements such as C, N and O. Preliminary findings qualitatively confirm predictions of stellar evolution calculations that the efficiency of mixing increases with decreasing metallicity (Urbaneja et al., 2005).

The time will come when an ELT will allow the observation of individual massive stars within a much wider range of environments. However, even with a 40 m-class E-ELT we will be able to measure Ca II triplet metallicities only out to Cen A, not reaching the Virgo galaxies.

For the end-states of massive stars there are also important uncertainties related to the explosion mechanism and hence on the location of mass cut, energy of explosion and the amount of fallback as a function of stellar mass and metallicity. The best constraint to such models still comes from SN 1987A. Other important constraints come from the multi-band observations of the Cassiopeia A remnant (Young et al., 2006). Thanks to Chandra, XMM-Newton and Spitzer the spatial distribution of different chemical elements can be traced in SN remnants, offering crucial constraints on the explosion models (their energies, asymmetries, etc.) and chemical yields.

Another powerful way of constraining stellar models is via the abundance measurements of very-metal poor stars, supposedly born from an ISM enriched only by massive stars. The First Stars ESO Large Programme has already had a strong impact on the field of stellar evolution. Fast rotating massive stars seem to be needed in order to explain the observed patterns of $[C/O]$, $[N/O]$ and $[^{12}C/^{13}C]$ with $[Fe/H]$ in the Galactic halo (Chiappini et al., 2006, 2008). The ultimate fate of these rapidly rotating Pop III stars could be related to the progenitors of gamma ray bursts (GRBs) (Yoon & Langer, 2005). In addition, the observed GRB-SN connection (Woosley & Bloom, 2006) together with the abundances of Co and Zn in extremely metal poor stars can be used to constrain the different models for the GRB progenitors (Nomoto et al., 2008). How rotation and binarity may be related to the diversity of SN Ibc and long GRBs is still a matter of debate: Yoon et al. (2008) argue that, with respect to their rotational properties, SN Ibc progenitors from binary systems may not significantly differ from single star progenitors.

Current surveys are in progress and will certainly increase the samples of known very metal poor stars by orders of magnitude (e.g. LAMOST, SEGUE). Spectroscopic follow-up of a large number of metal poor stars offers probably the only way at present to constrain stellar models at such low metallicities. Iron peak elements offer important constraints on the still uncertain explosive nucleosynthesis, whereas heavy metals help to constrain the properties of r- and s- processes in such stars. In this respect the detailed abundances obtained for dwarf spheroidals and dwarf irregulars in the Local Group represent important complementary information, crucial to better constraining the production sites and the metallicity dependence of the stellar yields (e.g. Tolstoy et al., 2006; Lanfranchi et al., 2006).

Some of the uncertainties in stellar models discussed in this Section are responsible for the still uncertain mass boundary between AGB stars and core collapse SN and its metallicity dependence. Theory predicts the existence of super-AGB stars (that can ignite carbon in partially degenerate conditions) producing either a ONe core WD or an electron capture core collapse supernova (Nomoto, 1984). The minimum mass for C ignition as well as the transition mass for core collapse SN are very uncertain and metallicity dependent (Siess, 2007). One of the main

uncertainties in this case is mass loss. Mass loss will determine if the star will have a longer life or die violently. The mechanisms powering mass loss from AGB stars are still not clear: radiation pressure acting on dust and levitation caused by pulsation might both be at work (see van Loon, 2008, for a recent review).

The super-AGB stars undergo thermal pulses and are believed to end this phase after an episode of very strong mass loss. The core may grow beyond the Chandrasekhar limit depending on the mass-loss and convective mixing processes. The competition between these processes will determine the fate of the star as either a ONe WD or an electron capture supernova. According to Poelarends et al. (2008) electron capture SN could account for $\sim 4\%$ of the local SN rate at solar metallicity. This fraction could rise if mass loss at reduced metallicities was also reduced, thus allowing more stars to attain a core mass beyond the Chandrasekhar limit. The nucleosynthesis predicted for electron capture SN and super-AGBs is still very uncertain and essentially no prediction of the stellar yields are available. As a consequence their impact on the chemical evolution of galaxies is still unknown.

Current theoretical estimates suggest the formation of CO WDs for stars below $\sim 7 M_{\odot}$, ONe WD between $7\text{--}9 M_{\odot}$, and core-collapse SN for larger masses, at solar metallicities. One way to pin down these mass ranges observationally is by detecting more SN progenitor objects. Smartt et al. (2004), Maund & Smartt (2005), Maund et al. (2005) and Hendry et al. (2006) have achieved 4 detections of SN II-P progenitors – all likely to be red supergiants towards the bottom end of the expected mass range ($8 - 15 M_{\odot}$). This concerted campaign, which has chalked up at least as many non-detections, has exploited HST-archive deep multicolour images of galaxies in the nearby Universe. These authors (Smartt et al. 2008 in preparation) estimate the lower mass limit for core-collapse SN to be $7.5 \pm 1 M_{\odot}$, leaving little room for super-AGB stars. But it is too early to rule them out. Interestingly, Werner et al. (2004, 2007) reported the discovery of H1504+65, the hottest known WD to date. Analyses of HST, FUSE and Chandra spectra were performed to obtain the surface abundances needed to determine the star's evolutionary status. These data indicate that this object is potentially the first single ONe WD to be found, thus permitting the existence of WDs as post-super-AGB remnants.

Future facilities such as VISTA could be used to map both the LMC and SMC at near-infrared wavelengths, where the bulk of the flux of AGB and super-AGB stars can be accessed. Super-AGB candidates found this way would then need to be followed up by spectroscopic observations.

A different constraint on the mass dividing the WD progenitors from SN progenitors can be obtained from WDs of known age - generally those in intermediate-

age star clusters, where metallicity is also known (Kalirai et al., 2005; Williams et al., 2004, e.g.). The essentials of the method is to: determine the WD mass and cooling age; then subtract this cooling age from the total (cluster) age, to infer the lifetime of the progenitor; and finally infer the progenitor mass using stellar evolutionary models. Currently the observed lower limit on the maximum mass for a WD progenitor is $\sim 6.5M_{\odot}$ (Catalán et al., 2008). This method also offers the possibility of establishing the initial-final mass relation for WDs and how it may depend on metallicity and rotation. So far no strong dependency has been found (Williams, 2007). This result is surprising as in principle such a relation should depend on the mass loss history which in turn is expected to be metallicity-dependent. A significant uncertainty in all this is cluster age: with Gaia, cluster ages will become more precise, thereby delivering tighter limits on the fate of stars in the 7-12 M_{\odot} range.

In the preceding discussion, binarity has been referred to a number of times as the possible explanation for observed surface abundances and other properties that evolutionary models for single stars fail to match. It was also noted in Section 3.2.2 that it is likely that nearly all stars are born into multiple systems. Nevertheless it is a fact that single-star evolutionary models are often sufficient, given that of the two-thirds of the stars still bound in binaries after their youth is over, around a half of them are in systems that are too wide to ever bring the component stars into interaction. This leaves around a third of all stars in binaries that are close enough for interaction to occur at some stage: these are far less well-described and we cannot yet be sure we have not fallen prey to some serious misconceptions.

Among the long-recognised signs that binary evolution models remain very much a work-in-progress are (i) the unsettled origin of blue stragglers (those blue stars seen in clusters in near main sequence positions above the turn-off in colour-magnitude diagrams), (ii) the zoo of options in play as possible compact binary progenitors of SN Ia, (iii) the absence of accepted quantitative modelling for the common envelope phase that precedes the evolution to compact configurations. Along with the above it is worth noting the growing concern over the extent to which the planetary nebula evolutionary phase of intermediate mass stars may be restricted to binary systems (De Marco et al., 2008). This could turn out to have implications for the wider interpretation of the abundances derived from PNe.

The blue straggler problem is an old one. As well as exhibiting strange photometric properties, these objects also present unusual and quite varied surface abundance patterns. By the time the topic was reviewed by Baily (1995), there were two main schools of thought on their origin: either direct collisions between two low-mass stars lead to mergers, or there is an interaction between components of a binary that ends as a coalescence. Even now the situation remains confusing, after many studies of many globular and open clusters: for example, Leigh

et al. (2007) set out expressly to examine what they thought were likely to be collision-produced blue stragglers in globular cluster cores and failed to find the expected trends, leading them to the tentative conclusion that formation within binary systems may be the dominant process.

For SN Ia, the major source of iron in the universe, important uncertainties remain on what the progenitor binaries are. These are classified into two main groupings: double-degenerate progenitors (binary white dwarfs), and single-degenerate progenitors wherein accretion onto a white dwarf pushes it over the Chandrasekhar limit. In particular, for the latter group, major uncertainties still exist with respect to the evolutionary pathways, the net mass transfer achieved over time, flame speed (deflagration vs. delayed detonation models), center and off center explosion (1D vs. 3D models) – all hindering a clear picture of what it is that explodes in a SN Ia event. Direct constraints on such models can come from the inferred distribution of chemical elements in SN multi-wavelength spectra. For example, it is possible to deduce the abundance stratification in the ejecta of SN Ia by fitting series of spectra taken at close time intervals (Stehle et al., 2005). So far this technique has been applied to a limited number of objects. In the mean time, binary-star population synthesis models continue to be developed in order to disentangle the possible pathways that might lead to SN Ia (e.g. Han & Podsiadlowski, 2004), and it has been noticed that delay times between star formation and the appearance of SN Ia might also provide clues to the nature of the progenitors (Strolger et al., 2004; Greggio et al., 2008)

Some of the solution to the SN Ia progenitor problem lies further back in binary evolution, in the common envelope phase that occurs when either the primary or, indeed, the secondary expands to become a red giant and engulfs its companion. This is a seriously difficult astrophysical hydrodynamics problem, that is generally sidestepped by adopting a crude parametrisation, that allows the binding energy of the expanded envelope to be offset against the binary orbital energy released as the engulfed companion spirals in (the α_{ce} parameter, see e.g. Webbink, 2007; Politano & Weiler, 2007). Measurements of space densities to be compared with model predictions remain subject to significant uncertainties (see e.g. Pretorius et al., 2007). Perhaps the better prospect for getting to grips with the outcome of the common envelope phase is to carefully survey the properties of the systems recently emerged from it (either sdB systems or shorter-period red dwarf/white dwarf binaries). Programmes of this nature are underway: they frequently involve follow-up of candidate systems requiring significant time allocations on 4m-class optical telescopes for time series spectroscopy (e.g. Dillon et al., 2008).

4.2 To constrain population synthesis models

Population synthesis models aim at reproducing observations of galaxies in a given scenario of formation and evolution. Following the first ideas of Tinsley (1972), they assume a star-formation history, a total age of the populations, and a chemodynamical scenario of evolution. In external galaxies, they are mostly used to produce spectra over large ranges of wavelength which are then compared with observations. The fit of observed spectra to the prediction of a population synthesis model helps one determine the weight of each population of different ages at different wavelengths and hence to infer the star formation history. In the case of external galaxies, stars are not resolved, and most of the information is in the spectra-energy distribution and in the shape of the lines (which depends on the kinematics). The deconvolution of the line shapes is not unique, and the result of spectral-distribution fitting is also generally not unique. It has been extensively demonstrated that in synthesis models, ‘a factor of three change in age produces the same change in most colours and indices as a factor of two in z ’ (Worthey, 1992), known as the *age-metallicity degeneracy* (Renzini & Buzzoni, 1986; Buzzoni, 1995).

In the case of our Galaxy, observations give a lot of complementary information which allow one to understand the history of star formation. Population synthesis models are major tools, using information from different kind of surveys (photometric, astrometric, and spectroscopic) and from various ranges of wavelength, to confront different scenarios. These models rely on theories/scenarios of Galaxy formation and evolution. Contrary to the case in external galaxies, in our own many independent measurements can be used to check a scenario of chemical evolution. It can be done using the distribution of metallicities, statistics of populations in well defined stage of evolution (giants in the red clump, planetary nebulae, variables, etc.), kinematics versus age versus metallicity distributions for different populations, abundance ratios as a function of galactic position and kinematical properties, abundances and gradients in the gas, in clusters of different ages, etc. In external galaxies, one mainly has a coarse-grained view of the abundances of most abundant species, as a function of projected position in the galaxy.

Population synthesis models are made of building blocks: an initial mass function, a star formation rate, a set of evolutionary tracks, a set of atmosphere models, a chemical evolution model, and dynamical constraints. Studies of the Galaxy can help to constrain a few of the building blocks of these synthesis models: the chemical evolution models can be tested in many different locations, at different metallicities, at different ages (in the bulge, in the external part of the disc, in the thick disc and the halo). The initial mass function and processes of

star formation can be studied in massive clusters, in low mass clusters, in various star forming regions of different star formation rates. Studies of clusters of different metallicities can constrain stellar evolution theory and stellar atmospheres, as well as the binary rate and evolution, and dynamical evolution. When these theories are well constrained they can be used for population synthesis in external galaxies. Even if it may not be appropriate to use hypotheses for our Galaxy in applications to external galaxies, for example in highly different environments, comparisons with real galaxies of different kinds help one understand the main physical processes at work in galaxy formation and evolution, which features are common to all galaxies and which vary as a function of morphological type and/or environment.

A number of questions are addressed using these population synthesis models. Not all have obtained clear answers: Is the initial mass function universal? Can one understand the bulge formation in disc galaxies as the formation of elliptical galaxies? Is the Hubble sequence an evolutionary sequence? etc. However, population synthesis models offer an efficient way to identify how to understand these questions. They help find the most efficient wavelength at which to distinguish between two scenarios, which type of observations are useful, which sample will best constrain the hypothesis.

These models also have known problems, as identified by Cervino & Luridiana (2005), such as the consequence of the incompleteness of the input ingredients, the problems due to interpolation between tracks and to interpolation between different set of tracks with different physics. Moreover they completely rely on existing evolutionary tracks. If these are not accurate enough, the results of the synthesis are not reliable. Uncertainties in the stellar physics, such as the mixing length in stellar interiors, mass loss over the stellar lifetime, rotation, are major difficulties which should be taken into account in any interpretation using population synthesis tools. It is in our Galaxy that these questions have to be solved first, before we can apply our new assessments to external galaxies.

At present a few population synthesis models exist for the Galaxy. All have their limitations. None take into account a full dynamically self-consistent model, even if local attempts have been made (Bienayme et al., 1987; Robin et al., 2003). Some have very detailed evolutionary tracks but lack chemo-dynamical consistency (Girardi et al., 2005). Some include a chemo-dynamical model but do not compute stellar populations at different wavelengths (Naab & Ostriker, 2006). None takes into account gamma ray emission, the global magnetic field of the Galaxy, several states of the interstellar medium. Further studies need to be conducted to be able to combine these complementary approaches and to construct a fully consistent model with all available data from gamma to radio wavelengths and all identified physical processes. Building a self-consistent population synthesis model

for our Galaxy will continue to be a challenging project, with the eventual aim of constraining galaxy formation scenarios and helping interpret future, large scale multi-wavelength surveys.

4.3 To constrain galaxy formation models

As the Galaxy contains stars spanning almost the age of the Universe, it is fruitful to compare its oldest populations to the high redshift universe. The halo provides local samples of material that were assembled earlier than the epochs corresponding to the largest known lookback times in the high-redshift universe.

The quest to find extremely metal-poor stars in the Galaxy is at least partially motivated by a desire to detect the Population III objects responsible for re-ionisation of the Universe at redshifts between (perhaps) 20 and 6. Whether Population III stars will ever be detected is unclear. Nevertheless, it is quite likely that the imprint they left on the next stellar generation, the lowest metallicity Population II stars, will be identified. Indeed, that imprint may already have been detected in the increasingly peculiar abundances which are found in stars with $[\text{Fe}/\text{H}] < -5$ (2 stars to date; Christlieb et al., 2002; Frebel et al., 2005). One goal of the detection and study of local Population III material, either directly or indirectly via Population II, is a better understanding of the objects responsible for reionisation, which set the conditions for early galaxy formation.

Galactic stellar populations are also interesting templates for two classes of high-redshift objects: the low-column-density intergalactic medium which is detected in the Lyman- α forest, the high-column-density gas ($N(\text{HI}) > 2 \times 10^{20} \text{ cm}^{-2}$) which forms damped Lyman- α (DLA) absorption lines.

DLAs are commonly assumed to be galaxies at an early stage of their formation, before extensive star formation has occurred. Their metallicities are generally low, mostly in the range $-2.0 < [\text{Zn}/\text{Fe}] < -0.5$. The lack of strong evolution in the metallicity-redshift relation for DLAs is consistent with these objects having low star formation rates (Pettini et al., 1999). It also emphasises that these objects provide a snapshot of the status of galaxy progenitors at a range of epochs, but not an evolutionary sequence. Nevertheless, the range of element ratios measured in them indicates that they have already experienced a range of star-formation histories and can usefully be compared to abundances seen in Galactic populations (Prochaska et al., 2000).

The existence of high-redshift objects with both higher and lower column densities than the DLAs opens the possibility of making comparisons with a wider range of Galactic populations. As for the DLAs, though, there appears to be no

evolution of metallicity with redshift for the Lyman-alpha forest based on C IV measurements (Pettini et al., 2003), which may point towards pre-enrichment of the intergalactic medium at redshifts $z > 5$. Such pre-enrichment, if it exists universally, might also be expected in the abundances of Population II stars in the Galaxy, except perhaps that Population II stars may be even older than $z \sim 5$ objects. Clearly there are complementary constraints to be obtained for the early epochs of galaxy formation from observations of both high-redshift objects and very metal-poor Galactic stars.

4.4 To constrain dynamical models and theories of the nature of dark matter and gravity

The Galaxy is the system where dynamical models and gravitational theories can be tested to the greatest extent. This is because it is the only galaxy for which full phase-space information for individual stars is (and in fact, will likely ever be) available. Such information allows us to derive directly the gravitational force field, and hence to test Newtonian dynamics, alternative theories of gravity such as modified Newtonian dynamics (MOND), or the predictions of cold dark matter (CDM) cosmogony.

In comparison, the internal dynamics of external galaxies can only be probed either via their rotation curve (spiral galaxies), with integral field or slit spectroscopy (generally used for elliptical galaxies, because of their low gas content), or with a small number tracers (i.e. less than 10^{-9} of the total number of objects in a typical galaxy) such as planetary nebulae or globular clusters. In the first case, one is only sensitive to the mass in the meridional plane of the system, and is unable to decompose in a unique way the contribution of the various galactic components. With integral field spectroscopy, the luminosity-weighted kinematics along the line-of-sight are measured, and hence one is also limited by the degeneracies imposed, for example, by the lack of knowledge of the actual three-dimensional shape of the system, or its orbital structure (for example, the degree to which orbits are circular or elliptical).

The Galaxy and its nearest neighbours are therefore, dynamical templates *par excellence*. In particular, in the coming years the following issues could be resolved via detailed studies of this system:

- Shape of dark matter halos: Cold dark-matter theories predict that these should be triaxial, and on very rare occasions, spherical. The determination of the shape of the gravitational field at large radii would then perhaps allow us to determine the ‘temperature’ of the dark-matter (cold, warm,

self-interacting), since a correlation exists between the type of dark-matter and the way this is distributed. Furthermore, the outskirts of a galaxy are always in the low acceleration regime, i.e. where the deviations from Newtonian dynamics are expected to be largest, as in MOND.

Currently, there is a debate on the actual shape of the Galaxy halo. Depending on the data of the Sgr dwarf streams, as well as on the dynamical tests employed, different shapes are favoured. The solution to this problem will come when more data (in particular proper motions for Sgr streams stars) becomes available, but also if other similarly extended tidal streams are discovered in the outer halo. Furthermore the models are still very rudimentary and do not incorporate our latest understanding of how dark halos react to the condensation of baryons in the centres of galaxies. Alternative probes of the shape of the halo are the high velocity stars, presumably ejected from the center of the Galaxy via 3-body interactions with the supermassive black hole (Gnedin et al., 2005).

- Cusps/Cores: Current dynamical models of the mass distribution inside the Solar radius leave very little room for dark-matter, and do not favour the characteristic NFW profile predicted by numerical simulations of structure formation. The Galaxy is not unique in this sense since many other galaxies are apparently fit better with other mass distributions. A better understanding of how baryonic physics has affected the distribution of matter in the central regions may help the cold dark matter scenario to survive this conundrum. However, it is also possible that the dark matter is not cold.

The dSph galaxies around the Galaxy offer a different testbed, because they appear to be dark matter dominated all the way to the very center (their characteristic mass-to-light ratio $M/L \sim 100 M_{\odot}/L_{\odot}$). With current data, and simple dynamical models, it is not possible to rule out cuspy dark matter distributions because of the mass-anisotropy degeneracy. However, when proper motions are available for individual stars, the full phase-space structure of these objects will be known, and hence the underlying force field (and mass distribution) can be recovered.

- Dark-matter detection experiments: In the next years several experiments may have reached the sensitivity to be able to directly detect dark matter particles on Earth. However, because of the very low rate of events and the very large parameter space (there is a zoo of candidates), it is possible that the signal may only be retrieved using prior knowledge (an educated guess) of the phase-space distribution of dark matter near the Sun. Another possibility is indirect detection of dark-matter through the gamma-rays produced during their self-annihilation. It is currently unclear which sources will be brightest in the sky, since this is very strongly dependent on the density distribution of

dark-matter in the very center of the Galaxy, and in satellite galaxies (Stoehr et al., 2003; Strigari et al., 2007).

- **Missing satellite problem:** One of the major crises of cold-dark-matter is that it predicts orders of magnitude more bound substructures than satellites observed around galaxies such as ours. This discrepancy can be solved by invoking new physics (the nature of dark-matter) or by realising that our understanding of the physics at the low end of the galaxy mass scale is far from complete. The smallest satellites are the most prone to processes such as feedback from supernovae and massive stars, photoionisation, etc. which can strongly perturb their baryonic content. Determination of the masses of the known satellites would allow one to check whether the predictions of CDM are correct at least at the high-mass end. Ongoing and future wide-field deep surveys will quantify how good or poor our knowledge of the satellite distribution really is.
- **Dark matter or modified gravity:** Once a precise distribution of dark matter density can be determined (within Newtonian gravity) any specific theory of modified gravity (such as that of Bekenstein & Milgrom, 1984) could be rigorously tested by asking whether, given the known baryon distribution, it predicts this equivalent dark matter distribution. Moreover, in the limited number of cases in which the predictions of dark matter have been computed by systems that are not in a steady state (e.g. Tiret & Combes, 2007; Ciotti et al., 2006), these have proved to differ significantly from the equivalent Newtonian predictions. Extension of this work to spiral structure in the outer disc of the Galaxy and M31 are likely to constrain theories of modified gravity very strongly.
- **Are galaxies in dynamical equilibrium?** In the hierarchical paradigm, galaxies merge and accrete smaller objects, all of which should possess significant amounts of substructure in their phase-space. Yet, we assume they can be modelled as systems in equilibrium, and that they have reached a coarse-grained state, in which substructures of this kind can be considered as simple perturbations. Furthermore, we model their orbital structure as if chaotic dynamics were unimportant during most of their lifetime. The ultimate test of these assumptions will come with the knowledge of the phase-space structure of our Galaxy that will be given by Gaia.

4.5 To interpret observations of galaxies beyond the Local Group

The Galaxy is the only large galaxy one can observe in detail, star by star, down to the faintest luminosities. Like the Galaxy, a large fraction of the galaxies in the Universe are disk, and of similar luminosity. This means that we may expect its properties to reflect most of the physics driving the formation and evolution of galaxies in general.

Age/metallicity/kinematics relations can be measured for individual stars in our Galaxy, giving access to the history of star formation in relation to its dynamical evolution. In external galaxies the evolution is deduced from mean kinematic and abundance characteristics, gradients and dispersions. In the best cases, recovering several populations with different velocity distributions from integral field spectroscopy leads to a significant degree of ambiguity due to the non-uniqueness of the solutions. For example, it is important to understand how age-metallicity degeneracies that plague integrated stellar population modelling and observations can be broken, and for this, studies of resolved stellar populations provide unique insights.

This is particularly relevant in the context of the next generation of spaceborne and ground-based telescopes, whose focus will lie in the near infrared. Both the James Webb Space Telescope (JWST) and E-ELT will observe in these wavelengths which, while they may be optimal to study the high-redshift universe, are less favourable for the resolved-stellar-populations approach to galaxy evolution. The stellar population diagnostics that are currently used to derive star formation and chemical evolution histories for nearby systems are mostly based on optical far blue and UV bands. Therefore, significant effort needs to be invested to develop a new set of tools that will enable us to extract this information for the stellar populations that will be resolved even at the distance of the nearest cluster of galaxies.

JWST will be able to measure spectroscopically $H\alpha$ that is produced by a galaxy with a star formation rate of $3 M_{\odot}/\text{yr}$ at redshift of 5 (only slightly larger than that estimated for the Galaxy at the present day), and will be able to image galaxies as faint as the Small Magellanic Cloud at this same redshift. Such studies will provide new views of the evolution of Milky Way-like galaxies. The interpretation of such challenging observations will benefit significantly from our detailed understanding of the Local Group systems, in particular because we will only have limited access to the signatures of the various physical processes taking place at those early epochs.

Modern cosmological models predict that mergers are important in the evo-

lution of galaxies. In the case of the Galaxy, it is possible to find relics of the merging events that have taken place during the early formation of the halo. It is even possible to disentangle recent merging from early ones. This allows us, for example, to constrain the mass distribution in our Galaxy, and eventually its evolution. A similar approach will be possible for external galaxies with a 40+meter ELT, although in this case one may need to rely on imaging and rough radial velocity information. The reduction from full phase-space information (6D) to 3D (position in the sky and radial velocity) will limit our ability to map the mass distribution in these systems, but this was to some extent the situation in the Galaxy until recently. Gaia will be able to get the 6D phase space for at least bright stars ($V < 16$), thus for a very large number of objects, to distances up to the Galactic centre. SIM would even go deeper but for a smaller area of the sky, which will be very useful as a complementary project to Gaia. As shown by Helmi et al. (2006) 6D phase space data allow to discriminate relics of different substructures forming the halo and the thick disc. Hence our understanding of the detailed properties of our Galaxy, and how to break degeneracies inherent to the models, will be extremely valuable.

The fact that mergers appear to be so common implies that it is likely that all galaxies have stellar halos as a result of this process. Finding these halos and characterising them can be very challenging, since they are expected to be faint, and in the case of our Galaxy, there is now evidence of a significant amount of graininess, particularly in the outskirts. This implies that only wide field surveys of external galaxies can provide true insights into their global properties.

Similarly one may expect all galaxies to have thick discs, if these are the result of mergers. With full phase-space information it will be possible to establish the reality of this model and the importance of dissipative processes in the case of the Galaxy. Now that there is evidence that thick discs may be ubiquitous, it will be important to establish how these scenarios can be tested via diagnostics obtained by applying ‘integrated light’ techniques to our thick disc. Simulations of thick disc formation will be confronted by 6D data from Gaia and SIM, giving constraints on these scenarios, on the epoch of thick disc formation, on their frequencies, resulting degree of homogeneity and general characteristics.

In external galaxies, bulges are seen in projection, and the observables are averages of the various populations along the line of sight. Interpreting these observations with a unique scenario is difficult, because kinematic distributions in the central regions of galaxies come from a sum of distinct populations all being in the same physical location but having different origins. Even though the problem of disentangling different populations is still present for the bulge of the Galaxy, each star can be assigned a probability based on its kinematical and chemical properties. A statistical analysis is then possible to understand the origin of the

bulge. When a realistic scenario for the origin of the Galaxy bulge has been developed, it will help in interpreting the formation of distant bulges and elliptical galaxies.

The prospect of having a 40 metre-class ELT equipped with a high-resolution spectrograph opens the possibility of measuring abundance ratios in some of the brightest stars beyond the Local Group. Just as studies of resolved stars in Local Group galaxies dispelled the preconception that their compositions would be similar to those of the Galactic halo (see Section 3.4.6), so we may expect direct measurements of the chemical compositions of stars in galaxies beyond the Local Group to produce a different and more complete understanding of the characteristics of the stellar populations produced in different galactic environments. This will move us further from a Galaxy-centric view of galaxy formation and evolution to one informed by detailed analyses of a wider range of objects, more representative of the wider Universe.

5 Top questions, and proposed solutions

In subsections ‘Facilities’, those appearing in *italic* are non-European, or with no major European contribution.

5.1 Global questions and proposed solutions

5.1.1 Which stars form and have been formed where?

The past and present pattern of star formation in the Galaxy is a critical input for understanding its present shape and historical background. With regard to current star formation, the true distribution of star formation towards the inner edge of the thin disc has still to be worked out (Section 3.2.5), and questions remain concerning the number and location of the spiral arms (Section 3.2.3). We also know rather little of the outer limits of the Galactic disc, and have yet to clearly characterise the populations found there (Section 3.2.3). Regarding the centre of the Galaxy, there is already intense interest in comprehending the ongoing star formation there, which seems to be an example of a dense environment producing a top-heavy IMF (Sections 3.2.5 and 3.2.2). In addition, the Galaxy remains the key location for understanding the process of star formation itself and how that shapes the IMF (Sections 3.2.1 and 3.2.2): only in the Galaxy can the IMF be examined all the way down to the lowest stellar masses.

Past star formation is bound up, inevitably, with how the Galaxy was assembled. To diagnose this, abundance patterns in all the major components of the Galaxy need to be measured and interpreted: this applies particularly to older field populations, beyond the solar neighbourhood, in the halo, the bulge and in the thin and thick discs.

Tools and tracers:

- Infrared studies of the inner disc, bulge, and centre of the Galaxy to pick out young populations
- Improved and more comprehensive, high spatial resolution, 3D extinction mapping
- Spatially well-resolved observations of gas emission-line surface brightness and kinematics across the Galaxy for fine-scale (\sim arcsec) star-formation and structure studies

- The collection of stellar distances and motions (to be linked with studies of the gas phase)
- Appropriate advanced dynamical models utilising the new observations
- Abundance studies in a wide variety of Galactic environments

Facilities

- VISTA, VST, *SkyMapper* and *PanSTARRS* optical-IR photometric surveys to build up comprehensive catalogues of calibrated magnitudes and colours (to Vega magnitudes of >20)
- Gaia and *JASMINE* for distances. Note: *JASMINE* in the z band, reaching to 14th magnitude (versus Gaia's 20th magnitude in the visible) will provide astrometry of the Galactic centre and bulge that cannot be achieved with Gaia
- Sensitive high spatial-resolution radio/sub-mm facilities (e-MERLIN, APEX, ALMA, SKA) for line mapping
- Highly multiplexed multi-object spectrographs with medium to high spectral resolution ($R > 20000$) for abundance studies at both optical and NIR wavelengths

5.1.2 What is the mass distribution throughout the Galaxy?

The mass distribution interior to R_0 can in principle be determined by combining radio-frequency measurements of gas emission lines with Gaia astrometry. Thus the necessary data are either in hand or in train. The challenge will be to extract the implied mass distribution by fitting the data to sophisticated dynamical models. Models of the required sophistication do not exist and their construction will require a significant effort.

Determining the mass distribution beyond R_0 is a harder problem. Gaia will provide distances to regions in the outlying disc, thus greatly improving our knowledge of the rotation curve at $R > R_0$. Gaia will also provide proper motions for halo objects, which are essential if masses are to be inferred from halo dynamics. SIM would provide proper motions for more distant halo objects. We will also need (photometric) distances to halo objects, so deep photometry of distant globular clusters and dwarf spheroidals will be required. Given what we now know about the disorderly state of the outlying regions of M31 and the Galaxy, the major

uncertainty in the density distribution at $\gtrsim 20$ kpc is likely to be associated with the assumption of virial equilibrium.

Tools and tracers:

- Existing surveys of gas line emission
- Stellar distances and motions, especially for objects in the plane and the distant halo
- Dynamical models to fit observational data

Facilities:

- Gaia: star census and astrometry down to magnitude $V = 20$; radial velocities for the brighter part of the programme
- *SIM*: distances and proper motions for distant halo objects
- Multi-band optical photometry to $V > 24$ for photometric distances to distant halo objects
- Wide-field multiplex spectrograph with spectral resolution $\gtrsim 6000$ and $\gtrsim 1000$ channels to get radial velocities for large samples of stars fainter than the Gaia RVS limit

5.1.3 What is the spiral structure of our Galaxy?

Once a three-dimensional extinction map of the plane has been developed, and secure distances are available for all star-formation regions, we will be able to trace spiral structure in young stars and gas, and to a lesser extent in the mass-bearing older stars. The main difficulty tracing spiral structure in stars will be obscuration, which will make it necessary to use rare luminous tracers much beyond the solar neighbourhood and will introduce uncertainties into the inferred stellar density. The stellar velocity field can be traced from proper motions and radial velocities. A few of these data will come from maser sources, and the majority will come from Gaia. Radio-frequency spectra and the extinction map will lead to a less complete gas velocity field. The challenge then will be to use dynamical theory to match the velocity fields to the density fields. Shocks in the gas flow should be related to the locations of star-forming regions.

Tools and tracers:

- Distances, proper motions and radial velocities
- Gas velocity field
- Extinction map
- Dynamical theory to match the velocity fields to the density fields

Facilities

- Gaia
- VISTA (VHS), VST
- VLBI, radio observations

5.1.4 How is mass cycled through the Galaxy?

What is the current rate at which the Galaxy is accreting gas? How has the accretion rate varied over time? What is the chemical composition of this gas? What is the neutral-gas fraction of the observed high-velocity clouds, and what role do these clouds play in the accretion of gas onto the Galaxy?

How does the radial distribution of freshly accreted gas compare with the distribution of gas consumption by star formation? In the likely event that the two distributions are distinct, there must be a flow of gas within the disc that brings gas to its points of consumption. What drives this flow, how is it regulated, and what impact does it have on the metallicity distribution in the disc?

In external galaxies there is evidence that star formation expels cold gas from the plane (Section 3.2.6). There are many indications that star formation similarly drives gas from the Galaxy's disc. Gas that is pushed up at one radius has a natural tendency to return to the disc at a larger radius. Hence a priori the phenomenon of extra-planar HI implies a significant flow of gas outwards. How does this flow interact with the expected inward flow of freshly accreted gas and modify its consequences? Extra-planar HI is thought to be pushed up by hotter, highly ionised gas. This gas is produced by supernovae and is likely to be very rich in freshly manufactured heavy elements. Are these heavy elements carried out of the Galaxy in a wind? Or are most of them absorbed within the WHIM (Section 3.2.6) and later returned to the Galaxy alongside freshly accreted gas?

The region of most intense star formation is the central molecular zone that occupies the inner ~ 200 pc of the plane, deep inside the bulge. There is evidence that star formation in this region is blowing gas at least 10 kiloparsecs away from the plane (Bland-Hawthorn & Cohen, 2003). Does this flow extend to infinity, or does it stagnate at some maximum height and then fall back towards the plane as in the fountain model? Does it remove metals from the Galaxy? Does it transfer metals from the bulge to the disc?

The answers to these important questions require major upgrades to current dynamical models. A point of departure should be precision models of the thin disc that include gas, stars and dynamically driven star formation. Such models would contain the appropriate gravitational torques from the bar and spiral structure, and the shocks that together drive gas inwards. They would also determine the degree of clustering of star formation, which is crucial for the development of regions of expanding hot gas that push filaments of H I upwards to form an H I halo. The predictions of such models could be matched to the Leiden-Argentine-Bonn (LAB) all-sky survey of 21 cm emission. They would also yield predictions for soft X-ray emission and UV absorption at the interfaces between extra-planar H I and expanding hot gas. The body of data on UV absorption that FUSE provided could usefully be extended to a larger number of background sources, especially halo stars with known distances. Gaia and SIM would be invaluable in determining such distances.

A valuable way of constraining distances to H I clouds is by searching for associated H α emission, so more sensitive high-latitude H α surveys would be useful.

Dynamical models that included gas flows and star formation could also lead to new interpretations of the observed phase-space and metallicity distributions of stars in terms of the Galaxy's star-formation history.

Tools and tracers:

- Distances of blue halo stars
- Leiden-Argentine-Bonn (LAB) all-sky survey of H I 21 cm emission
- All-sky survey of UV absorption
- High-latitude H α surveys
- Dynamical models including gas, stars and star formation

Facilities

- Soft X-ray and UV space observatory
- Gaia and *STIM* for distances of background halo stars
- Optical spectra with $R \gtrsim 6000$ of halo stars with $V \lesssim 18$
- H α high resolution imaging
- SKA for comparison with external galaxies

5.1.5 How universal is the initial mass function?

The problem of universality of the IMF is strongly driven by the accuracy with which it can be measured (Section 3.2.1). In clusters, the limitation comes from the small number of available stars at a given mass, specially for massive stars, and the unsettled problem of mass segregation consequent on dynamical evolution (Section 3.2.4). In the field, the mixing of ages and metallicity creates different problems. In external galaxies, sampling of the IMF is limited to higher mass stars only – and it is this work that has brought up the issue of the top-heavy IMF in dense environments (Section 3.2.1). In our Galaxy, we have the opportunity to measure the IMF in a broad range of environments beyond the solar neighbourhood, reaching into the Galactic bulge and out to the Magellanic Clouds. And all this can be accomplished as a function of metallicity and age, down to the lowest stellar masses.

To deduce IMFs from good-quality photometric data, an accurate mass-luminosity relation is required. Uncertainties here remain significant, particularly toward the high- and low-mass extremities of the IMF (mentioned in Sections 3.2.3 and 3.2.1). The situation can be improved with access to a large number of astrometric binary measurements, and further progress on stellar interior theories. Gaia has a critical role to play here, but will not be able to access dense, obscured environments towards the central regions of the Galaxy, where most stars are formed. A near infrared astrometric survey such as JASMINE is vital in this regard.

Tools and tracers:

- Good photometry, metallicity and ages
- Good distances from trigonometric parallaxes
- Well-determined metallicities and ages in a wide variety of environments

- Accurate mass-luminosity relation: large number of astrometric binary measurements outside the Solar vicinity to reach various metallicities
- Stellar interior theories
- Infrared studies of the inner disc, bulge, and centre of the Galaxy

Facilities

- Gaia, complemented by *JASMINE*
- VISTA, VST, *SkyMapper* and *PanSTARRS* optical-IR photometric surveys to build up comprehensive catalogues of calibrated magnitudes and colours (to Vega magnitudes of >20)
- Highly multiplexed multi-object spectrographs with medium/high spectral resolution ($R > 20000$) for abundance studies at both optical and NIR wavelengths

5.1.6 What is the impact of metal-free stars on Galaxy evolution?

To understand when the first metal-free stars formed, what their properties were and their impact on the subsequent stellar generations it is necessary to study extremely metal-poor stars (with $[\text{Fe}/\text{H}] \leq -3$). Their chemical abundance patterns offer a unique way to constrain the primordial IMF and nucleosynthesis in the early Universe (see Section 3.4.2 and 3.4.4). Although no metal-free star has been found so far, current dedicated surveys of the halo near the Sun have discovered a few stars with $[\text{Fe}/\text{H}]$ as low as ~ -5 . Since the expected number of extremely metal-poor stars is very small, and their spatial distribution is unknown, a huge number of stars probing a large volume have to be sampled. This is even more so now that it has become clear that the chances of finding metal-poor stars increase at distances beyond 15 kpc, while the oldest stars may well be located in the deepest part of the potential well, i.e. the bulge, a territory which has remained largely unexplored.

Tools and tracers:

- Large photometric surveys to select likely candidates
- Intermediate resolution spectroscopy ($R \sim 10000$) for large numbers of stars in the halo ($N \sim 10^5$) and the bulge

- High-resolution spectroscopy ($R \geq 20000$) to follow up interesting targets (with wavelength coverage in the blue-visual part of the spectrum, but also in the red-NIR to observe metal-poor stars in the bulge)
- Ages to better than 5% for the oldest stars

Facilities:

- Gaia for a systematic survey with distances, proper motions, radial velocities and metallicity estimations
- *SDSS – III*, *PanStarrs* and *LSST* for photometry
- Multi-object ($N_{\text{fibre}} \geq 100$) spectroscopy on 3-4 m class telescopes with wide field of view ($\sim 2 - 3 \text{ deg}^2$) at intermediate resolutions
- High-resolution spectroscopic follow-up on 8-m class telescopes for the confirmation of very metal-poor stars
- High performance (wide angle, ultra-high precision photometry) satellite for age determination of large samples of metal-poor stars by asteroseismology techniques

5.1.7 What is the merging history of the Galaxy?

Mergers are expected to have left behind a large amount of substructure in the phase-space distribution and kinematics of stars, especially in the stellar halo, and probably also in the thick disc and bulge of our Galaxy (see Sections 3.5.1, 3.5.2 and 3.5.3). To recover this substructure it is imperative to obtain full phase-space information for stars in the inner Galaxy ($R < 15 \text{ kpc}$) because this is where most of the stars in our Galaxy reside.

For the outer halo, lower dimensionality deep surveys providing positions in the sky and distances are sufficient to find the substructures because of the longer dynamical (and mixing) timescales characteristic of those regions. However, radial velocities will be needed to fully understand their kinematics. In this case, it is fundamental to probe the main sequence turn off (and below) to have enough stellar tracers to be able to identify streams of very low surface brightness such as those originating in low luminosity objects accreted long ago. Complementary metallicity information will be helpful in disentangling the reality of the substructures. Furthermore detailed chemical abundances and multi-colour photometry of stream stars can be used to trace the star formation and chemical evolutionary

history of the building blocks, and hereby characterise the progenitors and time the merger events.

Tools and tracers:

- Proper motions, distances, radial velocities and metallicity estimation for stars in all Galactic components
- Multi-colour photometry and radial velocities for halo stars
- Full sky coverage to disentangle local from global asymmetries
- High-resolution spectroscopy ($R \geq 20000$) for chemical characterisation of progenitors
- Dynamical models to recover evolutionary history

Facilities:

- Gaia to obtain full phase-space coordinates of stars in all Galactic components
- Complementary intermediate resolution ($R \sim 10000$) spectroscopic surveys from the ground for fainter targets ($G > 17$), typically on 4 m class telescopes with wide-field ($> 2\text{-}3 \text{ deg}^2$) multiplex ($N_{\text{fibres}} > 100$) capabilities
- Dedicated surveys on 8m class telescopes to do high resolution spectroscopy for $N \sim 50000$ stars on efficient wide-field instruments ($> 0.5 \text{ deg}^2$) with ≥ 100 fibres
- Wide-field deep surveys ($V > 22$) such as UKIDSS, VISTA, VST, *SDSS*, *LSST*, *PanStarrs*.

5.1.8 Is the Galaxy consistent with Λ CDM?

There are a number of critical observations that provide direct tests of the current cosmological paradigm. Amongst these, we would like to understand *i*) where are the missing baryons and if/how they have affected the evolution of the Galaxy (see Section 3.2.6); *ii*) if our Galaxy is exceptionally quiescent because of the lack of a very massive classical bulge and the presence of an old thin disc, which implies that it has not experienced recent mergers (see Section 3.5.1 for direct tests); and *iii*) what is its dark matter content and its distribution and how did this evolve.

Tools and tracers

- Baryons in a hot phase through studies along many halo lines of sight
- Baryons in the cold phase which could be detected dynamically, or through a wide-field survey in the infrared to measure the rotational emission lines produced by H_2 at $T \sim 100\text{K}$
- Chemical abundance patterns of the gas (either in hot or cold phase) to establish their role in the evolution of the Galaxy
- Imaging surveys of the stellar halos of nearby galaxies (surface brightness photometry or with resolved studies) to establish how generic is the Milky Way in comparison to other late type discs
- Spectroscopy of stars in nearby disc galaxies beyond the Local Group to derive metallicity distributions as well as kinematics in the outer halos of these galaxies
- Samples of halo stars (both field and in streams) with full-phase space coordinates
- Distant high-velocity stars
- Streamers to be used to derive the evolution of the Galactic potential. The requirements to find these have been listed in the previous top question.

Facilities

- Soft X-rays and far ultraviolet space observatories
- Far infrared observatory with very high resolution capabilities
- High resolution spectroscopic capabilities on these missions
- Imaging with 8m telescopes with wide field capabilities and from space (e.g. ACS and refurbishment on HST and JWST)
- Multiplex spectroscopic capabilities on 40m ELT (presumably around the Ca triplet region)
- Gaia complemented with radial velocity surveys for fainter targets

5.2 The central pc

5.2.1 Open questions

Why is Sgr A* so inert? How fast does it spin? What are the temperature and density of gas at the edge of its zone of influence? How does it accrete? Does it drive a jet or other outflow? Does it accelerate particles to $> 10^{15}$ eV as more active galactic nuclei appear to do?

These questions may be answered by simultaneous multi-waveband monitoring of flaring by Sgr A* since such observations can be used to constrain the dynamics of the plasma just outside the black hole. We might have the good fortune to detect interaction between any jet and the wind of a nearby star.

What are the structure, history and dynamics of the central star cluster? Is it dominated by stellar-mass black holes and neutron stars at $r \lesssim 0.3$ arcsec? Are any intermediate-mass black holes present? How the star cluster fed with gas? Why does the intense tidal field of Sgr A* not prevent stars from forming? What is the IMF in this region, and what impact do stellar collisions have on the evolution of the stellar population? Are hypervelocity stars ejected from this region, and if so, by what mechanism?

We currently detect only young, luminous stars in the central parsec, but advances in infrared detectors will enable increasingly fainter stars to be studied. If we can probe at absolute magnitudes $M_V \simeq 0$ or fainter, we will be able to study older stars and begin to unpick the history of the central parsec. Studies of the spectral lines of CS, HCN and other molecules at angular resolutions better than a few arcsec would make it possible to trace the gas flow in the region. This exercise should explain how and where stars form in this region.

5.2.2 Tools and tracers

- Simultaneous monitoring of flares from radio to X-ray
- X-ray surface-brightness maps to trace virial-temperature gas
- γ -ray maps to trace cosmic rays and e^\pm annihilation
- Proper motions and radial velocities of stars around the central black hole
- High-resolution maps of the Galactic centre in spectral lines of molecules

- Models of the central star cluster that combine dynamics with stellar evolution
- models of the plasma in the vicinity of Sgr A*
- Catalogues of hypervelocity stars

5.2.3 Facilities

- near-IR photometry and spectroscopy with adaptive optics (AO)
- Space-based near-IR astrometry of objects too faint for *JASMINE*
- VLBI astrometry of maser sources
- Photometry and spectroscopy with ELT
- mm and submm radio aperture-synthesis telescopes, especially ALMA
- γ -ray and cosmic-ray observatories to probe particle acceleration

5.3 The bar/bulge

A fundamental step to be understood in the formation of the Galaxy is the formation of the central region. One has to trace in detail the structures (a bar or several bars, a spheroidal part, a black hole, numerous massive clusters) with their characteristics (epoch of formation, dynamical processes such as dynamical friction, gas flows and interactions between gas and stars, star formation history) in order to place constraints on the scenario of formation, on the existence of a true bulge, a pseudo-bulge or a bulge formed from residuals of satellite accretions at early epochs.

5.3.1 Open questions

Do we have distinct bar and bulge populations? What is the orbital distribution? Does it break up in two populations?

These questions refer to different scenarios of formation, and whether some kind of observations are able to distinguish them. Tracers are either kinematics or abundances, but preferentially both. Necessary parameters to measure are abundances (iron and alpha), as well as 3D kinematics on a star by star basis (proper motions, distances and radial velocities). Kinematics must be obtained for very numerous stars, and should be accurate. Because the bulge is far away from the

Sun and highly obscured by dust, good distances are difficult to measure. One expects accuracy of 10% on distances from Gaia, but in limited regions because of the extinction, and only for the near side of the bar. JASMINE will be more efficient, giving access to near-infrared astrometry. For the 3D kinematics, radial velocities are needed but are difficult to obtain with current instruments for large samples in reasonable time. Highly multiplexed multi-object spectrographs should be available with medium spectral resolution in order to measure at the same time the radial velocity and the abundances. On account of extinction, a wide range of wavelength should be considered (from optical to mid-infrared) and efforts have to be put in to obtain better knowledge of the extinction law and its spatial variations. It implies as well the need for a better understanding of the properties of the dust grains (size, temperature, fragmentation).

What was the impact of the formation of the bulge on the chemical history of the disc ?

This question requires us to obtain information on gas flows at early epochs. It can be answered only by understanding better the physics of the gas and the overall history of formation. Hence it will be answered by expending effort to model the central regions.

What is the star formation history ?

The star formation history can be deduced from analysis of accurate photometric surveys. Gaia will provide a good opportunity to understand the star formation history of stellar populations in the bulge region from the inversion of Hess diagrams. However it requires good model atmospheres in the IR and evolutionary tracks for evolved stars, to produce unbiased results. Having the star formation rate as a function of time will help in discovering the proportion of stars coming from different processes of formation (bulge/bar/merging).

What is the evidence for merging in the bulge ?

Evidence of merging can be found in the bulge, as in the halo and thick disc, by analysing phase space with suitable accuracy. 3D kinematics (distance, proper motions, radial velocities) will reveal coherent streams if they are present in the bulge region. It will give new insights into the rate of merging in the central region during early epochs, and into the link between the bulge and spheroid populations.

5.3.2 Tools and tracers

- Abundances (iron and alpha)
- 3D kinematics (proper motions, distances and radial velocities)
- The extinction law and its spatial variations

- Model-atmosphere fluxes in the IR and evolutionary tracks of evolved stars
- Gas dynamics
- Dynamical models to integrate stellar and gas kinematics

5.3.3 Facilities

- Multi-object spectroscopy in the IR, for a field as wide as possible, reasonable resolution (medium for radial velocities, high for abundances), not very faint stars (cf recommendation at the symposium about ‘The VLT in the ELT Era’) + deep field (go to the other side of the bar)
- Kinematics: Gaia, *JASMINE*
- ALMA, APEX, Herschel, SKA and smaller ground-based radio telescopes to measure molecular line radiation and dust continuum

5.4 The thin disc

Inward of the solar neighbourhood, we do not know where the inner disc ends, or how the transition into the bulge/bar is accomplished (Section 3.1.2). Outward, distance determinations are especially unreliable and our knowledge of the outer reaches of the thin disc is patchy. Presently, the linkage between the gas and dust density distributions, and the stellar distributions is infirm (Section 3.1.5). Within this context, we have noted that the Galactic rotation model, used so often as a method of distance determination, is so far underpinned by gaseous CO and HI measurements only (Section 3.2.3). Better extinction mapping across the Galactic plane is desirable.

Improved cartography of the Galactic plane will support progress in tracing the current pattern of star formation in the thin disc, and in exposing the role of spiral density waves and other triggers in promoting cloud collapse (Sections 3.2.2 and 3.2.5). Questions to do with the process of star formation itself must be addressed in a focused way using mainly infrared, submillimetre and radio imaging and spectroscopic techniques. We also need to tackle the unresolved questions concerning star clusters, such as the origins of mass segregation and the reasons for cluster “infant mortality” (Section 3.2.4).

5.4.1 Open questions

What are the relations between the inner disc, the bulge-bar, and the halo?

Current/planned medium/high-resolution spectroscopic surveys are all in the optical (e.g. RAVE, SEGUE, LAMOST, Gaia) and will not be able to unveil the detailed chemical composition of objects in the very obscured regions of the inner disc/bulge/halo. Further progress in this area requires comprehensive (for at least $\sim 10^4$ stars) high-resolution infrared spectroscopic surveys in order to disentangle the different Galactic components which, towards the Galactic centre, reach their peak densities. Different teams are starting the development of such multi-object IR spectrographs (e.g. APOGEE as part of SDSS-III projects, WINERED in Japan - see description in Section 6.2). Data of this kind will be complementary to other surveys such as SEGUE-2 and future optical high-resolution surveys focusing in the halo and outer parts of the disc.

What is the history of star formation in the thin disc and how has the distribution of disc stars evolved over the life of the Galaxy?

Knowledge of the detailed abundance distributions of individual stars allows us to make inferences about the history of star formation. Currently abundance data are sparse for stars outside the solar neighbourhood. Moreover, when abundances within relatively distant stars are known, the implications of them are confused by uncertain distances and extinctions. Hence the provision of trigonometric parallaxes by Gaia and possibly JASMINE, and the 3D mapping of the ISM, will have a big impact on studies of the evolution of the disc. Studies of the abundance patterns in distant stars should start in advance of the advent of these parallaxes.

We know that the orbits of solar-neighbourhood stars evolve with time (the age-velocity dispersion relation - Section 3.4.5). However, recent theoretical work has suggested that the scale of stellar migration may have been underestimated (Section 3.5.3), so the present locations of stars may differ significantly from their places of birth, requiring interpretation using chemodynamic models. Fortunately, once the Gaia catalogue is available, 6D phase-space coordinates will be available for spectroscopically observed stars, giving their current orbits. From a combination of orbits, age, and abundance data, we can expect to be able to unravel much of the star-formation and dynamical history of the thin disc. In particular, it should be possible to determine as functions of radius and time: (i) the metallicity of the ISM; (ii) the star-formation rate; (iii) the IMF; (iv) the rate of increase of random velocities. None of these quantities is currently strongly constrained beyond the solar neighbourhood.

5.4.2 Tools and tracers

- The collection of stellar distances and motions, to be linked with studies of the gas phase across the optically-accessible disc
- All star parameters (especially for long-lived G and K dwarfs beyond the solar neighbourhood) as a function of Galactocentric radius: velocity field, orbits, abundances and ages
- 6D mapping of the disc in order to reveal the extent of substructures, whether they are dissolving stellar associations or dynamical structures associated with resonances. Detailed metallicity distributions and ages will provide vital discriminants between these two cases
- Improved, high spatial resolution, 3D extinction mapping of as much of the Galactic Plane as possible, to its inner edge and outer limits
- Reliable distances to obscured star-forming regions, by a range of methods. Focused, NIR and longer wavelength studies of individual star-forming clouds, to unpick processes within them
- Spatially well-resolved observations of gas emission line surface brightness and kinematics across the Galaxy for fine-scale (\sim arcsec) star formation and structure studies
- Appropriate advanced dynamical models utilising the new observations
- NIR and optical studies of clusters to examine the origins of mass segregation and infant mortality
- Large stellar samples from, and mapping of the disc, halo, bulge and bar towards and beyond the inner edge of the disc
- $[\text{Fe}/\text{H}]$, $[\alpha/\text{Fe}]$ and other abundance ratios for a large number of chemical species in the selected samples, along with precise radial velocities (better than a few km s^{-1}) to constrain the dynamical models in this inner region and to look for structures

5.4.3 Facilities

- Gaia, *JASMINE* for distances and proper motions of stars brighter than 20th magnitude. Gaia's RVS will provide radial velocities down to $V \sim 16.5$ Note: *JASMINE* in z band, reaching to 14th (versus Gaia's 20th magnitude in the visible) will provide astrometry of the Galactic centre and bulge, that cannot be achieved with Gaia

- IPHAS and UVEX in the north, VPHAS+ in the south provide $u', g', r', i', H\alpha$ optical photometry to better than 20th magnitude across the entire Galactic Plane
- The UKIDSS Galactic Plane Survey and VISTA VVV will provide NIR multi-band photometry at better than 1 arcsec spatial resolution, down to $K \sim 19$. Present plans leave some parts of the Galactic Plane uncovered. VISTA will provide important target lists for inner-disc/bulge spectroscopy projects
- Medium-resolution ($R > 5000 - 7000$) multi-object spectroscopy on 4 m and larger optical-NIR telescopes, in both hemispheres, for radial velocities to a few km s^{-1} and metallicities to 0.2 dex, to distances of a few kpc: complementing Gaia's Radial Velocity Spectrometer (RVS) for stars with $V > 15$. *LAMOST* under construction in the North
- High-resolution multi-object spectrograph in the NIR on 4- to 8-m class telescopes (large field of view required) for detailed abundances of numerous chemical species in large samples of stars. Already planned as part of *SDSS-III: APOGEE* in the North. A similar project should be envisaged for the southern hemisphere
- High-resolution multi-object spectrograph in the blue on 4- to 8-m class telescopes to obtain detailed abundances for stars in the outer
- Sensitive high spatial resolution IR/sub-mm/radio facilities (Herschel, ALMA, e-MERLIN, SKA) for mapping fine structure of the ISM
- Gaia proper motions to be used in the sample selection process allowing a very efficient selection of low density targets as thick disc, halo and Pop III objects among a vast amount of inner disc and common bulge objects
- ELT for obtaining metallicities at high dispersion ($R > 20000$) of F- and G-dwarfs stars across the disc

5.5 The thick disc

From recent works it appears that the thick disc seems chemically and kinematically distinct from the thin disc and the spheroid. However its origin is not well understood. As explained in Section 3.5.3 the thick disc may be formed from satellite accretion at an early epoch, from thin disc heating or from remnants of merging satellites. The epoch of such an event is also an open question (see Section 3.1.3). The main questions and the way they can be answered are the following.

5.5.1 Open questions

How fast was the star formation in the thick disc ?

The age is one of the most difficult parameter to measure for individual stars. However, the enrichment time scale of a population can be deduced from the distribution of its stars in a $[\alpha/\text{Fe}]$ versus $[\text{Fe}/\text{H}]$ diagram (see Section 3.4.3). With accurate elemental abundances (alpha elements and iron) the time scale of star formation can be derived. Star formation history can also be obtained using accurate photometry and inversion methods of the Hess diagram. Getting absolute ages for the population requires to be able to develop accurate atmosphere models. These ages and star formation history could then be confronted to scenarios of thick disc formation.

How can we separate the thin disc from the thick disc ?

Is the thick disc an extension of the thin disc ? How their kinematic properties differ ? How their chemical enrichment differs ? Was the thin disc pre-enriched by the thick disc ? These questions can be answered using surveys of both populations at different heights above the plane (kinematical and abundance vertical gradients) as well as along the plane (radial gradients). It is also important to understand the role played by radial motions in the building of these components (Haywood, 2008, see also Section 3.5.3). Large samples of thin and thick disc stars are necessary to reach this goal. Since the ratio between thick disc and thin disc is low in the solar vicinity, large volumes need to be studied. Such surveys also need to be unbiased with regards to the parameter measured (kinematics and metallicity).

Local samples are very useful to constrain abundances and kinematics of the local thick disc (RAVE, Geneva-Copenhagen samples, etc.). However they lack good distances which are needed to trace the vertical profile of this population and the related gradients. Gradients and discreteness of the transition between thick and thin disc would be very useful to constrain the scenario of formation of the former.

Do the characteristics of the thick disc vary with position in the Galaxy ?

Depending on the scenario of formation of the Galaxy, its characteristics may change with position (see Section 3.5.3). If the thick disc is constituted of remnants of one or several satellites having merged into our Galaxy, then the orbit of thick disc stars would keep the imprint of the orbit of the satellite. The degree of inhomogeneity in thick disc parameters also gives indications about its history of formation, in particular the proportion of its stars which have their origin in merged satellites. Considering the smooth part of the thick disc, important characteristics to measure are: the scale length and scale height, the possible variation of the scale height with radial position, kinematic and abundances gradients, both radially and vertically.

Gaia will greatly improve the radial and vertical profiles of this population, with accurate trigonometric distances, as well as good radial velocities for many stars. But one would need to go deeper to get more accurate abundance measurements in remote regions of the Galaxy, important to trace the star formation history in different regions, helping to identify probable satellite remnants, and to estimate the degree of mixing in different regions of the Galaxy. This can be done only with very large telescopes with efficient multi-object spectrograph in the visible with medium spectral resolution.

What is the origin of the globular cluster thick disc ?

As seen in Section 3.1.7 the globular clusters attributed to the thick disc population because of the flatness of their distribution and their abundances, may not be physically related to the thick disc population in the field. Some may originate from merging satellites as halo globular clusters, and be captured from more inclined orbits. It is still possible to discover new globular clusters, specially near the Galactic plane. The identification of their origin would help to understand their link with the thick disc, via their orbits, their detailed elemental abundances, and their age.

5.5.2 Tools and tracers

- 6D mapping of the disc in order to reveal the extent of substructures.
- Unbiased large samples of stars with accurate distances, kinematics, abundances and ages
- All star parameters as a function of Galactocentric radius and distance to the Galactic plane: velocity field, orbits, abundances and ages
- Appropriate advanced dynamical models utilising the new observations
- Stellar atmosphere models

5.5.3 Facilities

- Gaia for distances and proper motions, radial velocities, photometry, atmospheric parameters and abundances
- Radial velocity surveys (RAVE, etc.)
- Multi-object spectrographs in the visible with median spectral resolution ($R > 7000$) on 4- to 8-m class telescopes (large field of view required) to go deeper than Gaia for radial velocity surveys and abundances. Blue sensitivity to obtain detailed abundances for stars in the outer disc

- High performance (wide angle, ultra-high precision photometry) satellite for age determinations of large samples of stars by asteroseismology techniques
- Gaia proper motions to be used in the sample selection process allowing a very efficient selection of low density targets as thick disc, halo and Pop III objects among a vast amount of inner disc and common bulge objects
- ELT for obtaining metallicities and other element abundances at high dispersion ($R > 20000$) in the outer disc

5.6 The stellar halo

5.6.1 Open questions

The challenges faced in answering questions concerning the halo arise from a common set of factors: halo stars occupy the largest volume of any Galactic population, have the lowest stellar density, and are well mixed spatially, at least in the inner halo. Because of the halo's size, its stars are faint and spread along long lines of sight; only a biased fraction of them are found in the solar vicinity; and in the outer halo transverse velocities, which correspond to the tangential velocity component in the Galactic frame, are difficult to measure. In the questions posed below, we defer discussion of the Galactic globular cluster system to the following subsection.

How is the field component of the halo related to dwarf satellites?

The merger with the Sgr dwarf galaxy makes it clear that the halo contains *some* stars that formed outside the Galaxy, but halo field stars have different compositions to the surviving satellites (see Section 3.4.6). Observations and modelling of such differences may provide insights into the nature of satellites which may previously have been stripped, such as their stellar and dark-matter masses, densities, spatial distributions and angular momenta, compositions and kinematics. Discoveries of low-mass dwarfs may be expected from a more complete census of the Local Group. Gaia data should help discriminate between foreground and background objects.

What fraction of the stars in the halo was accreted?

By combining observations of surviving stellar streams with modelling, it may be possible to estimate the fraction that is accreted. In Figure 16, the contrast between streams is more evident beyond 20 kpc, and is detectable as spatial non-uniformities and structure in phase-space. Ideally, a survey to detect substructure would be deep, cover a wide field, and have good distance, velocity and abundance determinations. Gaia will catalogue stars down to $V \simeq 20$, corresponding to horizontal-branch (HB) stars at 80 kpc. However, for HB stars at 20 kpc, Gaia

parallax errors will be comparable to the parallax, so photometric parallaxes will have to be relied upon for the outermost halo stars. In the solar vicinity, substructure there will only be identifiable through clustering in phase-space, since the number of streams expected in Λ CDM is in the hundreds.

Does the accreted fraction vary throughout the halo?

It is probable that the accreted fraction varies throughout the halo, giving rise to the differences between inner- and outer-halo populations. Furthermore, Figure 16 shows that the space density of accreted material is expected to vary radially, azimuthally and with polar angle, implying that the halo needs to be mapped as fully as possible. Abundance analysis and age dating would provide useful information on the various formation paths. Further modelling, particularly cosmological simulations including gas physics, star formation and feedback processes with sufficiently high resolution to be able to populate the halo component with sufficient numbers of stars, is needed.

When did the halo come into place?

The colour distribution of halo field dwarf stars is consistent with this population being as old as the globular clusters. However, due to ongoing mergers, halo stars are being put in place even now (see Section 3.4.6). The accretion history may be discernible by tracing streams across the sky to determine their distributions around the Galaxy, and by comparing these with models of the time-evolution of streams of a given mass and phase-space trajectory to reproduce the degree of dissolution.

How does our halo compare with the halo of M31?

Substructure visible in the outer halo of M31 (Figure 22) is reminiscent of that in the Galactic accretion simulations (Figure 16). The characterisation of stripped structures in M31 will inform our interpretation of Galactic observations.

5.6.2 Tools and tracers

- Streams: identification by surveys with good distance and velocity determinations, supplemented by element abundance determinations
- Low-density dwarf galaxies: photometry, orbits, dynamics, element abundance patterns, ages
- Halo field stars: kinematics and abundance ratios, especially at low metallicity, throughout the outer halo as well as the inner halo
- Cosmological simulations of the stellar halo with high enough resolution to populate it with stars

- Models of the dynamical evolution of satellites, clusters and streams in realistic gravitational potentials starting from a variety of (cosmologically motivated) initial conditions

5.6.3 Facilities

- Gaia for distance, proper motions, photometry and radial velocities of halo stars
- High-resolution spectroscopic surveys of the radial velocity of stars in the inner and outer halo, particularly for stars fainter than the Gaia limiting magnitude which will be needed to trace, in sufficient numbers, the debris of accreted low-mass systems
- Photometric surveys to obtain photometric parallaxes
- $S/N > 30-40$, high-resolution spectroscopy ($R \sim 30000$), highly multiplexed (> 100 fibres) on 4 to 8 m class telescopes (field of view $> 2.5 \text{ deg}^2$ for 4m and $> 0.5 \text{ deg}^2$ for 8m telescope) and at low multiplex on an ELT, to obtain the compositions of giants and dwarfs in the inner and outer halo, in field stars, globular clusters and dwarf satellites

5.7 The globular cluster system

5.7.1 Open questions

How do globular clusters relate to dwarf satellite galaxies?

It will be of value to discover whether globular clusters other than those already associated with the Sgr dwarf galaxy can be linked to surviving substructures in the halo. If so, they may serve as beacons of past merger events and be diagnostic of the progenitor bodies. Reliable measurements of the dynamics, chemical abundances, ages, horizontal-branch morphology, and structural parameters could then be used as a way of tracing Galactic history and understanding the nature and evolution of now-stripped dwarf galaxies.

What is the origin of the two globular cluster populations?

The origin of the population dichotomy (see Section 3.1.7) remains unclear, but is presumed, perhaps correctly, to reflect the different origins of the field star populations of the halo and thick disc. At least some globular clusters are accreted; it remains to be established whether all are.

How and where did the globular clusters form? Constraints on models for the formation of globular clusters are provided by evidence of extended star formation and self-enrichment over perhaps a few tens of Myr, by the lack of globular clusters with $[\text{Fe}/\text{H}] < -2.5$, by the signatures of proton-capture nucleosynthesis not seen in the field halo population, and the existence of a small number of clusters which are younger than the others by a few Gyr (see Section 3.1.7). Precisely how they formed and over what (short) period of time has yet to be determined.

How do globular clusters relate to the field stars of the Galaxy?

Halo globular clusters are not entirely representative of the field halo component (see Section 3.1.7): the globular cluster metallicity distribution does not extend to such low values as the field stars, and proton-capture reactions in the Ne-Na and Mg-Al cycles are evident in some cluster giants but not their field counterparts. The origin of these differences are not well understood, but may reflect vastly different masses and/or stellar densities of their birth environments. These differences argue against the field population having been sourced in star clusters the same as the surviving globular clusters. We may be poised to discover more lower-mass, less-dense globular clusters once more precise phase-space and metallicity measurements for stars are available from Gaia. It will be of interest to compare their chemical characteristics with those of the field population. Convincing measurements of $[\text{Fe}/\text{H}]$ and key abundance ratios will require high S/N, high-resolution spectroscopy of a selection of giants.

What fraction of globular clusters survive to the present?

It is commonly believed that the globular clusters seen in the Galaxy today are a subset of the total number that ever existed there, some fraction having been shredded. The chemical differences between surviving globular clusters and the local halo stars (see above) provide only partial constraints on the number of systems which have dissolved; dynamical simulations provide other constraints. The unknown answer to this question is linked to many of the questions raised above.

5.7.2 Tools and tracers

- Globular clusters: orbits for all clusters, element abundance patterns, ages, horizontal branch morphologies
- Low-density dwarf galaxies: photometry, orbits, dynamics, element abundance patterns, ages
- Cosmological simulations of the stellar halo with high enough resolution to populate it with stars, clusters and dwarf galaxies

- Models of the dynamical evolution of satellites, clusters and streams in realistic gravitational potentials starting from a variety of (cosmologically motivated) initial conditions

5.7.3 Facilities

- Gaia and ultimately *SIM* for distances, proper motions, photometry and radial velocities of halo stars, globular clusters and low-density dwarf galaxies
- High-resolution spectroscopic surveys of the radial velocity of stars in the inner and outer halo, particularly for stars fainter than the Gaia limiting magnitude which will be needed to trace, in sufficient numbers, the debris of accreted low-mass systems
- Photometric surveys to obtain photometric parallaxes
- $S/N > 30-40$, high-resolution spectroscopy ($R \sim 30000$), highly multiplexed (> 100 fibres) on 4 to 8 m class telescopes (field of view $> 2.5 \text{ deg}^2$ for 4m and $> 0.5 \text{ deg}^2$ for 8m telescope) and at low multiplex on an ELT, to obtain the compositions of giants and dwarfs in the inner and outer halo, in field stars, globular clusters and dwarf satellites

5.8 The dark matter

5.8.1 Open questions

What is the evidence for dark matter?

There is a major discrepancy between the dynamical mass of the Galaxy and that which can be accounted for by counting its baryonic content (stars and gas; see Section 3.3.8). This has led to the notion of dark matter, whose nature, spatial distribution and characteristics remain poorly known. In principle, an alternative could be a modification to Newtonian dynamics. To firmly establish the need for dark matter or an alternative gravity it is necessary to map extensively the gravitational potential of the Galaxy in a complete and consistent way. Furthermore there is also some indication that the baryonic census is incomplete in our Galaxy (Section 3.1.5).

What is the distribution of dark matter? What are its main parameters?

The density profile, shape and extent of the dark-matter halo of our Galaxy are poorly constrained because of the lack of halo tracers with full phase-space information. It is therefore necessary to compile large samples of distant halo stars as

well as to find stellar streams from disrupting globular clusters or dwarf galaxies. For such objects, radial velocities, proper motions and distances are imperative. Further, complementary information can be obtained on the scales of dwarf satellites, since these are dark-matter dominated objects. For these, it is important to map their internal kinematics both with radial velocities as well as with proper motions.

Is there evidence for sub-structures?

Cold dark matter predicts a large amount of bound substructures in the halos of galaxies like the Milky Way, several orders of magnitude above the number of known satellites (Section 3.3.8). These ‘missing satellites’ may well be orbiting the Galaxy but not have a ‘visible counterpart’, and may eventually be detectable through the dynamical perturbations they exert on exceedingly cold stellar streams. It is therefore fundamental to map the stellar halo to search for such streams, and especially to find those which are orbiting beyond the Galactic disc where they avoid heating or scattering due to disc crossings. The measurement of the internal kinematics of such streams would then allow the characterisation of the mass function of substructures in the halo of our Galaxy.

What is the nature of dark matter?

It is possible that in the next decade, direct and indirect dark matter detection experiments will have constrained the nature of dark-matter. Complementary information is obtained from the characterisation of the density profiles and shapes of the halos of the Local Group system, since their actual properties (cusp/core; triaxial/spherical) depend significantly on the cross-section and ‘temperature’ of the fundamental particles.

5.8.2 Tools and tracers

- Mass and distribution of the stellar populations of the Galaxy
- Mass and distribution of cold gas (CO, but also possibly H₂ in an independent fashion)
- Mass and distribution of hot gas
- Velocities and accelerations of the above tracers to map the (seen and unseen) gravitational field

5.8.3 Facilities

- Gaia (proper motions + parallaxes + radial velocity for brighter stars) + radial velocities from the ground for fainter targets + wide field photometric

surveys; *JASMINE* for the bulge; *SIM* for dwarf galaxies and very cold streams

- Herschel, ALMA and SKA for a complete census of the (cold) gas content
- X-ray and far ultraviolet space missions for a census of the hot gas content
- Direct detection experiments (in the laboratory, such as e.g. the LHC in CERN) and indirect detection from space (through γ ray annihilation, such as e.g. *GLAST*)

6 Relevant programmes and associated instruments, ground-based and space

After having identified the most important open questions (Section 5), we now turn to the tools and facilities. The main goal here is to review ground- and space-based facilities that have played and/or will play a major role in achieving our scientific goals. This overview is restricted to on-going and planned facilities, and there is no claim for completeness. Preference has been given to all kinds of surveys because of their larger scientific impact. Each of the following tables collects information for both ground- and space-based surveys.

Surveys/facilities appearing in *italic* are non-European, or with no major European contribution.

6.1 Astrometric surveys

A summary of the main operational and planned ground- and space-based astrometric surveys is presented in Tables 1 and 2. Two already completed ESA missions are also listed for comparison purposes only. The two rightmost columns of Table 2 give respectively the parallax and the proper motions accuracy (achieved or to be achieved).

Table 1: Summary of main operational and planned astrometric surveys

Survey/ Mission	PI	Status	Years of operation	Goals
Ground-based				
<i>CTIOPI</i>	Henry, CTIO	operational	1999-	parallaxes, stars < 25 pc
<i>Pan-STARRS</i>	Hawaii U.	prototype	2007-2020	30 000 deg ² , North
<i>URAT</i>	USNO	partly funded	2009-2014	all-sky robotic
<i>LSST</i>	LSST Corp.	partly funded	2015-2025	20 000 deg ² , South
Space-based				
<i>Gaia</i>	ESA	fully funded	2011-2017	all-sky
<i>Nano-JASMINE</i>	JAXA	under development	2009-2010	all-sky, < 300 pc
<i>JASMINE</i>	JAXA	under development	2016-2021	10° x 20°, bulge
<i>J-MAPS</i>	USNO	phase A	2012-2017	all-sky
<i>SLM</i>	NASA + JPL	phase B	2015-2020 ⁽¹⁾	selected stars
<i>Hipparcos</i>	ESA	completed	1989-1993	all-sky + selected stars
<i>Tycho-2</i>	ESA	completed	1989-1993	all-sky

⁽¹⁾ The years of operation are only indicative, as the launch has been deferred indefinitely by NASA.

CTIOPI – *Cerro Tololo Interamerican Observatory Parallax Investigation*: this project began as an NOAO Surveys Program in 1999 using both the 0.9 m and 1.5 m telescopes at CTIO, and has continued on the 0.9 m as part of the SMARTS (Small and Moderate Aperture Research Telescope System) Consortium as of early 2003. It focuses on the discovery of nearby red, white, and brown dwarfs in the solar neighbourhood, with the main goal to discover 300 new southern star systems within 25 parsecs by determining trigonometric parallaxes accurate to 3 milliarcseconds (cf Henry et al., 2006). More information available at: <http://www.chara.gsu.edu/~thenry/CTIOPI>.

Pan-STARRS – *Panoramic Survey Telescope & Rapid Response System*: this is a wide-field imaging facility which has the immediate objective to detect and characterise Earth-approaching objects, both asteroids and comets, that might pose a danger to our planet. *Pan-STARRS* will catalogue 99% of the stars in the northern hemisphere that have ever been observed by visible light, not confined only to the Milky Way galaxy; stars in nearby galaxies will routinely have their colours and positions noted, and will be checked regularly for variability. The stellar database that results from *Pan-STARRS* will be a goldmine for statistical studies of how different kinds of stars are distributed in their parent galaxies. Selected regions of the sky, such as young star clusters, will be searched in even greater depth. The ensemble of positional information of stars observed with *Pan-STARRS*, whether nearby or distant, will lead to what will become the de-facto astrometric reference catalogue for faint objects (Chambers, 2005).

URAT – *USNO Robotic Astrometric Telescope*: this is a new 0.85 m aperture telescope with a 4.5 deg field of view (FOV). Its operation is envisioned to be fully automatic, generating stellar positions on the 5-10 mas level to at least 18th magnitude with a limiting magnitude of about 20 to 21. These reference stars, being on an inertial system (linked to quasars), will be very beneficial for *LSST*, *PanSTARRS* and other projects of the kind. With a few years of observing, absolute trigonometric parallaxes (5-20 mas, depending on magnitude) could be obtained for all stars accessible by *URAT* from an initially southern hemisphere location (Zacharias et al., 2006).

LSST – *Large Synoptic Survey Telescope*: this is a proposed ground-based 8.4 m, 10 square-degree-field telescope that aims at providing digital multi-colour u, g, r, i, z, y imaging of about half of the sky (that will be surveyed every three nights) to unprecedented depth ($r \sim 27.5$) and with an image quality of the order of 0.7" (median delivered seeing in the r band). This huge database (containing 10 billion galaxies and a comparable number of stars) will allow identifications of any object that change or move on rapid time-scales, like exploding supernova, potentially hazardous near-Earth asteroids, and distant Kuiper Belt Objects. Thanks to the targeted photometric (1% relative, 2% absolute) and astrometric (10 mas

Table 2: Selected characteristics of operational and planned astrometric surveys (cf Table 1)

Survey/ Mission	V-magnitude range	Wavelength [band/ μm]	Total number of stars	σ_π range [mas]	pm [mas/yr]
Ground-based					
<i>CTIOPI</i>	9 - 19	optical	300	3	...
<i>Pan-STARRS (PS4)</i>	15 - 24	optical	10^{10}	3 - 25 ⁽¹⁾	3 - 25 ⁽¹⁾
<i>URAT</i>	14 - 21	optical	10^9	5 - 100	5 - 100
<i>LSST</i>	17 - 24	0.3 - 1	10^{10}	1 - 10 ⁽¹⁾	0.2 ⁽¹⁾
Space-based					
Gaia	6 - 20	optical	10^9	0.007 - 0.3 ⁽²⁾	0.007 - 0.3
<i>Nano-JASMINE</i>	<8.3	z (0.9)	10^5	...	1
<i>JASMINE</i>	< 14	z (0.9)	10^7	0.01	0.004
<i>J-MAPS</i>	2 - 15	optical	40×10^6	0.35 - 5	0.05 - 0.1 ⁽³⁾
<i>SIM</i>	0 - 20	optical	~ 10000	0.004	0.004
Hipparcos	2 - 12.4	optical	118 000	0.2 - 4	0.8 - 4
Tycho-2	0 - 11.5	optical	2.5×10^6		2.5

⁽¹⁾ these two facilities will use very short exposures, thus astrometric accuracies will need to be carefully assessed once observations start

⁽²⁾ range corresponds to stellar magnitude range 10-20 (V mag)

⁽³⁾ when combined with the Hipparcos catalogue

per epoch) accuracy, it will also produce an important catalogue for stellar studies. The *LSST* Conceptual Design was reviewed and approved in September 2007, and the project is now moving closer to beginning construction (Wolff, 2005).

Gaia – this is one of the next ESA missions, which has the primary goal of investigating the origin and subsequent evolution of the Milky Way. It will conduct a census of more than 1 billion stars (both in our Galaxy and in other members of the Local Group), measuring their position with an accuracy down to $7 \mu\text{as}$. Together with stellar distances and motions, this mission will allow astronomers to build the most accurate three-dimensional map to date of the celestial objects in our Galaxy. Gaia will also perform spectral and photometric measurements for all objects. The final catalogue is expected to be ready by 2020. On a historical note, the name GAIA originally stood for Global Astrometric Interferometer Astrophysics, but as the project evolved, the interferometer concept was replaced by a new payload design, without changing the name of the mission (Lindegren & Perryman, 1996; Bailer-Jones, 2006).

Nano-JASMINE – *Nano-Japan Astrometry Satellite Mission for INfrared Exploration*: this is a nano size astrometry satellite (total payload mass less than 10 kg, 5 cm reflective telescope), which has the main purpose of proving and demonstrating in a real space environment the key technologies required for the main Japanese space mission *JASMINE*. *Nano-JASMINE* will measure annual parallaxes of bright stars (7 mag) with an accuracy greater than 1 mas after two years of operations, following the same observing technique of the Hipparcos mission (Kobayashi et al., 2006).

JASMINE – *Japan Astrometry Satellite Mission for INfrared Exploration*: *JASMINE* will carry out astrometry observations for stars located in a narrow strip within 4 deg of the Galactic plane in z -band ($\lambda_c \simeq 0.95 \mu\text{m}$), measuring the position, annual parallax and proper motion of about a few million stars with a precision of 10 microarcsec at $z = 14$ mag. It will cover, without gaps, a $20 \text{ deg} \times 10 \text{ deg}$ area in the Galactic bulge (Gouda et al., 2007).

J-MAPS – *Joint Milli-Arcsecond Pathfinder Survey*: this is a space-based, all-sky, visible wavelength astrometric and photometric survey for stars in the $V = 2\text{-}15$ magnitude range with a 2012 launch date goal. The primary goal is the generation of a 1-mas (down to $V = 12$ mag) all-sky astrometric catalogue for bright stars. The combination of the *J-MAPS* and Hipparcos catalogues will produce common proper motions on the order of 0.1 mas/yr level (Gaume et al., 2007).

SIM – *Space Interferometry Mission: SIM PlanetQuest* will be an optical interferometer operating in an Earth-trailing solar orbit. The goal is to measure the position, trigonometric parallax and proper motion of stars with an accuracy of

4 μ as down to magnitude 20. This breakthrough in capabilities is possible because *SIM* will use optical interferometry (Unwin et al., 2008).

Hipparcos and Tycho – ESA’s Hipparcos space astrometry mission was a pioneering space experiment dedicated to the precise measurement of the positions, parallaxes and proper motions of the stars. The intended goal was to measure the five astrometric parameters of some 120 000 primary programme stars to a precision of some 2 to 4 milliarcsec, over a planned mission lifetime of 2.5 years, and the astrometric and two-colour photometric properties of some 400 000 additional stars (the Tycho experiment) to a somewhat lower astrometric precision. Launched in August 1989, Hipparcos successfully observed the celestial sphere for 3.5 years before operations ceased in March 1993. All of the original mission goals have been significantly exceeded: the Hipparcos Catalogue contains 118 218 stars charted with the highest precision (1-4 mas), the Tycho Catalogue contains 1 058 332 stars, with lesser but still unprecedented accuracy. The Tycho 2 Catalogue, completed in 2000, brings the total to 2 539 913 stars, and includes 99 % of all stars down to magnitude 11. A new reduction of the Hipparcos raw data was performed by van Leeuwen & Fantino (2005), with a new dynamical modelling of the satellite’s altitude. The resulting astrometric accuracy is significantly improved for the brightest part of the Hipparcos catalogue, reaching 0.2 mas for stars of magnitude 5. The names, Hipparcos and Tycho, honour great astrometrists of classical and early modern times, Hipparchus the Greek (190-120BC) and Tycho Brahe the Dane (1546-1601). Hipparcos is also an acronym for High Precision Parallax Collecting Satellite (Perryman et al., 1997; ESA, 1997; Høg et al., 2000).

6.2 Spectroscopic surveys

A summary of the main operational and planned ground- and space-based spectroscopic surveys is presented in Tables 3 and 4. The two rightmost columns of Table 4 represent respectively the spectral resolution and the accuracy on radial velocity measurements.

RAVE – the Radial Velocity Experiment: this is a survey dedicated to the measurement of radial velocities, metallicities and abundance ratios for up to a million southern hemisphere stars using the 1.2-m UK Schmidt Telescope of the Anglo-Australian Observatory (AAO), over the period 2003 - 2010. The survey will provide a vast stellar kinematic database for all major components of the Galaxy. The First Data Release became available in February 2006, and includes data obtained during the first year of operations. It provides radial velocities for 24 748 individual stars and has a total sky coverage of $\sim 4\,760$ deg² (Steinmetz et al., 2006). The Second Data Release has become available in June 2008, and includes data

Table 3: Summary of main operational and planned spectroscopic surveys

Survey/ Mission	PI	Instrument/ Telescope	Status	Years of operation	Goals
Ground-based					
RAVE	Potsdam	6dF/UKST	operational	2003 - 2011	South
<i>SEGUE</i>	Sloan	SDSS/APO	operational	2005 -	3500 deg ² , North ⁽¹⁾
<i>LAMOST</i>	China	LAMOST	being commissioned	2009? -	
<i>WINERED</i>	Tokyo	PI-instrument	under development	2009? -	bulge ⁽²⁾
<i>APOGEE</i>	Sloan	SDSS/APO	partly funded ⁽³⁾	2011 - 2014	100000 giants
Space-based					
Gaia	ESA	RVS	fully funded	2011 - 2017	all-sky

⁽¹⁾ in complement to the Sloan Digital Sky Survey (SDSS)

⁽²⁾ in complement to JASMINE

⁽³⁾ telescope is operational, but instrument is only partly funded

Table 4: Selected characteristics of operational and planned spectroscopic surveys (cf Table 3)

Survey/ Mission	Magnitude range	Wavelength [μm]	Total number of stars	Resolution	σ_{RV} [km/s]
Ground-based					
RAVE	9 - 12 (<i>V</i>)	0.84 - 0.88	10^6	7500	< 3
SEGUE	14.5 - 23.5 (<i>g</i>)	0.38 - 0.92	250 000	2000	4 - 24
LAMOST		0.39 - 0.90	unknown ⁽¹⁾	1/0.25 nm	
WINERED	$< 14/17$ (²)	0.9 - 1.35		28 000 / 100 000 (³)	< 1
APOGEE	≤ 13.5 (<i>H</i>)	1.52 - 1.69	100 000	20 000	0.5
Space-based					
Gaia	< 17	0.847 - 0.874	10^8	11 500	1 - 15

⁽¹⁾ survey(s) have not been defined yet, but it will be possible to observe up to 4000 targets per exposure

⁽²⁾ depending on if spectrograph is mounted on a 4m or a 10m class telescope

⁽³⁾ depending on mode (normal Echelle or immersion grating mode)

obtained during the first two years of operation. It provides radial velocities for 49 327 individual stars, stellar parameters (temperature, gravity and metallicity) for 21 121 objects, and has a total sky coverage of 7200 deg² (Zwitter et al., 2008). More information available at: <http://www.rave-survey.aip.de/rave/index.jsp>.

SEGUE – *Sloan Extension for Galactic Understanding and Exploration*: this is one of the three major surveys that are part of the second phase of the Sloan Digital Sky Survey (SDSS-II). Its main objective is to obtain a detailed view of the stellar content and a 3-dimensional map of our Milky Way galaxy. *SEGUE* will ultimately obtain spectra of 240 000 stars in the disc and spheroid, revealing the age, composition and phase space distribution of stars within the various Galactic components. These will then allow to explore in detail the structure, formation history, chemical and dynamical evolution of the Galaxy. The first public release of *SEGUE* data was part of SDSS Data Release 6, released in June 2007. More information available at: <http://www.sdss.org/segue>.

LAMOST – *Large Sky Area Multi-Object Fiber Spectroscopic Telescope*: this is one of the National Major Scientific Projects undertaken by the Chinese Academy of Science. It has an aperture of 4 m, with a focal plane of 1.75 m in diameter, corresponding to a 5 deg field of view, which will be able to accommodate as many as 4000 optical fibres, that are connected to a number of spectrographs. One of the main scientific goals of *LAMOST* is a spectroscopic survey of a large number of stars, which will make a substantial contribution to the study of stellar astrophysics. Operations are planned to start in 2009. More information available from: <http://www.lamost.org/en>.

WINERED – *Warm Infrared Echelle spectrograph to Realize Extreme Dispersion*: the main goal of this project is to realise a portable NIR spectrograph with a high resolving power of 70 000 and a high throughput ($\geq 25\%$) at low costs and with a short development time. It is being developed as a PI-instrument, that can be easily attached to different 4 m/10 m class telescopes around the world. The initial design is for a single object spectrograph, but in the planning there is the intention to adapt the design for simultaneous multi-object spectroscopy. It is intended to do the spectroscopic follow up (in terms of radial velocities and abundances) of the planned astrometric space mission *JASMINE* which will provide exact positions, distances, and proper motions of the bulge stars (Tsujimoto & Kobayashi, 2007).

APOGEE – *Apache Point Observatory Galactic Evolution Experiment*: this is one of the four projects (collectively known as SDSS-III) to be undertaken with the Sloan 2.5-m telescope at Apache Point Observatory after completion of ‘Second Generation Sloan Digital Sky Survey – SDSS-II’ operations in 2008. *APOGEE* will construct a high-resolution, near-infrared multi-fibre spectrograph for a detailed

survey of the dynamics and chemistry of the Milky Way, especially at low Galactic latitudes (the disk, bulge and bar) where dust extinction makes optical wavelengths unusable. The 100 000 stars that are targeted by this survey will be selected based on 2MASS colours and will probe all Galactic populations (Majewski et al., 2007).

Gaia – See Section 6.1.

6.3 Photometric surveys

A summary of the main operational and planned ground- and space-based photometric surveys and/or facilities is presented in Tables 6.3 and 6. Some of them also include spectroscopy. For instance, for ESA next mission, Herschel, we decided to include it only in this table because there is no clear split between spectroscopic and photometric/imaging capabilities (two out of three instruments offer both).

IPHAS – INT/WFC Photometric H α Survey of the Northern Galactic Plane: this is a survey of the Northern Galactic Plane being carried out in H α , Sloan r' and i' filters, with the Wide Field Camera (WFC) on the 2.5 m Isaac Newton Telescope (INT). The survey began in 2003 and it is close to completion. The survey area comprises all galactic longitudes in the Northern Galactic Plane within the latitude range $-5 \text{ deg} < b < 5 \text{ deg}$, a total of 1800 deg^2 . The INT/WFC offers a pixel scale of $0.33''$ per pix, allowing on-sky structures above $1''$ in size to be resolved. The target faint-end limiting broadband magnitude is $r' = 20$. The final database will contain photometry on over 300 million Galactic Plane objects (Drew et al., 2005).

UKIDSS – United Kingdom Infrared Deep Sky Survey: UKIDSS is the next generation near-infrared sky survey, the successor to 2MASS, and it is carried out with WFCAM on the UK Infrared Telescope (UKIRT) in Hawaii. The survey began in 2005 and will survey 7500 degree^2 of the Northern sky, extending over both high and low Galactic latitudes, in JHK , down to $K=18.3$ (which is three magnitudes deeper than 2MASS). UKIDSS will be the true near-infrared counterpart to the Sloan survey, and will produce as well a panoramic clear atlas of the Galactic plane. UKIDSS is made up of five surveys, three of which are of Galactic nature: the Galactic Plane Survey (GPS), the Galactic Clusters Survey (GCS) and the Large Area Survey (LAS). GPS will image the Galactic plane around half the sky, covering 1800 deg^2 in JHK to a depth $K=19.0$. The K-band depth will be built up in three passes, to identify variability and measure proper motions over a period of several years. Additionally 300 deg^2 of the Taurus-Auriga-Perseus (T-A-P) star-formation complex will be scanned three times through a narrow-band H_2 filter ($2.12\mu\text{m}$). The GPS will require 186 nights of UKIRT time over 7 years. GCS will image 10 open star clusters and star-formation associations, covering a total area of 1400 deg^2 , in JHK to a depth $K=18.7$. The survey requires 74 nights

Table 5: Summary of operational and planned photometric surveys/facilities. Some of them also include spectroscopy.

Survey/ Mission	PI	Instrument/ Telescope	Status ⁽¹⁾	Years of operation	Goals
Ground-based					
IPHAS	Drew	WFC/INT	close to completion	2003 - 2008?	1800 deg ² , NGP
UKIDSS	Consortium	WFCAM/UKIRT	on-going	2005 - 2012	7500 deg ² , North
UVEX	Groot	WFC/INT	on-going	2006 - ?	1800 deg ² , NGP
VHS	ESO/McMahon	VIRCAM/VISTA	being commissioned	2009 - 2014	~ 20 000 deg ² , South
VMC	ESO/Cioni	VIRCAM/VISTA	being commissioned	2009 - 2014	184 deg ² , LMC & SMC
VVV	ESO/Minniti	VIRCAM/VISTA	being commissioned	2009 - 2014	520 deg ² , bulge + adj.plane
VPHAS+	ESO/Drew	ω Cam/VST	under construction	2009? -	1800 deg ² , SGP
<i>Pan-STARRS</i>	Hawai'i U.	<i>PanSTARRS</i>	prototype	2007-2020	30 000 deg ² , North
<i>SSS</i>	ANU/RSAA	SkyMapper	under construction	2009? -	Southern sky
<i>LSST</i>	LSST Corp.	<i>LSST</i>	partly funded	2015-2025	20 000 deg ² , South
Space-based					
XMM	ESA	EPIC	operational	1999-	360 deg ² , 2×10^5 sources
INTEGRAL	ESA	IBIS	operational	2002-	70% of the sky, key programmes
<i>GLIMPSE</i>	NASA	IRAC/Spitzer	on-going ⁽²⁾	2003-2008	legacy programmes
<i>MIPSGAL</i>	NASA	MIPS/Spitzer	operational ⁽²⁾	2005 - 2008	278 deg ² , Galactic Plane
Herschel	ESA	PACS/SPIRE/HIFI ⁽³⁾	fully funded	2008-2012	key programmes
Gaia	ESA		fully funded	2011 - 2017	all-sky
<i>AKARI</i>	JAXA	Akari	completed	2006-2007	all-sky

⁽¹⁾ status may refer to surveys (IPHAS, UKIDSS, GLIMPSE, MIPSGAL) or to facilities (all others)

⁽²⁾ all observations have been collected, final data release(s) are pending

⁽³⁾ these are the three instruments on board of Herschel mission

Table 6: Selected characteristics of operational and planned photometric surveys (cf Table 6.3). Some of them also include spectroscopy and/or spectro-photometry.

Survey/ Mission	Wavelength range / band	FOV	Bands	Pixel size/ angular res.	Spectral resolution
Ground-based					
IPHAS	optical	0.25 deg ²	H α , r' , i'	0.33"/pix	
UKIDSS	infrared	0.75 deg ²	Y, J, H, K, H ₂	0.4"/pix	
UVEX	blue/optical	0.25 deg ²	u' , g' , r' , HeI5875	0.33"/pix	
VHS	infrared	1.65 deg ²	J, K _s ^s + Y, H for Galactic Caps		
VMC	infrared	1.65 deg ²	Y, J, K _s		
VVV	infrared	1.65 deg ²	Z, Y, J, H, K _s		
VPHAS+	optical	1 deg ²	H α + broadband u' , g' , r' , i'	0.21"	
<i>Pan-STARRS</i>	optical	3 deg ²	broadband		
SSS	0.33 - 0.96 μ m	8 deg ²	u , v , g , r , i , z	0.5"	
<i>LSS</i>	0.3 - 1 μ m	9.6 deg ²	u , g , r , i , z , y		
Space-based					
XMM (EPIC)	0.15 - 15 keV	30'		40 μ m / <5"	20-50
INTEGRAL (IBIS)	17 keV - 100 keV	9 \times 9 deg ²		... / 12'	
<i>GLIMPSE</i>	3.6, 4.5, 5.8, 8.0 μ m	5.2' \times 5.2'	4	1.2"	
<i>MIPSGAL</i>	24 μ m, 70 μ m	5.4' \times 5.4', 5.25' \times 2.6' (1)	2	2.55", 5.3" or 9.96"	40-1 000
Herschel (PACS)	60-210 μ m	1.5 \times 3.5'	2 (wide)	5-12"	1 500
Herschel (SPIRE)	210-600 μ m	4 \times 8'	3	12-34"	10 ⁷
Herschel (HIFI)	150-600 μ m	12-40" beam	heterodyne		10 ⁷
Gaia	0.33-1.00 μ m (2)	2 \times (0.7 \times 0.7 deg ²)	4 (spectro-phot)	10 \times 30 μ m ²	11 500
<i>AKARI</i>	6 to 180	10' \times 10'	6 (for survey)	< 10"	

(1) there is also the option of 2.6' \times 1.3'

(2) this range will be covered by two channels: 0.33-0.68 μ m and 0.65-1.0 μ m

spread over 7 years and it will be completed in two stages: first a single pass in JHK over 1400 deg^2 , followed by an additional pass in K over the same 1400 deg^2 , for proper motions, with a baseline of at least 2 years. LAS is an off plane survey and will image an area of 4000 deg^2 at high Galactic latitudes in the $YJHK$ filters to a depth $K=18.4$, requiring 262 nights of UKIRT time over 7 years. This survey will be completed in two stages: first, a single pass in $YJHK$ over the full selected areas, second an additional pass in J for proper motions, with a baseline of at least 2 years (Lawrence et al., 2007).

UVEX – UV EXcess survey of the North Galactic Plane: this survey is the blue counterpart (u', g', r' follow-up) of IPHAS, using the same instrument (WFC), reaching the same limiting magnitude and covering the same survey areas. The re-observation of the r' band is for proper motions and also to tie IPHAS/UVEX photometry together. As for IPHAS, this is also a double pass survey. The scientific aims of UVEX are to provide the first ever blue-excess catalog of objects in the Galactic Plane, in particular the survey team is searching for the majority of the populations of white dwarfs, white dwarf binaries, subdwarf B-stars, interacting binaries with a neutron star or black hole as a primary. The survey started in 2006 on the 2.5m Isaac Newton telescope and it is on going (approximately 30% complete). Results obtained so far include the detection of a number of rare planetary nebulae, cataclysmic variables, red-dwarf white dwarf binaries in clusters, a possible AM CVn candidate, and a deep photometric and spectroscopic investigation of the Cyg X region (Groot et al., 2006). It should be noted that altogether IPHAS, UVEX, and VPHAS+ make up the so-called European GALactic Plane Surveys (EGAPS) project.

VHS – VISTA Hemisphere Survey: the VHS is one of the six Public Surveys approved to be conducted on the 4m near-infrared VISTA telescope, during its first 5 years of operations. VISTA is equipped with the VIRCAM camera, a large array of 16 infrared detectors that will fill a 1.5 deg^2 field (after stepping to cover the detector gaps). VHS will image the entire 20000 deg^2 of the Southern Sky, with the exception of the areas already covered by the VIKING and VVV surveys, in J and Ks . The resulting data will be about 4 magnitudes deeper than 2MASS and DENIS. The 5000 deg^2 covered by the Dark Energy Survey (DES), another imaging survey scheduled to begin in 2010 at the CTIO 4m Blanco telescope, will also be observed in H -band. The area around both of the Galactic Caps will be observed in Y and H bands as well as will be combined with the data from the VST ATLAS survey. The main science drivers of VHS include: examining low mass and nearby stars, studying the merger history of the Galaxy, measuring the properties of Dark Energy through the examination of large-scale structure to a redshift of ~ 1 , and searches for high redshift quasars. More information available from: <http://www.ast.cam.ac.uk/~rgm/vhs>.

VMC – VISTA Magellanic Clouds: this survey will image 184 deg² of the Magellanic System, i.e., the Large Magellanic Cloud, the Small Magellanic Cloud, the Bridge, and the Magellanic Stream in the Y , J , and Ks wavebands. Multi-epoch observations will constrain the mean magnitude of short-period variables. The survey will be used to study resolved stellar populations, the star formation history of the system as well as to trace its three-dimensional structure (Cioni, 2007).

VVV – VISTA Variables in the Via Lactea: this survey will target the galactic bulge and a piece of the adjacent plane in Z , Y , J , H , and Ks . The total area of this survey is 520 deg² and contains 355 open and 33 globular clusters. The VVV is multi-epoch in nature in order to detect a large number of variable objects and will provide > 100 carefully spaced observations for each tile. A catalogue with $\sim 10^9$ point sources including $\sim 10^6$ variable objects is expected. These will be used to create a 3-dimensional map of the Bulge from well-understood distance indicators such as RR Lyrae stars. Other science drivers include the ages of stellar populations, globular cluster evolution, as well as the stellar initial mass function (Minniti et al., 2006).

VPHAS+ – VST Photometric H α Survey of the Southern Galactic Plane: this is one of the three public surveys approved to be carried out on the 2.6 m optical VLT Survey Telescope (VST) equipped with OmegaCAM, which comprises 32 2k \times 4k CCDs (with 15 μm pixels). The VPHAS+ survey will combine H α and broadband u' , g' , r' , i' imaging over an area of 1800 deg² capturing the whole of the Southern Galactic Plane within the latitude range $|b| < 5$ deg. VPHAS+ will facilitate detailed extinction mapping of the Galactic Plane, and can be used to map the structure of the Galactic disc and its star formation history. The survey will yield a catalogue of around 500 million objects, which will include greatly enhanced samples of rare evolved massive stars, Be stars, Herbig and T Tau stars, post-AGB stars, compact nebulae, white dwarfs and interacting binaries. This survey is complementary to IPHAS, a survey of the Northern Galactic Plane nearing completion, but VPHAS+ will include more filters and will achieve better image quality. More information available from: <http://www.vphas.org/index.shtml>.

Pan-STARRS – See Section 6.1.

SSS – *Southern Sky Survey*: this survey has been allocated 75% (at least initially) of the time on the SkyMapper 1.3 m survey telescope, which will have an 8 deg² field of view. SSS which includes multi-colour, multi-epoch observations of all 20 000 deg² south of the Equator in u , g , r , i , z and one Strömgen-like v filter. The survey aims at reaching 3% absolute photometric calibration, an astrometric solution better than 50 mas, and a depth down to 21-22 after 6 epochs. The multi-epoch frequency will be: first epoch, +4 hours, +2-3 days, +1-2 weeks and +1-2

years. In addition, a 5-Second Survey will be undertaken in photometric conditions for calibration of stars of 9-16th magnitude in all bands, providing the calibration of the survey and allowing the survey to be tied to the Hipparcos and Tycho catalogues. One of the main outcomes will be a Galactic Census (metallicity, gravity, temperature, variability) of 5 billion stars (Murphy et al., 2008). More information available from: <http://www.mso.anu.edu.au/~stefan/skymapper/survey.php>.

LSST – See Section 6.1.

XMM (EPIC) – The Second XMM-Newton EPIC Serendipitous Source Catalogue contains 246 897 X-ray source detections which relate to 191 870 unique X-ray sources, making it the largest collection of X-ray objects ever compiled (<http://xmmssc-www.star.le.ac.uk/Catalogue/2XMM>). The total area covered on the sky by the combined observation fields is 360 deg². EPIC is the European Photon Imaging Camera, on board of XMM.

INTEGRAL (IBIS) – INTErnational Gamma-Ray Astrophysics Laboratory: IBIS is the imager instrument on-board of INTEGRAL, which is the first space observatory that can simultaneously observe objects in gamma rays, X-rays, and visible light. Its principal targets are violent explosions known as gamma-ray bursts, powerful phenomena such as supernova explosions, and regions in the Universe thought to contain black holes. It was launched in 2002 and it is still operational. At the beginning of 2007, INTEGRAL had observed over 70% of the sky, with a total exposure time of 40 million seconds. Three years' worth of data has resulted in the third INTEGRAL/IBIS catalogue of gamma-ray sources, containing a total of 421 gamma-ray objects (Bird et al., 2007). As of 2006, ESA has introduced the new Key Programme philosophy into the INTEGRAL observing programme and schedule, which means allocating a significant amount of time to one specific programme. So far, the three Key Programmes that have been selected focus on the Galactic Centre, the Cygnus, and the North Ecliptic Pole regions.

GLIMPSE – *Galactic Legacy Infrared Mid-Plane Survey Extraordinaire*: this is the main Galactic Legacy programme with the Spitzer Space Telescope that was launched into space in mid 2003. *GLIMPSE* is an infrared survey of the inner Galactic plane that uses the Infrared Array Camera (IRAC). It has three main parts: GLIMPSE I covers a latitude range of ± 1 deg, and a longitude range of $l = 10$ to 65 deg (Benjamin et al., 2003); GLIMPSE II images longitudes ± 10 deg of the central region of the Galaxy. The latitude coverage is ± 1 deg from $l = 10$ to 5 deg, ± 1.5 deg from $l = 5$ to 2 deg, and ± 2 deg from $l = 2$ to 0 deg; GLIMPSE-3D studies the vertical stellar and interstellar structure of the Inner Galaxy by observing latitude strips farther away from the Galactic plane. The data products consist of source lists and mosaiced images. The final and cumulative sum of all GLIMPSE I products was released in early 2007, mosaics (v. 2.0) and source lists

(v. 3.5) for the entire GLIMPSE II area have been released in April 2008, and the data deliveries for GLIMPSE 3D (mid 2007 and early 2008) include 10 regions (2×2 deg). More information available from: <http://www.astro.wisc.edu/sirtf>.

MIPSGAL: this is a 278 degree Galactic plane survey conducted through the Multiband Infrared Photometer for Spitzer (MIPS) instrument on the Spitzer Space Telescope, at 24 and 70 microns. The survey was designed to complement and match the spatial coverage of the *GLIMPSE* survey which focuses on shorter wavelengths (3-9 microns). The main science goals of *MIPSGAL* are to identify and study massive stars forming in the inner Galaxy and investigate the distribution and energetics of interstellar dust in our Galaxy. The main data deliveries of this survey are mosaic images at 24 and 70 microns, and their related source catalogs. The 24 microns mosaic images were released in Fall 2007, everything else is planned for Spring/Summer 2008.

Herschel: this is the very next ESA space mission to be launched (scheduled for end of 2008). Herschel Space Observatory is equipped with a 3.5 m reflecting telescope and instruments cooled to close to absolute zero, allowing observations at wavelengths that have never previously been explored, from the far infrared to sub-millimetre wavelengths (60 - 670 μm). The main scientific driver is to study formation and evolution of galaxies and stars and their interrelationship with the interstellar medium. Herschel is equipped with three cryogenically cooled instruments: the Photodetector Array Camera & Spectrometer (PACS), the Spectral and Photometric Imaging Receiver (SPIRE), and the Heterodyne Instrument for the Far-Infrared (HIFI). The first set of 42 Key Programmes (21 for Guaranteed and 21 for Open Time) has been approved and the list is available from: http://herschel.esac.esa.int/Key_Programmes.shtml.

AKARI: the main objective of the *AKARI* (formerly known as ASTRO-F) infrared astronomical mission was to make an all-sky survey at infrared wavelengths with a sensitivity one order of magnitude better and resolution a few times higher than IRAS (Infrared Astronomical Satellite). Equipped with a 68.5 cm telescope cooled down to 6K, it has observed in the wavelength range from 1.7 (near-infrared) to 180 (far-infrared) μm . *AKARI* was successfully launched into space in 2006 and has ceased operations at the end of August 2007. In addition to the all-sky survey, *AKARI* performed more than 5000 pointed observations over the wavelength range 2-180 μm in 13 bands (Murakami et al., 2007). ESA contributed by providing tracking support from the ground station in Kiruna. In return, 10% of the observing opportunities in the non-survey parts of the mission have been distributed to European scientists.

6.4 Other ground-based facilities

Table 7 presents a summary of operational and planned ground-based facilities and associated instruments. The list is not exhaustive, instead it focuses on those instruments most relevant to address the main scientific topics of this Working Group.

A major step forward in this field will obviously be accomplished when the new generation of extremely large telescopes (ELT) will become operational. Three major projects are currently been developed: the European efforts are concentrating on what for the time being is called the European ELT (E-ELT), whereas the American community is involved in the design of two such facilities: the Giant Magellan Telescope (GMT) and the Thirty Meter Telescope (TMT). There is a lot of excitement and on-going activities around these future facilities, although none of the projects currently under study has been fully funded. Despite this uncertainty, we think it is important to provide an overview of what these projects and their aims are. The on-going instrument design studies are driven by those science cases that the astronomical community (at large, considering the large overlap) has identified as the most important to tackle in the ELT era.

In what follows, Table 8 summarises the main on-going projects, whereas Table 9 lists the preliminary characteristics of possible first generation instruments that are under study for E-ELT, GMT and TMT respectively. Clearly, not all of these will actually become first generation instruments. For the E-ELT, for instance, the first generation instruments will be defined out of these concepts, in the E-ELT construction proposal, due in June 2010.

Table 7: *Summary of main operational or planned ground-based facilities*

Facility	PI	Status	Start of operation	Instruments	Comments
GTC	IAC	final stages	2009-	OSIRIS, EMIR	(1)
VISTA	ESO	being commissioned	2009 -	WF NIR camera	(2)
VLT	ESO	operational	1999-	several	(3)
VST	Italy/ESO	under construction	2009 -	OmegaCAM	(2)
<i>Gemini</i>	International	operational	2001-	several	
<i>Hobby Eberly</i>	Joint Project	operational	1999-	several	
<i>Keck</i>	Private	operational	1994-	several	
<i>LAMOST</i>	China	under construction	2009-	MOS (optical)	(4)
<i>LBT</i>	Consortium	passed first light	2009? -	LUCHFER (IR), PEPSI (high-res spectr.)	
<i>SALT</i>	Consortium	partly operational	2005-	SALTICAM, RSS, HRS	(5)
<i>SOAR</i>	Consortium	operational	2006-	several	(3)
<i>Subaru</i>	NAOJ	operational	2000-	several	(3)
<i>WYYN</i>	Consortium	operational	1994 -	several	(6)
E-ELT	ESO + ?	Design Phase	2017?-	several	(7)
<i>GMT</i>	Consortium	Planned	2017? -	several	(7)
<i>TMT</i>	Public/private partnership	Design Phase	2017? -	several	(7)

- (1) intermediate resolution spectroscopy in Z, J, H, K bands
- (2) Public Surveys (see Table 6.3)
- (3) 2nd generation instruments underway
- (4) up to 4000 fibres available
- (5) 1st generation instruments
- (6) One Degree Imager (under construction)
- (7) Choice of instruments driven by science cases

Table 8: *Design studies of first generation instruments for extremely large telescopes*

Telescope	Instrument	Configuration	Science Case(s)
E-ELT ⁽¹⁾	MICADO HARMONI CODEX EPICS + XAO EAGLE METIS SIMPLE ⁽³⁾ OPTIMOS ⁽³⁾	NIR camera sampling to the DL ⁽²⁾ single IFU, wide band spectr. High-Res Vis spectroscopy imaging + spectroscopy WF, multi IFU NIR spectrograph mid-IR imaging + spectroscopy NIR high-res spectrograph Visual-J-band MOS	almost all all expansion Universe exoplanets and circumstellar discs first light, stellar populations exoplanets planet spectr. search, stell. abund. galaxies survey, stellar abundances
<i>GMT</i> ⁽⁴⁾	GMACS NIRMOS Visible Echelle GMTNIRS MIISE HRCAM	Wide Field Optical Spectrograph 4 multi-slit spectrographs Wide Field NIR Spectrograph High-res optical spectrograph NIR Echelle Spectroscopy (LTAO - Natural Seeing) MIR imaging spectrograph, DL NIR AO imager	galaxy and chem. evolution, IGM tomography, dark energy and matter galaxy evolution at high-z, AGN radial velocity surveys, stellar abundances and populations young stars, dense clouds
<i>TMT</i> ⁽⁵⁾	IRIS IRMS WFOS MIREs PFI HRoS IRMOS WIRC NIREs	IR Imaging Spectrometer IR Multi-slit Spectrometer Wide-Field Optical Spectrometer MIR Echelle Spectrometer Planet Formation Instrument High-Res Optical Spectrometer IR Multi-Object Spectrometer Wide-Field IR Camera NIR Echelle Spectrometer	young planets bright exoplanets in reflected light early light, high-z galaxy assembling, resolved stellar populations, AGN/BH/GC early light, JWST follow-ups early light, stell. pops + chemical evolution protostars, protoplanetary discs direct detection and characterisation of exoplanets abundances in ISM, Local Group, IGM up to $z \sim 6$ JWST follow-ups GC astrometry, resolved stellar populations out to 10 Mpc IGM $z > 7$, Doppler detection planets, abundances in Local Group

⁽¹⁾ More information about the E-ELT Science Cases can be found at: <http://www.eso.org/public/astronomy/projects/e-elt.html>

⁽²⁾ DL = diffraction limit

⁽³⁾ Under discussion. Possible study to start in Fall 2008

⁽⁴⁾ More information about the GMT Science Cases can be found at: <http://www.gmto.org/sciencecase>

⁽⁵⁾ More information about the TMT Science Cases can be found at: <http://www.tmt.org/science/index.html> and <http://www.physics.uci.edu/TMT-Workshop/TMT-Handbook.pdf>

Table 9: *Characteristics of first generation instruments for extremely large telescopes*

Telescope	Instrument	Wavelength μm	Resolution	FOV
E-ELT	MICADO	0.8-2.4	wide, narrow bands	$> 30''$
	HARMONI	0.8-2.4	4000 (20 000)	point source
	CODEX	0.37-0.69	$> 120\,000$	$2''$ in V, $4''$ in H
	EPICS + XAO	0.6-1.8	$> 50 + \text{imaging}$ in Y and H bands	
	EAGLE	0.8-2.5	5 000 ($> 15\,000$)	$\geq 5'$ (> 20 arms)
	METIS	3-13 (16-20)	wide/narrow bands R=100 and 100 000	$> 30''$
	SIMPLE	0.8-2.4	120 000	point source
	OPTIMOS	0.37-1.4(1.7)	1 000-20 000	$> 5'D$
GMT	GMAOS	0.4 - 1.0	3 500 - 5 000	$9' \times 18'$
	NIRMOS	0.9-2.5	1 500 - 3 500	$5' \times 5'$
	Visible Echelle	0.3-1.0	20-100 000	$20''$
	GMTNIRS	1- 5	50-120 000	$30''$
	MISE	3 - 28	5 - 2 000	$2' \times 2'$
	HRCAM	1 - 2.5	5 - 2 000	$30''$
TMT	IRIS	0.8 - 2.5	4 000	$10'' \times 10''$ (imaging)
	IRM5	0.8 - 2.5	2 - 10 000	$2.3' \times 2.3'$
	WFO5	0.34 - 1.0	150 - 7 500	$40.5'^2$
	MIRE5	8.0 - 18	5 - 100 000	$3''$
	IRMOS	0.8 - 2.5	2 - 10 000	$5'$ (patrol field), $2''$ / IFU
	PFI	1.1 - 2.4	70 - 500	$2.2'' \times 2.2''$
	HR05	0.34 - 1.0	30 - 100 000	$20''$
	WIRC	0.8 - 5	5 - 100	$30'' \times 30''$
	NIRE5	1 - 5	5 - 30 000	$2''$

7 Recommendations

Europe has led the way in Galactic research as regards astrometry and spectroscopy and is on the brink of taking the lead in photometry: ESA's Hipparcos mission pioneered space astrometry and paved the way for the ambitious Gaia mission, which will perform the first parallax survey down to magnitude $V = 20$; ESO's innovative telescopes (NTT and VLT) coupled to leading capabilities in the construction of multi-object spectrographs have yielded detailed stellar abundances of faint stars; ESO is about to start massive programs of optical/near-IR photometry with two dedicated survey telescopes (VISTA and VST). This observational work is backed by unique European expertise in modelling stars and galaxies (stellar atmospheres, stellar and galactic evolution, population synthesis, dynamics, etc.).

The opportunities for European science are tremendous if we make strenuous efforts fully to capitalise on these assets. This involves both taking full advantage of the instrumentation that we have and planning new facilities. Particular attention has to be paid to the optimisation of synergies between Gaia and ground-based observations, especially with present or potential ESO instruments.

A number of suggestions in this direction are given below.

(1) ESA initiatives

- (a) **Gaia**: make maximum effort to achieve the science requirements (accuracies and limiting magnitudes for the astrometric, photometric and spectroscopic aspects of the mission). Only if these requirements are fulfilled can the satellite provide the promised revolution in our knowledge of the Galaxy by unveiling populations through the study of chemistry and dynamics.
[All subsections of Section 5].
- (b) **Infrared astrometry**: this would be the ideal complement to Gaia, which is not able to observe deeply in the Galactic centre, the bulge and parts of the disc because of heavy extinction and crowding. ESA should encourage the community to submit proposals for an IR instrument that has an astrometric accuracy of $10 \mu\text{as}$ down to magnitude 17 in the $0.9 \mu\text{m } z$ band. A first step in this direction might be a collaboration with the Japanese project JASMINE ($10 \mu\text{as}$ astrometric accuracy for stars brighter than $z = 14$).
[Sections 5.1.5, 5.2, 5.3, 5.4].
- (c) **Higher astrometric accuracy in the optical** (better than $4 \mu\text{as}$): this is the requirement for resolving the internal motions of the outer

globular clusters and dwarf galaxies of the Local Group, for which Gaia will provide only mean motions. This capability would also enable us to obtain direct distances to extragalactic stellar candles. ESA should encourage the community to prepare for the next generation of astrometric missions.

[Sections 5.7, 5.8].

- (d) **Asteroseismology:** this is a major tool to complement Gaia with respect to age determination. ESA should encourage the community to prepare for a next-generation mission, which would sample the different populations of the Galaxy much more widely than CNES-ESA's Corot (50 targets, mainly main-sequence stars with a metallicity close to solar) and NASA's Kepler (mainly main-sequence stars, some giants and pulsating stars).

[Sections 5.1.6, 5.4, 5.5, 5.6, 5.7].

- (e) **UV spectroscopy:** Ground-based adaptive optics (AO) has reduced Hubble's advantage at optical wavelengths. But now that NASA's satellite FUSE has died, UV wavelengths are only accessible through Hubble. ESA should support the longevity of Hubble, with a substantial share of its observing time being devoted to UV instruments, and support the use of COS, the new UV spectrograph to be installed on Hubble during the Servicing Mission 4.

[Sections 5.1.8, 5.1.4, 5.8].

(2) ESO initiatives

- (a) **Blue multiplexed spectrograph on 4 or 8 m class telescope:** ESO should consider the construction of a multi-object spectrograph (> 100 fibres) with high blue sensitivity ($S/N \sim 30-40$) and high resolving power (20 000 to 30 000) which can measure detailed abundances in 20 000 to 50 000 halo, thick-disc and outer thin-disc stars. This could be either on a dedicated 8 m class telescope with field of view (FOV) $\sim 0.5 \text{ deg}^2$, or on a dedicated 4 m telescope with FOV $\sim 2.5 \text{ deg}^2$.

[Sections 5.1.1, 5.1.2, 5.1.6, 5.1.7, 5.1.8, 5.4, 5.5, 5.6, 5.7].

- (b) **IR highly multiplexed spectrograph on 4 m class telescope:** ESO should consider the construction of a spectrograph with IR capabilities, to be placed on a dedicated 4 m survey telescope, with AO correction, massive multiplexing (> 500 fibres), $S/N \sim 20-30$, high resolving power (20 000 to 30 000) and large field of view. This instrument would obtain detailed abundances and radial velocities for 20 000 to 50 000 obscured bulge, thin-disc stars. A lower resolution mode (R

$\simeq 4000$) would also be perfect for fainter targets, not observed by the RVS on board Gaia. ESO may also consider collaboration with teams starting the development of such instruments (APOGEE in the USA; WINERED in Japan; Ukidna in Australia).
[Sections 5.1.1, 5.1.3, 5.2, 5.3, 5.4].

- (c) **IR multiplex spectrograph on 8 m class telescope:** ESO should consider improving the capabilities of current VLT multiplex spectrographs for larger field of view and infrared wavelengths.
[Sections 5.1.6, 5.1.7, 5.4, 5.5, 5.6, 5.7].
- (d) **Spectrograph on the E-ELT:** ESO should consider a spectrograph with very high resolving power (40 000 to 70 000) on the E-ELT to observe abundances of stars (Populations II and III stars, F- and G-dwarfs, etc.) across the whole disc and far from the Solar vicinity (bulge, outer halo).
[Sections 5.1.5, 5.1.6, 5.1.7, 5.1.8, 5.2, 5.4, 5.5, 5.7].
- (e) **NIR photometric survey:** It would be very valuable that the Southern Galactic Plane area as well the innermost regions of the Galaxy will have a full NIR coverage. The different VISTA surveys will be an important first step in this direction, but their final goals might be different. ESO should closely follow the sky and wavelength coverage of these surveys, and eventually invest extra observational efforts to ensure the total coverage.
[Sections 5.1.1, 5.1.2, 5.1.3, 5.2, 5.3, 5.4, 5.5].

(3) **ESA-ESO joint initiatives**

- (a) **Calibration of Gaia instruments:** ESA and ESO should jointly facilitate observations with ESO telescopes that are required for the calibration of Gaia instruments.
[All subsections of Section 5].
- (b) **European leadership in the exploitation of Gaia data:** ESA and ESO should jointly consider ways to give European astronomers a lead in the exploitation of the Gaia catalogue and facilitate follow-up observations on a ‘targets to be specified later’ basis.
[All subsections of Section 5].
- (c) **Spectroscopy for selected samples of Gaia targets:** ESA and ESO should jointly consider facilities for medium- to high-resolution

spectroscopic observations of a large number (40 000 - 100 000 stars) of particularly interesting stars selected from Gaia observations. There are two aspects:

- (1) follow-up high spectral resolution observations of particularly interesting samples selected from Gaia data;
- (2) medium spectral resolution observations of stars fainter than $V = 16.5$ and not measured by the Radial Velocity Spectrometer on Gaia. See details in the recommendations to ESO.
[All subsections of Section 5].

- (d) **Observation of the fine structure of the ISM:** We remind ESA and ESO of the issues raised by the ESA-ESO Working Group on Herschel-ALMA synergies with regard to the complementary nature of these facilities and their relative time lines. The capabilities of these facilities together will be important for unravelling the fine structure and kinematics of the Galactic ISM on all spatial scales and the processes of star formation within the Galaxy. Because Herschel comes into operation before ALMA, this Working Group sees a clear need for Herschel time allocation to be mindful of the legacy implications of its suite of supported programmes.
[Sections 5.2, 5.3, 5.4].

- (e) **Enhance the European scientific return from large Galactic surveys:** over the next decade the unique survey facilities of ESA and ESO will produce a huge body of new Galactic data. To maximise the science extracted from these data, ESA and ESO should jointly sponsor
- (1) a number of workshops that would optimise the performance of the European astronomical community in mining these data. The topics should include modelling and theory for stellar interiors and atmospheres; stellar evolution including that of massive stars and binaries; stellar population synthesis; galactic dynamics and specific models of Galactic populations; the interstellar medium and the distribution of dust and gas in the Galaxy;
 - (2) a number of fellowships that would optimise the European efficiency in exploiting these data, aiming both at improving the underlying theory and modelling and at developing high performance analysis techniques.

- (f) **Further ESA-ESO Working Groups:** ESA and ESO should jointly consider setting up further Working Groups to enhance the synergies between their missions and instruments. Two topics are recommended:
- (1) star formation in various environments. This topic will have a strong impetus with the start of the ESO public surveys of the Galactic Plane,

the launch of Herschel, and the progressive and massive enhancement of ground-based sub-mm observations with ALMA;

(2) galaxy formation. The diverse instruments considered for the E-ELT are in their definition phases and it is appropriate to explore fully the possible synergies between E-ELT and JWST instruments to explore in detail the whole Galaxy and its outskirts, in particular the *Terra Incognita* behind the Galactic center.

(4) **Remark**

Our terms of reference were to propose a set of recommendations to ESA and ESO for optimising the exploitation of their current and planned missions. However, the Galaxy is an all-sky object; in fact, from the ground, the outer parts of the Galaxy are best observed from the Northern hemisphere, as the extinction is on-average lower there. In parallel with Recommendations 2(a) to 2(d), there is a real need for dedicated highly multiplexed spectrographs in the Northern hemisphere.

References

- Abadi, M. G., Navarro, J. F., Steinmetz, M., & Eke, V. R. 2003, *ApJ*, 597, 21
- Agertz, O., et al. 2007, *MNRAS*, 380, 963
- Allen, D. A., Hyland, A. R., & Hillier, D. J. 1990, *MNRAS*, 244, 706
- Armandroff, T. E. 1989, *AJ*, 97, 375
- Arnett, D., Meakin, C., & Young, P. 2005, *From Lithium to Uranium: Elemental Tracers of Early Cosmic Evolution*, IAU Symposium, 228, 151
- Ashman, K. M., & Zepf, S. E. 1992, *ApJ*, 384, 50
- Asplund, M., Lambert, D. L., Nissen, P. E., Primas, F., & Smith, V. V. 2006, *ApJ*, 644, 229
- Athanassoula, E. 1992, *MNRAS*, 259, 345
- Athanassoula, E. 2003, *MNRAS*, 341, 1179
- Baade, W. 1944, *ApJ*, 100, 137
- Babusiaux, C., & Gilmore, G. 2005, *MNRAS*, 358, 1309
- Baganoff, F. K., et al. 2003, *ApJ*, 591, 891
- Bailer-Jones, C. A. L. 2006, *Memorie della Società Astronomica Italiana*, 77, 1144
- Bailyn, C. D. 1995, *ARA&A*, 33, 133
- Balser, D. S., Bania, T. M., Rood, R. T., & Wilson, T. L. 1999, *ApJ*, 510, 759
- Balser, D. S., Rood, R. T., & Bania, T. M. 2007, *Science*, 317, 1171
- Bania, T. M., & Lockman, F. J. 1984, *ApJS*, 54, 513
- Battaglia, G., et al. 2005, *MNRAS*, 364, 433
- Battaglia, G., Helmi, A., Tolstoy, E., Irwin, M., Hill, V., & Jablonka, P. 2008, *ApJ*, 681, L13
- Baugh, C. M., Lacey, C. G., Frenk, C. S., Granato, G. L., Silva, L., Bressan, A., Benson, A. J., & Cole, S. 2005, *MNRAS*, 356, 1191
- Bedregal, A. G., Aragón-Salamanca, A., & Merrifield, M. R. 2006, *MNRAS*, 373, 1125
- Beers, T. C., & Christlieb, N. 2005, *ARA&A*, 43, 531
- Beers, T. C., & Sommer-Larsen, J. 1995, *ApJS*, 96, 175
- Bell, E. F., et al. 2008, *ApJ*, 680, 295
- Bellazzini, M., Ferraro, F. R., & Ibata, R. 2003, *AJ*, 125, 188

- Bekenstein, J., & Milgrom, M. 1984, *ApJ*, 286, 7
- Belokurov, V., Evans, N. W., Irwin, M. J., Hewett, P. C., & Wilkinson, M. I. 2006a, *ApJ*, 637, L29
- Belokurov, V., et al. 2006b, *ApJ*, 642, L137
- Belokurov, V., et al. 2007a, *ApJ*, 654, 897
- Belokurov, V., et al. 2007b, *ApJ*, 658, 337
- Benjamin, R. A., et al. 2003, *PASP*, 115, 953
- Benjamin, R. A., et al. 2005, *ApJ*, 630, L149
- Bensby, T., Feltzing, S., & Lundström, I. 2004, *A&A*, 415, 155
- Bensby, T., Feltzing, S., Lundström, I., & Ilyin, I. 2005, *A&A*, 433, 185
- Bensby, T., Zenn, A. R., Oey, M. S., & Feltzing, S. 2007, *From Stars to Galaxies: Building the Pieces to Build Up the Universe*, ASP Conference Series, 374, 181
- Bernkopf, J., & Fuhrmann, K. 2006, *MNRAS*, 369, 673
- Bernkopf, J., Fidler, A., & Fuhrmann, K. 2001, *Astrophysical Ages and Times Scales*, ASP Conference Series, 245, 207
- Besla, G., Kallivayalil, N., Hernquist, L., Robertson, B., Cox, T. J., van der Marel, R. P., & Alcock, C. 2007, *ApJ*, 668, 949
- Bienayme, O., Robin, A. C., & Creze, M. 1987, *A&A*, 180, 94
- Binney, J. 2004, *MNRAS*, 347, 1093
- Binney, J., Bissantz, N., & Gerhard, O. 2000, *ApJ*, 537, L99
- Binney, J., & Dehnen, W. 1997, *MNRAS*, 287, L5
- Binney, J., & May, A. 1986, *MNRAS*, 218, 743
- Binney, J., & Merrifield, M. 1998, *Galactic astronomy / James Binney and Michael Merrifield*. Princeton, NJ, USA, Princeton University Press
- Binney, J., & Tremaine, S. 2008, *Galactic Dynamics: Second Edition*, by James Binney and Scott Tremaine. ISBN 978-0-691-13026-2. Princeton, NJ, USA, Princeton University Press
- Binney, J., Gerhard, O. E., Stark, A. A., Bally, J., & Uchida, K. I. 1991, *MNRAS*, 252, 210
- Binney, J., Gerhard, O., & Spergel, D. 1997, *MNRAS*, 288, 365
- Binney, J., Jiang, I-G., & Dutta, S. 1998, *MNRAS*, 297, 1237
- Binney, J., Dehnen, W., & Bertelli, G. 2000, *MNRAS*, 318, 658

- Binney, J. 2008, MNRAS, 386, L47
- Bird, A. J., et al. 2007, ApJS, 170, 175
- Bissantz, N., Debattista, V. P., & Gerhard, O. 2004, ApJ, 601, L155
- Bissantz, N., Englmaier, P., & Gerhard, O. 2003, MNRAS, 340, 949
- Bissantz, N., & Gerhard, O. 2002, MNRAS, 330, 591
- Bland-Hawthorn, J., & Cohen, M. 2003, ApJ, 582, 246
- Blitz, L., & Spergel, D. N. 1991, ApJ, 379, 631
- Blum, R. D., Ramírez, S. V., Sellgren, K., & Olsen, K. 2003, ApJ, 597, 323
- Blumenthal, G. R., Faber, S. M., Primack, J. R., & Rees, M. J. 1984, Nature, 311, 517
- Bonnell, I. A., & Bate, M. R. 2006, MNRAS, 370, 488
- Bosma, A., 1978, *The Distribution and Kinematics of Neutral Hydrogen in Spiral Galaxies*, Ph.D. Thesis, Groningen University, Groningen
- Bournaud, F., Elmegreen, B. G., & Elmegreen, D. M. 2007, ApJ, 670, 237
- Brand, J., & Blitz, L. 1993, A&A, 275, 67
- Brand, J., & Wouterloot, J. G. A. 2007, A&A, 464, 909
- Bregman, J. N. 1980, ApJ, 236, 577
- Bridges, T. J., & Hanes, D. A. 1990, AJ, 99, 1100
- Briggs, F. H. 1990, ApJ, 352, 15
- Brook, C. B., Gibson, B. K., Martel, H., & Kawata, D. 2005, ApJ, 630, 298
- Brown, A. G. A., 2002, ASP Conference Series, 285, 150
- Brown, W. R., Geller, M. J., Kenyon, S. J., & Kurtz, M. J. 2005, ApJ, 622, L33
- Brown, T. M., Smith, E., Ferguson, H. C., Rich, R. M., Guhathakurta, P., Renzini, A., Sweigart, A. V., & Kimble, R. A. 2006, ApJ, 652, 323
- Bullock, J. S., Kravtsov, A. V., & Weinberg, D. H. 2000, ApJ, 539, 517
- Bullock, J. S., & Johnston, K. V. 2005, ApJ, 635, 931
- Burbidge, E. M., Burbidge, G. R., Fowler, W. A., & Hoyle, F. 1957, Reviews of Modern Physics, 29, 547
- Buzzoni, A. 1995, Fresh Views of Elliptical Galaxies, ASP Conference Series, 86, 189
- Cabrera-Lavers, A., Garzón, F., & Hammersley, P. L. 2005, A&A, 433, 173

- Carlberg, R. G., & Sellwood, J. A. 1985, *ApJ*, 292, 79
- Carollo, D., et al. 2007, *Nature*, 450, 1020
- Carney, B. W., Latham, D. W., & Laird, J. B. 1989, *AJ*, 97, 423
- Catalán, S., Isern, J., García-Berro, E., & Ribas, I. 2008, *MNRAS*, 387, 1693
- Cayrel, R., et al. 2001, *Nature*, 409, 691
- Cayrel, R., et al. 2004, *A&A*, 416, 1117
- Cayrel, R., et al. 2007, *A&A*, 473, L37
- Cervino, M., Luridiana, V., 2005, *Resolved Stellar Populations*, ASP Conference Series
- Chambers, K. C. 2005, *Astrometry in the Age of the Next Generation of Large Telescopes*, ASP Conference Series, 338, 134
- Charbonnel, C. 2005, *Planetary Nebulae as Astronomical Tools*, 804, 117
- Charbonnel, C. 1995, *ApJ*, 453, L41
- Charbonnel, C., & Zahn, J.-P. 2007, *A&A*, 476, L29
- Chiappini, C., Matteucci, F., & Gratton, R. 1997, *ApJ*, 477, 765
- Chiappini, C., Matteucci, F., & Padoan, P. 2000, *ApJ*, 528, 711
- Chiappini, C., Renda, A., & Matteucci, F. 2002, *A&A*, 395, 789
- Chiappini, C., Romano, D., & Matteucci, F. 2003, *MNRAS*, 339, 63
- Chiappini, C., Hirschi, R., Meynet, G., Ekström, S., Maeder, A., & Matteucci, F. 2006, *A&A*, 449, L27
- Chiappini, C., Ekström, S., Meynet, G., Hirschi, R., Maeder, A., & Charbonnel, C. 2008, *A&A*, 479, L9
- Chou, M.-Y., et al. 2007, *ApJ*, 670, 346
- Christensen-Dalsgaard, J., 1988, *IAU Symposium*, 123, 295
- Christensen-Dalsgaard, J., Bedding, T. R., & Kjeldsen, H. 1995, *ApJ*, 443, L29
- Christlieb, N., et al. 2002, *Nature*, 419, 904
- Cioni, M.-R. L. 2007, *IAU Symposium*, 241, 300
- Ciotti, L., Londrillo, P., & Nipoti, C. 2006, *ApJ*, 640, 741
- Clark, P. C., Klessen, R. S., Bonnell, I. A. 2007, *MNRAS*, 379, 57
- Clark, J. S., Negueruela, I., Crowther, P. A., & Goodwin, S. P. 2005, *A&A*, 434, 949

- Coc, A. 2008, *Stellar Nucleosynthesis: 50 years after B2FH*, eds. C. Charbonnel and J. P. Zahn, EAS publication Series (in press)
- Coc, A., Vangioni-Flam, E., Descouvemont, P., Adahchour, A., & Angulo, C. 2004, *ApJ*, 600, 544
- Cordes, J. M., & Lazio(2002)]2002astro.ph..7156C Cordes, J. M., & Lazio, T. J. W. 2002, *ArXiv Astrophysics e-prints*, arXiv:astro-ph/0207156
- Côté, P., Marzke, R. O., West, M. J., & Minniti, D. 2000, *ApJ*, 533, 869
- Creze, M., Chereul, E., Bienayme, O., & Pichon, C. 1998, *A&A*, 329, 920
- da Silva, L., et al. 2006, *A&A*, 458, 609
- Dame, T. M., Hartmann, D., & Thaddeus, P. 2001, *ApJ*, 547, 792
- D'Antona, F., & Ventura, P. 2007, *MNRAS*, 379, 1431
- de La Fuente Marcos, R., & de La Fuente Marcos, C. 2004, *New Astronomy*, 10, 53
- De Marco, O., Hillwig, T. C., & Smith, A. J. 2008, *ArXiv e-prints*, 804, arXiv:0804.2436
- De Silva, G. M., Freeman, K. C., Asplund, M., Bland-Hawthorn, J., Bessell, M. S., & Collet, R. 2007, *AJ*, 133, 1161
- De Simone, R., Wu, X., & Tremaine, S. 2004, *MNRAS*, 350, 627
- del Peloso, E. F., da Silva, L., Porto de Mello, G. F., & Arany-Prado, L. I. 2005, *A&A*, 440, 1153
- Debattista, V. P., & Sellwood, J. A. 2000, *ApJ*, 543, 704
- Decressin, T., Charbonnel, C., & Meynet, G. 2007, *A&A*, 475, 859
- Dehnen, W. 1998, *AJ*, 115, 2384
- Dehnen, W. 1999, *ApJ*, 524, L35
- Dehnen, W., & Binney, J. J. 1998, *MNRAS*, 298, 387
- Dias, W. S., Alessi, B. S., Moitinho, A., & Lépine, J. R. D. 2002, *A&A*, 389, 871
- Dickey, J. M., & Lockman, F. J. 1990, *ARA&A*, 28, 215
- Diemand, J., Moore, B., & Stadel, J. 2005, *Nature*, 433, 389
- Digel, S., de Geus, E., & Thaddeus, P. 1994, *ApJ*, 422, 92
- Dillon, M., et al. 2008, *MNRAS*, 386, 1568
- Drew, J. E., et al. 2005, *MNRAS*, 362, 753
- Drimmel, R., & Spergel, D. N. 2001, *ApJ*, 556, 181

- Drimmel, R., Cabrera-Lavers, A., & López-Corredoira, M. 2003, *A&A*, 409, 205
- Edvardsson, B., Andersen, J., Gustafsson, B., Lambert, D. L., Nissen, P. E., & Tomkin, J. 1993, *A&A*, 275, 101
- Eggen, O. J., Lynden-Bell, D., & Sandage, A. R. 1962, *ApJ*, 136, 748
- Ehlerová, S., & Palouš, J. 2005, *A&A*, 437, 101
- Eisenhauer, F., et al. 2005, *ApJ*, 628, 246
- Elmegreen, B. G. 2007, *ApJ*, 668, 1064
- Elmegreen, B. G., & Efremov, Y. N. 1997, *ApJ*, 480, 235
- Elmegreen, B. G., & Elmegreen, D. M. 2006, *ApJ*, 650, 644
- Englmaier, P., & Gerhard, O. 1999, *MNRAS*, 304, 512
- ESA, 1997, *The Hipparcos and Tycho Catalogues*, ESA SP-1200
- Evans, C. 2007, *Massive Stars: Fundamental Parameters and Circumstellar Interactions*, in press
- Famaey, B., Jorissen, A., Luri, X., Mayor, M., Udry, S., Dejonghe, H., & Turon, C. 2005, *A&A*, 430, 165
- Fellhauer, M., et al. 2006, *ApJ*, 651, 167
- Ferguson, A. M. N., Irwin, M. J., Ibata, R. A., Lewis, G. F., & Tanvir, N. R. 2002, *AJ*, 124, 1452
- Ferrara, A., & Tolstoy, E. 2000, *MNRAS*, 313, 291
- Ferrière, K., Gillard, W., & Jean, P. 2007, *A&A*, 467, 611
- Fich, M., Blitz, L., & Stark, A. A. 1989, *ApJ*, 342, 272
- Figer, D. F., Najarro, F., Morris, M., McLean, I. S., Geballe, T. R., Ghez, A. M., & Langer, N. 1998, *ApJ*, 506, 384
- Figer, D. F., et al. 2002, *ApJ*, 581, 258
- Flynn, C., Holmberg, J., Portinari, L., Fuchs, B., & Jahreiß, H. 2006, *MNRAS*, 372, 1149
- Fraternali, F., Binney, J., Oosterloo, T., & Sancisi, R. 2007, *New Astronomy Review*, 51, 95
- Frebel, A., et al. 2005, *Nature*, 434, 871
- Freedman, W. L., et al. 2001, *ApJ*, 553, 47
- Freeman, K., & Bland-Hawthorn, J. 2002, *ARA&A*, 40, 487
- Freitag, M., Amaro-Seoane, P., & Kalogera, V. 2006, *ApJ*, 649, 91

- Friel, E. D. 1995, *ARA&A*, 33, 381
- Froebrich, D., Murphy, G. C., Smith, M. D., Walsh, J., & Del Burgo, C. 2007, *MNRAS*, 378, 1447
- Fulbright, J. P., McWilliam, A., & Rich, R. M. 2007, *ApJ*, 661, 1152
- Fuhrmann, K. 2004, *Astronomische Nachrichten*, 325, 3
- Fuhrmann, K. 2008, *MNRAS*, 384, 173
- Fux, R. 1999, *A&A*, 345, 787
- Galli, D. 2006, *Chemical Abundances and Mixing in Stars in the Milky Way and its Satellites*, ESO Astrophysics Symposia, Springer-Verlag, 343
- Gao, L., White, S. D. M., Jenkins, A., Stoehr, F., & Springel, V. 2004, *MNRAS*, 355, 819
- Gaume, R. A., Jr., Dorland, B., Zacharias, N., Hennessy, G., Johnston, K., & Makarov, V. 2007, *American Astronomical Society Meeting Abstracts*, 210, #86.01
- Geisler, D., Wallerstein, G., Smith, V. V., & Casetti-Dinescu, D. I. 2007, *PASP*, 119, 939
- Genzel, R., et al. 2003a, *ApJ*, 594, 812
- Genzel, R., Schödel, R., Ott, T., Eckart, A., Alexander, T., Lacombe, F., Rouan, D., & Aschenbach, B. 2003b, *Nature*, 425, 934
- Ghez, A. M., Salim, S., Hornstein, S. D., Tanner, A., Lu, J. R., Morris, M., Becklin, E. E., & Duchêne, G. 2005, *ApJ*, 620, 744
- Gilmore, G., Wilkinson, M. I., Wyse, R. F. G., Kleyana, J. T., Koch, A., Evans, N. W., & Grebel, E. K. 2007, *ApJ*, 663, 948
- Gilmore, G., & Reid, N. 1983, *MNRAS*, 202, 1025
- Girard, T. M., Korchagin, V. I., Casetti-Dinescu, D. I., van Altena, W. F., López, C. E., & Monet, D. G. 2006, *AJ*, 132, 1768
- Girardi, L., Groenewegen, M. A. T., Hatziminaoglou, E., & da Costa, L. 2005, *A&A*, 436, 895
- Gnedin, O. Y., & Ostriker, J. P. 1997, *ApJ*, 474, 223
- Gnedin, O. Y., Gould, A., Miralda-Escudé, J., & Zentner, A. R. 2005, *ApJ*, 634, 344
- Goldsmith, P. F., & Li, D. 2005, *ApJ*, 622, 938
- Goodwin, S. P., & Bastian, N. 2006, *MNRAS*, 373, 752
- Goodwin, S. P., Kroupa, P., Goodman, A., & Burkert, A. 2007, *Protostars and Planets V*, 133

- Goodwin, S. P., Nutter, D., Kroupa, P., Ward-Thompson, D., & Whitworth, A. P. 2008, *A&A*, 477, 823
- Goriely, S., & Arnould, M. 2001, *A&A*, 379, 1113
- Gouda, N., Kobayashi, Y., Yamada, Y., et al. 2007, *Advances in Space Research*, 40, 664
- Gough, D. O. 2001, *Astrophysical Ages and Times Scales*, ASP Conference Series, 245, 31
- Gratton, R. G., Sneden, C., Carretta, E., & Bragaglia, A. 2000, *A&A*, 354, 169
- Gratton, R. G., Carretta, E., Desidera, S., Lucatello, S., Mazzei, P., & Barbieri, M. 2003, *A&A*, 406, 131
- Gratton, R., Sneden, C., & Carretta, E. 2004, *ARA&A*, 42, 385
- Grebel, E. K., & Gallagher, J. S., III 2004, *ApJ*, 610, L89
- Greggio, L., Renzini, A., & Daddi, E. 2008, *MNRAS*, 730
- Groot, P. J., et al. 2006, *Exploiting Large Surveys for Galactic Astronomy*, 26th meeting of theIAU, Joint Discussion 13, 22-23 August 2006, Prague, Czech Republic, JD13, #54, 13,
- Gualandris, A., Portegies Zwart, S., & Sipior, M. S. 2005, *MNRAS*, 363, 223
- Haffner, L. M., Reynolds, R. J., Tufte, S. L., Madsen, G. J., Jaehnig, K. P., & Percival, J. W. 2003, *ApJS*, 149, 405
- Hamadache, C., et al. 2006, *A&A*, 454, 185
- Han, Z., & Podsiadlowski, P. 2004, *MNRAS*, 350, 1301
- Hansen, B. M. S., et al. 2002, *ApJ*, 574, L155
- Hansen, B. M. S., et al. 2004, *ApJS*, 155, 551
- Hansen, B. M. S., et al. 2007, *ApJ*, 671, 380
- Harris, W. E. 1991, *ARA&A*, 29, 543
- Harris, W. E. 1996, *AJ*, 112, 1487
- Harris, H. C., et al. 2006, *AJ*, 131, 571
- Hartmann, D., & Burton, W. B. 1997, *Atlas of Galactic Neutral Hydrogen*, by Dap Hartmann and W. Butler Burton, pp. 243. ISBN 0521471117. Cambridge, UK: Cambridge University Press, February 1997.,
- Hartmann, L., Ballesteros-Paredes, J., & Bergin, E. A. 2001, *ApJ*, 562, 852
- Haywood, M. 2005, *TheThree-Dimensional Universe with Gaia*, 576, 521
- Haywood, M. 2008, *MNRAS*, 388, 1175

- Hébrard, G., & Moos, H. W. 2003, *ApJ*, 599, 297
- Heller, C. H., Shlosman, I., & Athanassoula, E. 2007, *ApJ*, 671, 226
- Helmi, A. 2004, *ApJ*, 610, L97
- Helmi, A., & White, S. D. M. 1999, *MNRAS*, 307, 495
- Helmi, A., White, S. D. M., de Zeeuw, P. T., & Zhao, H. 1999, *Nature*, 402, 53
- Helmi, A., Navarro, J. F., Nordström, B., Holmberg, J., Abadi, M. G., & Steinmetz, M. 2006, *MNRAS*, 365, 1309
- Helmi, A., et al. 2006b, *ApJ*, 651, L121
- Hendry, M. A., et al. 2006, *MNRAS*, 369, 1303
- Henry, T. J., Jao, W.-C., Subasavage, J. P., Beaulieu, T. D., Ianna, P. A., Costa, E., & Méndez, R. A. 2006, *AJ*, 132, 2360
- Hernandez, X., Valls-Gabaud, D., & Gilmore, G. 2000, *MNRAS*, 316, 605
- Hilditch, R. W., Howarth, I. D., & Harries, T. J. 2005, *MNRAS*, 357, 304
- Hill, V., et al. 2002, *A&A*, 387, 560
- Høg, E., et al. 2000, *A&A*, 355, L27
- Holmberg, J., & Flynn, C. 2000, *MNRAS*, 313, 209
- Holmberg, J., & Flynn, C. 2004, *MNRAS*, 352, 440
- Holmberg, J., Nordström, B., & Andersen, J. 2007, *A&A*, 475, 519
- Huang, W., & Gies, D. R. 2006, *ApJ*, 648, 580
- Huang, W., & Gies, D. R. 2006b, *ApJ*, 648, 591
- Hunter, C., & Toomre, A. 1969, *ApJ*, 155, 747
- Hunter, D. A., Elmegreen, B. G., Dupuy, T. J., & Mortonson, M. 2003, *AJ*, 126, 1836
- Hunter, I., et al. 2008, *ApJ*, 676, L29
- Ibata, R., Irwin, M., Lewis, G. F., & Stolte, A. 2001, *ApJ*, 547, L133
- Ibata, R., Irwin, M., Lewis, G., Ferguson, A. M. N., & Tanvir, N. 2001b, *Nature*, 412, 49
- Ibata, R. A., Lewis, G. F., Irwin, M. J., & Quinn, T. 2002, *MNRAS*, 332, 915
- Ibata, R. A., Irwin, M. J., Lewis, G. F., Ferguson, A. M. N., & Tanvir, N. 2003, *MNRAS*, 340, L21
- Ibata, R., Martin, N. F., Irwin, M., Chapman, S., Ferguson, A. M. N., Lewis, G. F., & McConnachie, A. W. 2007, *ApJ*, 671, 1591

- Ivezic, Z., et al. 2008, ArXiv e-prints, 804, arXiv:0804.3850
- Jenkins, A., & Binney, J. 1990, MNRAS, 245, 305
- Jiang, I.-G., & Binney, J. 1999, MNRAS, 303, L7
- Jimenez, R., Flynn, C., & Kotoneva, E. 1998, MNRAS, 299, 515
- Jin, S., & Lynden-Bell, D. 2007, MNRAS, 378, L64
- Johnston, K. V., Law, D. R., & Majewski, S. R. 2005, ApJ, 619, 800
- Johnston, K. V., Spergel, D. N., & Haydn, C. 2002, ApJ, 570, 656
- Julian, W. H., & Toomre, A. 1966, ApJ, 146, 810
- Just, A., & Jahreiss, H. 2007, ArXiv e-prints, 706, arXiv:0706.3850
- Jurić, M., et al. 2008, ApJ, 673, 864
- Kahn, F. D., & Woltjer, L. 1959, ApJ, 130, 705
- Kalberla, P. M. W., & Haud, U. 2006, A&A, 455, 481
- Kalberla, P. M. W., Burton, W. B., Hartmann, D., Arnal, E. M., Bajaja, E., Morras, R., Pöppel, W. G. L. 2005, A&A, 440, 775
- Kalirai, J. S., Richer, H. B., Reitzel, D., Hansen, B. M. S., Rich, R. M., Fahlman, G. G., Gibson, B. K., & von Hippel, T. 2005, ApJ, 618, L123
- Kalirai, J. S., et al. 2006, ApJ, 648, 389
- Kazantzidis, S., Kravtsov, A. V., Zentner, A. R., Allgood, B., Nagai, D., & Moore, B. 2004, ApJ, 611, L73
- Keller, S. C. 2004, Publications of the Astronomical Society of Australia, 21, 310
- Kerr, F. J. 1957, AJ, 62, 93
- Kerr, F. J., Bowers, P. F., Jackson, P. D., & Kerr, M. 1986, A&AS, 66, 373
- Klypin, A., Kravtsov, A. V., Valenzuela, O., & Prada, F. 1999, ApJ, 522, 82
- Klypin, A., Zhao, H., & Somerville, R. S. 2002, ApJ, 573, 597
- Kobayashi, Y., et al. 2006, Proc. SPIE, 6265, 626544
- Kohoutek, L., & Wehmeyer, R. 1999, A&AS, 134, 255
- Korn, A. J., Grundahl, F., Richard, O., Barklem, P. S., Mashonkina, L., Collet, R., Piskunov, N., & Gustafsson, B. 2006, Nature, 442, 657
- Kotulla, R., Fritze, U., & Anders, P. 2008, MNRAS, 387, 1149
- Krabbe, A., Genzel, R., Drapatz, S., & Rotaciuc, V. 1991, ApJ, 382, L19
- Krauss, L. M., & Chaboyer, B. 2003, Science, 299, 65

- Kravtsov, A. V., & Gnedin, O. Y. 2005, *ApJ*, 623, 650
- Kroupa, P. 2001, *MNRAS*, 322, 231
- Kroupa, P. 2002, *Science*, 295, 82
- Kroupa, P. 2002b, *MNRAS*, 330, 707
- Kroupa, P. 2007, *ArXiv-preprints*, 703, arXiv:0703.0124
- Kroupa, P. 2008, *ArXiv-preprints*, 803, arXiv:0803.1833
- Krumholz, M. R., & Bonnell, I. A. 2007, *ArXiv e-prints*, 712, arXiv:0712.0828
- Krumholz, M. R., & Tan, J. C. 2007, *ApJ*, 654, 304
- Kuijken, K., & Gilmore, G. 1989, *MNRAS*, 239, 605
- Kunkel, W. E., Demers, S., Irwin, M. J., & Albert, L. 1997, *ApJ*, 488, L129
- Lacey, C. G. 1984, *MNRAS*, 208, 687
- Lada, C. J., & Lada, E. A. 2003, *ARA&A*, 41, 57
- Lamers, H. J. G. L. M., Gieles, M., Bastian, N., Baumgardt, H., Kharchenko, N. V., & Portegies Zwart, S. 2005, *A&A*, 441, 117
- Lanfranchi, G. A., & Matteucci, F. 2007, *A&A*, 468, 927
- Lanfranchi, G. A., Matteucci, F., & Cescutti, G. 2006, *MNRAS*, 365, 477
- Larson, R. B. 2005, *MNRAS*, 359, 211
- Launhardt, R., Zylka, R., & Mezger, P. G. 2002, *A&A*, 384, 112
- Lawrence, A., et al. 2007, *MNRAS*, 379, 1599
- Lebreton, Y., Michel, E., Goupil, M. J., Baglin, A., & Fernandes, J. 1995, *Astronomical and Astrophysical Objectives of Sub-Milliarcsecond Optical Astrometry*, IAU Symposium, 166, 135
- Lecureur, A., Hill, V., Zoccali, M., Barbuy, B., Gómez, A., Minniti, D., Ortolani, S., & Renzini, A. 2007, *A&A*, 465, 799
- Lee, H.-c., Gibson, B. K., Flynn, C., Kawata, D., & Beasley, M. A. 2004, *MNRAS*, 353, 113
- Lee, Y.-W., Gim, H. B., & Casetti-Dinescu, D. I. 2007, *ApJ*, 661, L49
- Leigh, N., Sills, A., & Knigge, C. 2007, *ApJ*, 661, 210
- Leisy, P., & Dennefeld, M. 2006, *A&A*, 456, 451
- Levine, E. S., Blitz, L., & Heiles, C. 2006, *Science*, 312, 1773
- Limongi, M., Chieffi, A. 2007, *Stellar Nucleosynthesis: 50 years after B2FH*, eds. C. Charbonnel and J. P. Zahn, EAS publication Series (in press)

- Lindegren, L., & Perryman, M. A. C. 1996, *A&AS*, 116, 579
- Linsky, J. L., et al. 2006, *ApJ*, 647, 1106
- López-Corredoira, M., Betancort-Rijo, J., & Beckman, J. E. 2008, *ASP Conference Series*, 390, 359
- López-Corredoira, M., Cabrera-Lavers, A., & Gerhard, O. E. 2005, *A&A*, 439, 107
- López-Corredoira, M., Cabrera-Lavers, A., Garzón, F., & Hammersley, P. L. 2002, *A&A*, 394, 883
- López-Corredoira, M., Cabrera-Lavers, A., Mahoney, T. J., Hammersley, P. L., Garzón, F., & González-Fernández, C. 2007a, *AJ*, 133, 154
- López-Corredoira, M., Momany, Y., Zaggia, S., & Cabrera-Lavers, A. 2007b, *A&A*, 472, L47
- Lubowich, D. A., Pasachoff, J. M., Balonek, T. J., Millar, T. J., Tremonti, C., Roberts, H., & Galloway, R. P. 2000, *Nature*, 405, 1025
- Lucas, P. W., et al. 2007, *ArXiv e-prints*, 712, arXiv:0712.0100
- Mackey, A. D., & Gilmore, G. F. 2004, *MNRAS*, 355, 504
- Maeder, A., & Meynet, G. 2001, *A&A*, 373, 555
- Majewski, S. R., et al. 2004, *AJ*, 128, 245
- Majewski, S. R., et al. 2007, *American Astronomical Society Meeting Abstracts*, 211, #132.08
- Malhotra, S. 1995, *ApJ*, 448, 138
- Maness, H., et al. 2007, *ApJ*, 669, 1024
- Marshall, D. J., Robin, A. C., Reylé, C., Schultheis, M., & Picaud, S. 2006, *A&A*, 453, 635
- Martayan, C., Frémat, Y., Hubert, A.-M., Floquet, M., Zorec, J., & Neiner, C. 2007, *A&A*, 462, 683
- Martin, N. F., Ibata, R. A., Bellazzini, M., Irwin, M. J., Lewis, G. F., & Dehnen, W. 2004, *MNRAS*, 348, 12
- Martin, N. F., Ibata, R. A., Irwin, M. J., Chapman, S., Lewis, G. F., Ferguson, A. M. N., Tanvir, N., & McConnachie, A. W. 2006, *MNRAS*, 371, 1983
- Martin, N. F., Ibata, R. A., Chapman, S. C., Irwin, M., & Lewis, G. F. 2007, *MNRAS*, 380, 281
- Mashonkina, L., & Gehren, T. 2001, *A&A*, 376, 232
- Massey, P. 2003, *ARA&A*, 41, 15
- Massey, P., Johnson, K. E., & Degioia-Eastwood, K. 1995, *ApJ*, 454, 151

- Mathewson, D. S., Cleary, M. N., & Murray, J. D. 1974, *ApJ*, 190, 291
- Matteucci, F. 2001, *The chemical evolution of the Galaxy* (Kluwer)
- Mayer, L., Governato, F., Colpi, M., Moore, B., Quinn, T., Wadsley, J., Stadel, J., & Lake, G. 2001, *ApJ*, 559, 754
- Maund, J. R., & Smartt, S. J. 2005, *MNRAS*, 360, 288
- Maund, J. R., Smartt, S. J., & Danziger, I. J. 2005, *MNRAS*, 364, L33
- McClure-Griffiths, N. M., Dickey, J. M., Gaensler, B. M., & Green, A. J. 2002, *ApJ*, 578, 176
- McClure-Griffiths, N. M., Dickey, J. M., Gaensler, B. M., & Green, A. J. 2004, *ApJ*, 607, L127
- Meléndez, J., et al. 2008, *A&A*, 484, L21
- Melioli, C., Brighenti, F., D'Ercole, A., & de Gouveia Dal Pino, E. M. 2008, *ArXiv e-prints*, 805, arXiv:0805.1138
- Meynet, G. 2007, *Stellar Nucleosynthesis: 50 years after B2FH*, eds. C. Charbonnel and J. P. Zahn, *EAS publication Series* (in press)
- Meynet, G., & Maeder, A. 2005, *A&A*, 429, 581
- Minniti, D., Lucas, P., Adamson, A., & co-authors, 5. 2006, *Memorie della Societa Astronomica Italiana*, 77, 1184
- Minniti, D., & Zoccali, M. 2008, *IAU Symposium*, 245, 323
- Mokiem, M. R., et al. 2006, *A&A*, 456, 1131
- Moore, B., Ghigna, S., Governato, F., Lake, G., Quinn, T., Stadel, J., & Tozzi, P. 1999, *ApJ*, 524, L19
- Moore, T. J. T., Bretherton, D. E., Fujiyoshi, T., Ridge, N. A., Allsopp, J., Hoare, M. G., Lumsden, S. L., & Richer, J. S. 2007, *MNRAS*, 379, 663
- Morris, M., & Serabyn, E. 1996, *ARA&A*, 34, 645
- Murakami, H., et al. 2007, *PASJ*, 59, 369
- Murphy, S. J., Keller, S. C., Schmidt, B., Tisserand, P., Bessell, M., Francis, P., & Da Costa, G. 2008, *ArXiv e-prints*, 806, arXiv:0806.1770
- Naab, T., & Ostriker, J. P. 2006, *MNRAS*, 366, 899
- Navarro, J. F., Frenk, C. S., & White, S. D. M. 1997, *ApJ*, 490, 493
- Neckel, T., Klare, G., & Sarcander, M. 1980, *A&AS*, 42, 251
- Newberg, H. J., et al. 2002, *ApJ*, 569, 245
- Nipoti, C., & Binney, J. 2007, *MNRAS*, 382, 1481

- Nissen, P. E. 2005, Proceedings of the Gaia Symposium, eds. Turon, C., O’Flaherty, K. S., Perryman, M. A.C., 121
- Nomoto, K. 1984, ApJ, 277, 791
- Nomoto, K., Iwamoto, K., Nakasato, N., Thielemann, F.-K., Brachwitz, F., Tsujimoto, T., Kubo, Y., & Kishimoto, N. 1997, Nuclear Physics A, 621, 467
- Nomoto, K., Tominaga, N., Umeda, H., Kobayashi, C., & Maeda, K. 2006, Nuclear Physics A, 777, 424
- Nomoto, K., Tominaga, N., Tanaka, M., Maeda, K., & Umeda, H. 2008, IAU Symposium, 250, 463
- Nordström, B., et al. 2004, A&A, 418, 989
- Norris, J. 1987, ApJ, 314, L39
- Odenkirchen, M., et al. 2001, AJ, 122, 2538
- Odenkirchen, M., Grebel, E. K., Dehnen, W., Rix, H.-W., & Cudworth, K. M. 2002, AJ, 124, 1497
- Olive, K. A., & Skillman, E. D. 2004, ApJ, 617, 29
- Oosterloo, T., Fraternali, F., & Sancisi, R. 2007, AJ, 134, 1019
- Ortolani, S., Renzini, A., Gilmozzi, R., Marconi, G., Barbuy, B., Bica, E., & Rich, R. M. 1995, Nature, 377, 701
- Ostriker, E. C., & Binney, J. J. 1989, MNRAS, 237, 785
- Pace, G., & Pasquini, L. 2004, A&A, 426, 1021
- Pagel, B. E. J. 1997, Nucleosynthesis and Chemical Evolution of Galaxies, by Bernard E. J. Pagel, pp. 392. ISBN 0521550610. Cambridge, UK: Cambridge University Press, October 1997.
- Palla, F., Galli, D., Marconi, A., Stanghellini, L., & Tosi, M. 2002, ApJ, 568, L57
- Parker, Q. A., et al. 2005, MNRAS, 362, 689
- Patsis, P. A., Skokos, C., & Athanassoula, E. 2003, Astrophysical Supercomputing using Particle Simulations, IAU Symposium, 208, 437
- Paulson, D. B., Sneden, C., & Cochran, W. D. 2003, AJ, 125, 3185
- Paumard, T., et al. 2006, ApJ, 643, 1011
- Paunzen, E., Maitzen, H. M., Pintado, O. I., Claret, A., Iliev, I. K., & Netopil, M. 2006, A&A, 459, 871
- Peacock, J. A., Schneider, P., Efstathiou, G., Ellis, J. R., Leibundgut, B., Lilly, S. J., & Mellier, Y. 2006, ESA-ESO Working Group Report on "Fundamental Cosmology"

- Pedersen, K., Rasmussen, J., Sommer-Larsen, J., Toft, S., Benson, A. J., & Bower, R. G. 2006, *New Astronomy*, 11, 465
- Peek, J. E. G., Putman, M. E., & Sommer-Larsen, J. 2008, *ApJ*, 674, 227
- Peimbert, M., Luridiana, V., & Peimbert, A. 2007, *ApJ*, 666, 636
- Martinez-Delgado Hans-Walter Rix, J. P. D. 2007, *astro-ph/0703601*
- Perryman, M. A. C., et al. 1997, *A&A*, 323, L49
- Perryman, M., et al. 2005, ESA-ESO Working Group on Report ‘Extra-solar Planets’
- Pettini, M., Ellison, S. L., Steidel, C. C., & Bowen, D. V. 1999, *ApJ*, 510, 576
- Pettini, M., Madau, P., Bolte, M., Prochaska, J. X., Ellison, S. L., & Fan, X. 2003, *ApJ*, 594, 695
- Piau, L., Beers, T. C., Balsara, D. S., Sivarani, T., Truran, J. W., & Ferguson, J. W. 2006, *ApJ*, 653, 300
- Poglitsch, A., et al. 2006, 36th COSPAR Scientific Assembly, 36, 215
- Politano, M., & Weiler, K. P. 2007, *ApJ*, 665, 663
- Poelarends, A. J. T., Herwig, F., Langer, N., & Heger, A. 2008, *ApJ*, 675, 614
- Pont, F., & Eyer, L. 2004, *MNRAS*, 351, 487
- Popowski, P., et al. 2005, *ApJ*, 631, 879
- Prantzos, N. 2007, *Stellar Nucleosynthesis: 50 years after B2FH*, eds. C. Charbonnel and J. P. Zahn, *EAS publication Series* (in press)3185
- Pretorius, M. L., Knigge, C., O’Donoghue, D., Henry, J. P., Gioia, I. M., & Mullis, C. R. 2007, *MNRAS*, 382, 1279
- Pritzl, B. J., Venn, K. A., & Irwin, M. 2005, *AJ*, 130, 2140
- Prochaska, J. X., Naumov, S. O., Carney, B. W., McWilliam, A., & Wolfe, A. M. 2000, *AJ*, 120, 2513
- Prodanovic, T., & Fields, B. D. 2008, *ArXiv e-prints*, 804, arXiv:0804.3095
- Putman, M. E., Staveley-Smith, L., Freeman, K. C., Gibson, B. K., & Barnes, D. G. 2003, *ApJ*, 586, 170
- Quillen, A. C., & Garnett, D. R. 2001, *Galaxy Disks and Disk Galaxies*, *ASP Conference Series*, 230, 87
- Quillen, A. C., & Minchev, I. 2005, *AJ*, 130, 576
- Quinn, P. J., Hernquist, L., & Fullagar, D. P. 1993, *ApJ*, 403, 74
- Quinn, T., & Binney, J. 1992, *MNRAS*, 255, 729

- Rana, N. C., & Wilkinson, D. A. 1986, MNRAS, 218, 721
- Rattenbury, N. J., Mao, S., Sumi, T., & Smith, M. C. 2007, MNRAS, 378, 1064
- Reddy, B. E., Lambert, D. L., & Allende Prieto, C. 2006, MNRAS, 367, 1329
- Reid, M. J., & Brunthaler, A. 2005, Future Directions in High Resolution Astronomy, ASP Conference Series, 340, 253
- Renzini, A., & Buzzoni, A. 1986, Spectral Evolution of Galaxies, 122, 195
- Renzini, A. 1997, ApJ, 488, 35
- Rich, R. M., Reitzel, D. B., Howard, C. D., & Zhao, H. 2007, ApJ, 658, L29
- Richer, H. B., et al. 1996, ApJ, 463, 602
- Rix, S. A., Pettini, M., Steidel, C. C., Reddy, N. A., Adelberger, K. L., Erb, D. K., & Shapley, A. E. 2007, ApJ, 670, 15
- Robin, A. C., Reyl e, C., Derri re, S., & Picaud, S. 2003, A&A, 409, 523
- Robin, A. C., et al. 2007, ApJS, 172, 545
- Rocha-Pinto, H. J., Scalo, J., Maciel, W. J., & Flynn, C. 2000, ApJ, 531, L115
- Rogers, A. E. E., D devoir, K. A., Carter, J. C., Fanous, B. J., Kratzenberg, E., & Bania, T. M. 2005, ApJ, 630, L41
- Romano, D., Tosi, M., Chiappini, C., & Matteucci, F. 2006, MNRAS, 369, 295
- Romano, D., Chiappini, C., Matteucci, F., & Tosi, M. 2005, A&A, 430, 491
- Roxburgh, I. W., & Vorontsov, S. V. 2003, A&A, 411, 215
- Ruphy, S., Robin, A. C., Epchtein, N., Copet, E., Bertin, E., Fouque, P., & Guglielmo, F. 1996, A&A, 313, L21
- Russeil, D. 2003, A&A, 397, 133
- Russeil, D., Adami, C., & Georgelin, Y. M. 2007, A&A, 470, 161
- Sahu, K. C., et al. 2006, Nature, 443, 534
- Sakamoto, T., Chiba, M., & Beers, T. C. 2003, A&A, 397, 899
- Sales, L. V., et al. 2008, ArXiv e-prints, 805, arXiv:0805.0508
- Salpeter, E. E. 1955, ApJ, 121, 161
- Sandage, A., Lubin, L. M., & Vandenberg, D. A. 2003, PASP, 115, 1187
- Sancisi, R., Fraternali, F., Oosterloo, T., & van der Hulst, T. 2008, A&A Rev., 15, 189
- Sanders, R. H., & McGaugh, S. S. 2002, ARA&A, 40, 263

- Scalo, J. 1998, The Stellar Initial Mass Function (38th Herstmonceux Conference), ASP Conference Series, 142, 201
- Schlegel, D. J., Finkbeiner, D. P., & Davis, M. 1998, ApJ, 500, 525
- Schweizer, F. 1986, in “Nearly Normal Galaxies”, Faber, S., 18
- Seabroke, G. M., & Gilmore, G. 2007, MNRAS, 380, 1348
- Searle, L., & Zinn, R. 1978, ApJ, 225, 357
- Seigar, M. S., & James, P. A. 2002, MNRAS, 337, 1113
- Sellwood, J. A. 2008, ApJ, 679, 379
- Sellwood, J. A., & Binney, J. J. 2002, MNRAS, 336, 785
- Sellwood, J. A., & McGaugh, S. S. 2005, ApJ, 634, 70
- Sembach, K. R., et al. 2003, ApJS, 146, 165
- Shen, J., & Sellwood, J. A. 2006, MNRAS, 370, 2
- Shetrone, M., Venn, K. A., Tolstoy, E., Primas, F., Hill, V., & Kaufer, A. 2003, AJ, 125, 684
- Siess, L. 2007, Stellar Nucleosynthesis: 50 years after B2FH, eds. C. Charbonnel and J. P. Zahn, EAS publication Series (in press)
- Smartt, S. J., Maund, J. R., Hendry, M. A., Tout, C. A., Gilmore, G. F., Mattila, S., & Benn, C. R. 2004, Science, 303, 499
- Smith, L. J., & Gallagher, J. S. 2001, MNRAS, 326, 1027
- Smith, M. C., et al. 2007, MNRAS, 379, 755
- Smith, V. V., Lambert, D. L., & Nissen, P. E. 1993, ApJ, 408, 262
- Smith, V. V., Lambert, D. L., & Nissen, P. E. 1998, ApJ, 506, 405
- Snedden, C. 2005, From Lithium to Uranium: Elemental Tracers of Early Cosmic Evolution, IAU Symposium, 228, 337
- Sommer-Larsen, J., Götz, M., & Portinari, L. 2003, ApJ, 596, 47
- Soubiran, C., & Girard, P. 2005, A&A, 438, 139
- Soubiran, C., Bienaymé, O., Mishenina, T. V., & Kovtyukh, V. V. 2008, A&A, 480, 91
- Sparke, L. S., & Casertano, S. 1988, MNRAS, 234, 873
- Spergel, D. N., & Steinhardt, P. J. 2000, Physical Review Letters, 84, 3760
- Spergel, D. N., et al. 2007, ApJS, 170, 377

- Spite, F., & Spite, M. 1982, *A&A*, 115, 357
- Spite, M., et al. 2005, *A&A*, 430, 655
- Spitzer, L. J., & Schwarzschild, M. 1953, *ApJ*, 118, 106
- Stanek, K. Z. 1995, *ApJ*, 441, L29
- Stark, A. A., & Lee, Y. 2005, *ApJ*, 619, L159
- Stehle, M., Mazzali, P. A., Benetti, S., & Hillebrandt, W. 2005, *MNRAS*, 360, 1231
- Steigman, G. 2006, *International Journal of Modern Physics E*, 15, 1
- Steinmetz, M., et al. 2006, *AJ*, 132, 1645
- Stephenson, C. B., Sanduleak, N. 1971, *PW & SO*, 1, 1
- Stoehr, F., White, S. D. M., Springel, V., Tormen, G., & Yoshida, N. 2003, *MNRAS*, 345, 1313
- Stolte, A., Brandner, W., Grebel, E. K., Lenzen, R., & Lagrange, A.-M. 2005, *ApJ*, 628, L113
- Strickland, D. K., & Heckman, T. M. 2007, *ApJ*, 658, 258
- Strigari, L. E., Koushiappas, S. M., Bullock, J. S., & Kaplinghat, M. 2007, *Phys. Rev. D*, 75, 083526
- Strigari, L. E., Bullock, J. S., Kaplinghat, M., Diemand, J., Kuhlen, M., & Madau, P. 2007b, *ApJ*, 669, 676
- Strolger, L.-G., et al. 2004, *ApJ*, 613, 200
- Sumi, T., et al. 2006, *ApJ*, 636, 240
- Talon, S., & Charbonnel, C. 2003, *A&A*, 405, 1025
- Taylor, J. H., & Cordes, J. M. 1993, *ApJ*, 411, 674
- Tinsley, B. M. 1972, *A&A*, 20, 383
- Tiret, O., & Combes, F. 2007, *A&A*, 464, 517
- Tolstoy, E., Venn, K. A., Shetrone, M., Primas, F., Hill, V., Kaufer, A., & Szeifert, T. 2003, *AJ*, 125, 707
- Tolstoy, E., et al. 2006, *The Messenger*, 123, 33
- Toomre, A. 1964, *ApJ*, 139, 1217
- Toomre, A. 1983, *Internal Kinematics and Dynamics of Galaxies*, 100, 177
- Tremaine, S., & Weinberg, M. D. 1984, *MNRAS*, 209, 729

- Trippe, S., Paumard, T., Gillessen, S., Ott, T., Eisenhauer, F., Martins, F., & Genzel, R. 2008, *Revista Mexicana de Astronomia y Astrofisica Conference Series*, 32, 12
- Tsujimoto, T., Kobayashi, N. 2007, *IAU Symposium 248*, Shanghai, October 2007
- Tumlinson, J. 2007, *ApJ*, 664, L63
- Unavane, M., Wyse, R. F. G., & Gilmore, G. 1996, *MNRAS*, 278, 727
- Urbaneja, M. A., et al. 2005, *ApJ*, 622, 862
- Unwin, S. C., et al. 2008, *PASP*, 120, 38
- Vallée, J. P. 2005, *AJ*, 130, 569
- van Albada, T. S., Bahcall, J. N., Begeman, K., & Sancisi, R. 1985, *ApJ*, 295, 305
- van der Hucht, K. A. 2001, *New Astronomy Review*, 45, 135
- van der Hucht, K. A. 2006, *A&A*, 458, 453
- van Leeuwen, F., & Fantino, E. 2005, *A&A*, 439, 791
- van Loon, J. T. 2008, *ArXiv-prints*, 801, arXiv:0801.0557
- van Woerden, H., Wakker, B. P., Schwarz, U. J., & de Boer, K. S. 2004, *High Velocity Clouds*, 312
- Venn, K. A., Irwin, M., Shetrone, M. D., Tout, C. A., Hill, V., & Tolstoy, E. 2004, *AJ*, 128, 1177
- Walker, M. G., Mateo, M., Olszewski, E. W., Gnedin, O. Y., Wang, X., Sen, B., & Woodroffe, M. 2007, *ApJ*, 667, L53
- Wakker, B. P., et al. 2007a, *ApJ*, 670, L113
- Weaver, H., & Williams, D. R. W. 1973, *A&AS*, 8, 1
- Weaver, H., & Williams, D. R. W. 1974, *A&AS*, 17, 1
- Webbink, R. F. 2007, *ArXiv-prints*, 704, arXiv:0704.0280
- Weidner, C., & Kroupa, P. 2006, *MNRAS*, 365, 1333
- Weinberg, M. D., & Blitz, L. 2006, *ApJ*, 641, L33
- Werner, K., Rauch, T., & Kruk, J. W. 2007, *A&A*, 474, 591
- Werner, K., Rauch, T., Barstow, M. A., & Kruk, J. W. 2004, *A&A*, 421, 1169
- West, A. A., Hawley, S. L., Bochanski, J. J., Covey, K. R., Reid, I. N., Dhital, S., Hilton, E. J., & Masuda, M. 2008, *AJ*, 135, 785
- Wielen, R. 1977, *A&A*, 60, 263
- Williams, K. A., Bolte, M., & Koester, D. 2004, *ApJ*, 615, L49

- Williams, K. A. 2007, 15th European Workshop on White Dwarfs, ASP Conference Series, 372, 85
- Wilkinson, M. I., & Evans, N. W. 1999, MNRAS, 310, 645
- Wilson, T. L., & Elbaz, D. 2006, ESA-ESO Working Group Report on 'The Herschel-ALMA Synergies'
- Wolff, S. C. 2005, Astrometry in the Age of the Next Generation of Large Telescopes, ASP Conference Series, 338, 63
- Wolff, S. C., Strom, S. E., Dror, D., & Venn, K. 2007, AJ, 133, 1092
- Wood, A., & Mao, S. 2005, MNRAS, 362, 945
- Woosley, S. E., & Bloom, J. S. 2006, ARA&A, 44, 507
- Worthey, G. 1992, Ph.D. Thesis, Univ. of California, Santa Cruz
- Wyse, R. F. G., & Gilmore, G. 1986, AJ, 91, 855
- Yoachim, P., & Dalcanton, J. J. 2005, ApJ, 624, 701
- Yoon, S.-C., & Langer, N. 2005, A&A, 443, 643
- Yoon, S.-C., Langer, N., Cantiello, M., Woosley, S. E., & Glatzmaier, G. A. 2008, IAU Symposium, 250, 231
- Young, P. A., et al. 2006, ApJ, 640, 891
- Yu, Q., & Tremaine, S. 2003, ApJ, 599, 1129
- Zacharias, N., Laux, U., Rakich, A., & Epps, H. 2006, Proc. SPIE, 6267, 62670
- Zinn, R. 1985, ApJ, 293, 424
- Zoccali, M., et al. 2003, A&A, 399, 931
- Zoccali, M., Hill, V., Lecureur, A., Barbuy, B., Renzini, A., Minniti, D., Gómez, A., & Ortolani, S. 2008, A&A, 486, 177
- Zwitter, T., et al. 2008, AJ, 136, 421

List of abbreviations

AAO: Anglo Australian Observatory
ACS: Advanced Camera for Surveys
AGB: Asymptotic Giant Branch
AGN: Active Galactic Nuclei
AKARI: Japanese infrared satellite mission
ALMA: Atacama Large Millimetre Array
AMR: Age-Metallicity Relation
ANU: Australian National University
AO: Adaptive Optics
APEX: Atacama Pathfinder EXperiment
APO: Apache Point Observatory
APOGEE: Apache Point Observatory Galactic Evolution Experiment
ATLAS: one of three approved VST Public Surveys
BBN: Big Bang Nucleosynthesis
BH: Black Hole
CCD: Charged Coupled Device
CDM: Cold Dark Matter
CERN: European Organisation for Nuclear Research
Chandra: NASA X-ray observatory, launched in 1999
CIMF: Cluster Initial Mass Function
CMB: Cosmic Microwave Background
CNES: Centre National d'Etudes Spatiales
CNO: Carbon Nitrogen Oxygen
CO: Carbon Oxide
COBE: Cosmic Background Explorer
CODEX: Cosmic Dynamics EXperiment (high resolution spectrograph for the E-ELT)
CoRoT: COncvection, ROtation and planetary Transits
COS: Cosmic Origins Spectrograph (on board of Hubble)
CS: Carbon Sulphide
CTIO: Cerro Tololo Interamerican Observatory
CTIOPI: CTIO Parallax Investigation
DCN: Diclosan (Deuterated Hydrogen Cyanide)
DENIS: DEep Near Infrared Survey of the Southern Sky
DES: Dark Energy Survey
DF: Distribution Function
DIRBE: Diffuse InfraRed Background Experiment
DL: diffraction limit
DLA: Damped Lyman-Alpha
dSph: dwarf spheroidals

EAGLE: Elt Ao for GaLaxy Evolution (multi-object/field, near-infrared spectrograph for the E-ELT)
 E-ELT: European Extremely Large Telescope
 e-MERLIN: upgrade of MERLIN (Multi-Element Radio Linked Interferometer Network)
 EGAPS: European Galactic Plane Surveys
 EIROforum: partnership of the seven largest European Intergovernmental Research Organisations
 ELT: Extremely Large Telescope
 EMIR: Espectrografo Multi-objeto InfraRojo
 EMP: Extremely Metal-Poor
 EPIC: European Photon Imaging Camera (on board of XMM satellite)
 EPICS: Earth-like Planet Imaging Camera and Spectrograph (for the E-ELT)
 ESA: European Space Agency
 ESO: European Southern Observatory
 FGK: stars of spectral type F, G, and K
 FLAMES: Fibre Large Array Multi Element Spectrograph
 FOCES: Fibre Optical Cassegrain Echelle Spectrograph
 FORS: FOcal Reducer Spectrograph
 FOV: Field of View
 FUSE: Far Ultraviolet Spectroscopic Explorer
 GAIA: ESA mission (originally it stood for Global Astrometric Interferometer for Astrophysics)
 GC: Galactic Centre
 GCS: Galactic Clusters Survey (UKIDSS)
 GLIMPSE: Galactic Legacy Infrared Mid-Plane Survey Extraordinaire (Spitzer Legacy Science Programme)
 GLIMPSE-3D: extension of GLIMPSE to latitude strips farther away from the galactic plane
 GMACS: wide-field optical spectrograph for the GMT
 GMT: Giant Magellan Telescope
 GMTNIRS: Giant Magellan Telescope Near-Infrared Spectrograph
 GPS: Galactic Plane Survey (UKIDSS)
 GRB: Gamma Ray Burst
 GRB-SN: Gamma Ray Burst - Supernova connection
 GTC: Gran Telescopio Canarias
 HARMONI: High Angular-Resolution, Monolithic Optical and Near-infrared Integral field spectrograph for the E-ELT
 HARPS: High Accuracy Radial velocity Planet Searcher
 HB: Horizontal Branch
 HCN: Hydrogen Cyanide
 Herschel: Space Observatory and mission to be launched by ESA in 2009

HIFI: Heterodyne Instrument for the Far Infrared on board of Herschel satellite
 HiGAL: the Herschel infrared Galactic Plane Survey
 HRCAM: High-Resolution Camera for the GMT
 HR: Hertzsprung-Russel diagram
 HROS: High-Resolution Optical Spectrograph for the TMT
 HRS: High Resolution Spectrograph (at SALT telescope)
 HST: Hubble Space Telescope
 Hydra: multi-fibre spectrograph installed on the Mayall 4-m telescope at KPNO
 IBIS: Imager on-Board INTEGRAL Satellite
 IFU: Integral Field Unit
 IGIMF: Integrated Galactic Initial Mass Function
 IGM: InterGalactic Medium
 ILR: Inner Lindblad Resonance
 IMF: Initial Mass Function
 INT/WFC: Isaac Newton Telescope Wide Field Camera
 INTEGRAL: International Gamma-Ray Astrophysics Laboratory
 IPHAS: INT/WFC Photometric H-Alpha Survey (part of EGAPS)
 IR: InfraRed
 IRAC: InfraRed Array Camera (on board of Spitzer satellite)
 IRAS: InfraRed Astronomical Satellite
 IRMOS: InfraRed Multi-Object Spectrograph for the TMT
 IRMS: InfraRed Multi-slit Spectrometer for the TMT
 ISM: InterStellar Medium
 J-MAPS: Joint Milli-Arcsec Pathfinder Survey
 JASMINE: Japan Astrometry Satellite Mission for Infrared Exploration
 JAXA: Japan Aerospace Exploration Agency
 JHK: J, H, and K bands
 JWST: James Webb Space Telescope
 LAB: Leiden-Argentine-Bonn (all-sky 21 cm survey)
 LAMOST: Large Sky-Area Multi-Object Fiber Spectroscopic Telescope
 LAS: Large Area Survey
 LBT: Large Binocular Telescope
 LHC: Large Hadron Collider
 LMC: Large Magellanic Cloud
 LSST: Large Synoptic Survey Telescope
 LTAO: Laser-Tomography Adaptive Optics
 LUCIFER: LBT NIR spectroscopic Utility with Camera and Integrated Field Unit
 for Extragalactic Research
 MCAO: Multi-Conjugate Adaptive Optics
 MDF: Metallicity Distribution Function
 METIS: Mid-IR E-ELT Imager and Spectrograph
 MICADO: MCAO Imaging Camera for Deep Observations (imaging camera for

the E-ELT)

MIISE: Mid-IR Imaging Spectrometer for the GMT

MIPS: Multiband Imaging Photometer for SIRTf

MIPSGAL: MIPS Inner Galactic Plane Survey

MIR: Mid-InfraRed

MIRES: Mid-InfraRed Echelle Spectrograph for the TMT

MOND: MODified Newtonian Dynamics

MOS: Multi-Object Spectrograph

MOST: Microvariability and Oscillations of STars

MSTO: Main-Sequence Turn-Off

Nano-JASMINE: technical demonstrator of JASMINE mission

NAOJ: National Astronomical Observatory of Japan

NASA: National Aeronautics and Space Administration

NFW: Navarro, Frenk and White

NGC: New General Catalogue

NIR: Near InfraRed

NIRES: Near-Infrared Echelle Spectrometer for the TMT

NIRMOS: Near-IR Multi-Object Spectrometer for the GMT

NOAO: National Optical Astronomy Observatory

NTT: New Technology Telescope

OmegaCAM: wide field optical camera for the VST

ONe WD: Oxygen Neon White Dwarf

OSIRIS: Ohio State InfraRed Imager/Spectrometer

PACS: Photodetector Array Camera and Spectrometer on board of Herschel satellite

Pan-STARRS: Panoramic Survey Telescope & Rapid Response System

PEPSI: Potsdam Echelle Polarimetric Spectroscopic Instrument

PFI: Planet Formation Imager for the TMT

PNe: Planetary Nebulae

RAVE: Radial Velocity Experiment

RGB: Red Giant Branch

RSAA: Research School of Astronomy and Astrophysics (Australia)

RSS: Robie Stobie Spectrograph (at SALT telescope)

RVS: Radial Velocity Spectrometer on board of Gaia satellite

SALT: Southern African Large Telescope

SALTICAM: SALT Imaging Camera

SDSS: Sloan Digital Sky Survey

SEGUE: Sloan Extension for Galactic Understanding and Exploration

Sgr: Sagittarius

SIM: Space Interferometry Mission

SIMBAD: Set of Identifiers, Measurements and Bibliography for Astronomical Data

SIRTf: Space InfraRed Telescope Facility (now Spitzer Space Telescope)
 SKA: Square Kilometre Array
 SkyMapper: new survey telescope planned by ANU
 SMARTS: Small and Moderate Aperture Research Telescope System
 SMC: Small Magellanic Cloud
 SN: supernova
 SN Ia: type Ia supernova
 SN Ibc: type Ibc supernova
 SN II: type II supernova
 SN II-P: type II supernova with a plateau
 SOAR: SOUThern Astrophysical Research telescope
 SPIRE: Spectral and Photometric Imaging REceiver on board of Herschel satellite
 Spitzer: NASA infrared space observatory
 SSS: Southern Sky Survey
 TMT: Thirty Metre Telescope
 UKIDSS: United Kingdom Infrared Digital Sky Survey
 UKST: United Kingdom Schmidt Telescope
 ULIRG(s): Ultra-Luminous InfraRed Galaxy(ies)
 URAT: USNO Robotic Astrometric Telescope
 USNO: United States Naval Observatory
 UVEX: Northern Galactic Plane UV Excess Survey (part of EGAPS)
 VISTA: Visible and Infrared Survey Telescope for Astronomy
 VHS: VISTA Hemispheric Survey
 VIKING: VISTA KIlo-degree INfrared Galaxy Survey
 VIRCAM: Vista InfraRed Camera
 VLBI: Very Long Baseline Interferometry
 VLT: Very Large Telescope
 VLT-FLAMES: VLT Fibre Large Array Multi-element Spectrograph
 VMC: Vista Magellanic Clouds Survey
 VPHAS+: VST OmegaCAM Photometric H-Alpha Survey
 VST: VLT Survey Telescope
 VVV: Vista Variables in the Via Lactea
 WD: White Dwarf
 WFC: Wide Field Camera
 WFCAM: Wide Field Camera instrument
 WFOS: Wide-Field Optical Spectrograph for the TMT
 WHAM: Wisconsin H-Alpha Mapper
 WHIM: Warm Hot Intergalactic Medium
 WINERED: Warm INfrared Echelle-spectrograph with high-Resolution and high
 Efficiency Devices
 WIRC: Wide-field Infrared Camera for the TMT
 WIYN: Wisconsin-Indiana-Yale NOAO (observatory/telescope)

WMAP: Wilkinson Microwave Anisotropy Probe
WN9/Ofpe: highly evolved stars, with properties intermediate between O-type and Wolf-rayet stars
XAO: eXtreme Adaptive Optics
XMM and/or XMM-Newton: X-ray Multi-Mirror satellite, ESA X-ray space observatory
 Λ CDM: Lambda Cold Dark Matter
2MASS: Two Micron All Sky Survey
6dF: 6-degree field (mounted on the 1.2m UK Schmidt Telescope)